Persistent immune dysregulation from sepsis in critical care

A thesis presented by

Sarah-Jane Speich Cashmore

Registered at

Barts and the London School of Medicine and Dentistry
Queen Mary University of London

For the degree of

Doctor of Philosophy

Centre of Translational Medicine & Therapeutics
John Vane Science Centre
The William Harvey Research Institute
Charterhouse Square
London, EC1M 6BQ

Declaration

I, Sarah-Jane Cashmore, confirm that the research included within this thesis is my own work or that where it has been carried out in collaboration with, or supported by others, that this is duly acknowledged below and my contribution indicated. Previously published material is also acknowledged below.

I attest that I have exercised reasonable care to ensure that the work is original, and does not to the best of my knowledge break any UK law, infringe any third party's copyright or other Intellectual Property Right, or contain any confidential material.

I accept that the College has the right to use plagiarism detection software to check the electronic version of the thesis.

I confirm that this thesis has not been previously submitted for the award of a degree by this or any other university.

Signature:

Date: 30th April 2022

Acknowledgements

I am grateful to Dr Michael O'Dwyer, Professor Gareth Ackland, Professor Charles Hinds, and Professor James Whiteford for their continued supervision and support, and for allowing me the opportunity to enrol on this PhD. Without their supervision this thesis would not have been possible.

For their support and advice, I would like to thank every member of the Ackland lab, Dr Julie Borgel, Dr Ana Gutierrez Del Arroyo, Dr Jenifer Sanchez, Dr Sophie Walker, and Dr Richard Cashmore who have all been invaluable to this journey. Dr Julie Borgel's support has been incredible, with her sound guidance and direction. Rich, you have been my rock, thank you for always being by my side.

This research project was funded by The British Journal of Anaesthesia and The Royal College of Anaesthetists, for which I am most grateful.

Without the kindness of the patients and their families, and the healthy volunteers who have donated to this project, none this would have been possible and for that I am humbled. I am grateful for the hard work that went into this project by the Critical Care research team at The Royal London Hospital.

For their emotional support, I would like to thank my four mandarin ducks; Pepper, Piper, Pickle, and George Clooney. For keeping me sane, I would like to thank my dogs, Casper and Pyxis.

Last but never least, for her continued sacrifice and endless support, I would like to thank my mother, Shirley. Without her I would never have been where I am today and also I would not exist.

Per aspera ad astra

Abstract

Introduction

Patients who survive sepsis can develop an increased morbidity and mortality that persists long-term. This thesis examines whether sepsis induces epigenetic changes in host leukocytes which could result in long-term immune defects in patients, and whether this is due to the infection itself or widely used concomitant treatments sedation and neuromuscular blockade.

Methods

Patients (n=69) with positive blood cultures underwent blood sampling within 24 hours of blood culture result, 4-10 days later and 6-12 months following hospital discharge. Healthy volunteers served as a comparator group (n=37). In Vitro THP1 cell line models explored persistent effects of sepsis, Propofol, and Rocuronium treatment. Gene expression and concentration of candidate cytokines were assayed in cells rechallenged LPS/PMA. Immunometabolic profiling was carried out on cells recovered from Propofol and Rocuronium and rechallenged with septic spike. Chromatin Immunoprecipitation was performed to assess changes in histone modifications.

Results

Gene expression of key histone modifying enzymes were not altered in septic patient cells, but cell may display an immune defect when restimulated. Propofol and Rocuronium both affect the immunometabolism of monocytes, and Sugammadex reverses Rocuronium's effect. Addition of Vecuronium produced a different immunometabolic profile in cells than Rocuronium. The expression of key cholinergic and cytokine genes were affected by

Rocuronium and Sugammadex. Persistent histone modification changes were observed in cells with sepsis or treated with Propofol.

Conclusions

The thesis describes a trend of persisting epigenetic and immunometabolic changes in leukocytes following sepsis, which could result in long-term immune defects in patients. Routinely used Propofol and Rocuronium administration may contribute to these cellular changes, which will have clear clinical implications in treatment of intensive care patients.

List of contents

Figures listed in this thesis

Figure 5.3.6.4 Relative expression of the M1, M2, M3, M4, and M5 genes for THP1 NLRP3-/- cells at passage 17 (peach), passage 23 (blue) and passage 28 (mauve).

Figure 5.3.6.5 Relative expression of A) nAChR α7 B) nAChRβ2, C) nAChRε, D) nAChRγ, E) ChAT, and F) AChT genes for THP1 NLRP3-/- cells at passage 17 (peach), passage 23 (blue) and passage 28 (mauve).

Figure 5.3.6.6 Relative expression of A) IL-10 B) IFNγ C) TNFα D) PINK1 E) Parkin genes for THP1 NLRP3-/- cells at passage 17 (peach), passage 23 (blue) and passage 28 (mauve).

Figure 5.3.7.1 The concentration on IL-10 (ng/mL) in cell supernatants of A) THP1 Nulls, B) THP1 NLRP3-/-, C) HL-60, and D) Monocytes as determined via ELISA assay for cells treated with either Nil drugs control, Rocuronium 1.4µg/ml, Sugammadex 50µg/ml, or Rocuronium 1.4µg/ml and then reversed with Sugammadex 50µg/ml.

Figure 5.3.7.2 The concentration on IL-6 (ng/mL) in cell supernatants of A) THP1 Nulls, B) THP1 NLRP3-/-, C) HL-60, and D) Monocytes as determined via ELISA assay for cells treated with either Nil drugs control, Rocuronium 1.4µg/ml, Sugammadex 50µg/ml, or Rocuronium 1.4µg/ml and then reversed with Sugammadex 50µg/ml

Tables listed in this thesis

Glossary of terms

ANOVA	Analysis of variance
APCs	Antigen presenting cells
ASH1L	ASH1 Like Histone Lysine Methyltransferase
ATP	Adenosine triphosphate
CLRs	C-type lectin receptors
COX-2	Cyclooxygenase-2
DAMPs	Damage associated molecular patterns
DNA	Deoxyribonucleic acid
DOT1L	DOT1-like histone H3K79 methyltransferase
EDTA	Ethylenediaminetetraacetic acid
EHMT2	Euchromatic histone-lysine N-methyltransferase 2
ELISA	Enzyme-linked immunosorbent assay
ESICM	European Society of Intensive Care Medicine
GM-CFS	Granulocyte-macrophage colony-stimulating factor
H3K27-me3	Histone 3 lysine 27 trimethylation
H3K4-me3	Histone 3 lysine 4 trimethylation
H3K9-Ac	Histone 3 lysine 9 acetylation
H3K9-me3	Histone 3 lysine 9 trimethylation
HDAC3	Histone Deacetylase 3
HDAC8	Histone Deacetylase 8
HLA-DR	Human Leukocyte Antigen – DR isotype
HMGB1	High mobility group box 1
HMT	Histone methyltransferase
HV	Healthy volunteer
ICU	Intensive Care Unit
IFN	Interferon

IL	Interleukin
IRAK-M	Interleukin-1 receptor-associated kinase 3
IV	Intravenous
JAMA	Journal of the American Medical Association
KDM5B	Lysine Demethylase 5B
KDM6B	Lysine Demethylase 6B
KMT2A	Histone-lysine N-methyltransferase 2A
LPS	Lipopolysaccharide
MAPK	Mitogen-activated protein kinase
MHC	Major histocompatibility complex
MODS	Multiple organ dysfunction syndrome
mRNA	Messenger ribonucleic acid
MyD88	Myeloid Differentiation Marker 88
NF-κB	Nuclear factor- kappa B
NLRs	Nucleotide-binding oligomerization domain-like receptors
PAMPs	Pathogen associated molecular patterns
PBMCs	Peripheral Blood Mononuclear Cells
PKA	Protein kinase A
PKC	Protein kinase C
PMA	Phorbol 12-myristate 13-acetate
Prop	Propofol
PRRs	Pattern recognition receptors
qSOFA	Quick Sequential (Sepsis-related) Organ Failure Assessment
RLRs	Retinoic acid-inducible gene-like receptors
RNA	Ribonucleic acid
Roc	Rocuronium
ROS	Reactive oxygen species
SEM	Standard error of the mean
SET	Su(var)3-9, Enhancer-of-zeste, Trithorax domain

SIRS	Systematic inflammatory response syndrome
SIRT1	Sirtuin-1
SOFA	Sequential (Sepsis-related) Organ Failure Assessment
Sug	Sugammadex
Th	T helper cells
TLRs	Toll like receptors
TNF-α	Tumour necrosis factor-α
TRAM	TRIF-related adapter molecule
Treg	Regulatory T Cell
UTI	Urinary tract infection
Vec	Vecuronium
WBCs	White blood cells
WHO	World Health Organisation

Chapter 1: Introduction

1.1 Host Response to Infection

In 2017, there was an estimated 48.9 million cases of sepsis worldwide (Rudd *et al*, 2020)]. Critical to improving sepsis morbidity and mortality is developing a deeper understanding of the underlying pathophysiology of sepsis. Mechanisms of immune compromise are becoming increasingly recognised as a major factor and further potentially influenceable factor within sepsis. Immunosuppression in sepsis appears to be underpinned by defects in oxidative phosphorylation and glycolysis (Cheng *et al,* 2016). It is currently unclear whether these observed defects are caused by the infection itself or influenced by concomitant treatments. The hypothesis of this thesis is that sepsis induces epigenetic changes in leukocyte gene expression, which results in long-term immune defects in patients. Within this, the hypnotic agent Propofol and neuromuscular blocking agent Rocuronium, both routinely used in general anaesthesia and the most severe cases of sepsis appear to be capable of affecting immune cell function. It appears possible that these commonly administered medications may contribute to the persistent immune dysregulation observed in sepsis survivors without active infection.

Sepsis is the leading cause of death in US hospitals and is forecasted to account for more than 5 million deaths globally per year (Angus *et al*, 2016). Despite this, the precise mechanisms of the host immune response both immediately following an infection, and over the longer term is controversial and poorly understood.

Sepsis is a highly heterogenous syndrome, and additionally the vast differences in patient phenotypes make sepsis challenging to fully characterize and investigate

Clinical outcomes, such as mortality, increasingly recognised morbidity, and population incidence surrounding sepsis and bacteraemia are of most pressing importance. These outcomes could be markedly improved with the mechanisms behind host response following infection fully unravelled.

Clinically defining sepsis

In February 2016, The Third International Consensus Definitions for Sepsis and Septic Shock changed the criteria for a sepsis diagnosis, relating it directly to the presence of organ failure (Singer *et al,* 2016). Sepsis is defined as a life-threatening organ dysfunction that is caused by a dysregulated host response to infection. The Sepsis-related Organ Failure Assessment (SOFA) score is used clinically as a scoring system to track the person's extent of organ function or failure in the Intensive Care Unit (Vincent *et al*, 1996).

The SOFA score aim to guide healthcare providers identifying patients with increased risk of morbidity and mortality. Further, it can be used to estimate the probability of these risks.

Sepsis-3 removed the definition of Severe Sepsis entirely and removed the criteria for SIRS (Systemic Inflammatory Response Syndrome), arguing that sepsis is a life-threatening condition caused by a dysregulated response to infection that leads to organ dysfunction, and it is therefore unhelpful to use two or more SIRS criteria because these do not necessarily indicate a life threatening and dysregulated response. The new definition is summarised in Table 1.1:

Table 1.1 The new definition for sepsis and septic shock

Sepsis-3	Clinical criteria
Sepsis	Suspected or documented infection AND 2 or 3 of "HAT" criteria (qSOFA) a) Hypotension (SBP ≤100 mmHg) b) Altered mental state (GCS ≤13) c) Tachypnoea (≥22/min) OR A rise in SOFA score by 2 or more
Septic shock	Sepsis AND Vasopressors needed for mean arterial pressure >65 mmHg + Lactate >2 mmol/L

Homeostasis disruption

When the pathogen prevails to the point of bacteraemia, the homeostasis of the host is disrupted. Often the host response splits, to display both immune suppression and excessive inflammation concurrently, resulting in an unbalanced immune system.

Innate immune response

The innate immune system of the immunocompetent host senses an invading pathogen through pattern recognition receptors (PRRs). PRR's recognise molecules expressed by pathogens (pathogen-associated molecular patterns (PAMPs)), and, molecules released by injured host cells, (damage-associated molecular patterns (DAMPs)). PRR's themselves comprise a diverse collection of receptors, including toll-like receptors (TLRs), C-type lectin

receptors (CLRs), nucleotide-binding oligomerization domain-like receptors (NLRs) and retinoic acid-inducible gene-like receptors (RLRs) (van der Poll *et al*, 2017).

When PAMPs bind to PRRs, Nuclear factor kappa B (NF-κB) signalling is activated which promotes the transcription of pro-inflammatory factors to fight the infection (Ricklin *et al*, 2019; Tang *et al*, 2012; Abraham, 2003).

DAMPs also trigger the PRRs, and can activate many PRRs that also recognise PAMPs. With this, the host immune response becomes further complicated. Additional to the initial infection, and in some cases without, the continued recognition of DAMPs prolong the immune activation. This may also explain the clinical similarities in inflammatory host response to infectious and non-infectious injury (Chan *et al*, 2012; Deutschman *et al*, 2014).

Macrophages play a key role in the innate immune response. There are two broad classifications of macrophages: the classically activated macrophages known as M1, and the alternatively activated macrophages known as M2. M1 macrophages, typically activated by lipopolysaccharides (LPS) and interferon gamma (IFN-γ), initiate the immune response as well as phagocytosing pathogens and producing pro-inflammatory cytokines, producing NF- κB, and presenting antigens. They produce Reactive Oxygen Series (ROS) and inducible nitric oxide synthase (iNOS) (Mosser *et al,* 2008; Liu *et al,* 2014). ROS production is a careful balance, because although it serves as a critical signalling molecule in healthy biology (such as in normal immune signalling), it can also cause damage to cellular processes and organelles which can lead to a physiological imbalance (Auten *et al,* 2009). Imbalanced ROS production has been associated with several diseases, such as cancer, retinopathy, inflammatory disorders, and pulmonary hypertension (Auten *et al,* 2009).

M2 macrophages are associated with tissue repair and building the extracellular matrix, and do not present antigens to T cells or produce nitric oxide (NO) (Liu *et al,* 2014). Macrophages can polarise in response to their microenvironment, with bacterial infections shifting macrophage polarisation towards M1 (Shaughnessy *et al,* 2007; Benoit *et al*, 2008). M1 macrophages will either apoptose or shift into M2 macrophages to control the levels of proinflammatory cytokines (Liu *et al,* 2014). However, dysregulated control of M1 polarisation can result in excessive production of proinflammatory cytokines. Excessive proinflammatory cytokine production can result in the termed 'cytokine storm' associated with sepsis (Wynn *et al*, 2016).

Endothelial damage

Following infection, leukocytes show increased adherence and migration to the endothelium due to increased endothelial permeability (Leligdowicz, 2018). This furthers endothelial damage and results in intravascular leak, oedema and hypotension (De Backer *et al,* 2010; Leligdowicz, 2018). The adhesion molecules that are upregulated when the endothelium is activated include ICAM, VCAM, and E-selectin, and C-C Motif Chemokine Ligands such as CCL2 that recruit monocytes, memory T cells, and dendritic cells to the sites of inflammation (Zhao *et al,* 2014; Leone *et al*, 2002). These adhesion and recruitment molecules encourage leukocytes to the site of tissue injury, and neutrophil entry into the endothelium has been a recent research focus due to its simultaneous beneficial effect of fighting infection and exacerbation of host tissue damage (Sônego *et al,* 2016). Endothelial damage is often the precursor to septic organ dysfunction.

Unfortunately, at present targeted therapies at this level are lacking in sepsis. Current management is aimed at maintaining organ perfusion through the use of supplementary intravenous fluids and vasoactive substances (Ince *et al*, 2015).

Inflammatory and immunosuppressive phases of sepsis

It was initially believed that sepsis induced an immune response that consists of two distinct phases, first the "early" hyperinflammatory phase (Systemic Inflammatory Response Syndrome- SIRS) and then the "late" hypoinflammatory/ immunosuppressive phase (Compensatory Anti-inflammatory Response Syndrome- CARS) (Bone, 1996). However, the current theory is that these two changes occur concomitantly (Osuchowski *et al,* 2006). In sepsis, the immune response that is initiated by an invading pathogen fails to return to homeostasis, and therefore culminates in a pathological syndrome characterized by both immune suppression and sustained excessive inflammation.

Inflammation

A major cause of mortality in acute sepsis is due to the organ dysfunction and tissue injury caused by excessive inflammation (Wiersinga, 2011; Kawasaki *et al*, 2014).

Leukocytes are recruited to the site of infection and pro-inflammatory mediators and cytokines are released to fight infection, such as TNF-α, IL-1β, IL-6, IL-10, IL-12 and IFN-γ. Complement activation occurs to recruit and activate leukocytes, platelets and endothelial cells by release of activation complexes known as anaphylatoxins. Coagulation and immunothrombosis are also triggered to activate; a physiological effector of the innate immune response (Gaertner *et al*, 2016; Engelmann *et al*, 2013). During the infection, the

host attempts to return to homeostasis by repairing damaged tissue and resolving inflammation.

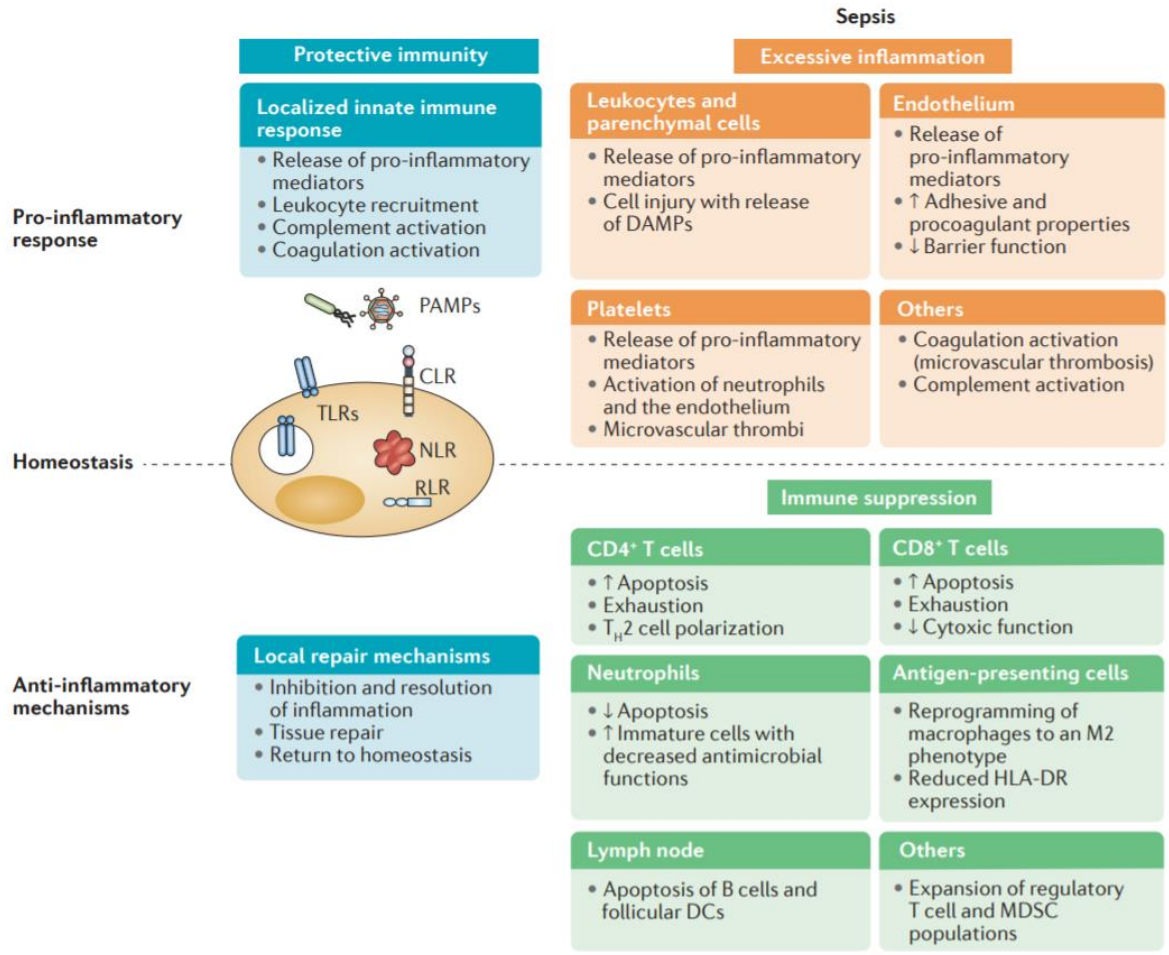

Figure 1.1.1 The host response to sepsis. From van der Poll *et al* (2017).

Figure 1.1.1 describes the immune reaction to sepsis; the orange panels describe the features of excessive inflammation with features of immune suppression in the green panels. In excessive inflammation, the complement system, the coagulation system and the vascular endothelium all undergo sustained activation. Further contributing to the effect of excessive inflammation, platelets, endothelium, leukocytes and parenchymal cells continue to release pro-inflammatory mediators in response to sepsis. As previously described, cell injury results

in the release of DAMPs which further prolong immune activation. This excessive inflammatory response may be mostly responsible for the early mortality in sepsis due to multiple organ dysfunction and cardiovascular collapse (van der Poll *et al*, 2017).

Immunosuppression

The reprogramming of antigen-presenting cells and leukocyte exhaustion results in the host immune suppression in sepsis. However, a major complication in sepsis research is that most studies do not have a 'pre-sepsis' sample of the patients, therefore the immune function of the patients prior to infection is unknown. To combat the excessive inflammation, anti-inflammatory cytokines are released, myeloid-derived suppressor cells (MDSCs) increase, antigen-presenting cells (APCs) have a reduction in response to PAMPS, and leukocytes apoptose (Kane et al, 2014; van der Poll et al, 2017). Due to this apoptosis, there is a significant reduction in circulating lymphocytes, specifically dendritic cells, B cells and T cells (particularly CD4+ Th1 cells, Th2 cells and Th17 cells, and CD8+ cells) that is strongly associated with sepsis (Boomer *et al*, 2011), while the regulatory T cell and myeloid-derived suppressor cell populations expand which can impede immune responses. Research carried out by Dr. Michael O'Dwyer has demonstrated that, following exposure to PAMPs, down regulation of T helper cell type 1 (Th1), Th17 and pro-inflammatory innate pathways in conjunction with augmented anti- inflammatory regulatory T cell (Treg) pathways occur acutely and are quantitatively associated with increased mortality in patients with severe sepsis (O'Dwyer *et al*, 2006; O'Dwyer *et al*, 2008).

Increased levels of MDSCs are found in both sepsis and cancer, which produce arginase-1, reactive oxygen species, TGF-β, and IL-10 that supress NK- and T-cells thereby supressing immune function (Schrijver *et al*, 2019; Gabrilovich *et al,* 2009; Uhel *et al,* 2017). Furthermore,

the antigen-presenting cells undergo reprogramming during sepsis, resulting in the characteristic reduction in HLA-DR expression in circulating monocytes found. Longbottom *et al* (2016) investigated HLA-DR expression in PBMCs from healthy sex- and age-matched donors (n=7) which were cultured in 30% serum from septic patients (n=7) drawn at a) within 24 hours of sepsis being confirmed, b) 5 days after sepsis confirmed or c) 12 months after sepsis. When heathy donor cells were cultured with serum from acutely septic patients there was a marked reduction in HLA-DR expression in healthy CD14+ monocytes, however this change did not persist when cultured with serum obtained at 12 months. Furthermore, the addition of GM-CSF was able to reverse this fall in mHLA-DR expression.

T cells, monocytes and macrophages become exhausted, and are less able to produce pro-inflammatory cytokines (immunoparalysis). This immune deficit can persist in sepsis survivors even long after the infection has cleared. The reprogramming of these cells during sepsis may be due to the epigenetic control of gene expression.

The NLRP3 inflammasome

More recently in regards host immune homeostasis, there is growing appreciation of the role of inflammasomes as critical components of the innate immune system. NLRP3 has been linked to inflammation mediated by cytokine IL-1β and various autoinflammatory diseases (Mangan *et al*, 2018).

NF-κB is a transcription factor which acts as a mediator in the inflammatory response, regulating parts of both the adaptive and innate immune system, and in addition regulates inflammasomes (Oeckinghaus *et al*, 2009). The canonical way of activating NF-κB involves stimuli from a diverse range of stimulus, including TNF receptors, T- and B-cell receptors, and PRRs, which requires degradation of 'nuclear factor of kappa light polypeptide gene enhancer

in B-cells inhibitor alpha' (IκBα). The alternative activation pathway does not involve the degradation of IκBα, and will respond selectively to specific group of stimuli, such as CD40, transmembrane protein RANK, and the BAFF receptor (member of the TNF receptor family) (Sun *et al,* 2011; Xiao *et al*, 2001). NF-κB modulates inflammatory T cells through regulating their effector function, activation, and differentiation (Lawrence, 2009; Tak *et al*, 2001). In addition, NF-κB regulates inflammasome NLRP3 activation by upregulating its transcription, and regulates cytokine production (Sutterwala *et al*, 2014).

The NLRP3 inflammasome is composed of NOD-like receptor family pyrin domain containing 3 (NLRP3), pro-caspase 1 and an apoptosis-associated speck (ASC)-like protein (Lebreton *et al*, 2018). NLRP3 is activated by a broad range of stimuli, consisting of both PAMPs and DAMPs, in contrast to most other PRRs. The various stimuli are unrelated, however all induce cellular stress. DAMPs from external irritants and sterile inflammation, as well as PAMPs from bacterial, viral and fungal infections, can all activate NLRP3. The upstream mechanisms regarding NLRP3 activation have not been fully elucidated, but are believed to include mitochondrial dysfunction, changes in metabolism, calcium ion flux, and potassium or chloride ion efflux.

The main role of the NLRP3 inflammasome is to produce and mature IL-1β cytokines, which involves a two-step process consisting of a priming signal and an activation signal. The priming signal can be induced by the detection of PAMPs or DAMPs through PRRs such as TLRs or NOD2, or through 1L-β or TNF induced activation of NF-κB (nuclear factor-κB) (Xing *et al,* 2017; Bauernfeind *et al,* 2009; Franchi et al, 2009). The priming signal induces the upregulation of expression of pro-IL-1β, NLRP3, and caspase 1 (Lebreton *et al,* 2018; Swanson et al, 2019). If the priming occurs with LPS interactions with TLR4, then an

oxidative phosphorylation to glycolysis metabolic shift will occur in macrophages, which will increase IL-1β gene transcription and stabilise HIF-1α (Tannahill *et al,* 2013).

The activation signal follows the priming signal, which results in the activation of caspase-1 and the formation of the NLRP3 inflammasome. The mechanisms in which NLRP3 detects cellular stress and the pathways involved in the inflammasome formation are not fully elucidated, however the activation of caspase-1 will cleave the pro-1L-1β into the mature form IL-1β, resulting in its secretion. The pathways involved in the priming and activation of the NLRP3 inflammasome is summarised in Figure 1.1.2.

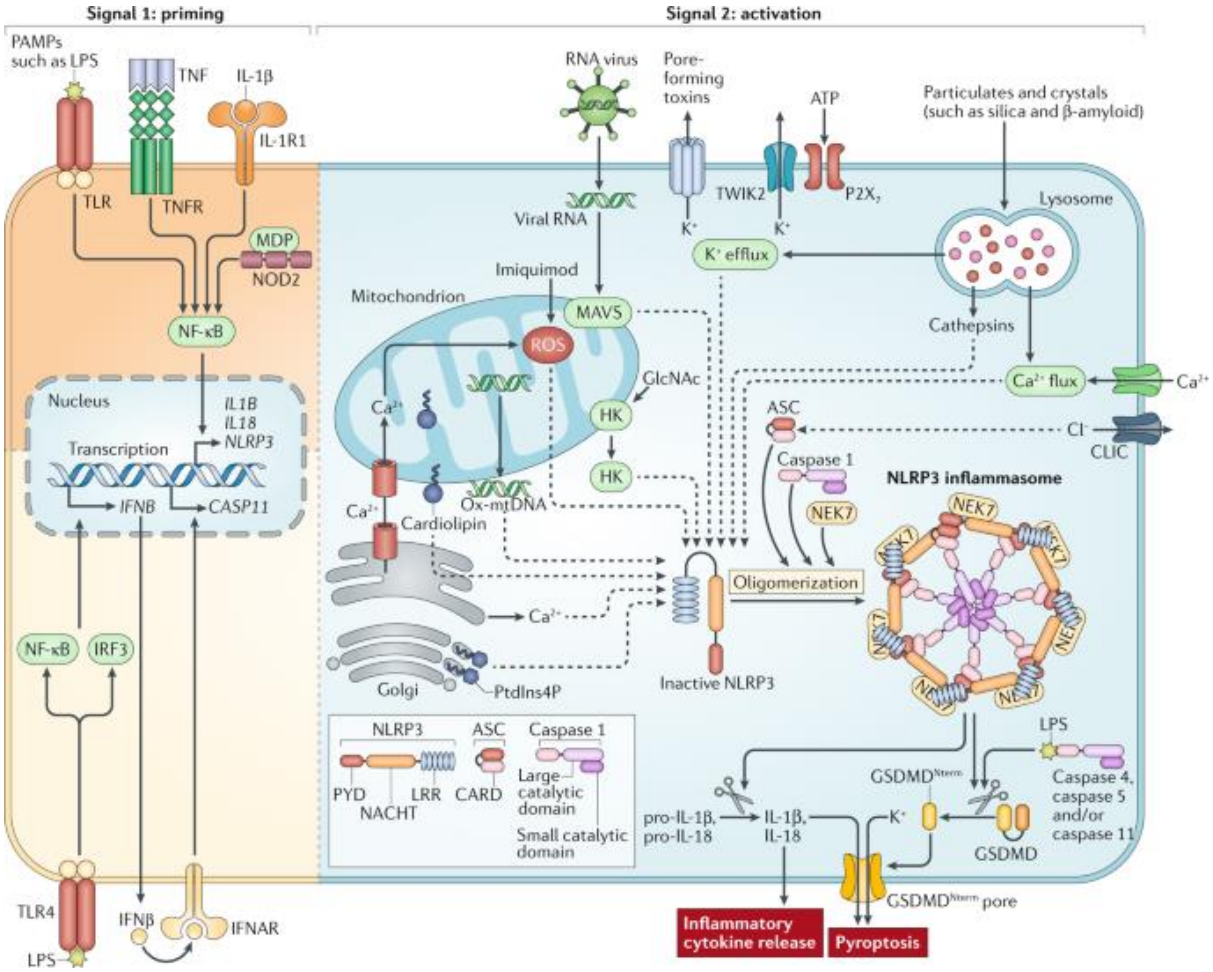

Figure 1.1.2 The pathways involved in priming and activating the NLRP3 inflammasome, from Swanson *et al,* 2019.

Mitochondrial dysfunction is involved in the activation of NLRP3. A by-product of oxidative phosphorylation is the production of ROS by the mitochondria, and in times of cellular stress the release of mitochondrial ROS into the cytosol is greatly increased, which in turn will trigger NLRP3 to activate (Swanson *et al*, 2019; Cruz *et al,* 2007). ROS levels can be downregulated by the transcription factor NRF2 (nuclear factor erythroid 2-related factor 2), which will therefore inhibit NLRP3 activation (Liu *et al,* 2017). NRF2 has also been shown to inhibit NLRP3 inflammation activity by attenuating NF-κB activation and downregulating NLRP3, caspase-1, and IL-1β (Li *et al,* 2008).

Damaged and dysfunctional mitochondria are removed via mitophagy, therefore decreasing the amount of ROS and regulating NLRP3 activation (Zhou *et al*, 2011). Furthermore, oxidative stress can result in mitochondrial DNA (mtDNA) being released into the cytoplasm from damaged mitochondria, which in turn will act as a DAMP to cause NLRP3 activation (Zhong *et al*, 2018; Zhang *et al,* 2010).

There is increasing evidence that mitochondria may be used as a docking site for NLRP3 inflammasome assembly, due to activated NLRP3 and caspase-1 independently associating with the mitochondria via the mitochondrial phospholipid cardiolipin (Zhong *et al*, 2018; Dudek *et al,* 2017; Zhou *et al*, 2011; Subramanian *et al*, 2013; Iyer *et al*, 2013; Elliott *et al*, 2018). While cardiolipin is usually found on the inner membrane, in times of cellular stress it has been shown to migrate to the outer membrane where it can act as a binding site (Dudek *et al,* 2017).

There may be a role for glycolysis in NLRP3 inflammasome activation. Sanman *et al* (2016) found that the NLRP3 inflammasome will be activated, as well as IL-1β production and pyroptosis, by a disruption of glycolytic flux. This was triggered by a decrease in NADH levels

and an induction of mitochondrial ROS production. It is difficult to fully elucidate this however, as LPS-induced IL1β gene transcription is inhibited when glycolysis is inhibited during NLRP3 priming (Tannahill *et al,* 2013).

As discussed, hexokinase mediates phosphorylation of glucose in glycolysis, however hexokinase will bind with GlcNAc (N-acetylglucosamine) which is a compound released from degradation of bacterial cell walls during an infection (Wolf *et al*, 2016). The GlcNAc can travel into the cytosol via hexokinase binding, where it will then activate the NLRP3 inflammasome (Wolf *et al*, 2016).

Persistent inflammation, immunosuppression, and catabolism syndrome

Patients with a long ICU stay are susceptible to developing the clinical syndrome "persistent inflammation, immunosuppression, and catabolism syndrome" (PICS) (Mira *et al,* 2017; Hawkins *et al*, 2018). The cause of PICS is multifaceted; however, the symptoms suggest there may be involvement of a persistent immune dysfunction (Chang *et al*, 2015). Once the initial septic insult has been resolved, patients with PICS still have a higher mortality and morbidity due to increased risk of secondary infections or viral reactivations (Denstaedt *et al*, 2018; Walton *et al*, 2014). It has been demonstrated that even years after a septic episode patients can still suffer a persistent immunoparalysis characterised by a reduction in cytokine secretion and a decrease in monocyte expression of TLR5 (Arens *et al* 2016). An increased mortality is apparent when pre-sepsis health is taken into account and the patients have been age-matched with control individuals (Prescott *et al,* 2018; Prescott *et al*, 2016; Ou *et al,* 2016).

Post-sepsis susceptibility to repeated infections

Patients who survive the first 30 days following a diagnosis of severe sepsis are 2.7 times more likely to die during the first year and 2.3 times more likely to die over the subsequent 3 years than an age, sex and illness matched cohort (Storgaard *et al,* 2013). Furthermore, this excess mortality can persist for at least 8 years even when taking into account co-existent illnesses (Storgaard *et al*, 2013). Rahmel *et al* (2020) performed a retrospective cohort study on 83,974 sepsis, septic shock, and severe infection hospital survivors from data of a large German statutory health care insurer and found an increased 5 year mortality post hospital discharge in these hospital survivors (56.1% septic shock, 62.1% sepsis, 52.4% severe infections) compared to matched controls without infectious diseases. A cohort study on 87,581 US adult sepsis survivors on Medicare found that 28% of survivors died within 1 year of hospital discharge (Courtright *et al*, 2020).

Animal models of sepsis survivors remain susceptible to repeated infections long after the acute inflammatory response has been resolved (Benjamin *et al*, 2003; Deng *et al*, 2006) and the most common re-admission within 30 days following septic shock is recurrent infection (Czaja *et al*, 2009). DeMerle *et al* (2017) found that 19% of sepsis readmissions within 90 days of sepsis were confirmed to be the same infection site and same organism. They hypothesised that a proportion of sepsis readmissions were due to a recrudescent infection, with half of readmissions due to new infections at a different site or with a different organism. Shankar-Hari *et al* (2020) conducted a systemic review and meta-analysis of 56 non-randomised studies into sepsis hospital readmissions, and found a mean rehospitalisation rate of 39% within one years of initial discharge with infection as the most common rehospitalisation diagnosis, with one- to two-thirds of rehospitalisation diagnoses being sepsis.

The sepsis-induced immune dysregulation appears to persist even after the initial infection has been treated. An emerging theory on the pathophysiology of sepsis is that the inflammation and immune suppression are symptoms of acute cellular reprogramming that occurs due to the triggering infection, which leads to fundamental changes to the metabolic and immune processes of cells (van der Poll *et al*, 2017).

1.2 Epigenetics in sepsis

Definition of epigenetics

Most simply put, an epigenetic change refers to a change in phenotype without a change in genotype- a heritable change in gene expression (i.e. active versus inactive genes) which does not involve changes to the genetic code/underlying DNA sequence (Dupont *et al,* 2009).

Epigenetics is concerned with the activation vs inactivation of genes and the processes behind these regulations, whereas epigenomics is concerned with the complete set of epigenetic modifications (the epigenome). The epigenome is the link between the genome and the environment, and reflects the overall epigenetic state of the cell. Epigenomics focuses on the cell or organism by analysing many genes and assessing the series of proteins and compounds that modify gene expression by attaching to the genome.

Epigenetic changes can be influenced by external factors and are both natural and regular, and will occur throughout an organism's lifetime from a variety of factors such as diet, the environment, aging, and disease, and this modified gene expression can be inherited via meiosis and mitosis (Carson *et al*, 2011). Three known systems that are believed be capable of sustaining and initiating epigenetic change are DNA methylation (Illingworth *et al*, 2009), non-coding RNA-associated gene silencing and histone modification (Ho *et al,* 2016; Drury *et al,* 2017; Egger *et al*, 2004).

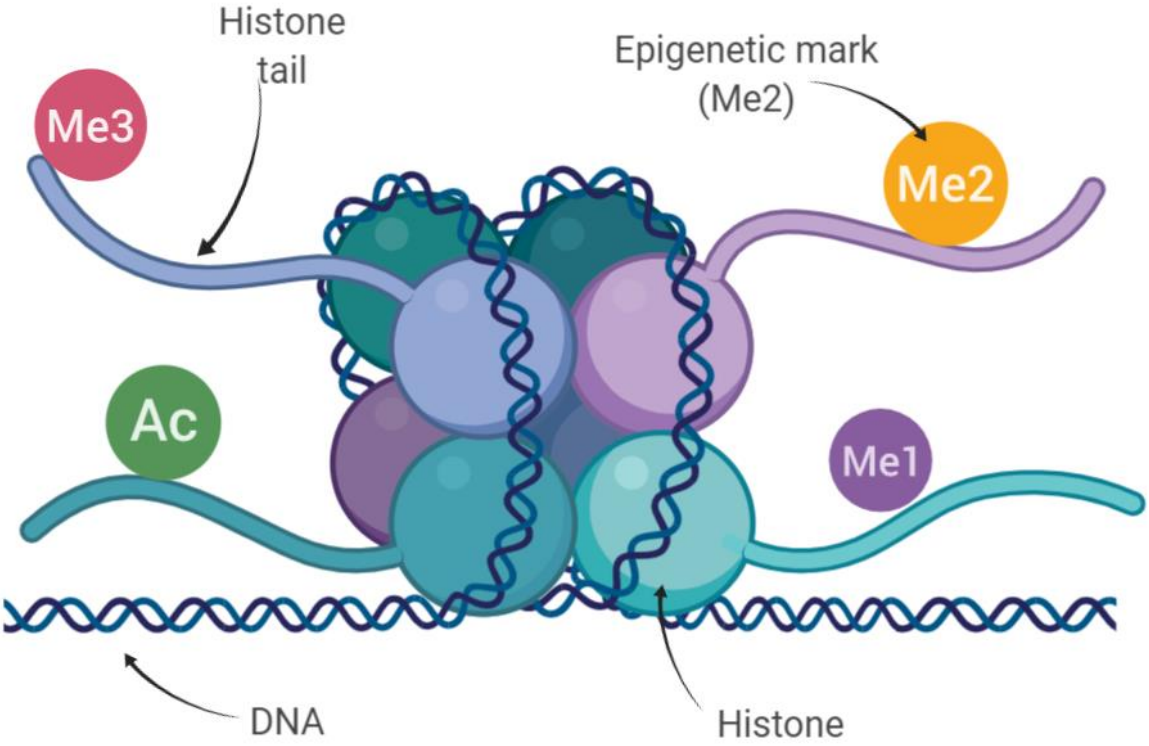

Figure 1.2.1 The structure of a histone protein; composed of eight subunits with histone tails and epigenetic marks. Image created using *BioRender software*.

Epigenetic changes in disease

Epigenetics has been implicated in numerous diseases along with aging. To date, there is strong evidence of epigenetic dysregulation in several major diseases, and is notably linked to cancer, both haematological and solid malignancies.

Cancer patients are observed to exhibit different outcomes despite the same cancer stage and grade. Cancer has a broad and complex aetiology, which varies depending on the type of cancer, but is believed to be brought on by a combination of hereditary and environmental influences. The epigenetic theory of cancer was first proposed in 1979 by R Holliday, who believed they were the cause of tumorigenesis (Holliday, 1979). Since then, evidence has

continued to grow to support this. Holliday determined the probability of malignant transformation may be explained by specific methyltransferases, and cancer phenotype can be reversed to normal if these epigenetic mutations are reversed. Epigenomic changes have been demonstrated to alter cell function and result in oncogenic transformation (Shen *et al*, 2013), but multiple different epigenetic events combine to induce tumorigenesis. Epigenetic heterogeneity can be observed at a cellular level, where different tumour cells demonstrate a range of different changes from individual to genome-wide genes and histone modifications, but despite heterogeneity global histone modification patterns were found to predict the risk of reoccurrence of prostate cancer (Seligson *et al*, 2005). Hypoacetylation and hypermethylation of histones, along with methylation of DNA CpG islands, were further demonstrated to repress tumour suppressor genes (Fahrner *et al*, 2002). Evidence of the role of epigenetics in cancer is so compelling that currently six epigenetic drugs are approved for clinical use in the treatment of cancer by the FDA, and a multitude of clinical trials have investigated the effects of epigenetic drugs, particularly anti-DNA methylation therapy for various cancers (Cheng *et al*, 2019).

DNA methylation has been studied most extensively in cancer, whereas histone modifications have been investigated in broader areas of diseases. Histone modification have indeed been investigated in haematological malignancies and solid tumours, but have also been implicated in many inflammatory diseases (Cheng *et al*, 2019).

Inflammatory conditions were originally believed to be caused by either innate immune responses (autoinflammatory) or adaptive immune responses (autoimmune) (Hedrich *et al*, 2016). However, modern research suggests that inflammatory disorders exist on a spectrum and will usually involve a combination of autoinflammatory and autoimmune elements

(Hedrich *et al*, 2017; McGonagle *et al*, 2006). Epigenetic modifications have been closely linked to the pathophysiology of inflammatory/autoimmune diseases, both as factors determining clinical outcomes and as factors determining predisposition to disease (Surace *et al,* 2019). A downregulation in genes coding for histone proteins was observed in patients with Cryopyrin-Associated Autoinflammatory Syndromes (CAPS) (Aubert *et al*, 2012), and when stimulated with IL-1β CAPS patients displayed a large demethylation in monocytes and macrophage genes IL1B, NLRC5, PYCARD, AIM2, and CASP1 which was then reversed with IL-1 blocking treatment (Vento-Tormo *et al,* 2017). NLRP3 was also shown to be regulated by epigenetic modulator miRNAs which were upregulated in CAPS patients (Poudel *et al,* 2018).

Epigenetic changes associated with drugs

Not only are there epigenetic changes associated with cancer itself, but chemotherapeutic drugs have also been associated with epigenetic alterations. Most chemotherapy drugs are genotoxic, and genotoxic carcinogens are known to cause epigenetic alterations (Pogribny *et al,* 2008). A number of chemotherapy drugs were shown to induce DNA hypermethylation in cell culture, including topoisomerase II inhibitors and microtubule inhibitors (Nyce *et al,* 1989; Nyce *et al*, 1993).

Chemotherapeutic drugs are able to induce multidrug resistance (MDA), whereby the efficacy of cancer treatments can be diminished by the expression of the gene MDA1. Upregulation of MDR1 was demonstrated by epigenetic modifications at the MDR1 locus in response to chemotherapeutic drugs, specifically increases in H3 acetylation and induction of methylated H3K4 (Baker *et al*, 2005). Epigenetics were also demonstrated to underpin tamoxifen-induced hepatocarcinogenesis, inducing a global DNA hypomethylation, and a decrease in protein

expression of maintenance DNA methyltransferase DNMT1 and de novo DNA methyltransferases DNMT3a and DNMT3b (Pogribny *et al*, 2007).

An autoimmune disease similar to lupus can be triggered by the drugs procainamide (a drug to treat arrhythmias) and hydralazine (a vasodilator) due to their inhibition of DNA methylation (Cornacchia *et al*, 1988). Procainamide inhibited the reaction of DNA methyltransferase I (Lee *et al,* 2005), whereas hydralazine influenced the expression of DNA methyltransferase genes (Arce *et al*, 2006), both of which result in a genomic hypomethylation.

Histone modifications

Research herein focuses on the chemical modification of histone proteins. Histone modification is an important mechanism of influencing gene expression as the re-modelling of chromatin can facilitate or block polymerases and transcription factors from accessing DNA promoters (Carson *et al,* 2011; Schmidt *et al*, 2017). Histone proteins are octamers composed of eight subunits, consisting of two copies each of the proteins H2A, H2B, H3 and H4. Each histone subunit has an N-terminal histone tail and a C-terminal histone fold, and the histone octamer is created when a double H3 H4 tetramer bonds with two H2A H2B dimers. The histone tails contain epigenetic marks that can be modified to control the exposure of DNA. Figure 1.2.1 depicts the components of a histone.

The histone octamers form a series of weak bonds with DNA that can be repositioned, and the DNA will wrap itself around many histone octamers to form a “beads on a string” nuclear array. This structure is referred to as chromatin, which can be seen below in Figure 1.2.2

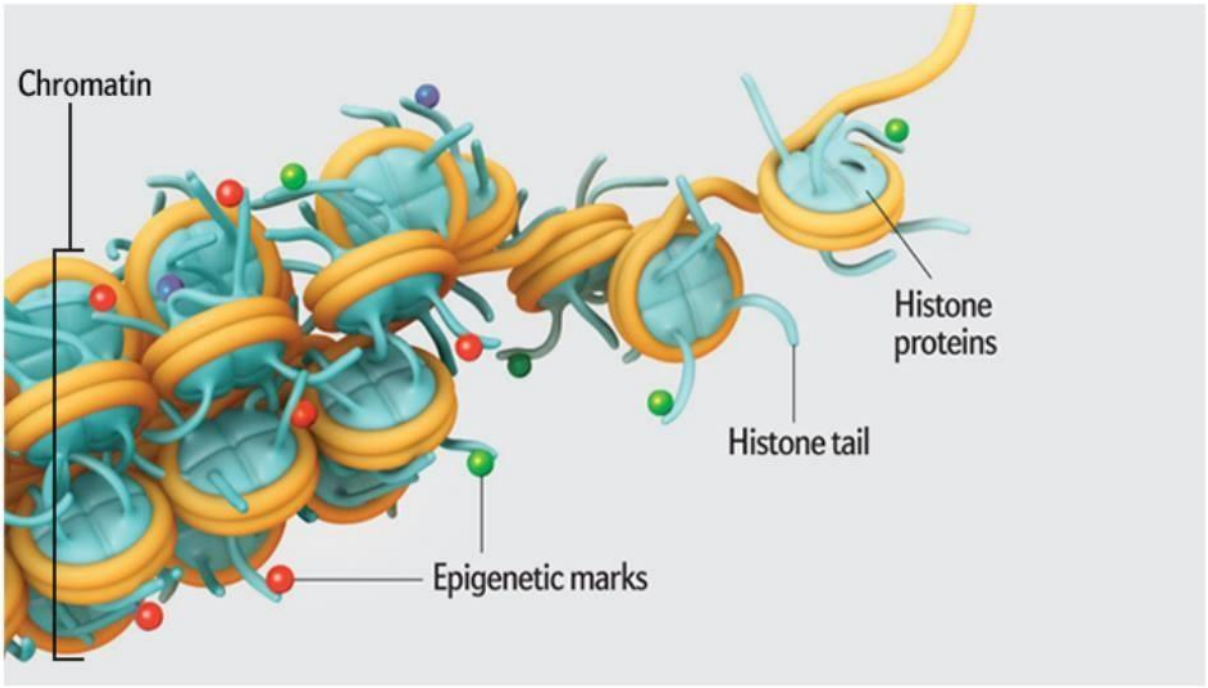

Figure 1.2.2 The structure of chromatin, showing the DNA (orange) winding around histone proteins (blue) and epigenetic marks (red, green, purple) on histone tails (From Rusting, 2011).

Cellular DNA is wrapped around these protein complexes called histones, and 'chromatin' refers to this DNA-histone complex. The presence or absence of epigenetic marks can be influenced by environmental factors, experiences or inherited. Epigenetic marks are various chemical groups that can influence the activity level of a gene in a given region by affecting how tightly the chromatin spools are packed together. Transcriptional regulation takes place by organizing the gene loci on chromatin into transcriptionally active or silent states. The epigenetic marks can be modified by various histone modifying enzymes. When the histone modification results in the unwinding/ loose packing of those spools to result in transcriptionally active chromatin, the complex is termed euchromatin. An example of this is acetylation, which can result in an exposed/ active gene (Figure 1.2.3)

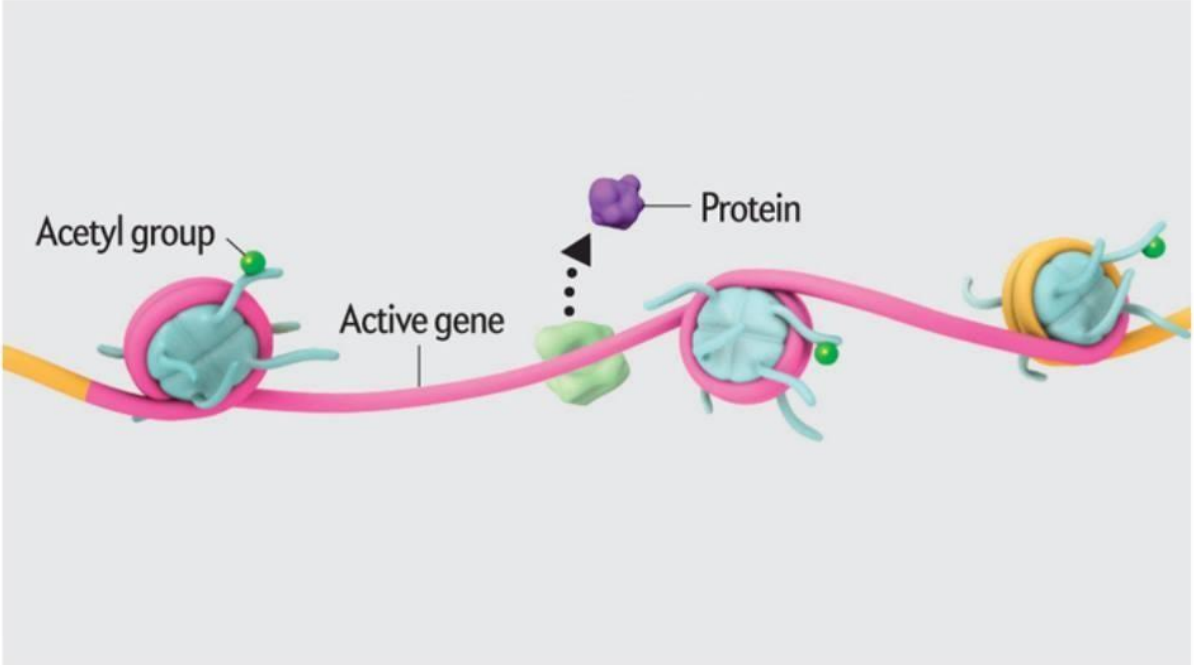

Figure 1.2.3 Euchromatin resulting from acetyl group interaction, exposing the gene to polymerases and transcription factors and thus activating the gene. (From Rusting, 2011).

Conversely, transcriptionally silent chromatin is termed heterochromatin, whereby the spools are packed tightly together which blocks gene transcription machinery from interacting with the DNA and therefore gene transcription is inhibited. An example of this is methylation, which often results in an inactive gene (Figure 1.2.4).

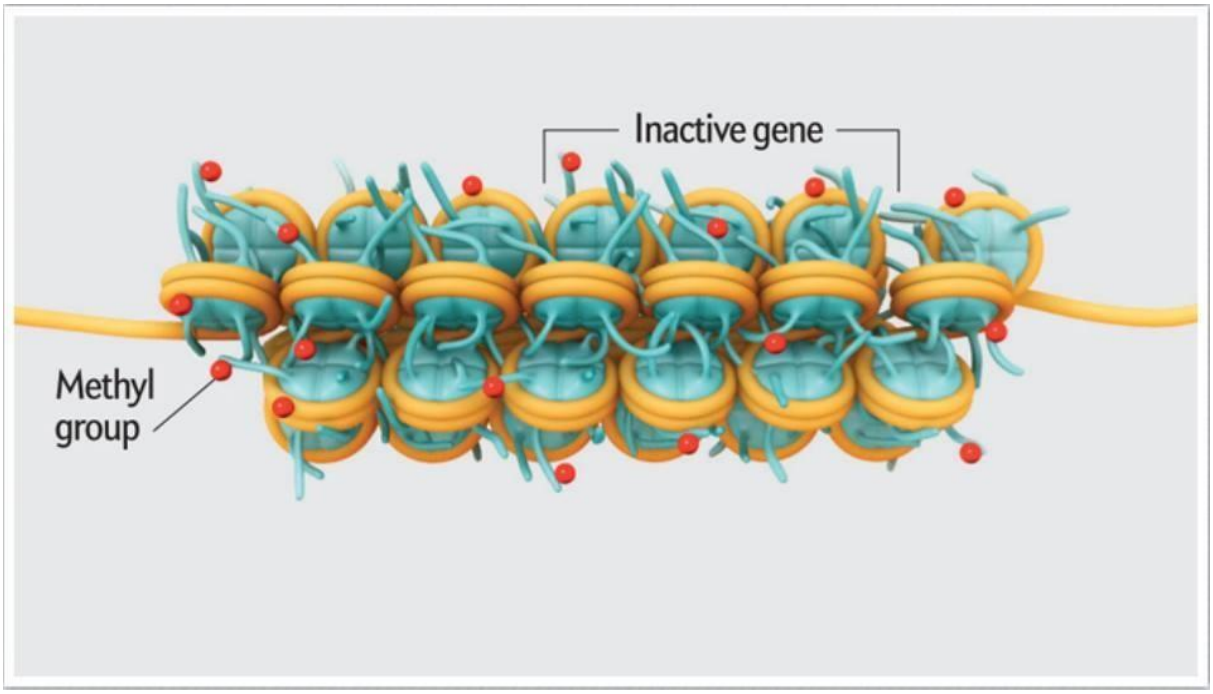

Figure 1.2.4 Heterochromatin resulting from methyl group interaction whereby chromatin is structurally organised to keep transcription factors and polymerases away from genes which are therefore inactivated. (Rusting, 2011.)

Epigenetic alterations observed after sepsis

It is feasible that an acute episode of sepsis will result in epigenetic alterations that impart an immunological defect and susceptibility to secondary infection (Cross et al, 2019). An immune deficit caused by epigenetics would have the capacity to persist far beyond resolution of the acute infection; and may explain immunosuppression some patients face. In theory, epigenetic changes could last a lifetime and be passed on to future generations via meiosis. Epigenomic changes tend to be stable, however there are several known gene loci that display plasticity due to environmental influences (Joehanes *et al,* 2016; Sapienza *et al*, 2016; Minarovits *et al*, 2016). Epigenetic alterations may account for the long-term excess mortality observed in septic patients: Wen *et al* (2008) found repressive methylation marks for up to 6 weeks following the original infection in murine dendritic cells. LPS-induced tolerance in

murine monocytes was demonstrated be to caused by histone modification with a global reduction of H3K4me3 (Foster *et al,* 2007). LPS-induced tolerance in macrophages resulted in an increase of the modification H3K9me2 that is associated with gene repression at the promotor regions of TNFα and IL-1β (Chan *et al*, 2005; El Gazzar *et al,* 2009). There is currently very little human data available to validate the translation of this. Sepsis-induced histone modification changes were observed in human monocytes for the first time in 2015, in a pilot study that found enrichment of genes involved in immune function in septic patients (n=2) compared to healthy donors (n=4) (Weiterer *et al,* 2015).

Epigenetic modifications of certain genomic regions in host cells may be pathogenically blunted by the pathogen as a survival advantage (Fol *et al*, 2020). Following on from this, several investigations involving animal and *in vitro* models have sought to identify promising candidate genes involved in such histone modifications (Chan *et al*, 2005; El Gazzar *et al,* 2009; Lyn-Kew *et al*, 2010; Klose *et al,* 2007).

Histone modifying enzymes in sepsis

Several genes of histone modifying enzymes associated with sepsis and bacteraemia were identified, and are summarised in Table 1.2.1 below:

Table 1.2.1 A summary of the genes of the enzymes involved in histone modifications in sepsis and bacteraemia.

Enzyme	**Epigenetic effects**	**Reference(s)**	**Description**
ASH1L	Histone methyltransferase (H3K4; and potentially H3K9, H3K36 & H3K20 Tanaka *et al* 2011)	Xia *et al*, 2013 Byrd & Shearn, 2003 Gregory *et al,* 2007	Ash1l suppressed IL-6 & TNF production in TLR-triggered macrophages, and enhanced ubiquitin-editing enzyme A20, protecting mice from sepsis and endotoxic shock. Ash1l negatively

		Tanaka *et al*, 2011	regulates TLR-triggered production of proinflammatory cytokines by suppressing NF-kB & MAPK pathways by acting on the SET domain.
MLL (KMT2A gene)	Histone methyltransferase (H3K4)	Xia *et al*, 2013 (MLL1 & MLL4) Schaller *et al*, 2015 (MLL1) Wang *et al*, 2012 Austenaa *et al*, 2012 Lyn-Kew *et al,* 2010	Once MLL1 is upregulated by IL-12 it then regulates the proliferation of Th1 cells. MLL1 and MLL4 could upregulate LPS- induced IL-6 production. MLL HMTs in general interact with H3k4- IRAK-M plays critical role in mediating macrophage re-programming during sepsis which may be due to regulation of chromatin remodelling that controls inflammatory gene transcription, therefore MLL may play role.
G9a (EHMT2 gene)	Histone methyltransferase (H3K9)	Chan *et al,* 2005 El Gazzar *et al*, 2009 Merkling *et al*, 2015 Lehnertz *et al*, 2010	G9a acts on H3K9. Chromatin-specific remodelling by HMGB1 and H1 silences pro-inflammatory genes during endotoxin tolerance. G9a interaction with RelB leads to trimethylation of H3K9me3 and subsequently recruits HP1. HP1+G9a form a repressive complex at the promotors of RelB-dependent genes. G9a deficient drosophila mutants are more sensitive to RNA virus infection and succumb faster to infection than wild type controls, which was associated with strongly increased Jak-Stat dependent responses. G9a-deficient t-helper cells are specifically impaired in their induction of TH2 lineage-specific cytokines IL-4, IL-5 &

			IL-13 and fail to protect against infection with the intestinal helminth *Trichuris muris*. G9a-deficient Th cells are characterised by the increased expression of Il-17A, which is associated with a loss of H3k9me2 at the IL-17a locus.
DOT1L KDM5B	Histone methyltransferase Histone demethylation	Carson *et al,* 2012 (abstract J Immunol May 2012 188 121.15)	Superarray analysis of mRNA isolated from CD117+ hematopoietic stem cells isolated from animals subjected to an experimental model of sepsis identified a distinct set of modulated mRNAs encoding distinct histone modifying enzymes including methyltransferases (Dot1l, Prmt8 and Smyd1) and demethylases (Kdm5b), among others. These results indicate that severe sepsis can modulate the expression of chromatin modifying enzymes in hematopoietic stem cells.
Jmjd3 (KDM6B)	Histone demethylation (H3K27)	Weiterer *et al*, 2015 De Santa *et al*, 2009 Klose *et al*, 2006	Jmjd3 contributes largely to the control of gene expression in LPS-activated macrophages by fine tuning the transcriptional output of LPS-activated macrophages in an H3K27 demethylation- independent manner (De Santa). They found 70% of LPS-inducible genes were Jmjd3 targets. Jmjd3 is induced by TF NF-kB in response to microbial stimuli. Erases H3K27-me3 (highly associated w/ repressed promotor regions and lineage determination).

HDAC3	Histone deacetylation	Chen *et al*, 2012	Chen et al found that HDAC3-deficient macrophages were unable to activate almost half of the inflammatory gene expression program when stimulated with LPS. Central role for HDAC3 in inflammation, and studies building upon this research testing HDAC inhibitors as anti-inflammatory agents backs this up.
HDAC8	Histone deacetylation (H4Ac)	Aung *et al,* 2006 Lyn-Kew *et al* 2010	As with HDAC3, LPS regulates pro-inflammatory gene expression in macrophages by altering HDAC expression, and found that HDAC8 (class 1 HDAC, as HDAC1 suppressed Cox-2 promotor activity) over-expression in murine macrophages blocked the ability of LPS to induce Cox-2 mRNA (Aung).

In general, acetylation is "activating" of genes (pro-transcriptional), however there are certain gene loci where it has been found to be repressive (Wang *et al*, 2009; Zhang *et al*, 2017). Several genes involved in the inflammatory response are known to be regulated by acetylation of histones (Ghizzoni *et al,* 2011; Barnes *et al,* 2005). Histone deacetylases (HDACs) and histone acyltransferases (HATs) are the two classes of enzyme that controls the acetylation of histones. HDACs were discovered in yeast before humans, and the human HDAC sequence homology with the yeast counterparts allows them to be similarly grouped into four classes. Most research is conducted on the Class I, II and IV HDACs, but there is also the Class III HDACs which behave a bit differently in that they require NAD+ as a substrate for lysine deacetylation, as opposed to the other classes that are Zn2+-dependent

metalloproteases (Hull *et al,* 2016). In total, there are 18 HDACs found in humans. There are five groups of HATs, however they all function in the same manner, primarily targeting H3 and H4 lysine residues and use acetyl-CoA as a substrate (Marmorstein *et al*, 2014). HDACs and HATs do not only target histones; they are also involved in other cellular processes, notably cellular metabolism (Hull *et al*, 2016).

Endothelial permeability in acute lung injury may be partially modulated by a reduction in histone acetylation that results in an upregulation in adhesion molecules. Murine models of poly-microbial sepsis that were pretreated with inhibitors of histone deacetylases (HDACi) found a reduction in the gene expression of ICAM-1 and E-selectin in the lungs (Zhang *et al*, 2010; Roger *et al*, 2011). HDACi, such as depsipetide and vorinostat, are also used in cancer treatment, where they induce apoptosis (via shifting the balance of pro- and anti-apoptotic proteins in favour of apoptosis) and upregulate the gene p21 which blocks the CDK/cyclin complex leading to the cell cycle arrest of cancer cells (Kim *et al*, 2011).

Further, a murine sepsis model found that lung acetylation reduction at the promotors of the genes Angp1, Tek, and Kdr, which are all paramount in the signalling cascades for vascular endothelial growth factor and Tie2/Angiopoietin (Bomsztyk *et al*, 2015). However, this study was widely criticised for its limitations (Bataille *et al*, 2015). The three main reasons were described as follows. Firstly, the controls: mechanical ventilation and anaesthesia was not used as this was a murine model, and anaesthesia has been demonstrated to induce epigenetic changes on histones (Zhong *et al*, 2014). There was also a lack of positive control in endothelial cells in MODS. Secondly, when studying the epigenome cell type is an important consideration. A cell-specific approach much be considered when studying sepsis due to the infiltration of several immune cells into specific organs; different cells types carry different

epigenetic marks and their changes need to be integrated in order to understand the epigenetic landscape of the immune system. For example, the paper assesses the marker of acute kidney injury, neutrophil gelatinase-associated lipocalin (NGAL), but it displayed different epigenetic marks in the three organs studied. The third criticism applies to the field broadly, which is that epigenetics are dynamic, and data interpretation relies heavily on the 'snap-shot' of the epigenetic landscape at that time, which may be long-term modifications or fleeting.

Micro RNA (miRNA) are another epigenetic mechanism which have been associated with endothelial response to sepsis (Goodwin *et al,* 2015); certain miRNAs are found to reduce the expression of adhesion molecules (Sun *et al*, 2012; An *et al*, 2018; Wang *et al,* 2018; Gao *et al,* 2015), and possibly miRNA play a larger role than histone modification in endothelial response to sepsis.

Stability of epigenetic alterations

Histone modifications were demonstrated to underlie LPS-induced tolerance in monocytes by Foster *et al* (2007), specifically a reduction in H3K4me3. LPS-induced tolerance in macrophages resulted in increased H3K9me2 at the promotor regions of TNFα and IL-1β (Chan *et al*, 2005; El Gazzar *et al,* 2009). LPS induced the expression of the histone modifying enzyme Jmjd3 through macrophage NF-κB signalling (De Santa *et al,* 2007; De Santa *et al*, 2009). LPS exposure can also regulate HAT activity by enhancing the stability of its transcriptional co-activator CREB-binding protein, a key requirement of NF-κB signalling and regulation of the inflammatory response- thereby increasing cytokine release and histone acetylation (Calao *et al*, 2008; Wei *et al,* 2017). Similarly, LPS exposure has been shown to enhance the stability of the HBO1 histone acetyltransferase (Long *et al*, 2018). LPS exposure

can also repress TNFα, NF-κB p65 and IL-1ß genes by promoting the HDAC SIRT1 (Liu *et al,* 2011; Kawahara *et al,* 2008).

The stability of these epigenetic alterations over time may account for the long-term excess mortality in septic patients; Wen *et al* (2008) found repressive methylation marks for up to 6 weeks following the original infection in murine dendritic cells, but further human data is needed to verify the translation of this theory to apply to human patients. Sepsis-induced histone modifications may contribute to Persistent Inflammation, Immunosuppression, and Catabolism Syndrome (PICS), particularly the immune dysfunction characterised by increased apoptosis and leukocyte functional abnormalities (Christou *et al,* 1995; Mira *et al,* 2017). Increased levels of Myeloid-Derived Suppressor Cells (MDSCs) are found in sepsis, which produce arginase-1, reactive oxygen species, TGF-β, and IL-10 that supress NK- and T-cells thereby supressing immune function (Schrijver *et al,* 2019; Gabrilovich *et al,* 2009; Uhel *et al*, 2017). Epigenetic mechanisms control MDSCs transcriptional regulators; and may be responsible for the increase in MDSCs found in sepsis. C/EBP-β and Runx1 are transcriptional factors that promote MDSC proliferation and have been found to be downregulated by HDAC11 recruitment (Chen *et al*, 2014); although the effect of sepsis on HDAC11 concentration remains unclear. Again, certain miRNAs have also been found to promote the increase in MDSCs in sepsis (Fazi *et al,* 2005; McClure *et al*, 2014; Tian *et al,* 2015; Bazzoni *et al*, 2009). Epigenetics may also control the other side to immunosuppression- endotoxin tolerance.

Trained immunity

Trained immunity is possible in innate host defence (Netea *et al*, 2011). Concentration of antigen and the type of microbial stimulus both determine the induction of endotoxin

tolerance and trained immunity (Netea *et al*, 2016). Trained immunity can persist long-term and can propagate via progenitor cells (Mitroulis *et al,* 2018; Kaufmann *et al,* 2018), and β-glucan was shown to reverse endotoxin tolerance in monocytes (Novakovic *et al*, 2016). Trained immunity was found to epigenetically reprogram monocytes via an increase in the activating histone modification H3K4me3 at the promotors of TNFα, IL-1β, IL-6, IFNγ and TLR4 (Kleinnijenhuis *et al*, 2012; Quintin *et al*, 2013). Distinct epigenetic and metabolic profiles were observed in LPS-stimulated monocytes via their TLR pathway (immunosuppressive) or NLR pathway (inflammatory) (Saeed *et al,* 2014; Cheng *et al*, 2014). More insight into the longevity of trained immunity and endotoxin tolerance can therefore be elucidated by a better understanding of histone modifications.

1.3 Effects of sepsis on immunometabolism

Genes involved in sepsis and immunometabolism

Several genes are involved in sepsis and immunometabolism. One important gene is Interleukin-1 receptor-associated kinase 3 (IRAK-3, also known as IRAK-M). IRAK-M-/- macrophages exhibit modulated expression of histone deacetylase mRNA following sepsis as compared to wild-type macrophages, suggesting that IRAK-M may direct sepsis-induced chromatin modifications through modulations of the histone modifying machinery in the cell (Lyn-Kew K *et al*, 2010). Hypoxia-inducible factor-1A (HIF-1α) acts on IRAK-M and is a key regulator on anaerobic glycolysis. It also has importance in processes other than just metabolism during the functional reprogramming of human monocytes in sepsis when switching from inflammatory to immunosuppressive states. HIF-1α was upregulated in sepsis compared to healthy controls in three different data sets analysed by Shalova *et al*, 2015.

The Eukaryotic Translation Initiation Factor 4E Binding Protein 1 (EIF4EBP1) gene encodes for 4E-BP1 protein, which along with S6K protein are part of the m-TOR pathway (targets of mTORC1) that is essential for sepsis survival (Zhou *et al*, 2010). Inhibition of the mTOR-pathway in human PBMCs by metformin inhibited the phosphorylation of S6K and 4EBP1 (Shih-Chin *et al*, 2014) and inhibition of mTOR with metformin, rapamycin or torin-1 decreased the cytokine production induced by *C. albicans* sepsis and resulted in significantly diminished survival of mice with sepsis and lower cytokine production by splenocytes compared to mice not treated with metformin (Inoki *et al*, 2005). The mTOR-AKT pathway stimulates glycolysis (Barthel *et al* 1999), and mTOR-regulated increase in anaerobic glycolysis was a key metabolic pathway in acute inflammation (Inoki *et al,* 2005). Mitochondrial PTEN-induced kinase 1 (PINK1) mediates glycolysis by a regulating the Warburg effect via ROS-

dependent stabilization of HIF1α (Agnihotri *et al*, 2016). The ubiquitin E3 ligase "Parkin" also regulates the cellular metabolism and the glycolysis pathway, by interacting with Pyruvate Kinase M2 to increase glucose starvation (Kun Liu *et al,* 2016).

Immunometabolic changes from infection

Broad defects in oxidative phosphorylation and glycolysis appear to underlie immunosuppression in sepsis (Cheng S *et al*, 2016). Both hyper- and hypo-inflammatory phases result in major shifts away from basal homeostasis. The phenotypic phase shifts of immune cells may in fact follow on from key metabolic shifts. When host defence is triggered an early shift from oxidative phosphorylation to anaerobic glycolysis occurs.

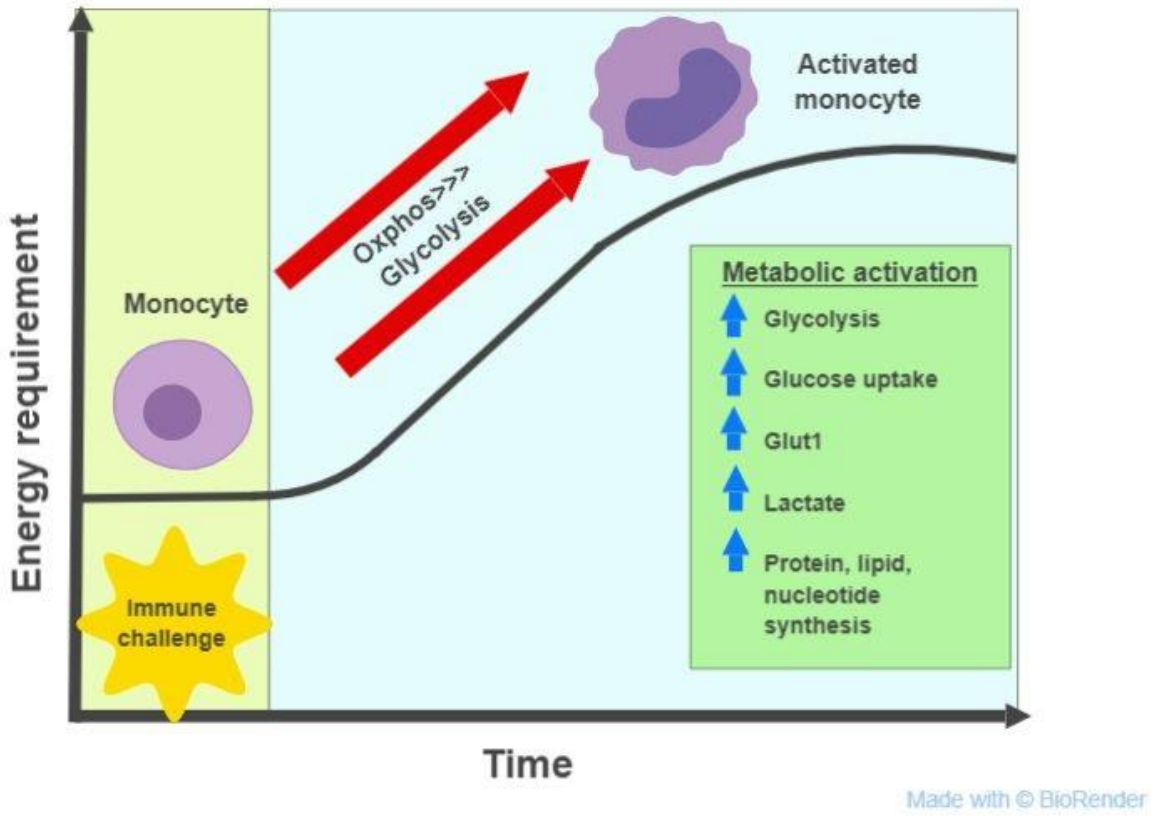

Figure 1.3.1 When a monocyte faces and immune challenge more energy is required, and a shift from oxidative phosphorylation is observed when the monocyte becomes activated. Image created using *Biorender software*.

More energy is required of the immune cells in order to defend against an immune challenge. Figure 1.3.1 depicts a monocyte's increased energy requirement in order to activate against the infection, and a shift from oxidative phosphorylation to glycolysis occurs. Metabolic activation results in an increase in glycolysis, glucose uptake, GLUT1, lactate, and synthesis of nucleotides, lipids and protein. Septic patients presenting with immunoparalysis displayed defects in both glycolysis and oxidative metabolism (Cheng S *et al*, 2016).

Glycolysis provides a major source of ATP for innate immune cells during periods of extreme cellular stress, such as in the early phase of sepsis. Whilst oxidative phosphorylation is highly efficient in ATP generation (more so than glycolysis), glycolysis is a far more rapid way to generate ATP and meet the cells' demand quickly in times of extreme stress.

Fatty acid transportation in sepsis

The CPT1 mitochondrial enzyme is responsible for fatty acid transportation. Immunoblot analysis of monocytes showed diminished activation of CPT1 in patients during sepsis, while these effects were reversed once patients recovered (Shih-Chin *et al,* 2014). Etomoxir is a widely used inhibitor of CPT1a, and therefore inhibitor of fatty acid oxidation, however the usefulness of this inhibitor is debatable. Acute production of Reactive Oxygen Species and evidence of severe oxidative stress was observed in T cells when exposed to concentrations above 5µM of Etomoxir, and as well as concerns with cellular redox and oxidative metabolism this demonstrates that Etomoxir lacks CTP1a specificity at these concentrations (O'Connor *et al*, 2018).

The NLRP3 (NOD-, LRR- and pyrin domain-containing protein 3) inflammasome was found to be activated by free fatty acids and the saturated fatty acid palmitate (Wen *et al*, 2011; Moon *et al,* 2015; Moon *et al*, 2016). Palmitate supresses AMPK (anti-inflammatory AMP-activated protein kinase) activation, which is a mediator of fatty acid metabolism that acts by suppressing inflammation through minimising ROS production and activating autophagy (Li *et al,* 2009). The suppression of AMPK by palmitate therefore increases ROS production and activates NLRP3.

Oxidative phosphorylation

Energy in the form of adenosine triphosphate (ATP) is required by cells to perform a multitude of processes, including the cellular response to infection. Two ways that cells can generate ATP is through the metabolic pathways of oxidative phosphorylation and glycolysis.

Within eukaryotic mitochondria, a major source of ATP is generated through the oxidative phosphorylation pathway utilising a mitochondrial proton gradient. Nutrients are oxidised using enzymes via the oxidative phosphorylation pathway in order to produce ATP as a result of the transfer of electrons from NADH or FADH 2 to oxygen by a series of electron carriers (Berg JM, 2002). The mitochondrial membrane contains protein complexes that pump out protons into the mitochondrial matrix. Electron flow from NADH or $FADH_2$ to O_2 through these protein complexes results in the protons being pumped out of the matrix. This results in a change in pH gradient and transmembrane electrical potential, which in turn draw the protons back into the matrix through an enzyme complex called ATP synthase, generating ATP (Figure 1.3.2). The ATP synthase uses a phosphorylation reaction to turn adenosine diphosphate (ADP) into adenosine triphosphate (ATP).

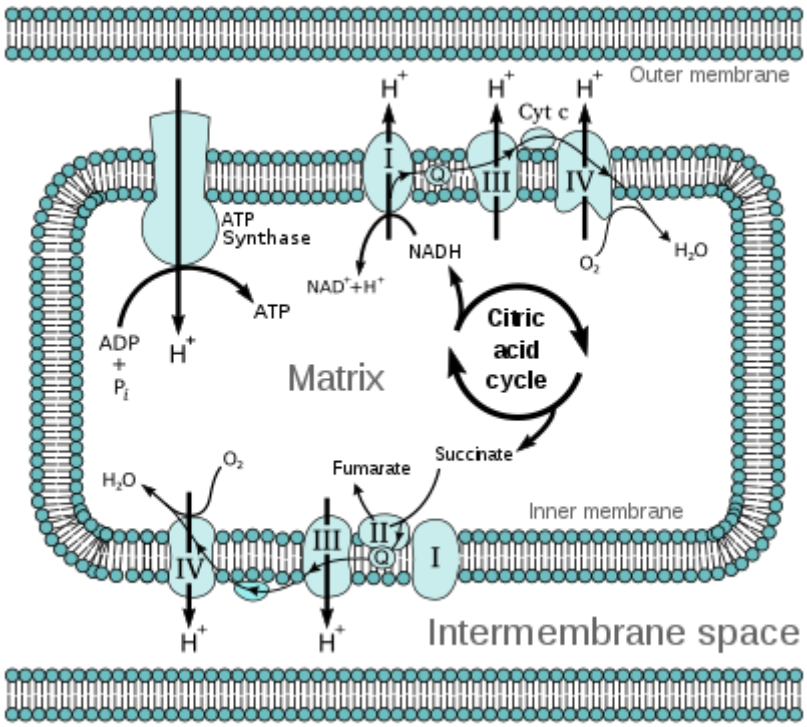

Figure 1.3.2 Process of oxidative phosphorylation. Oxidation and ATP synthesis are coupled by transmembrane proton fluxes. Image from Berg JM, 2002.

Glycolysis

The glycolysis pathway in eukaryotes is anaerobic and independent of oxygen; and occurs in the cytosol. Glycolysis converts glucose into pyruvate, pyruvic acid, and a proton. The resultant energy is than used to form ATP and NADH (Berg JM, 2002).

Glycolysis requires ATP in order to then form more ATP. It can be divided into three stages; destabilisation of glucose, cleavage of 6-carbon fructose, and finally generation of ATP (Figure 1.3.3).

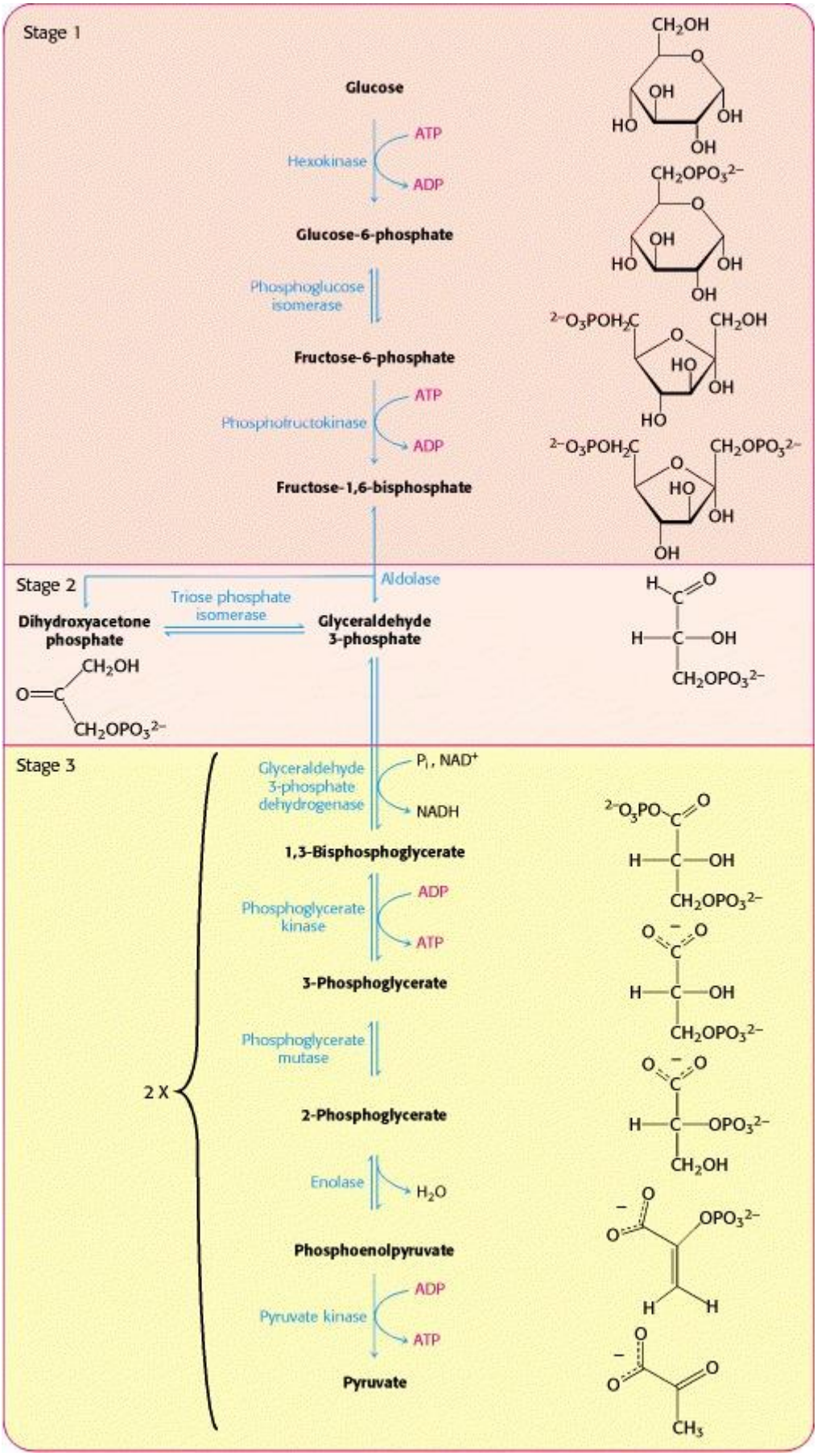
Stage 1
Glucose
ATP
Hexokinase
ADP
Glucose-6-phosphate
Phosphoglucose isomerase
Fructose-6-phosphate
ATP
Phosphofructokinase
ADP
Fructose-1,6-bisphosphate
Aldolase
Stage 2
Triose phosphate isomerase
Dihydroxyacetone phosphate
Glyceraldehyde 3-phosphate
Stage 3
2 X
Glyceraldehyde 3-phosphate dehydrogenase
P_i, NAD^+
NADH
1,3-Bisphosphoglycerate
Phosphoglycerate kinase
ADP
ATP
3-Phosphoglycerate
Phosphoglycerate mutase
2-Phosphoglycerate
Enolase
H_2O
Phosphoenolpyruvate
Pyruvate kinase
ADP
ATP
Pyruvate

Figure 1.3.3 Process of glycolysis. Image from Berg JM, 2002.

In the first stage, ATP is required by hexokinase in order to phosphorylate glucose in the cell to form glucose 6-phosphate. In the second stage, fructose 6-phosphate is formed from the isomerisation of glucose 6-phosphate by phosphoglucose isomerase. ATP is then required to phosphorylate the fructose 6-phosphate and create fructose 1,6-bisphosphate by phosphofructokinase. The fructose 1,6-bisphosphate is then cleaved into glyceraldehyde 3-phosphate and dihydroxyacetone phosphate by aldolase. The dihydroxyacetone phosphate is not in the direct glycolysis pathway; but can be converted into glyceraldehyde 3-phosphate by triose phosphate isomerase. In the final stage, glyceraldehyde 3-phosphate is converted into 1,3-bisphosphoglycerate by glyceraldehyde 3-phosphate dehydrogenase. One of the phosphoryl groups of 1,3-bisphosphoglycerate is then transferred to ADP to create ATP and 3-phosphoglycerate catalysed by phosphoglycerate kinase. So far, the ATP generated has made up for the ATP used in the glycolytic pathway. Finally, 3-phosphoglycerate is converted into pyruvate with the concomitant conversion of ADP into ATP (Berg JM, 2002).

1.4 Treatment-specific factors that may influence outcomes of sepsis

Many of the therapeutics used to facilitate organ support may have important actions themselves on not yet fully understood pathways that may influence the outcomes of sepsis. The effects of the sedative propofol and the neuromuscular blocking agent Rocuronium in sepsis were examined in this thesis.

Propofol in general anaesthesia

Ventilatory support is required in 85% of all septic patients (Wheeler *et al*, 1999). Sedation is mandatory where intubation and mechanical ventilation are required (Hogarth *et al*, 2004), which makes up 55-70% of septic patients in intensive care (Rivers *et al*, 2001). Historically a combination of opioids and benzodiazepines were administered in general anaesthesia in the intensive care unit, but their long delays in patient wake up time lead to a shift towards propofol use, which remains the standard sedation agent to this day (Patel *et al,* 2012; Jakob *et al*, 2012). Propofol is sedative, anxiolytic, and an anticonvulsant (Kotani *et al*, 2008).The advantages of propofol over other sedative agents are that propofol has a rapid onset of action, rapid elimination and thus shorter patient wake up times, and improved patient comfort (decreased postoperative nausea and vomiting) (Byrne *et al*, 2008).

Propofol mechanism of action

Propofol is a GABA receptor agonist that is administered intravenously and acts as a blocking nervous system (Royse *et al*, 2008). Anaesthetic agents have broad effects on the immune system (Kurosawa *et al,* 2008), but their specific mechanisms are not fully understood.

Anti-inflammatory effects of Propofol

Propofol is known to have antioxidant and anti-inflammatory effects (Runzer *et al*, 2002; Murphy *et al*, 1992; Chen *et al*, 2002). Propofol has been demonstrated to encourage oxidative phosphorylation in LPS-activated macrophages, and inhibits NADPH which in turn inhibits the overproduction of ROS and therefore ROS-mediated GLUT1 expression (Zeng *et al*, 2021). In comparison to sevoflurane, Propofol increased anti-inflammatory cytokine levels in serum (IL-6, IL-8, IL-10) in a study on craniotomy (Markovic-Bozic *et al*, 2016), and proinflammatory cytokine levels were reduced by Propofol in a study on myocardial ischemia reperfusion (Corcoran *et al*, 2004). It is not only cytokines that Propofol affects; studies have also found it attenuates the inflammatory response in both an animal model of renal ischemia/reperfusion injury by blocking formyl peptide receptor 1 (Yang *et al*, 2013) and a human study of robot-assisted laparoscopic radical prostatectomy that found a serum cytokine levels were attenuated in patients who had received propofol infusion (Roh *et al*, 2019).

Propofol-induced immunosuppression

Propofol impairs neutrophil function and locomotion (O'Donnell *et al*, 1992; Skoutelis *et al*, 1994; Jensen *et al*, 1993), attenuate TNF-α, IL-6 and NO expression in canine PBMCs (Pei and Wang, 2012), and inhibits bacterial clearance via propofol's intralipid solvent (Koch *et al,* 2002). Patients who have undergone surgery can display a perioperative immunosuppression due to neuroendocrine stress. The surgical stress is caused by the activation of the hypothalamic-pituitary-adrenal (HPA) axis as well as activation of the autonomic nervous system, which cause the release of hormones that can inhibit immune function (Kennedy *et al*, 1999). Further contributing to the perioperative immunosuppression are the interventions

involved in stabilising the patients under general anaesthesia, such as pain management, management of hypothermia and hypoglycaemia, and the anaesthetics themselves (Schneemilch *et al*, 2004). Several studies suggest that the inflammatory response can be impaired by anaesthetic agents (Kurosawa *et al*, 2008; Colucci *et al,* 2013; Schneemilch *et al*, 2004), and that they may directly affect immune cell function (Schneemilch *et al*, 2004; Amin *et al*, 2011; Colucci *et al,* 2011). However, propofol has also demonstrated protective effects on endothelial cell permeability when exposed to LPS and reduced LPS-induced iNOS and NF-κB protein levels (Gao *et al*, 2006), and reduces TNF-α, IL-1β, IL-6, and nitric oxide synthesis via NO synthase downregulation in LPS-activated macrophages (Chen *et al,* 2003; Chen *et al*, 2005).

The effect of Propofol in sepsis

There are several studies into propofol's effects on sepsis. Propofol can have anti-inflammatory effects by competitively blocking formyl peptide receptor 1 (FPR1) in human neutrophils which is required for human neutrophil activation, and reduces neutrophil chemotaxis (Yang *et al*, 2013). In contrast to the sterile animal surgical model noted previously (Yang *et al*, 2013), propofol was found to increase mortality and morbidity in an animal model of sepsis (Schläpfer *et al*, 2015). The authors speculated that the reason propofol had such an adverse effect in this context may be due the concentration of endotoxin in the plasma, resulting in a hypotension that did not respond to fluid resuscitation (Schläpfer *et al*, 2015). In a murine model of bloodstream MRSA, propofol increased populations of myeloid-derived suppressor cells (MDSCs); a lineage of immune cells originating from bone marrow stem cells (Visvabharathy *et al*, 2017). A retrospective cohort study on septic patients admitted to two academic centre ICUs from 2013 to 2017 found that propofol (n=64) was more likely to result

in hypotension than dexmedetomidine (n = 31), which can lead to organ failure (Benken *et al*, 2019).

Rocuronium neuromuscular blockade in general anaesthesia

Rocuronium bromide is widely used in general anaesthesia as a non-depolarising neuromuscular blocking agent (Brull *et al*, 2017). It is used in both intubation and surgical procedures routinely in the intensive care unit, and the World Health Organisation estimates that globally each year around 187 million surgeries using general anaesthetics are carried out (Weiser *et al,* 2008). Approximately 80% of patients undergoing general anaesthesia will receive neuromuscular blocking agents with 50% receiving reversal agents (Ball L, 2017). Rocuronium functions as an aminosteroid, and acts on acetylcholine (ACh) and nicotinic acetylcholine (nAChR) receptors on the synapse in the nicotinic neuromuscular junction (Zhang *et al*, 2014). It has a rapid onset and is reversible.

Anaesthetic management of septic patients frequently require neuromuscular blockade to assist in tracheal intubation (Niiya *et al*, 2006). Septic patients who received neuromuscular blocking agents had a 4.3% reduction in their in-hospital mortality rates in an epidemiologic cohort study of 39 US hospitals (Steingrub *et al*, 2014). The 2014 Surviving Sepsis Campaign suggested neuromuscular blocking agents may be beneficial in sepsis induced ARDS if administered within 48hours (Rhodes *et al,* 2017). However, septic shock patients have an increased risk of critical illness polyneuropathy when exposed to neuromuscular blocking agents (Price *et al,* 2012; Garnacho-Montero *et al,* 2001).

Reversal agents of neuromuscular blockade

Two commonly used reversal agents for neuromuscular blockade are Neostigmine Sugammadex. Sugammadex, developed specifically for Rocuronium and Vecuronium anaesthesia, is a modified g-cyclodextrin that will provide a rapid and effective reversal of the neuromuscular blockade (Bom *et al*, 2002; Epemolu *et al*, 2003; Zhang, 2003; Suy *et al*, 2007). It works by encapsulating the Rocuronium or Vecuronium, and literature to date has not found a direct interaction between Sugammadex and the cells themselves (Bhaskar, 2013; Lee *et al,* 2009; Gijsenbergh *et al*, 2005; Nicholson *et al*, 2007). It is currently the closest drug to a reversal agent ideal: efficient, fast onset, longer half life than the neuromuscular blocking agents themselves, can work during both mild and intense neuromuscular blockade, and should be free from side effects (Hemmerling *et al*, 2010). Sugammadex will act in a dose-response relationship for the reversal of Rocuronium and Vecuronium neuromuscular blockade in both Sevoflurane and Propofol general anaesthesia (Pühringer *et al*, 2010). Sugammadex was found to have a lower incidence of major pulmonary complications than Neostigmine (Kheterpal *et al*, 2020) and is a faster-acting and more reliable antagonist (Kopman, 2010).

Pulmonary complications in neuromuscular blockade

Despite their widespread use, patients who have received neuromuscular blocking agents have an increased risk of hospital readmission within 30 days due to pulmonary complications. After wound infection, pulmonary complications are the next most common complication in postoperative patients (Dimick *et al*, 2004; Khuri *et al*, 2005) and are common in high-risk surgical groups (Serpa Neto *et al*, 2014). Neuromuscular blocking agents are associated with postoperative respiratory complications such as atelectasis, respiratory

failure, post-extubation hypoxia and negative pressure-induced pulmonary edema (Kafer *et al,* 1997; Kumar *et al,* 2012; Murphy *et al*, 2010). This could be due to the neuromuscular blockade persisting after patient arousal from the general anaesthesia, as a persisting low level paralysis could result in the inability to cough, difficulty swallowing, or if atelectasis formed from anaesthesia it may disrupt ventilatory muscle contraction (Farhan *et al,* 2014). Due to the nature of the treatments, most research into the postoperative pulmonary complications resulting from neuromuscular blockade are registry-based retroactive studies (McLean *et al*, 2015), and furthermore there may be a selection bias in the literature regarding pulmonary complications specifically as this is what patients are expected to return to hospital with. Therefore, evidence is currently lacking.

Immune cell expression of acetylcholine receptors

Immune cells, including T cells, B cells, macrophages, and dendritic cells, are also known to express cholinergic components such as muscarinic and nicotinic acetylcholine receptors (Fujii *et al*, 2017). These immune cells express all of the muscarinic acetylcholine receptors (mAChR) M1-M5 and several nicotinic acetylcholine receptors such as nAChR α7 (Grando *et al*, 2015; Kawashima *et al*, 2019). The study into mAChR and nAChR gene-knockout mice by Fujii *et al* (2017) suggests that a functioning immune system is partially modulated by the immune cell cholinergic system, in that Ach synthesis and ChAT mRNA expression is upregulated via CD3- and T-cell receptor mediated pathways. They found that less TNF-α and IL-6 was produced in M1/M5 knockout mice, whereas more TNF-α and IL-6 was produced in nAChR α7 knockout mice.

Hypothesis of this thesis

The overarching hypothesis of this project is that there are persisting epigenetic and immunometabolic changes in leukocytes following sepsis, which contribute to the long-term immune defects in patients.

Chapter 2: Methods

2.1 General research plan

2.1.1 Study design and patient recruitment.

The study design is analytic observational, encompassing a long term follow up of blood culture positive bacteraemia patients. Patient recruitment commenced in 2014 and ended May 2017, and the blood culture results were available in real-time at a work station in the intensive care and anaesthesia research department of The Royal London Hospital. The patients all had confirmed bacteraemia and the first blood sample was taken from patients within 24 hours of a blood culture positive result. Patients (n=69) with positive blood cultures underwent blood sampling within 24 hours of blood culture result, 4-10 days later and 6-12 months following hospital discharge at a routine outpatient follow-up appointment. The 24 hour samples was chosen as it is an acute sepsis rection, where the patients are actively fighting an infection. The 4-10 day sample was chosen because the patients had by then cleared the infection from their system, but were still hospitalised. By this time their immune system may be fatigued from fighting sepsis for so many days. The final sample, 6-12 months, was drawn when patients had been discharged from hospital for several months and are considered 'recovered' from sepsis.

Healthy volunteers served as a comparator group (n=37). Clinical and demographic features are shown in Table 2.1.1 below. The median age of the volunteer group was 41 and 22 (60%) were male.

Table 2.1.1 Demographic and clinical features of the patient cohort. Numbers refer to median with full range in parenthesis, or absolute count and percentages.

	n=69
Age	59 (19-92)
Male sex	41 (59%)
Level of care	Intensive care: 23 (33.3%)
	General ward: 46 (66.6%)
SOFA score day 0 (ICU cohort)	6.4 (2-13)
Gram -ve infection	37 (53.6%)
Gram +ve infection	31 (44.9%)
Fungal infection	1 (1.4%)

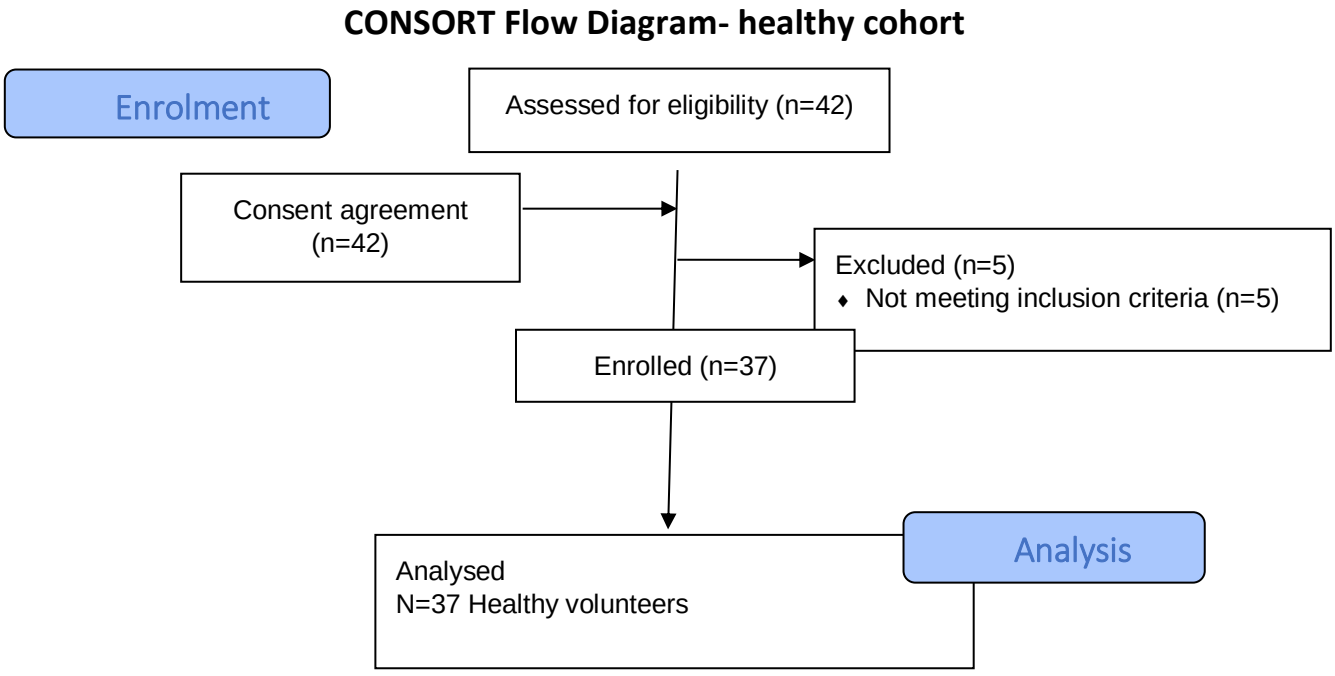

CONSORT Flow Diagram- full septic cohort

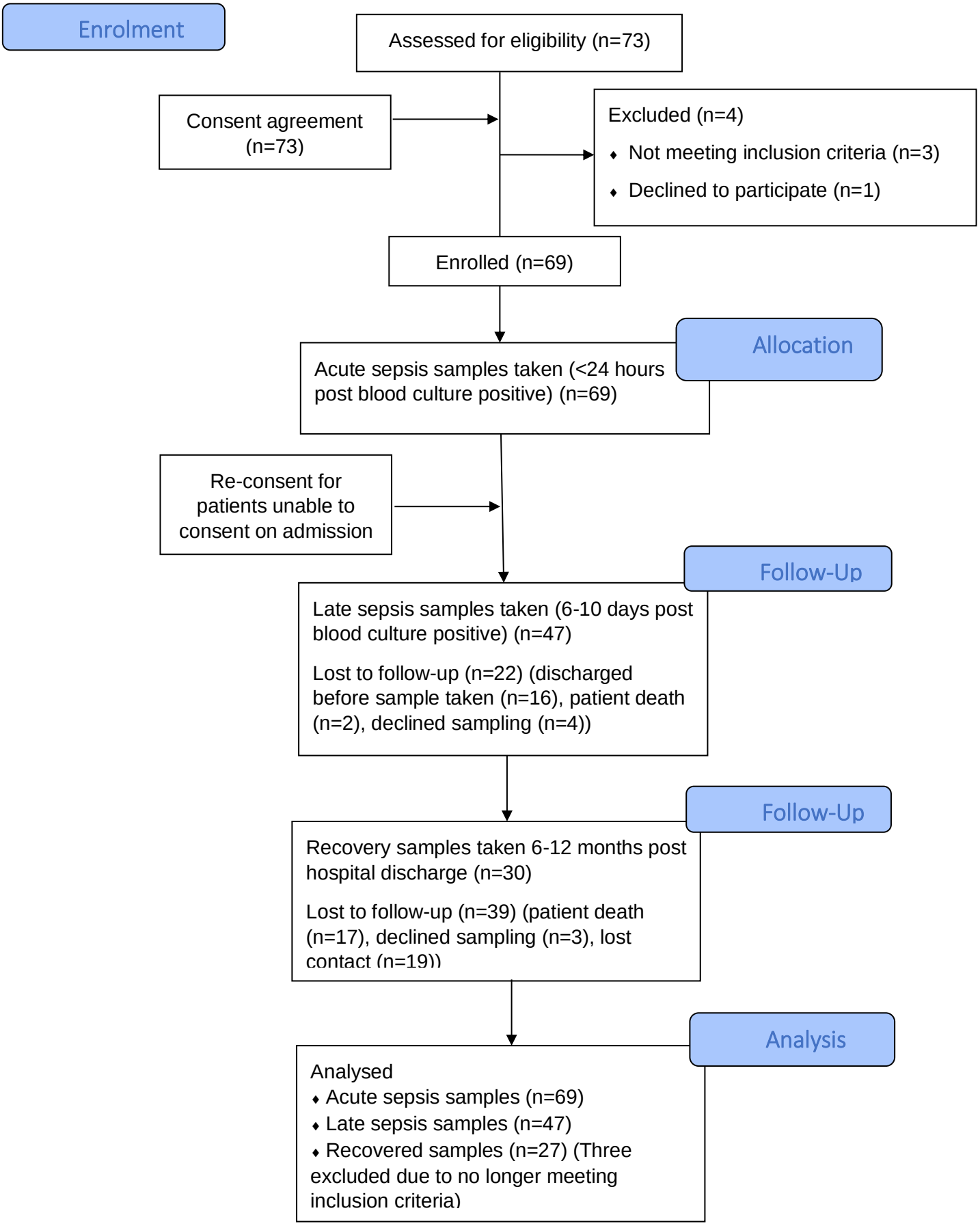

Blood samples are obtained at three different time points for each patient, and these samples include peripheral blood mononuclear cells (PBMCs) isolated using Ficoll-Paque density gradient centrifugation, a total RNA blood tube, and a serum sample.

65 patients were recruited prior to this PhD research in 2016, and samples were taken by medical staff at the Royal London Hospital and stored. The subsequent patients were recruited when this research commenced, and samples were processed by myself. PBMCs were previously frozen in PBS 2% FBS, but since this research began, I froze the subsequent PBMCs in FBS 10% DMSO to protect the integrity of the cells. Patient eligibility screening, consent, and phlebotomy was performed by medical staff at the Royal London Hospital.

Patients recruited prior to 2016 also had a citrated plasma sample taken, which was replaced in 2016 by an additional tube for PBMC extraction. Samples are kept in a -80˚C freezer for long term storage. Patients were clinically phenotyped by information recorded in their comprehensive case report forms (CRF), which includes data relating to functional status following hospital discharge and acquired infectious episodes.

2.1.2 Ethics

The project was granted ethical approval by the NRES Committee London (REC reference: 13/LO/0363, IRAS project ID 123422) prior to the study commencing. Informed, written patient consent was sought before any bloods were drawn and patients were free to withdraw from the study at any point. For patients unable to consent, consent from next of kin was sought and re-consent took place when patients were able to consent. For any patients who withdrew consent, any data and samples were destroyed. Informed verbal consent was sought before any bloods

were drawn from healthy volunteers, recruited via word of mouth, who were also covered under the project ethics. No animal experiments were carried out.

2.1.3 Patient inclusion and exclusion criteria

Patients over 18 years old were eligible for consideration for inclusion to this study, and in order to avoid recruiting patients with long preceding hospital admissions and resultant confounding epigenetic stressors, patients were excluded if they had spent more than 48 hours in the hospital prior to the positive blood culture being drawn. Patients with a known history of immunosuppression, cancer, chemotherapy/radiotherapy, or those who had received immunosuppressive medications in the prior six months were excluded from the study.

Thirty-seven healthy volunteers served as a comparator group to the bacteraemia patients. The volunteers were all physically healthy and had not had bacteraemia in the past, had no known acute or chronic illnesses including immunodeficiency, and had not taken immunosuppressive medication within the six months prior.

2.1.4 Blood sampling, processing, and storage.

As previously described, patients with positive blood cultures for bacteraemia underwent blood sampling within 24 hours of blood culture result, 4-10 days later and 6-12 months following hospital discharge. A healthy volunteer group served as a comparator group. Venous bloods were drawn into two 10ml vacutainer EDTA tubes (BD Biosciences), one 7ml PAXGene Blood RNA tube (PreAnalytix, Germany) and one 4.5ml serum separator tube (BD SST II Advance, BD Biosciences), inverted to mix, and then walked at room temperature back to The William Harvey Research Institute where they were processed immediately.

Whole blood was drawn from each of the patients and volunteers into 7ml PAXGene Blood RNA Tubes (PreAnalytix, Germany), which were then inverted 10 times and left to stand at room temperature for 2 hours to lyse the blood cells. The blood was stored for future use by being frozen in a -20^{o}C freezer for 24 hours then transferred to a -80^{o}C freezer for long term storage.

Peripheral Blood Mononuclear Cells (PBMCs) were isolated via Ficoll-Paque density gradient centrifugation; each 10ml EDTA tube of blood was diluted with 20ml sterile PBS and carefully and slowly run over 15ml of Ficoll-Paque Plus solution (GE Healthcare Biosciences, USA) in a 50ml Falcon tube (Corning, USA) to form a layer. The blood was then spun at 400g for 30 minutes at room temperature with the brake off in a Heraeus Megafuge 1.0R (Thermo Scientific, USA).

Meanwhile, the gold top serum tube was also processed by being left upright on the benchtop at room temperature to clot (approximately 30 minutes), and then spun in an ALC PK 120 centrifuge (ALC International, Italy) at 1000g for 10 minutes. The top layer (serum) was then pipetted into a 1.8ml cryogenic vial (Thermo Fisher Scientific, USA) after being passed through a syringe attached to a sterile Acrodisc 32mm Syringe Filter with 1.2µm Supor Membrane (PALL Life Sciences, cat no.4656). The serum was then transferred immediately to the -20°C freezer and then two hours later transferred to the -80°C freezer for long-term storage. The serum cannot be thawed and refrozen for subsequent uses.

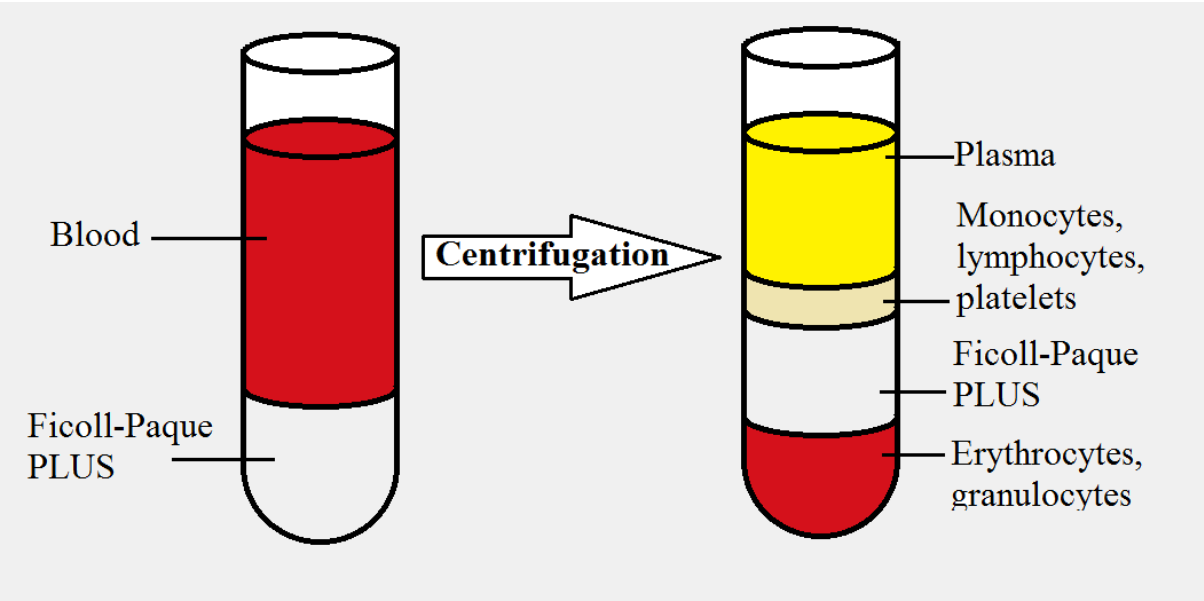

Figure 2.1.1 Ficoll-Paque blood separation before (left) and after centrifugation (right).

The Ficoll-Paque blood tube should come out layered. The top layer (diluted plasma) was aspirated to leave the mononuclear cell layer undisturbed at the interface, and this cell layer was then pipetted out and transferred to a 15ml conical tube (Corning) and washed twice with PBS, spun at 300g for 10 minutes (Heraeus Megafuge 1.0R, Thermo Scientific) at room temperature. Cells were then re-suspended in 500µl PBS and counted on a haemocytometer using trypan blue (cat no. T8154, Sigma Aldrich, USA).

For culture, PBMCs are grown in RPMI with 10% serum (unless otherwise stated) in an incubator at 37°C at 5% CO_2. For storage, the PBMCs were gradually resuspended in 1ml of FBS 10% DMSO, then put into a Nalgene Mr Frosty Freezing container (Sigma Aldrich, USA) filled with isopropyl alcohol that was immediately transferred to the -80°C freezer overnight for a 1°C/min cooling rate. They were then kept in the -80°C freezer for long term storage.

2.1.5 Cell culture of THP1 and HL-60 cell lines

HL-60, THP1 and THP1 NLRP3-/- (all purchased from InvivoGen) are immortalised cell lines that were used as a model alongside PBMCs. HL-60s are promyeloblasts isolated from peripheral blood from a 36-year-old woman who had acute promyelocytic leukaemia. THP1s were derived from peripheral blood from a one-year-old male acute monocytic leukaemia patient. THP1 Null and THP1 NLRP3-/- lines can be used to study the impact of the NLRP3-/- inflammasome. THP1 Null cells are derived from THP1 human monocytic cells and express high levels of NLRP3, ASC and pro-caspase 1 as a positive control to THP1 NLRP3-/- cells which lack NLRP3, ASC and pro-caspase 1. The NLRP3-/- cells were generated from the human monocytic THP1-Null cell line (via CRISPR by the manufacturer) through the deletion of the N-terminal region of the NLRP3 gene- only an inactive NLRP3 C-terminal fragment is expressed.

These lines proliferate continuously in suspension culture, and are beneficial when running experiments that require several days of culture (used here in challenge and recovery experiments). They also help to validate findings as each type of cell line is of the same lineage.

THP1 Null, THP1 NLRP3-/- and HL-60 cells were incubated in 75cm^3 tissue flasks in RPMI 1640 supplemented with 10% foetal bovine serum (FBS) at a concentration of <1x10^6 cells/mL. For drug administration, cells were plated into cell culture plates as required. Cells were not treated with antibiotics, and all cell culture work was performed under sterile conditions. Cells would be terminated if they got to passage 21 as they begin to degrade, but experiments were performed starting on young cells thawed at passage 7. Cell viability was assessed using a haemocytometer with Trypan Blue, viability was typically 85%+.

2.2 Cytometric Bead Array

2.2.1 Theory

The Cytometric Bead Array methodology is a multiplexed bead-based immunoassay that can measure a variety of proteins both soluble and intracellular, such as cytokines, chemokines and growth factors. They use the same basic principle as sandwich immunoassays and allow proteins to be quantified via flow cytometry to provide a higher sensitivity and broader dynamic range than the ELISA methodology.

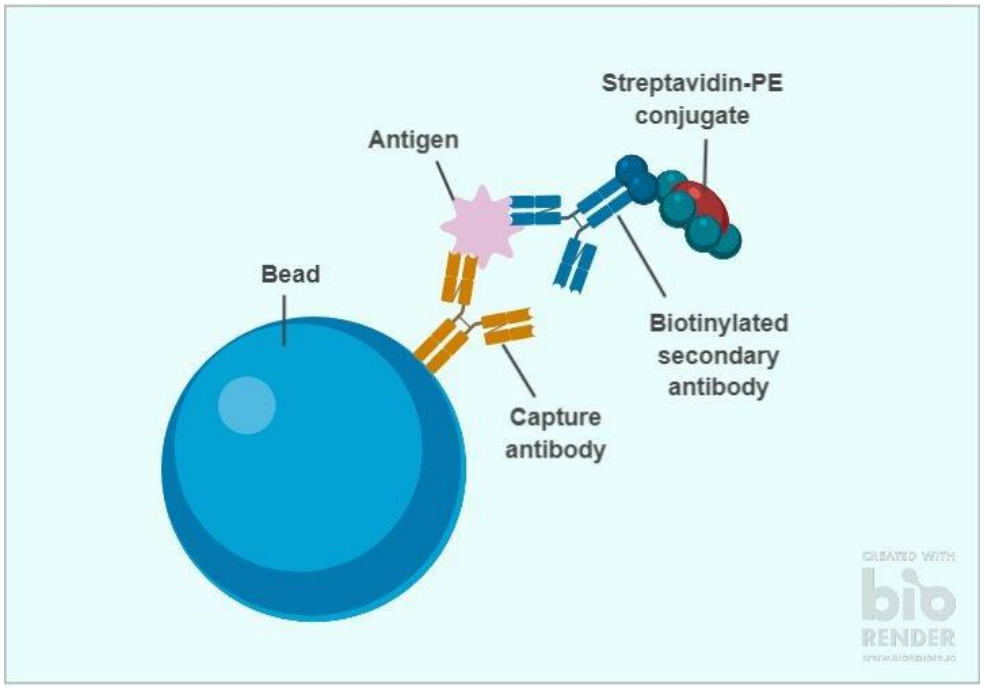

Figure 2.2.1 Binding of antibodies and analytes to beads in Cytometric Bead Array

Size and internal fluorescence intensities differentiate the beads. Two sizes of beads are utilised in the *LEGENDplex Human Th Cytokine Panel 13-plex* by Biolegend, CA (cat no. 740001) which was used in this research. The two sizes of beads are the smaller “Beads A” and larger “Beads B”. Each of these beads acts as a capture for analytes of interest by being

conjugated with the antibody specific to that analyte. The different bead sizes capture different analytes of interest. When the beads are added to a sample containing analytes of interest, the analytes will bind to their specific capture beads during an incubation period. Then, a biotinylated detection antibody cocktail can be added after washing the beads, which will bind to the analytes specific to each antibody in the cocktail. This forms the capture bead-analyte-detection antibody sandwiches, which can then be detected by the additional of streptavidin-phycoerythrin (SA-PE) which will provide fluorescent signals when bound to the biotinylated detection antibodies. The intensity of the fluorescent signals are proportional to the amount of bound analytes. These fluorescent signals can then be read on a flow cytometer, and from there first the bead size and then the internal fluorescence intensities can be segregated so that the PE fluorescent signal of each analyte-specific population can be read. A standard curve can then be generated in order to determine the concentration of each analyte.

2.2.2 Assay preparation and procedure

The flow cytometry-compatible multiplex *LEGENDplex Human Th Cytokine Panel 13-plex* by Biolegend, CA (cat no. 740001) was utilised for quantification of 13 cytokines; IL-2, IL-4, IL-5, IL-6, IL-9, IL-10, IL-13, IL-17A, IL-17F, IL-21, IL-22, IFN-gamma and TNF-alpha. These cytokines are released by T helper cells to regulate the immune response and stimulate effector cells such at macrophages, cytotoxic T cells and B cells. IL-1β was not included- this was an oversight- it should have been in the panel due to its relationship with the NLRP3 inflammasome.

Cell supernatants were harvested as previously described and centrifuged (Labnet Prism™ R Refrigerated Microcentrifuge, Labnet International, USA) to remove debris, and then

aliquoted at 100µl each in 1.5ml microcentrifuge tubes (Starlab, UK) for freezing and storage at -80^{o}C until cytokine quantification was carried out. This prevented multiple freeze-thaw cycles. Sample dilution was not required for the cell culture supernatants.

The standard was prepared by reconstituting the lyophilized *Human Th Cytokine Standard Cocktail* in 250µl assay buffer and performing six 1:4 serial dilutions, where the top undiluted sample "C7" has a concentration of 10,000 pg/ml for each analyte in the panel, and a final standard of only assay buffer "C0" was used for a 0 pg/ml standard. Serial dilutions were performed as in Table 2.2 below:

Table 2.2.1 Serial dilution plan from the Biolegend *LEGENDplex Human Th Cytokine Panel* manual.

Tube	**Serial dilution**	**Assay buffer added (µl)**	**Standard added**	**Final concentration of standard (pg/ml)**
C7	N/A	N/A	N/A	10,000
C6	1:4	75	25µl of C7	2,500
C5	1:16	75	25µl of C6	625
C4	1:64	75	25µl of C5	156.3
C3	1:256	75	25µl of C4	39.1
C2	1:1024	75	25µl of C3	9.8
C1	1:4096	75	25µl of C2	2.4
C0	N/A	75	N/A	0

Wash buffer was prepared by diluting 25ml of the supplied 20X Wash Buffer with 475ml of deionized water. The assays were performed in polypropylene V-bottom microplates. Samples were run in duplicate and arranged as per plate map below (Table 2.2.2), with an additional two C0 (G11 and 12) and C7 (H11 and 12) standards used for set up on the flow cytometer.

Table 2.2.2 Plate map for samples run in cytometric bead array

Plate map

	1	2	3	4	5	6	7	8	9	10	11	12
A	C7	C7	Sample 1	Sample 1	Sample 9	Sample 9	Sample 17	Sample 17	Sample 25	Sample 25	Sample 33	Sample 33
B	C6	C6	Sample 2	Sample 2	Sample 10	Sample 10	Sample 18	Sample 18	Sample 26	Sample 26	Sample 34	Sample 34
C	C5	C5	Sample 3	Sample 3	Sample 11	Sample 11	Sample 19	Sample 19	Sample 27	Sample 27	Sample 35	Sample 35
D	C4	C4	Sample 4	Sample 4	Sample 12	Sample 12	Sample 20	Sample 20	Sample 28	Sample 28	Sample 36	Sample 36
E	C3	C3	Sample 5	Sample 5	Sample 13	Sample 13	Sample 21	Sample 21	Sample 29	Sample 29	Sample 37	Sample 37
F	C2	C2	Sample 6	Sample 6	Sample 14	Sample 14	Sample 22	Sample 22	Sample 30	Sample 30	Sample 38	Sample 38
G	C1	C1	Sample 7	Sample 7	Sample 15	Sample 15	Sample 23	Sample 23	Sample 31	Sample 31	C0	C0
H	C0	C0	Sample 8	Sample 8	Sample 16	Sample 16	Sample 24	Sample 24	Sample 32	Sample 32	C7	C7

.

First 25µl of assay buffer was added to all wells, and then 25µl of either standard or sample was added to the appropriate wells. For each well, the mixed beads were vortexed thoroughly to resuspend before 25µl was added and mixed by pipetting into the well. Finally, 25µl of detection antibodies were added to each well so that the volume of each well now totals 100µl.

A lid was put on the plate and it was covered in aluminium foil and shaken at 600rcf on a plate shaker for 2 hours at room temperature (max speed to mix without spilling the contents of the wells). Then, 25µl SA-PE was added directly into each well without washing the plate, then the plate was re-covered in aluminium foil and set back on the 600rcf plate shaker for a further 30 minutes at room temperature. The plate was then centrifuged (IEC Centra GP8R, Thermo Fisher Scientific) at 1000g for 5 minutes and the supernatant was removed using a multichannel pipette. The beads were resuspended by pipetting up and down in 200µl of prepared 1X wash buffer in each well, and then centrifuged again at 1000g for 5 minutes.

Supernatants were removed, then the beads resuspended in a fresh 200µl of 1X wash buffer per well, and transferred to labelled 1.2ml polypropylene microtubes (TN0946-01R National Scientific Supply Company, Thermo Fisher Scientific) for flow cytometry.

2.2.3 Flow cytometry data acquisition

Samples were read on a BD LSR Fortessa (BD Biosciences, USA) immediately after being transferred to the microtubes. The Fortessa used FACSDiva™ software and the PE channel was used for reporter and the APC channel was used for bead classification, and so compensation between these channels was not required. The additional C7 was used to set up the PE voltage settings, and the C0 was useful for APC voltage settings. After initial set up, the document was saved as a template for subsequent Cytometric Bead Array experiments.

Beads were gated by creating a dot plot with the x-axis of FSC (forward scatter) and the y-axis of SSC (side scatter) in linear mode, then two gates were created and labelled as “Beads A” and “Beads B”. Then, for each gating of Beads A and B, a dot plot with the x-axis of PE and the y-axis of APC in log mode was created, along with an additional plot of x-axis of FITC and y-axis of APC in log mode gated on both Beads A and B.

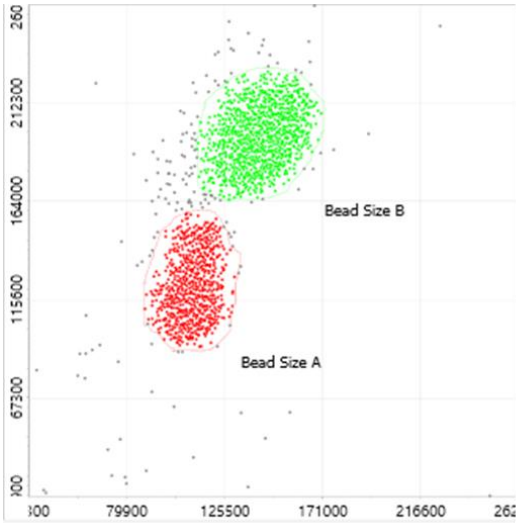

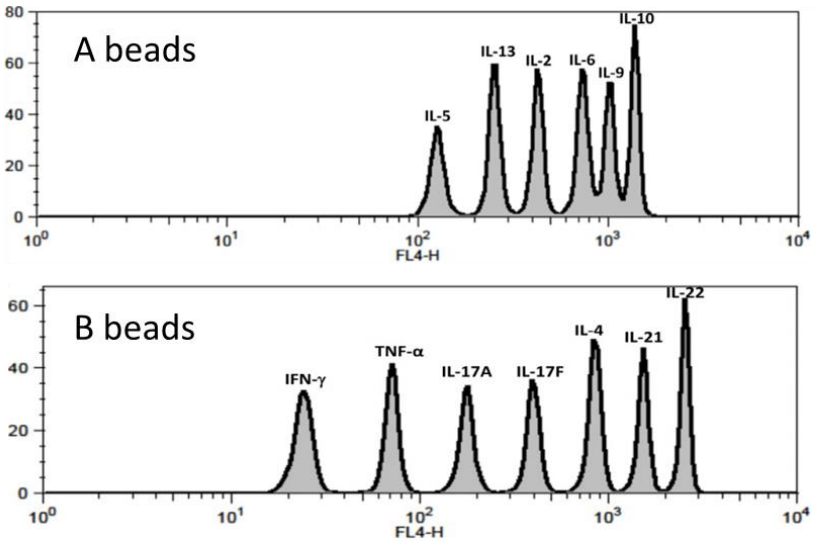

Figure 2.2.3 Images from CBA experiment set up. FSC vs SSC divides beads in their two sizes (left). Then, each bead can be further divided based on their internal fluorescence intensities (right). The internal dye can be detected using FL3, FL4 or APC channel, depending on type of flow cytometer used.

The additional C7 and C0 standards were vortexed and used to set up the PMT voltage of the classification channel APC, reporter channel PE, and FITC channel. Flow cytometer flow rate was set to low, and (with several refreshes) the FSC and SSC settings were adjusted until both bead populations were visible and well separated. The smaller beads were gated as "Beads A" and the larger beads gated as "Beads B". To complete the set-up, the majority of the beads should have a FITC signal and PE signal between $1x10^1$ and $1x10^2$, and APC fluorescence intensity between $1x10^2$ and $5x10^4$. Once set up was complete it was saved as a template for future Cytometric Bead Array experiments. Standards and then samples were then each vortexed run through the flow cytometer and the data was exported.

Quality control

The intra-assay and inter-assay reproducibility was determined by Biolegend by evaluating a test plate of ten replicates of three different sample levels (intra-assay) and two replicates of three different sample levels from four separate experiments (inter-assay).

2.2.4 Data analysis

The FCS files generated on the flow cytometer were analysed using Biolegend's *LEGENDplex Data Analysis Software*. The FCS files produced by the flow cytometer were uploaded and the

experiment parameters were adjusted to set the highest analyte concentration, the dilution factor, and the decimal places; and the replicates were marked. The standards were identified and an 8-point standard curve was selected.

Next, the bead gating was carried out; the number of bead sizes, report signal, and bead ID and analyte were defined. Then in a plot of forward scatter (FSC) x-axis and side scatter (SSC) y-axis the two different bead sizes A and B were gated. FSC vs SSC divides the beads into their two sizes, and from there each bead can be further divided based on their internal fluorescence intensities. The internal dye can be detected using a FL3, FL4 or APC channel, depending on type of flow cytometer used- in this case, APC was used. The gating settings were saved as a gating protocol for any future experiments or repeats.

After set up was complete the software was run, and the concentration of each cytokine in a sample was determined from the concentration curve made from the mean fluorescence intensity (MFI) of standards of each cytokine at the known concentrations.

2.3 Seahorse XF96 metabolism assay

2.3.1 Theory

Cellular metabolism drives biological processes and cellular health. Therefore, measuring immunometabolism and bioenergetics can help determine cell health and performance after a septic insult. The metabolism of cells can be assessed by measuring the oxygen consumption rate (OCR) and extracellular acidification rate (ECAR) of the cells using the Agilent Seahorse XF methodology. The cells' basal respiration, ATP production, proton leak, maximal respiration, spare respiratory capacity, and non-mitochondrial respiration can be estimated through serial injection of three mitochondrial inhibitors. These serially injected mitochondrial inhibitors are oligomycin, fluoro-carbonyl cyanide phenylhydrazone (FCCP), and finally a combination of rotenone and antimycin A.

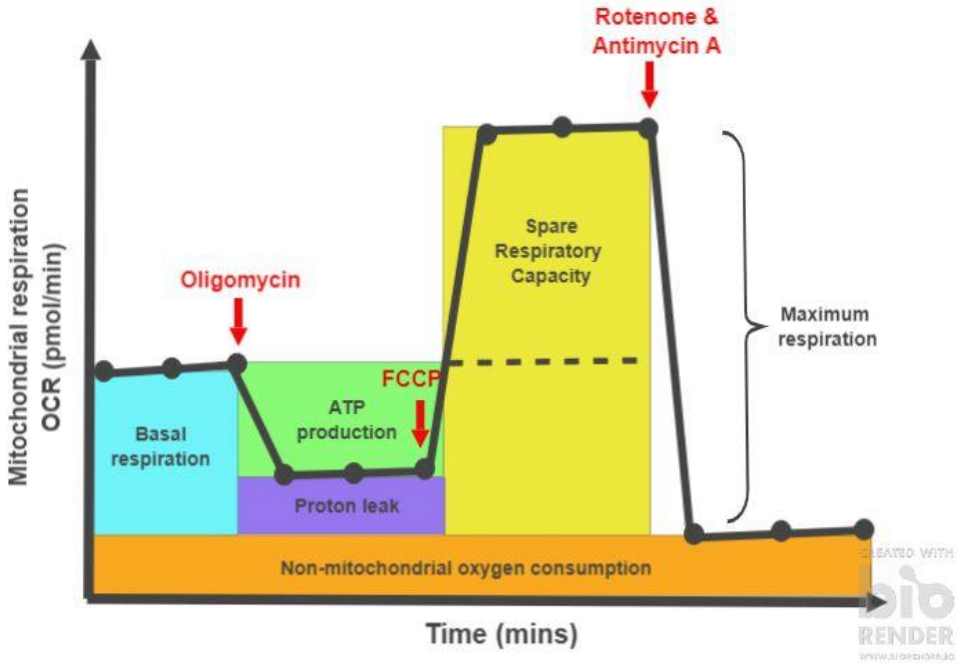

Figure 2.3.1 Injection strategy showing the OCR over time and how this allows various aspects of respiration to be measured.

Oligomycin is an antibiotic which inhibits oxidative phosphorylation by binding ATP synthase (complex V) in such a way as to block the proton channel. The addition of oligomycin results in a decrease in oxygen consumption rate, which correlates to respiration associated with cellular ATP production in the mitochondria.

Fluoro-carbonyl cyanide phenylhydrazone (FCCP) is a pure uncoupling agent that acts as an ionophore, completely dissipating the proton gradient and disrupting the mitochondrial membrane potential to leave the electron transport system uninhibited, and therefore oxygen is maximally consumed by complex IV.

Finally, mitochondrial respiration is then shut down with an injection of rotenone (complex I inhibitor) combined with antimycin A (complex III inhibitor), allowing non-mitochondrial respiration to be assessed. The Seahorse extracellular flux (XF) analyser is able to measure cellular oxygen consumption rates (OCR) and extracellular acidification rates (ECAR) simultaneously in real-time, generating a detailed picture of mitochondrial respiration and glycolysis. The outputs from the Seahorse analyser consist of several measurements of cellular bioenergetics, including maximum respiration, spare respiratory capacity, ATP production, proton leak, and glycolysis. From the OCR readings of ATP production, maximal respiration, and non-mitochondrial respiration induced by the addition of these drugs plus the basal respiration readings, the proton leak and spare respiratory capacity can be calculated. Furthermore, lactate production can be measured by the extracellular acidification rate (ECAR), which is essentially a measurement of pH this is predominately a result of the excretion of lactic acid per unit time after its conversion from pyruvate. The Seahorse XF assay allows for a comprehensive assessment of cellular metabolism by

determination of both aerobic glycolysis/oxidative phosphorylation and anaerobic glycolysis by determination of the OCR and ECAR, respectively.

Table 2.3.1 How each parameter of respiration is calculated.

Parameter	Equation
Baseline	(Last rate measurement before first injection) – (Non-Mitochondrial Respiration Rate)
Acute response	(Last rate measurement before second injection) – (Non-Mitochondrial Respiration Rate)
ATP Production	(Last rate measurement before Oligomycin injection) – (Minimum rate measurement after Oligomycin injection)
Max respiration	(Maximum rate measurement after FCCP injection) – (Non-Mitochondrial Respiration)
Spare Respiratory Capacity	(Maximal Respiration) – (Basal Respiration)
Non-mitochondrial respiration	Minimum rate measurement after Rotenone/antimycin A injection
Proton leak	(Minimum rate measurement after Oligomycin injection) – (Non-Mitochondrial Respiration)
Estimated glycolysis	Last rate measurement ECAR after sera injection
Coupling efficiency	(ATP Production Rate) / (Basal Respiration Rate) × 100

2.3.2 Assay procedure

The plate was prepared with cell-tak (cat no.354240, Corning, USA) in the cell culture hood in advance of the day of the seahorse run (these can be prepared up to one week in advance of the run and can be stored at 4°C, but the plate must be warmed to room temperature prior to seeding). Cell-tak is an extracellular matrix protein preparation that is non-immunogenic and is isolated from the *Mytilus edulis* marine mussel. Without touching the sides of the wells, 20µl per well of cell-tak solution (bicarbonate, sodium hydroxide, cell-tak) was added at a concentration of 22.4µg/ml to the whole Seahorse XF96 Cell Culture Microplate (Agilent, USA) and left to sit for one hour.

For one plate, the cell-tak solution recipe is as follows in Table 2.3.2:

Table 2.3.2 Cell-tak solution recipe for Seahorse XFe96 metabolism assay.

Reagent	**Volume**
Sodium Bicarbonate	1.872ml
Sodium hydroxide	16µl
Cell-tak	32µl

Then, the excess cell-tak solution was flushed out with 100µl per well of sterile distilled water and the plate was left to dry under the hood. In advance of the run day it is also recommended to prepare the plate map and assay design for the Agilent Seahorse XFe96 Analyzer (Agilent, USA) to read using the *Agilent Wave Software* version 2.4.

The day before the run, the calibration plate with sensor cartridges (Agilent, USA) was hydrated with 250µl per well Seahorse XF96 Calibrant pH7.4 (Agilent, USA), and left to soak overnight in a 37^{o}C non-CO_2 incubator. The assay medium can also be made up the day before the run, and was done so by dissolving one vial of powdered RPMI-1640 Medium (modified, with L-glutamine, without phenol red and sodium bicarbonate) (cat no. R8755-1L, Sigma) in 1 litre of sterile distilled water, which was then decanted into 45ml aliquots in 50ml Falcon tubes (Corning, USA) and frozen at -20°C until required.

On the day of the run, one tube of assay medium was defrosted and warmed in a 37^{o}C incubator. Once warmed, the pH was checked on both a calibrated pH meter (pHenomenal® pH 1100L, VWR Collection USA) and pH strip (cat no.P4536, Sigma Aldrich, USA); concentrated hydrochloric acid or sodium hydroxide can be added if required to bring the medium pH to exactly 7.4.

The cells were pelleted and re-suspended in assay media, then 100µl of cells were added to each of the cell-tak coated wells (apart from the four outer corner wells which served as blanks) at a concentration of approximately 300,000 cells per well. To the four outer corner wells (A1, A12, H1 and H12) 100µl assay media was added instead. Once the cells were added, the plate was transferred to a 37^{o}C non-CO_2 incubator and left for 30 minutes for the cells to settle.

In the meantime, the drugs were prepared and loaded into the injection ports on the sensor cartridge using the plate grid. For the four blanks, assay buffer was added to the injection ports. The concentration of mitochondrial poisons were 1µM oligomycin, 1.5µM fluoro-carbonyl cyanide phenylhydrazone (FCCP), and a combination 100nM rotenone with 1µM antimycin A, this was due to published literature on the optimisation by the Erika Pearse laboratory (van der Windt *et al*, 2016).

The injection strategy was programmed as follows:

Measurement	**Cycles**	**Mix time (mins)**	**Wait time (mins)**	**Measure time (mins)**
Baseline	3	01:00	02:00	04:00
Stimulation	4	01:00	10:00	04:00
Oligomycin	3	01:00	02:00	04:00
FCCP	3	01:00	02:00	04:00
Rotenone/ Antimycin A	3	01:00	02:00	04:00

On the computer the assay should be set up using the assay design created in the *Agilent Wave Software* by uploading the file from a pen drive, which instructs the Agilent Seahorse XFe96 Analyzer. The calibration plate with sensor cartridge for injections was loaded into the Agilent Seahorse XFe96 Analyzer and calibrated (this takes approximately 30 minutes).

Meanwhile, an additional 80µl of warm assay medium was slowly added to the sides of each well of the plate with the cells to bring the total volume to 180µl, and then the plate was returned to the incubator as the machine calibrated. Once the calibration is complete, the plate was ejected (without the sensor cartridge with injections) and the cell culture plate was loaded into the machine. At the end of the run the plate and sensor cartridge were ejected. The *Wave* file of the results was saved to a pen drive, and a lid was placed on the cell culture plate and it was stored in the -20^{o}C freezer for the protein assay. The calibration plate, sensor cartridge, and injection plate grid were all disposed of.

This process was optimised for the cell types used in these experiments.

Quality control

The Seahorse machine is maintained by the laboratory of Professor Federica Marelli-Berg, who perform calibration and quality control checks monthly. The Seahorse machine will also perform an internal quality control check with the calibration plate of each experiment. Lastly, unstimulated controls were run on each plate and compared across plates.

2.3.3 Pierce BCA analysis

Total protein can be quantified using colorimetric detection of the reduction of Cu^{2+} to Cu^{+} by protein. BCA (bicinchoninic acid) can detect this Cu^{+} cuprous cation by a 2:1 chelation of BCA: cuprous cation which results in a purple colouration that exhibits a strong absorbance at 562nm. This strong 562nm absorbance allows for a protein detection range of 20-2000µg/ml, as the absorbance from the colour change of green to purple is nearly linear with increasing protein concentrations.

In order to normalise the Seahorse data, protein analysis using the Pierce BCA Protein Assay Kit (cat no. 23225, Thermo Fisher Scientific) was carried out on the cells frozen in the plate.

First, the plate that was stored in the -20^{o}C freezer was placed on ice to thaw. 100µl of RIPA buffer (25mM Tris pH 8.0, 150mM NaCl, 0.1% SDS, 0.5% sodium deoxycholate, 1% Triton X-100) with protease inhibitor cocktail (cat no. P8340, Sigma) was added into each well, pipetted up and down, and left to incubate on ice for 30 minutes. The Working Reagent is made up by mixing 50 parts of BCA Reagent A with 1 part of BCA Reagent B (50:1, Reagent A:B). 100µl of Working Reagent was added to each sample, therefore for 100 wells 200µl of BCA Reagent B was added to 10ml of BCA Reagent A. When mixed, the Working Reagent should appear clear green, and when added to the samples it should turn purple after incubation.

While waiting on the RIPA buffer incubation, some samples of a few wells can be taken to test the intensity of the resultant purple colour before performing the assay on the whole plate; in this case samples of 5µl, 10µl and 20µl were taken to determine the volume of the wells to use. It is important that the protein concentration is not so large as to push the well readouts over the maximum the plate reader can record, but not so low that the samples will readout close to the blank values.

The determined volume of sample was transferred into a clean microplate and 100µl of Working Solution was added to each sample. The plate was left to incubate at 37^{o}C for 30 minutes, before being read at 562nm on a plate reader (Tecan Infinite M200 Pro). The samples were normalised to the well with the highest absorbance, which was taken as 1.

2.4 Isolation of total RNA from whole blood and conversion to cDNA

2.4.1 Total RNA extraction and quantification

In groups of 12, the total RNA of each PAXGene whole blood tube was extracted using a PAXGene Blood RNA Kit (Qiagen, Germany). Wash buffer BR4 is supplied as a concentrate, and so when starting a new kit four volumes of ethanol (96–100%, purity grade p.a.) was added to BR4 get a working solution. As well as this, when a kit is first opened the DNAse I stock solution was prepared by dissolving the solid DNase I (1500 Kunitz units) in 550µl of the DNase resuspension buffer (DRB) and aliquoted into 130µl volumes, which can be stored at -20^{o}C to prevent multiple freeze-thaw cycles.

PAXGene Blood RNA Tubes were centrifuged at 5000g for 10 minutes and the supernatant was decanted by pouring and gentle tapping onto a clean paper towel. 4ml of RNAse-free water was added to each pellet and the tube closed with a fresh BD Hemogard closure, then the pellets were vortexed until visibly dissolved. The tubes were centrifuged again at 5000g for 10 minutes, and the entire supernatant was discarded. 350µl of resuspension buffer BR1 was added to each pellet and vortexed until the pellets were visibly dissolved, then each sample was transferred to a labelled 1.5ml microcentrifuge tube.

To each Eppendorf tube, 300µl of binding buffer BR2 and then 40µl of proteinase K was added and mixed by a 5 second vortex. Samples were immediately incubated at 55^{o}C for 10 minutes in a pre-heated shaker-incubator set to 1200rcf. Pipettes and the benchtop were treated with RNase to prevent contamination. The lysate of each tube was transferred to a PAXGene Shredder Spin Column placed in a 2ml processing tube and centrifuged at maximum speed for 3 minutes. Without disturbing the pellets in each of the processing tubes, the entire supernatant of each of the flow-through fractions were transferred to fresh 1.5ml

microcentrifuge tubes. Into each tube 350µl of ethanol (96–100%, purity grade p.a.) was added and mixed by vortex, then centrifuged for 1-2 seconds at 500g to remove drops from inside the lid.

700µl of each sample was transferred to its own PAXGene RNA Spin Column in a 2ml processing tube and centrifuged at max speed for one minute. Then the processing tube containing the flow-through was discarded and the spin column was placed in a new 2ml processing tube, then the remaining sample was pipetted into the corresponding spin column and centrifuged at max speed for one minute. The processing tube containing flow-through was then discarded and the spin column placed into a new 2ml processing tube.

Into each spin column, 350µ of wash buffer 1 (BR3) was added and then the columns were centrifuged at max speed for one minute. The processing tube containing flow-through was then discarded and the spin column placed into a new 2ml processing tube. The DNase I incubation mix was prepared by adding 10µl of a gently thawed DNase I stock solution aliquot to 70µl DNA digestion buffer (RDD) for each sample (i.e., for 12 samples plus 1 for pipetting error is 130µl DNase I stock solution with 910µl Buffer RDD) in a 1.5ml Eppendorf tube and mixed by gently flicking. A vortex was not carried out due to its sensitivity to physical denaturation. Into each spin column 80µl of DNase I incubation mix was carefully added directly onto the column membrane and the columns were left for 15 minute at benchtop room temperature.

Into each spin column, 350µl of wash buffer 1 (BR3) was added and the columns were centrifuged at max speed for one minute. The processing tube containing flow-through was then discarded and the spin column placed into a new 2ml processing tube. Into each spin column, 500µl of wash buffer 2 (BR4) was added and the columns were centrifuged at max

speed for one minute. The processing tube containing flow-through was then discarded and the spin column placed into a new 2ml processing tube. Again, into each spin column 500µl of wash buffer 2 (BR4) was added and the columns were centrifuged at max speed for three minutes. The processing tube containing flow-through was then discarded and the spin column placed into a new 2ml processing tube, then the columns were spun again at max speed for one minute to ensure all remaining wash buffer had been eliminated. The processing tube containing flow-through was then discarded and the spin column placed into a new 2ml processing tube.

The spin columns were then placed into labelled 1.5ml microcentrifuge tubes and directly onto each membrane 40µl of buffer BR5 was pipetted on (wetting the whole membrane) and centrifuged at max speed for one minute to elute the RNA. The spin column was then transferred to a new microcentrifuge tube and the elution repeated so that each sample has two microcentrifuge tubes of RNA. The microcentrifuge tubes were then incubated at 65^{o}C for 5 minutes without shaking to denature the RNA, and then chilled immediately on ice.

The purity and concentration of each RNA sample was then measured on a Thermo Nanodrop 2000 (Thermofisher Scientific, USA) with elution buffer BR5 acting as the blank, and samples were stored in the -80^{o}C freezer until required.

2.4.2 DNA and RNA quality control and quantification

The Nanodrop is an instrument that is able to both ascertain an accurate concentration (ng/µl) of a sample of RNA or DNA, and indicate an approximation of the sample purity. The instrument measures the absorbance of UV visible light transmitted through the sample via spectrophotometry by holding a small volume (1-2µl) of the sample between two optical pedestals through surface tension. The instrument measures absorptions at wavelengths

230nm, 260nm and 280nm, from which the sample purity can be deduced, as well as measuring the concentration (ng/µl) of a sample.
Prior to each use, the eight sample pedestals on the Nanodrop 2000 (Thermo Fisher Scienific, USA) were cleaned thoroughly, first with a swab of 70% ethanol, then with a swab of nuclease-free water. The machine was then calibrated with a 1µl drop of nuclease-free water onto each sample pedestal. Next, the machine was 'blanked' with a 1µl drop of the elution solution the DNA or RNA was suspended in; this was nuclease-free water for the DNA extracted in the chromatin immunoprecipitation experiments, or elution buffer 'BR5' (Qiagen, Germany) for the RNA extracted for the qPCR experiments. Then, the sample type was selected (for example, dsDNA) and 1µl of each sample was loaded onto the pedestals and read. The concentration (ng/µl) and purity (260/280 and 260/230 ratios) were noted for each sample. Between each sample, the pedestals were cleaned and re-blanked. After the last samples were read the Nanodrop was cleaned once more, and the samples were immediately transferred to the -80°C freezer for storage.

One problem with the Nanodrop is that it assumes the samples are not degraded, therefore accuracy depends heavily on sample quality. It should be noted that higher dilutions of samples result in less precision and accuracy of the Nanodrop, and every time a sample is thawed the RNA will degrade a bit more.

2.4.3 Reverse transcription of RNA into cDNA

Strip 250µl PCR tubes for each RNA sample were placed on a cooled holder block that had been in the -20^{o}C freezer. The volume required for 200ng RNA from each sample was calculated prior to starting and these volumes were pipetted into the corresponding 250µl

PCR tubes. Then, nuclease-free water was added where needed to make the total volume in each tube 10µl. Reagents from the Applied Biosystems *High Capacity cDNA Reverse Transcription Kit* were thawed on ice and the volume required was calculated. 2X Reverse Transcription Mastermix was made up as follows in Table 2.4.1:

Table 2.4.1 Recipe for Reverse Transcription Mastermix

Solution	**1X reaction**
10X RT buffer	2.0µl
25X dNTP Mix (100mM)	0.8µl
Nuclease-free water	4.2µl
Random primers	2.0µl
Reverse Transcription Enzyme- MultiScribe™ Reverse Transcriptase	1.0µl

The MultiScribe™ Reverse Transcriptase was carefully added last to the mixture, as it is very sensitive to heat and physical denaturation. The Mastermix was mixed gently by pipette and kept on ice. 10µl of Mastermix was pipetted into each sample tube to bring the total reaction volume to 20µl and again gently mixed.

Caps were placed on the tubes to seal them and the tubes were briefly centrifuged to spin down the contents and ensure there are no air bubbles, and then the tubes were placed back on the cooled holder block until all samples were prepared for the reverse transcription.

The thermocycler was programmed with the conditions as follows in Table 2.4.2:

Table 2.4.2 Thermocycler programming for RT-PCR

	Step 1	**Step 2**	**Step 3**	**Step 4**
Temperature (^{o}C)	25	37	85	4
Time (minutes)	10	120	5	(Hold)

The reaction volume was set to 20µl and the thermocycler was loaded with the samples and run. The cDNA created was then stored in the -20°C freezer until required.

2.5 Quantitative Real Time Polymerase Chain Reaction

2.5.1 Theory

In order to investigate gene expression, the Quantitative Real Time Polymerase Chain Reaction method, also known as “RT-PCR” or “qPCR”, was carried out. This methodology allows the number of copies of DNA or cDNA to be determined in real time as that PCR product is amplified.

The DNA is amplified in wells containing a thermostable DNA polymerase, deoxyribonucleotides, a pair of specific primers all in a suitable buffer solution, which will all undergo temperature cycling in a thermocycler. To any single strand of DNA with a double stranded starting point, the DNA polymerase will synthesise a complementary sequence of bases. To instruct the DNA polymerase to amplify a specific gene of interest, primers can be added, which are small DNA pieces that are complimentary to said gene of interest. The temperature is first raised to 95°C in order to separate the double-stranded DNA into single strands. Then, the temperature is lowered to 60°C to allow the primers to bind to the desired genes, which in turn provides the DNA polymerase somewhere to bind to begin DNA replication and will result in the doubling of the amount of product. The amplification of DNA is linked to generation of fluorescence with is detected by the qPCR machine, and as the cycling of these temperature alterations occurs, the amount of product and therefore fluorescence doubles with each cycle. Typically, a qPCR will run 40 cycles, resulting in an exponential increase in fluorescence (and product), which will begin to plateau in the last cycles as the reactants run out.

There are different ways to generate fluorescence for the qPCR machine to detect. The most common intercalating dye that can be used is SYBR® Green (Thermo Fisher Scientific, USA),

which is a fluorescent dye that binds with double stranded DNA, altering the dye structure and causing it to fluoresce more. Alternatively, hydrolysis probes such as Taqman® (Thermo Fisher Scientific, USA) use fluorescently labelled DNA oligonucleotides that bind downstream of one of the primers. These probes contain a fluorescent reporter molecule bound to the 5' end with a quencher molecule on the 3' end which will stifle the fluorescence of the reporter. As the probe binds downstream of the primer it gets cleaved by the DNA polymerase during the reaction, resulting in the separation of reporter and quencher and therefore the fluorescence increases, with increasing fluorescence generated through each cycle as more probes are cleaved.

2.5.2 Optimisation

For researchers wishing to determine the amount of a target gene or target sequence in a sample, qPCR is a simple and effective methodology. However, there are some critical factors that have to be evaluated in order to ensure correct set up of the RT-PCR reaction(s).

In general, RT-PCR performance can be evaluated in four ways; efficiency, precision, R^2 and sensitivity (Life Technologies, 2013). Firstly, PCR primer-probe amplification efficiency must be evaluated as this can affect the Ct. Every primer-probe must be evaluated by drawing a standard curve for serial dilutions of several samples plotting all three repeats, and the efficiency will equal 100% (amplification factor of 2) if the slope of the standard curve equals -3.322. As an example, Figure 2.5.1 is the collection of graphs drawn to assess the efficiency of the housekeeping gene UBC (ubiquitin C); to calculate efficiency (E) the following equation is applied:

$$E = (10(-1/\text{slope}) - 1) \times 100$$

The efficiencies for each sample are then averaged, and an efficiency of 90-100% is generally seen as acceptable for the Livak method of relative quantification (Livak & Schmittgen, 2001)- if efficiencies are not close to 100% or if they vary between primer-probes then alternative methods such as Pfaffl (standard curve) can be utilised that take these varied efficiencies into account (Pfaffl, 2001). In this thesis, all Taqman primer-probes had efficiencies between 95-110% so the Livak method was adopted.

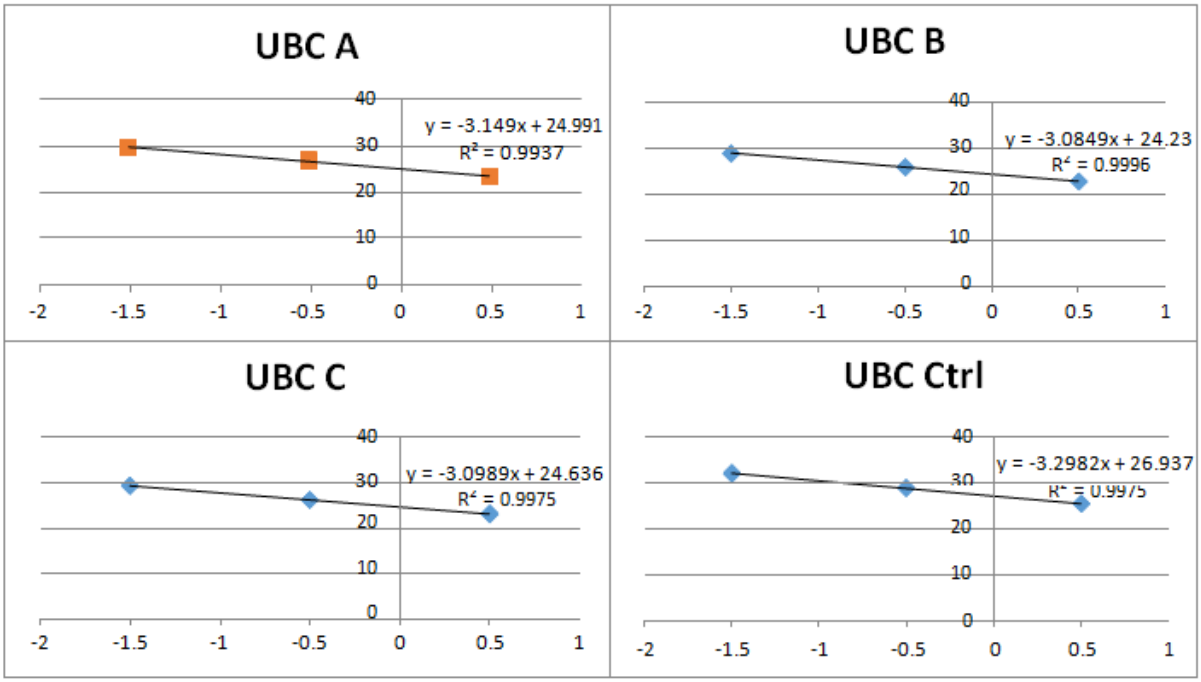

Figure 2.5.1 Collation of four graphs for evaluation of Taqman ubiquitin C (UBC) primer-probe; patient samples A, B, C and Control at serial dilutions of log 3.08, 0.308 and 0.0308 ng cDNA.

Another factor that must be considered at this stage is the R^2 values; these are statistical calculations that, in simple terms, reveal how accurate one value is at predicting another. A value of 1 is ideal, where the Ct value can be used to accurately predict the concentration of DNA, whereas a value of 0 indicates it cannot be predicted (Livak & Schmittgen, 2001). All of the primer-probes utilised in this investigation had a good confidence (R^2>0.99).

It is also important to note that triplicates should be very close in value as can be seen above, and care must be taken to check triplicates for each Ct and eliminate any outliers when calculating the mean. A common measure of precision is the standard deviation between triplicates; any value over 2 standard deviations from the mean was excluded. Consideration of qPCR sensitivity should also be taken into account, and a series of DNA dilutions must be performed in order to determine an appropriate concentration for use in qPCR, and if you have a low copy number for a gene then sample accuracy can be improved by increasing the amount of repeats. Following on from this, RT-qPCR assumes the same concentration of cDNA in each sample and that the quality is adequate (Huggett, Dheda, Bustin, & Zumla, 2005), therefore all DNA or RNA for cDNA reverse transcription must be quantified and quality checked. Human error can be minimised by use of a well calibrated pipette, which extends to pipetting of the PCR plate as use of electric pipettes or PCR pipetting robots are recommended particularly with large sample sizes.

For Livak method Relative Quantification to be applied correctly it is vital to optimise one or more housekeeping (reference) genes in order to normalise the target gene expression. Housekeeping genes must be expressed consistently through all samples across all conditions, therefore housekeepers are often chosen from ubiquitously expressed genes. A panel of 8 housekeeping genes were tested for gene expression experiments for enzymes involved in histone modification: GAPDH, 18S, ACTB, ATP5B, B2M, HPRT, SDHA and UBC. Literature analysis excluded GAPDH as it was found to be inappropriate for use with septic patients as its expression has been reported to rise in response to inflammation and oxidative stress (Cummings, Sarveswaran, Homer-Vanniasinkam, Burke, & Orsi, 2014). A selection of 12 patients- three patients out of each of the four conditions (Sample A, Sample B, Sample C and Healthy Control)- were run with each of the 7 remaining housekeeping genes to provide an

accurate representation of all samples expression levels and from this the stability of the reference genes were analysed using the geNorm VBA applet (Vandesompele et al., 2002). (Figure 2.5.2).

Average stability of remaining reference targets:

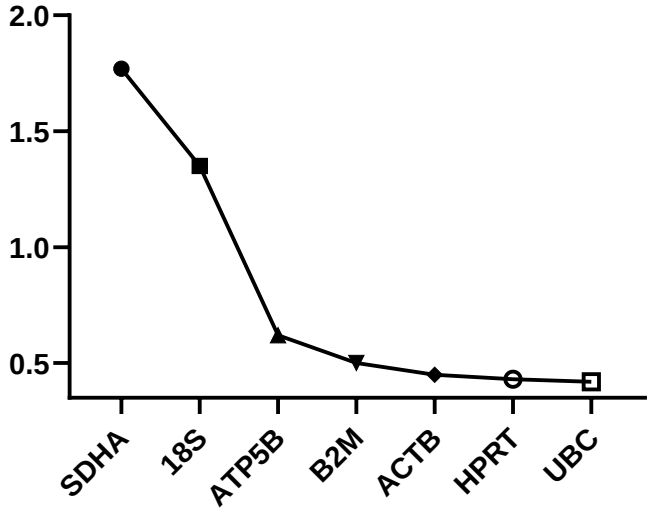

Figure 2.5.2 The average expression stability (M) values of the seven reference genes evaluated by geNorm

The Y axis displays the average expression stability which is determined as the average pairwise variation between a candidate gene and all other control genes, the lower the number the more stable the gene is. Genes are ranked in order of stability, with most stable to the right of the X axis.

The number of reference genes to be used is also a consideration, as more may improve the accuracy of the data but would incur practical difficulties. Therefore, geNorm was used to analyse the statistical difference between using different numbers of reference genes.

Values under geNorm V=0.15 fall under the recommended stability threshold and have no significant change in the normalisation factor with the addition of further reference genes to the experiment, therefore the two most stable housekeeping genes (ubiquitin C “UBC” and hypoxanthine guanine phosphoribosyltransferase “HPRT”) were selected for the enzyme gene expression study.

Finally, the choice between Taqman or SYBR Green can influence qPCR results (Thermofisher Scientific, 2013). The use of Taqman primer-probes does not require post-PCR processing and highly specific hybridisation between probe and target is required to generate fluorescent signal, making it better for genes with low expression. SYBR Green does not have a probe and is significantly cheaper, however it may provide false positive signals by binding to non-specific dsDNA, therefore it is critical to have well designed primers and a melt curve analysis must be carried out for each plate.

2.5.3 Procedure

For a volume of 20µl per well, two separate tubes of 10µl per well of either DNA solution or Primer solution was made up in order to decrease pipetting error (Table 2.5.1). Experimental chapters contain details of their respective Mastermix and primers used in each experiment. All reactions were performed either in triplicate or duplicate.

Table 2.5.3 Recipes for the DNA and Primer solutions for a 20µl volume well.

DNA solution	Volume per well
DNA	1µl
Mastermix	5µl
Water	4µl
Total volume per well= 20µl	

Primer solution	Volume per well
Primer (5µM)	1µl
Mastermix	5µl
Water	4µl

Using an electronic pipette, 10µl per well of DNA solution was added to appropriate wells of a 96 well PCR optical reaction plate. Then, pipetting onto the opposite wall of the well so as not to contaminate samples, 10µl per well of Primer solution was added. An optical adhesive cover was stuck onto the plate and then the plate was briefly centrifuged to ensure no solution remained on the sides of the wells.

The plate was put into a Step One Plus Real-Time PCR machine (Thermo Fisher Scientific, USA) running Step One Software v2.3, and the plate plan was drawn up for the run to instruct the machine. The initial denaturation step was programmed as 95°C for 10 minutes. Then, 40 cycles of temperature alternating occurred, each cycle consisting of two steps; first 15 seconds at 95°C, then 60 seconds at 60°C. At the end of the second step of each cycle, the fluorescence was read and recorded. In experiments where SYBR Green primers were used instead of Taqman, a melt curve was then performed for the plate.

Quality control

Amplification plots should be checked to ensure the sigmoidal curve is the same for all samples. A melt curve analysis must be carried out for each plate to detect any false positive signals from SYBR Green primers binding to non-specific dsDNA. Replicates of the same sample should be run on each plate to assess inter-plate reliability. A further quality control

assessment which was not used here would be a no-template control to assess contamination.

2.5.4 Results interpretation

Raw data from qRT-PCR can be analysed in two main ways: the methods of absolute quantification and of relative quantification (Livak & Schmittgen, 2001). Research conducted in this thesis utilised the relative quantification Livak method (Delta-Delta Ct) in order to determine gene expression of cytokines and enzymes involved in histone modifications.

2.6 Chromatin Immunoprecipitation

2.6.1 Theory

Chromatin Immunoprecipitation, often abbreviated to "ChIP", can be performed to determine the localisation of proteins bound to a specific DNA sequence/ gene locus, and these specific protein-DNA interactions can be quantified by Quantitative Polymerase Chain Reaction (qPCR). The specific genomic locations that various histone modifications are associated with can be determined by ChIP, which can also indicate targets for histone modifiers. ChIP is a complex technique that employs several molecular biology and proteomics methods; briefly, the steps of ChIP are crosslinking cells (except in Native ChIP), shearing of cells and chromatin into ~500bp fragments, immunoprecipitation of DNA fragments associated with the proteins of interest, then purification of the DNA and quantification of enrichment of these DNA sequences. For each sample ChIP will generate factions of immunoprecipitated DNA (the DNA which were bound to histones that had the modification of interest), which can be compared to the input faction (a sample of all the DNA taken just before the immunoprecipitation), and finally a control faction such as IgG which should not yield DNA.

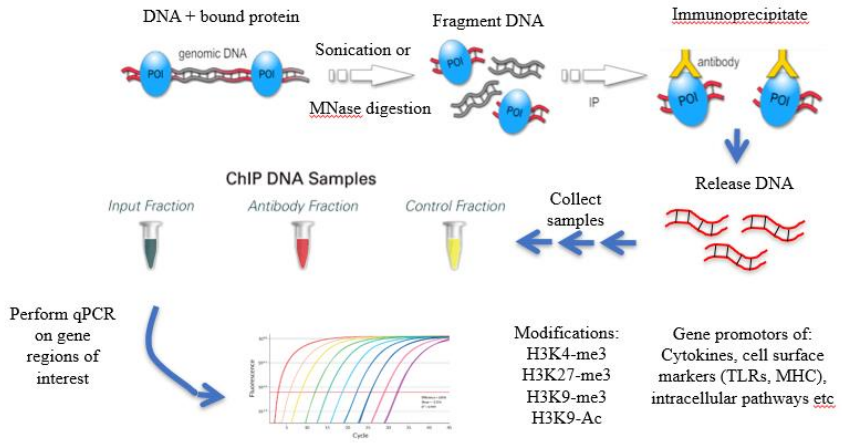

Figure 2.6.1 Workflow of Chromatin Immunoprecipitation

ChIP is technically demanding and several steps require optimisation in order to work, such as cell number, cell lysis, cross-linking, chromatin shearing, amount of chromatin to use per immunoprecipitation, antibody binding for the immunoprecipitation, the means to precipitate the chromatin-antibody complex (e.g., protein A/G or magnetic beads), DNA purification and optimisation of specialised buffers. The change of one of these factors will affect the rest of the processes in the assay, which may then need to be adapted, adding to the technical challenges of ChIP.

For histone modifications, there are two kinds of ChIP; N-ChIP and X-ChIP. N-ChIP (Native ChIP) does not require cross-linking and the chromatin is sheared by micrococcal nuclease digestion, whereas in X-ChIP (Cross-Linked ChIP) the cells are cross-linked and the chromatin sheared by sonication. The choice between the two types of ChIP depends on starting material and experimental aims. When studying histone modifications N-ChIP or X-ChIP can both be suitable, the better option depending on methodology optimisation. Both N-ChIP and X-ChIP were explored during optimisation for peripheral blood mononuclear cells (PBMCs), and ultimately the methodology chosen and described in this chapter is X-ChIP of Active Motif ChIP-IT PBMC kit (cat no 53042). The Chromatin Immunoprecipitation methodology and optimisation is explored in-depth in *Chapter 3: Sepsis-induced histone modifications of peripheral blood mononuclear cells* in this thesis.

2.6.2 Chromatin extraction

Before commencing the experiment, 5ml fixation solution per 10 million PBMC sample was prepared fresh by adding 500µl 10x PBS (supplied with kit) to 4.36ml sterile water, then under a fume hood 140µl of 37% formaldehyde solution (with 10-15% methyl alcohol to prevent

polymerisation) (cat no.252549, Sigma Aldrich, USA) was added. The solution was then vortexed to mix. 10ml of PBS Wash Buffer per sample was also prepared prior to starting each experiment by adding 8.5ml sterile water, 1ml 10x PBS, 500µl detergent (supplied with kit), and finally 20µl 100mM PMSF, then mixed by inverting and chilled on ice. PBMCs are notoriously difficult to lyse, typically yielding only 30-50% of what a cell line would, and therefore a minimum of 10 million cells should be used per sample to prepare chromatin.

Flash-frozen pellets of at least 10 million cells in 15ml conical tubes were prepared from the samples; the cells were thawed and transferred to the conical tubes where they were spun down to pellet (1200g, 10 minutes). Then, the supernatants were discarded and the cells immersed in dry ice for 10 minutes. To each cell pellet, 5ml fresh fixation solution was added and the cells were gently resuspended. The samples were incubated for 15 minutes on a room temperature roller, then 250µl Stop Solution (provided with kit; EDTA solution) was added to stop the reaction and samples returned to the roller for a further 5 minutes.

Then, 250µl detergent was added to each sample, mixed by inversion, and the cells were pelleted by centrifugation at 1250g for 5 minutes at 4°C. From now on the samples were kept on ice. After the spin if there were cells floating or stuck to the walls of the conical tubes, they were scraped with a metal spatula back into the solution and the spin was repeated until all the cells were pelleted. The supernatants were discarded, then for each sample the cells were resuspended in 5ml of ice-cold PBS Wash Buffer and centrifuged at 3200g for 5 minutes at 4°C. The supernatant was carefully discarded, then each pellet was washed a second time with another 5ml ice-cold PBS Wash Buffer and pelleted again. The supernatant was carefully discarded, then the pellets were flash frozen in dry ice and incubated for 10 minutes to facilitate cell lysis. At this stage samples can be stored at -80°C if required.

Each flash-frozen pellet was resuspended in 5ml ice-cold Swelling Buffer (provided with kit) supplemented with 5µl 100mM PMSF and 5µl Protein Inhibitor Cocktail (PIC) and incubated on ice for 30 minutes. Then cells were then lysed by adding 125µl Detergent (provided with kit) and vortexed on the highest setting for 30 seconds. Samples were then centrifuged at 3200g for 10 minutes at 4°C, and the supernatants discarded. Each pellet was then resuspended in 500µl ChIP buffer (supplied with kit) supplemented with 5µl 100mM PMSF and 5µl PIC, and then transferred to a 2ml microcentrifuge tube and incubated on ice for 10 minutes.

2.6.3 Sonication of chromatin

The 2ml microcentrifuge tube was held suspended in a small beaker containing ice and water to ensure the tube would remain ice-cold during sonication. The sonicator tip was submerged in the sample and kept ~5mm from the tube bottom, without touching the sides of the tube. Sonication time was optimised as 4 rounds of 10 minutes sonication, 30 seconds on the 30 seconds off, with a five minute cooling period between each round. The optimisation procedure is described in *Chapter 5: Chromatin Immunoprecipitation Optimisation* in this thesis.

The samples were then spun at maximum speed for 5 minutes at 4°C to pellet the cellular debris and the supernatant (chromatin) was transferred to a fresh microcentrifuge tube. 10µl of the chromatin was checked under the microscope to ensure cell lysis. 25ul of the chromatin of each sample was transferred to a 250µl PCR tube which will become the Input DNA and be used for chromatin quantification and analysis of shearing efficiency. The rest of the chromatin was flash frozen by dry ice immersion for 10 minutes then transferred to the -80°C freezer for storage.

2.6.4 Input preparation

The input was prepared as follows. 175µl of pH 8.0 TE buffer was added to each 25µl chromatin preparation, then 20µg RNAse A was added and the PCR tube capped and vortexed to mix. The sample was incubated in a thermocycler for 1 hour at 37°C. Then, 50µg Proteinase K was added to the tube, the sample was vortexed, then incubated for a further 3 hours at 37°C in the thermocycler. To reverse the crosslinks, 10µl 5M NaCl was added to the tube, vortexed, then incubated at 65°C overnight (but not to exceed 16 hours).

The next day, the input was removed from the thermocycler and a phenol-chloroform DNA extraction was carried out. 250µl phenol chloroform:isoamyl alcohol (24:1) was added to the sample and vigorously vortexed at max speed. The sample was then spun at maximum speed for 15 minutes at room temperature, and the resultant upper phase aqueous layer was carefully transferred to a fresh 1.5ml microcentrifuge tube. To this, 83µl Precipitation Buffer (supplied with kit) was added, followed by 2µl Carrier (supplied with kit), and finally topped up to 1.5ml with ice-cold 100% ethanol. The tube was vortexed, then transferred to the -80°C freezer for 2 hours (it can be left 30 minutes to overnight).

The tube was then spun at 4°C at maximum speed for 15 minutes, and the supernatant was carefully removed without disturbing the pellet. The pellet was then washed with 500µl of ice-cold 70% ethanol and spun at maximum speed for a further 5 minutes. The entire supernatant was removed carefully so as not to disturb the pellet, and the pellet was left to air dry uncapped for approximately 10-15 minutes.

10µl DNA Purification Elution Buffer (supplied with kit) was added onto the pellet once it had dried, then the tube was capped and incubated at room temperature for 10 minutes. Finally, the tube was vortexed to resuspend the pellet, and the input DNA has now been prepared.

The DNA concentration and purity of the input was then determined by being read on a Thermo NanoDrop 2000 (Thermo Fisher Scientific, USA), then 1000ng of DNA was set aside for a gel electrophoresis and the rest of the input stored at -20°C.

To prepare the chromatin sample for the agarose gel electrophoresis, the sample was transferred to a 250µl PCR tube and 2µl 500mM NaCl was added, then the final volume was topped up to 10µl with sterile water. The sample was heated at 100°C in the thermocycler for 20 minutes followed by ramping the temperature down to 50°C. The sample was then incubated at room temperature for 5 minutes, and electrophoresis was carried out as described in *Chapter 2: Methods 2.8 Agarose gel electrophoresis* of the thesis. DNA ladders of 100bp and 1kb were used to analyse chromatin size. Analysis of chromatin shearing is described in *Chapter 5: Chromatin Immunoprecipitation Optimisation* in this thesis.

2.6.5 Immunoprecipitation

From the input DNA quantification the amount of DNA set aside for the immunoprecipitations can be calculated. The sonicated chromatin sample was thawed on ice and spun at 4°C at maximum speed for 2 minutes. From the amount of DNA yielded, the volume of chromatin was calculated so that each immunoprecipitation would 10µg chromatin and divided into separate 1.5ml microcentrifuge tubes. Any leftover chromatin was processed as additional input. Each tube for the immunoprecipitation was topped up to 200µl with ChIP Buffer and 5µl of PIC was added.

In separate, fresh 1.5ml microcentrifuge tubes, the ChIP-grade antibodies were prepared. 4µg of antibody per immunoprecipitation was added to each tube, followed by 5µl of Blocker (supplied with kit), and left to incubate at room temperature for 1 minute. The antibodies used are as follows in Table 2.6.1:

Table 2.6.1 Antibodies used in ChIP immunoprecipitation

Antibody (Rabbit polyclonal)	**Manufacturer**	**Catalogue number**
H3K4-me3	Diagenode	C15410003
H3K27-me3	Diagenode	C15410195
H3K9-me3	Diagenode	C15410193
IgG	Merke Millipore	PP64

The antibodies were then added to their respective immunoprecipitation tube and incubated overnight at 4°C on an end-to-end rotator.

The next day, Protein G agarose beads (supplied with kit) were thoroughly resuspended by pipetting up and down, and into a fresh 1.5ml microcentrifuge tube 30µl of beads per immunoprecipitation were added using a pipette with 2mm cut off the end of the pipette tip (120µl for H3K4-me3, H3K27-me3, H3K9-me3 and IgG). To wash the beads, an equal volume of pH 8.0 TE buffer was added and mixed by inverting, then spun at 1200g for 1 minute. The supernatant was removed, and the wash was repeated once more. Then, the equivalent volume of TE buffer added was removed from the supernatant and the beads ready to use.

The immunoprecipitation reactions were briefly centrifuged at 1200g to collect liquid from inside the caps. To each immunoprecipitation reaction, 30µl of the washed Protein G agarose beads were added using a cut-tipped pipette, then the samples were incubated at 4°C on an end-to-end rotator for 3 hours.

The ChIP filtration columns supplied with the kit were labelled and the tabs at the bottom pulled off. An empty P1000 pipette tip box was used to hold the columns. The immunoprecipitation reactions were briefly spun again at 1200g to collect liquid from inside

the caps, then 600µl ChIP Buffer was added to each tube and the entire reaction was transferred to its respective filtration column (including the Protein G agarose beads). Flow-through was allowed to occur by gravity. The columns were washed five times by adding 900µl Wash Buffer AM1 (supplied with kit), letting them stand for 3 minutes, then repeating four more times. Residual Wash Buffer was then removed by transferring each column to a fresh 1.5ml microcentrifuge tube and centrifuging at 1200g for 3 minutes.

The ChIP filtration columns were then transferred to new 1.5ml microcentrifuge tubes, and directly onto each column membrane 50µl of 37°C Elution Buffer AM4 was added and left to incubate at benchtop for 5 minutes. The samples were spun at 1200g for 3 minutes at room temperature, then the elution was repeated with another 50µl of 37°C Elution Buffer AM4 was added to each column and left to incubate at benchtop for 5 minutes. The samples were spun again at 1200g for 3 minutes at room temperature, then the columns were discarded and the resultant 100µl DNA (flow-through) was de-crosslinked and purified.

2.6.6 Reversal of immunoprecipitate cross-links and DNA purification

Each eluted ChIP DNA was transferred to its own fresh 250µl PCR tube. 20µg of Proteinase K was added to each tube and vortexed, then the samples were transferred to a thermocycler and heated at 55°C for 30 minutes, then the temperature was increased to 80°C for 2 hours, to reverse the cross-links.

The DNA was then transferred into fresh 1.5ml microcentrifuge tubes and to each tube 500µl DNA Purification Binding Buffer was added and mixed by vortex. 5µl of 3M Sodium Acetate was then added to adjust the pH, with samples turning bright yellow to indicate the correct pH. The entirety of each pH-adjusted sample was then transferred to its own DNA Purification Column in a collection tube, and centrifuged cap closed at 14,000rcf for one minute. The flow-

through in the collection tubes were then discarded and the columns returned to the collection tubes.

DNA Purification Wash Buffer was prepared before the first use by the additional of ethanol as previously described. Into each column, 750µl DNA Purification Wash Buffer was added and capped, then the columns were spun at 14,000rcf for one minute. The flow-through in the collection tubes were then discarded and the columns returned to the collection tubes. Columns were then spun for another two minutes at 14,000rcf with the cap open to remove any residual wash buffer.

Each column was then transferred to its own fresh 1.5ml microcentrifuge tube. To the centre of each column membrane, 50µl of pre-warmed (37°C) DNA Purification Elution Buffer was added and incubated for one minute on benchtop. The columns were then spun at 14,000rcf for one minute to elute the DNA. This was then repeated a second time; to the centre of each column membrane, 50µl of pre-warmed (37°C) DNA Purification Elution Buffer was added and incubated for one minute on benchtop. The columns were then spun at 14,000rcf for one minute to elute the DNA. The total elution volume of the DNA was 100µl each, and the purified DNA was stored at -20°C to await downstream analysis.

Quality control

Fragmentation efficiency of the DNA after sonication or MNase digestion should be determined by running an Agarose gel. Targeted ChIP should also be performed on the positive and negative controls for the histones to check reliability.

2.7 Agarose gel electrophoresis

2.7.1 Theory

The approximate length of a DNA fragment can be determined by performing an agarose gel electrophoresis on the DNA sample(s) against a collection of DNA fragments of already determined lengths, known as a DNA ladder. DNA has the same charge per mass, allowing it to be separated by length using positive and negative electrodes. An electric field allows the negatively charged DNA fragments to migrate through the agarose matrix towards a positive electrode, with the shorter fragments moving faster than the longer fragments, thus separating the DNA samples into bands of their respective lengths which can then be determined by referring to the DNA ladder. The DNA samples and ladder are mixed with loading buffer prior to loading into the wells; the loading buffer usually contains a dye to monitor the progress of the DNA migration (as DNA is not visible in natural light) and a dense compound to increase the density of the sample so that it sinks to the bottom of the well.

The composition and ionic strength of the electrode buffer is responsible for the DNA mobility on the gel, the most common buffers are tris-acetate-EDTA buffer (TAE) and tris-borate-EDTA buffer (TBE) with the choice between the two depending on the samples. TAE is preferred for a higher resolution of supercoiled DNA, large DNA fragments (>2kb), and for isolating DNA to be used in downstream enzymatic processing (such as ligations) as the borate in TBE in an enzyme inhibitor. TBE is preferred for a higher resolution of smaller DNA fragments (<2kb) and for longer runs (as it is a better conductive medium).

The DNA can be viewed by staining the gel so that it will fluoresce under a UV light transilluminator, and the staining can occur either by adding the stain to the gel mixture before it sets or staining the set gel post-run. The traditional stain used was ethidium bromide,

however several alternatives have become commercially available, such as the SYBR family of stains which require a blue light transilluminator.

2.7.2 DNA length determination

The 2% agarose gel was prepared by mixing 3g of agarose powder with 150ml of 1x TBE buffer. The mixture was heated to near boiling point in a microwave until the agarose had completely melted and mixed with the TBE buffer. When the mixture had cooled sufficiently (enough that the flask it is in can be touched but before it begins to set), 4µl of SYBR Safe DNA Gel Stain (cat no. S33102, Invitrogen, USA) was added in and mixed. The agarose mixture was then poured into a cast with combs to create the loading wells, and was left on the benchtop to set.

Once the gel had set, the combs were removed to reveal the wells and the gel was placed in the electrophoresis apparatus, which was then topped up with more 1x TBE buffer to the max fill line to completely submerge the gel. The wells were flushed out with TBE buffer using a pipette to remove any air bubbles. The DNA ladder and DNA samples were topped up to 10µl with nuclease-free water and mixed with 2µl of loading buffer- Orange DNA Loading Dye (6X) (cat no. R0631, Thermo Fisher Scientific, USA) was chosen because it contains two different dyes, orange G and xylene cyanol FF, to allow for better visual tracking of the DNA migration. Using a pipette, the 12µl of each sample and DNA ladder were loaded into their own individual wells and the lid was placed on the apparatus, aligned so that they will migrate towards the positive electrode with the negative electrode positioned behind the wells. The gel was run at 160V, for approximately 20 minutes to separate the DNA fragments, then the electric field

was turned off. The DNA on the gel was visualised under a blue light transilluminator and fragment length determined by referring to the ladder.

2.8 Statistical analysis

All statistical analysis and graphs were created using GraphPad Prism software.

The Friedman Test is utilised where sample sizes are sufficiently powered to warrant statistical analysis. This test is used when measuring a continuous variable to determine if three or more matched groups are significantly different from each other. The test is non-parametric, and so does not assume a normal distribution. The matched groups are repeated measures from the same related sample, in this case the same septic patients who were measured at three different time points.

Some sample sizes within this body of work are too small to be able to perform statistical analysis. Doing a statistical analysis on a small n number will result in a higher chance of a type II error. A type II error is known as a 'false negative', where there is a failure to reject a null hypothesis that is false, whereas a type I error is known as a 'false positive' where there is a mistaken rejection of a true null hypothesis.

Two typical ways to minimise errors are to have a more stringent p value (reducing the probability of type I error) and increase sample size/ statistical power (reducing the probability of type II error). Although type I and type II errors are always minimised as much as possible in statistical testing, it cannot be completely eliminated without a known cause and effect. Statistical tests work on probability, and therefore there is never a certainty in

the conclusions, and any form of uncertainty results in the possibility of errors. Results must be interpreted with this in mind, particularly where statistical power is lacking in parts of this thesis.

Multiple comparisons in statistical testing can result in problems if not accounted for. The more comparisons are made, the higher the probability of a type I error. Multiple comparisons can be corrected by setting stricter thresholds for statistical significance, the caveat being that the stricter the threshold you set, the less power your experiment will have to detect true differences. Statistical post-hoc tests such as Bonferroni, Tukey, and Dunn use this approach to correct for multiple comparisons.

An important point to consider in research is the statistical power of the sample. The statistical power determines the probability of the hypothesis test correctly rejecting the null hypothesis. A low statistical power will result in invalid conclusions when interpreting the meaning of the results, and so often a minimum power of 0.8 will be implemented when designing an experiment (meaning the probability of a type II error is 20%). When performing an experiment, a minimum sample size will be required depending on the statistical power, significance level, and effect size, and this can be determined by a power analysis.

Chapter 3: Sepsis-induced histone modifications of peripheral blood mononuclear cells

3.1 Introduction

Patients who survive an acute septic illness go on to experience significant reductions in their long-term survival. This reduction in survival persists for at least 8 years after hospital discharge (Czaja *et al*. 2009), and the origins of this observed phenomenon are hotly sought. Recurrent infections account for a major proportion of this increased long-term morbidity (Mira *et al*. 2017), and accordingly hint at a fundamental reduction in immune function, or perhaps an increase in host susceptibility. In line with this, one theory is that epigenetic alterations induced by the acute episode, impart an acquired yet persistent, immunological defect. This immune deficit, being epigenetic, has the ability to persist far beyond resolution of the acute infection, and may begin to explain some of the observed effects.

This investigation builds upon the data outlined previously (see sections 1.2.6 and 1.2.8), which developed the hypothesis that the immune suppression following a septic insult/bacteraemia may be due to a transient release of certain circulating mediators which are no longer detectable 12 months later.

Myeloid and lymphoid-derived cells produce quantities of pro-inflammatory chemokines and cytokines in order to respond to an infection, in an endeavour to achieve an optimal bactericidal effect. It is feasible that, in order to confer a survival advantage to an infecting organism, epigenetic modifications of relevant genomic regions in host cells induced by an infection itself may encourage a pathogenically blunting process. Following on from this,

several investigations involving animal and *in vitro* models have sought to identify promising candidate genes involved in such histone modifications (Chan *et al*, 2005; El Gazzar *et al,* 2009; Lyn-Kew *et al*, 2010; Klose *et al,* 2007). Histone modifications are controlled by several enzymes, some of which have found to be associated with sepsis and infections in the literature.

The persistence of these epigenetic alterations over time is of particular importance, as they may account for the long-term excess mortality observed in septic patients. Wen *et al* (2008) found repressive methylation marks for up to 6 weeks following the original infection in murine dendritic cells. Currently, human data is needed to verify the translation of this.

Histone modifications have been demonstrated to underlie LPS-induced tolerance in monocytes. Foster et al (2007) investigated LPS-induced tolerance in monocytes and found a global reduction in the modification associated with gene activation; H3K4me3.

Furthermore, LPS-induced tolerance in macrophages resulted in an increase of the modification H3K9me2 that is associated with gene repression at the promotor regions of TNFα and IL-1β (Chan *et al*, 2005; El Gazzar *et al,* 2009).

Hypothesis: Severe infections induce long-term changes or modifications of histone modifications in host leukocytes which mediate both immediate and persistent immune suppression, thereby compromising the patient's ability to overcome the primary infection and also increasing the risk of acquiring further infections.

Aims:

1: To confirm the presence of functional immune compromise immediately following a blood stream infection (BSI), as defined by cells ability to produce cytokines when rechallenged *in vitro,* and to investigate whether this phenotype persists following clinical recovery from the acute infection.

2: To describe host gene expression patterns in key immune related and regulatory genes following a BSI

3: To describe the acquisition of histone modifications in host peripheral blood mononuclear cells following a BSI and their persistence following recovery from the acute infection.

3.2 Methods

3.2.1 Patient cohort

Methods are described in full in Chapter 2 of this thesis. Briefly, for gene expression studies the full patient cohort was used along with a healthy volunteer cohort as previously described. Patient blood was drawn at three different time points, <24 hours post positive blood culture, 4-7 days post positive blood culture, and finally 6-12 months post hospital discharge. Statistics are only performed on patient samples who have blood sampled at all three time points, at n=18; the reason for the incomplete data set are patients being lost to follow-up for a full set of samples (n=51) (one of more reasons of these listed: patient death (n=17), discharged before sample taken (n=16), declined sampling (n=3), lost contact (n=19)).

Pooled septic serum was created from serum samples from the patients who had *E.coli* sepsis in the full cohort. Only patients with a full set of samples were selected, resulting in n=14 patients. Healthy pooled serum was created from n=20 of the 37 healthy volunteers selected at random.

Few patient samples were used for Chromatin Immunoprecipitation and cytokine concentration studies. These were the final few patients recruited as this research began, and their PBMCs were handled and stored to keep the cells intact in FBS 10% DMSO, unlike most of the cohort which had cells frozen in PBS 2% FBS. A CONSORT diagram for their selection is included below.

CONSORT Flow Diagram- septic cohort

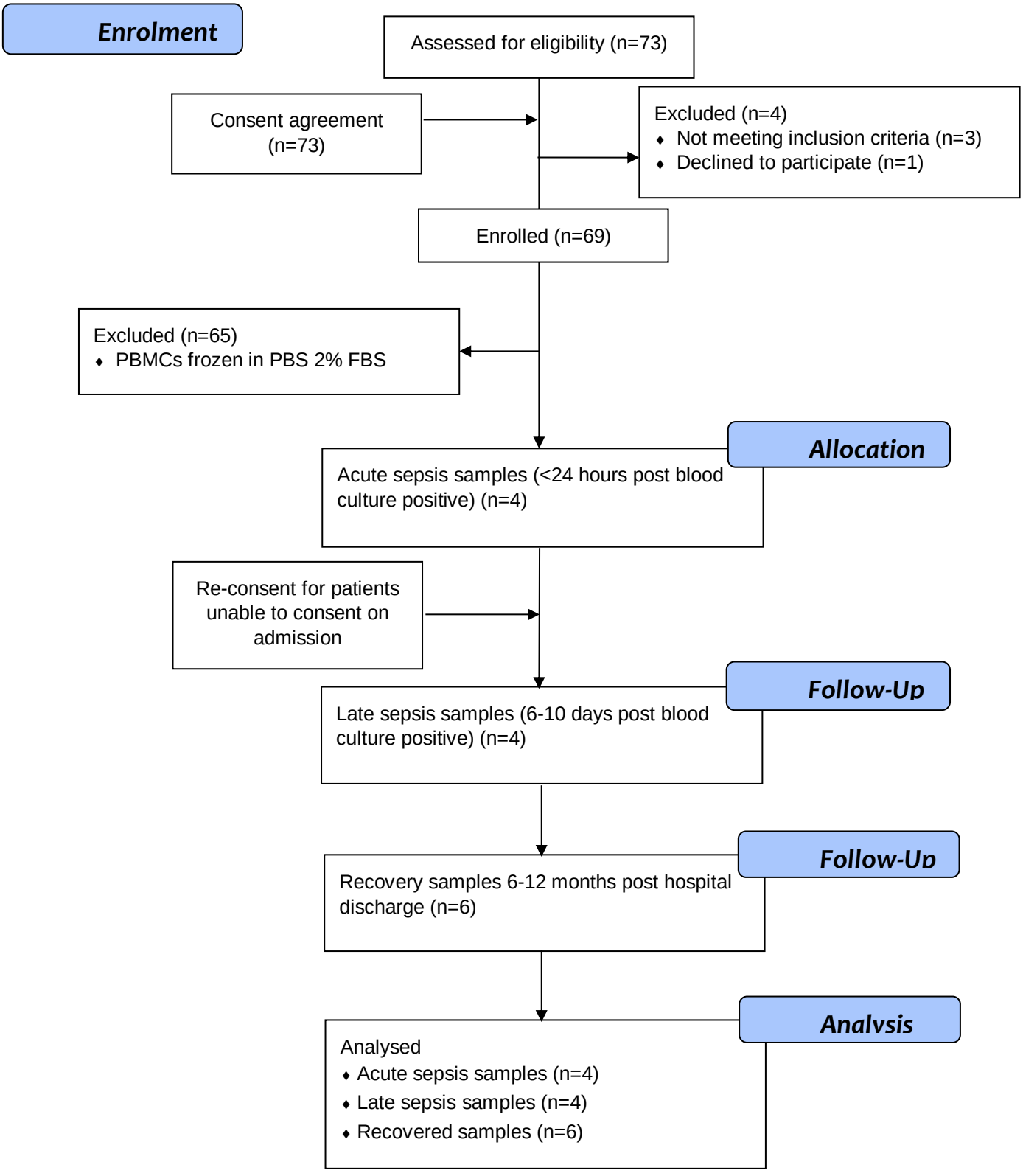

3.2.2 Gene expression

Gene expression of the full patient cohort was ascertained using quantitative PCR. Quantitative PCR was used to quantify; **a)** gene expression in candidate genes for cytokines descriptive of specific immune pathways (innate and adaptive) and **b)** gene expression for candidate histone methylating and acetylating genes. The cytokines were TNFα, IL-1β, IL-10, IL-6, IL-12 and CCL2. Findings in the literature highlighted several genes of enzymes involved in histone modifications that were associated with sepsis and bloodstream infections, these genes were analysed in these experiments and were as follows; ASH1L, KMT2A, EHMT2, DOT1L, KDM5B, KDM6B, HDAC3 and HDAC8.

Hypothesis: Cytokine and histone modifying gene levels will rise in the acute stage of sepsis, but by 6-12 months post hospital discharge will have lowered to baseline.

3.2.3 Cytokine concentration

As well as gene expression of cytokines, the concentration was also measured. The flow cytometry-compatible multiplex *LEGENDplex Human Th Cytokine Panel 13-plex* by Biolegend, CA (cat no. 740001) was utilised for quantification of 13 cytokines; IL-2, IL-4, IL-5, IL-6, IL-9, IL-10, IL-13, IL-17A, IL-17F, IL-21, IL-22, IFN-gamma and TNF-alpha. Patient PBMCs were extracted from patients and immediately cultured for 24 hours in one of three conditions (two repeats per condition); 100ng/µl LPS, 20 µM PMA with 1µg/ml ionomycin or unstimulated control. A Cytometric Bead Array was performed then samples were read on a BD LSR Fortessa (BD Biosciences, USA) to inform cytokine concentrations in pg/ml. A standard ELISA was performed to quantify the IL-10 and IL-6 levels in patient blood plasma.

Hypothesis: Recovered patient cells will respond to LPS/PMA by increasing cytokine production. There will not be a difference in the responses between the different sepsis time points.

3.2.4 Histone modifications

Chromatin Immunoprecipitation (ChIP) was optimised then performed on A) septic host PBMCs, and B) healthy donor PBMCs cultured in 10% septic serum for 2 hours. The histone modifications examined were H3K4me3, H3K9me3, H3K9Ac, and H3K27me3. Both N-ChIP and X-ChIP were explored during optimisation for PBMCs, and ultimately the methodology chosen was X-ChIP of Active Motif ChIP-IT PBMC kit (cat no 53042). The downstream analysis was targeted qPCR of specific gene loci associated with sepsis.

3.2.5 Statistics

While all data points are displayed, the Friedman test with Dunn post hoc was performed only on patients from the full cohort who had a full set of blood samples for all three timepoints (n=18) and compared against healthy volunteers, taking into account matched vs unmatched pairs in the analysis.

Hypothesis: Sepsis will induce changes in histone modifications related to genes associated with sepsis and infection.

3.3 Results

Patient characteristics

Table 3.3.1 details the clinical characteristics of the full patient cohort.

Table 3.3.1 Demographic and clinical features of the patient cohort.

	n=69
Age	59 (19-92)
Male sex	41 (59%)
Level of care	Intensive care: 23 (33.3%)
	General ward: 46 (66.6%)
SOFA score day 0 (ICU cohort)	6.4 (2-13)
Gram -ve infection	37 (53.6%)
Gram +ve infection	31 (44.9%)
Fungal infection	1 (1.4%)

Table 3.3.1 Numbers refer to median or absolute count with percentages in parenthesis, or median with full range in parenthesis.

69 patients donated their first blood samples, but by the 6-10 day sampling only 47 patients donated blood and only 30 patients returned again for the 6-12 month sampling. This was due to patient deaths, discharges before the 6-10 day sampling, declining the sampling, and losing contact with the patients. A full breakdown CONSORT diagram is found in the Methods Chapter. Furthermore, there were difficulties extracting blood from some of the patients, resulting in too little RNA to perform the gene expression analysis.

3.3.1 Cytokine gene expression in septic patients

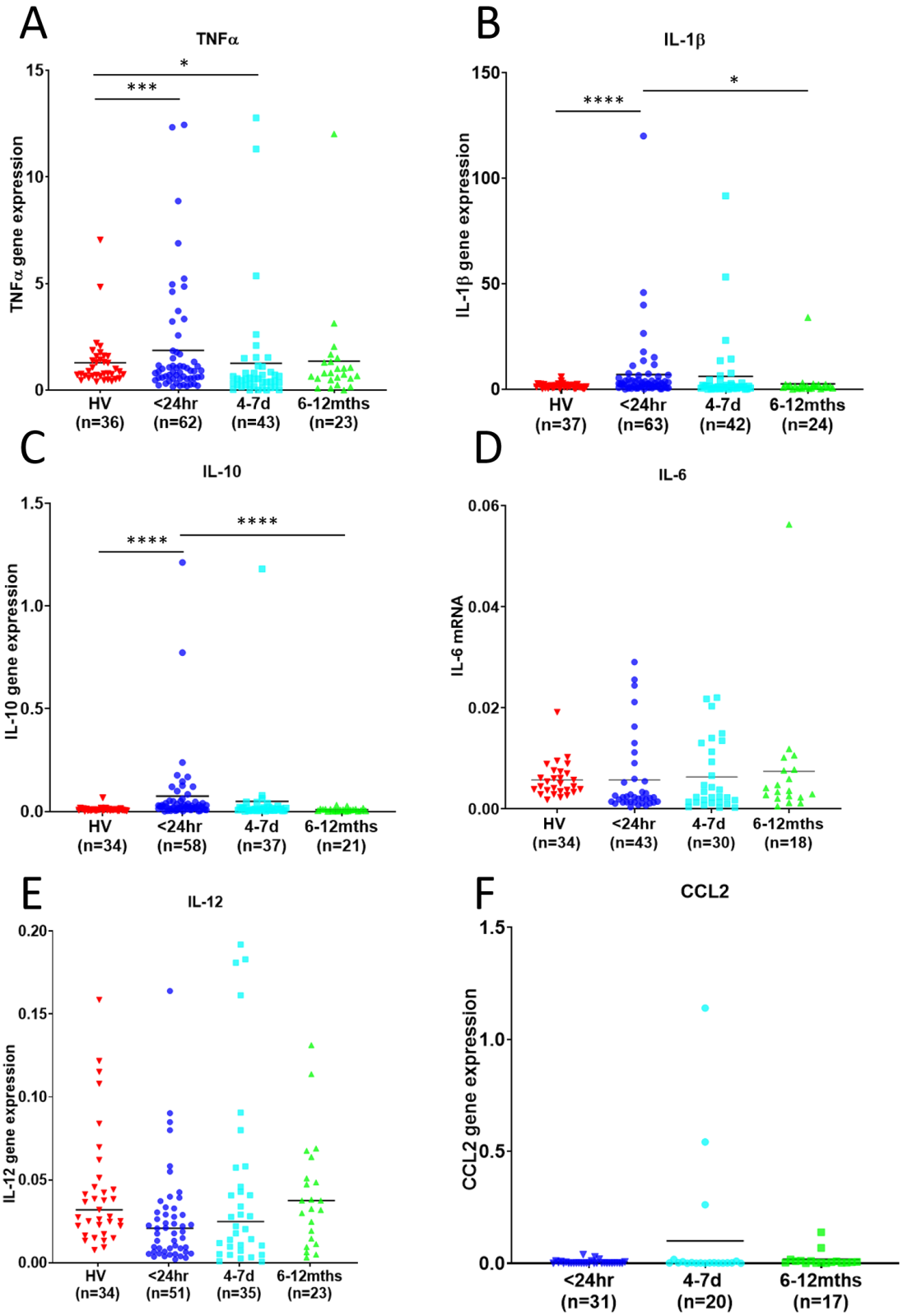

Key:	
HV= Healthy volunteer	<24hr= <24 hours post +blood culture
4-7d= 4-7 days post +blood culture	6-12mth= 6-12 months post hospital discharge

Figure 3.3.1 Gene expression of (A) TNFα, (B) IL-1β, (C) IL-10, (D) IL-6, (E) IL-12, and (F) CCL2, derived from quantitative PCR data with two housekeeping genes UBC and HPRT. The expression of each of these genes were assessed for blood samples drawn from the same patient cohort at three time points, <24 hours post positive blood culture, 4-7 days post positive blood culture, and finally 6-12 months post hospital discharge, and from a comparator group of 37 healthy volunteers. Lines represent mean values. Friedman statistical test with Dunn post-hoc was performed only on matched pairs from septic patients at all three time points (n=18). A p-value less than 0.05 is flagged with one star (*), a p-value is less than 0.01 is flagged with two stars (**), a p-value is less than 0.001is flagged with three stars (***) and a p-value is less than 0.0001 is flagged with four stars (****).

The presence of CCL2 was persistent, present in the samples of septic patients at all three time points including 6-12 months post hospital discharge but was not present in any of the healthy volunteers. No significance was found within some cytokines: IL-6, and IL-12, which is inconsistent with established literature. Interindividual variability accounted for some of the lack of differences within the samples. IL-1β and IL-10 did show a significant difference between the samples taken <24 hours post positive blood culture and 6-12 months post hospital discharge ($p=0.0376$ and $p<0.0001$ respectively).

3.3.2 IL-10 and IL-6 concentrations in septic patient plasma

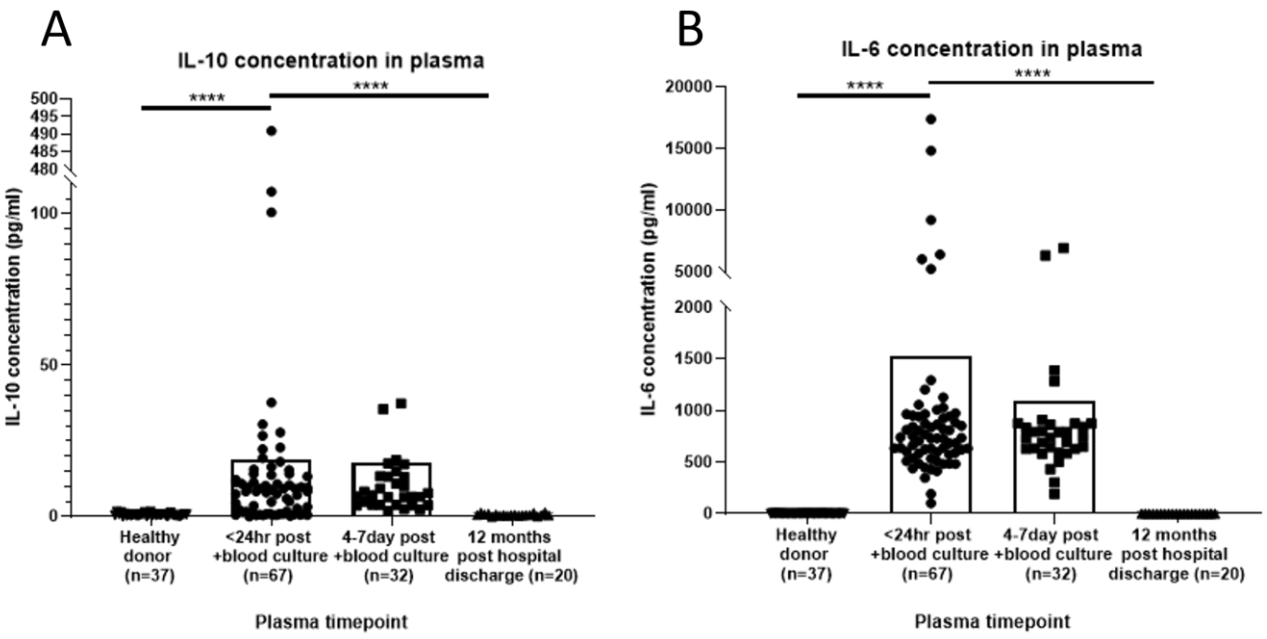

Figure 3.3.2 The concentration (pg/ml) of (A) IL-10 and (B) IL-6 in the plasma drawn from septic patients at three different time points. In grey is healthy volunteer data as a comparator. Lines represent the mean values. A p-value less than 0.05 is flagged with one star (*), a p-value is less than 0.01 is flagged with two stars (**), a p-value is less than 0.001is flagged with three stars (***) and a p-value is less than 0.0001 is flagged with four stars (****). Statistics calculated via Friedman test with Dunn post-hoc only on patient samples with all three time points (n=18). The three patient time points were <24 hours post blood culture positive, 4-7 days post blood culture positive, and 6-12 months post hospital discharge.

The IL-10 concentration was higher at <24 hours post blood culture positive in patients than healthy donors ($p<0.0001$) or 6-12 months post hospital discharge ($p<0.0001$). The difference between <24 hours and 4-7 days post blood culture positive was not significant. By 6-12 months post hospital discharge, the patient levels of IL-10 had returned to the same level as healthy volunteers.

Similarly, there was no difference between <24 hours and 4-7 days post blood culture positive for IL-6 levels. The IL-6 levels at <24 hours post blood culture positive in patients was significantly higher than healthy donors ($p<0.0001$), and likewise with the 6-12 months post hospital discharge sample ($p<0.0001$). Again, by 6-12 months post hospital discharge, the patient levels of IL-6 had returned to the same level as healthy volunteers.

3.3.3 Cytokine production in rechallenged "recovered" patient cells LPS rechallenge

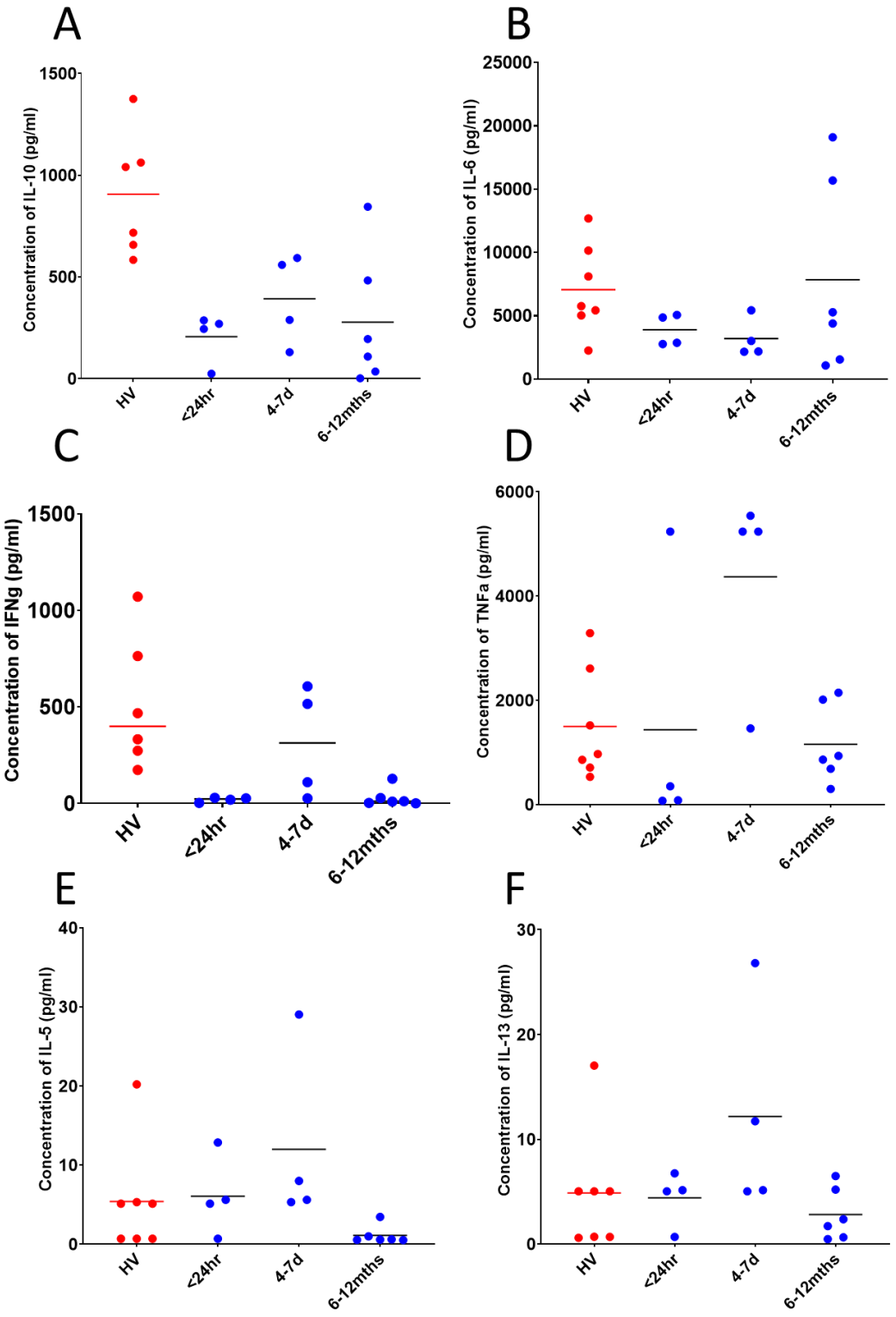

Key:	
HV= Healthy volunteer	<24hr= <24 hours post +blood culture
4-7d= 4-7 days post +blood culture	6-12mth= 6-12 months post hospital discharge

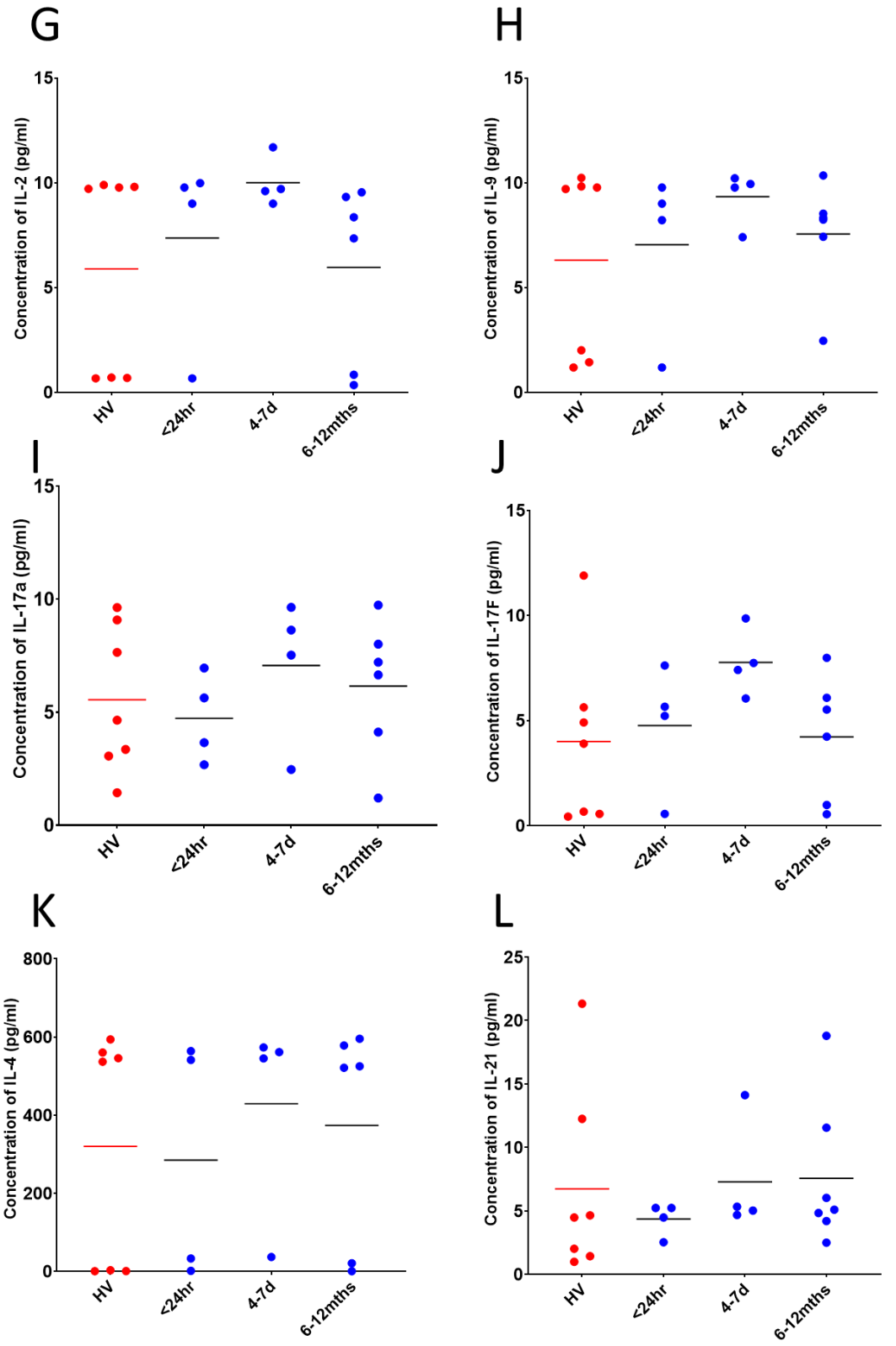

Key:

HV= Healthy volunteer

<24hr= <24 hours post +blood culture

4-7d= 4-7 days post +blood culture

6-12mth= 6-12 months post hospital discharge

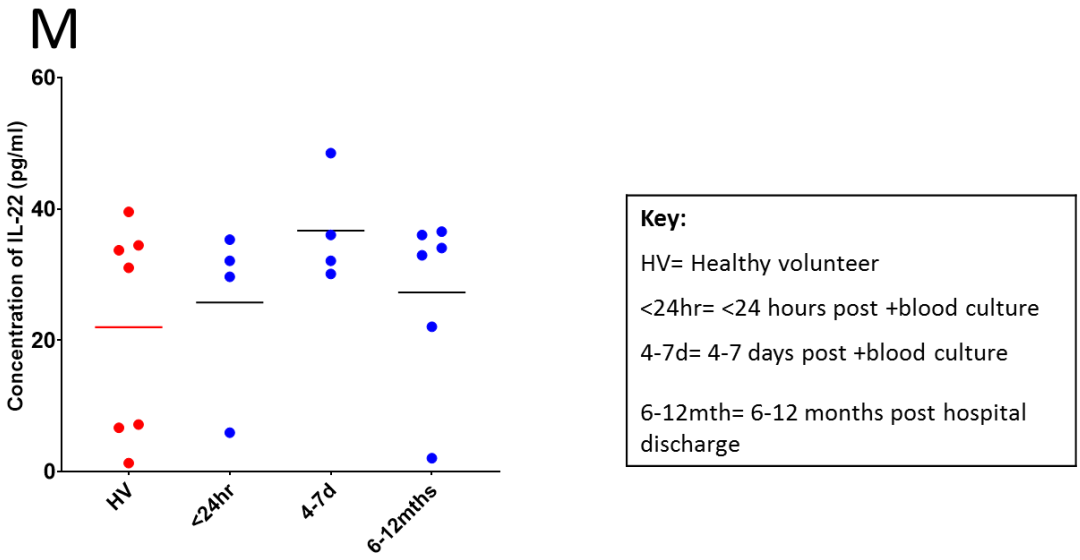

Figure 3.3.2.1 The concentration (pg/ml) of (A) IL-10, (B) IL-6, (C) IFNγ, (D) TNFα, (E) IL-5, (F) IL-13, (G) IL-2, (H) IL-9, (I) IL-17a, (J) IL-17F, (K) IL-4, (L) IL-21 and (M) IL-22 from supernatants of PBMCS rechallenged with LPS (100ng/µl) for 24 hours *in vitro*. Shown in blue, the PBMCs were extracted from septic patients at three time points, <24 hours post positive blood culture, 4-7 days post positive blood culture, and finally 6-12 months post hospital discharge. A comparator group of healthy volunteers is shown in red. Lines represent mean values.

PMA rechallenge

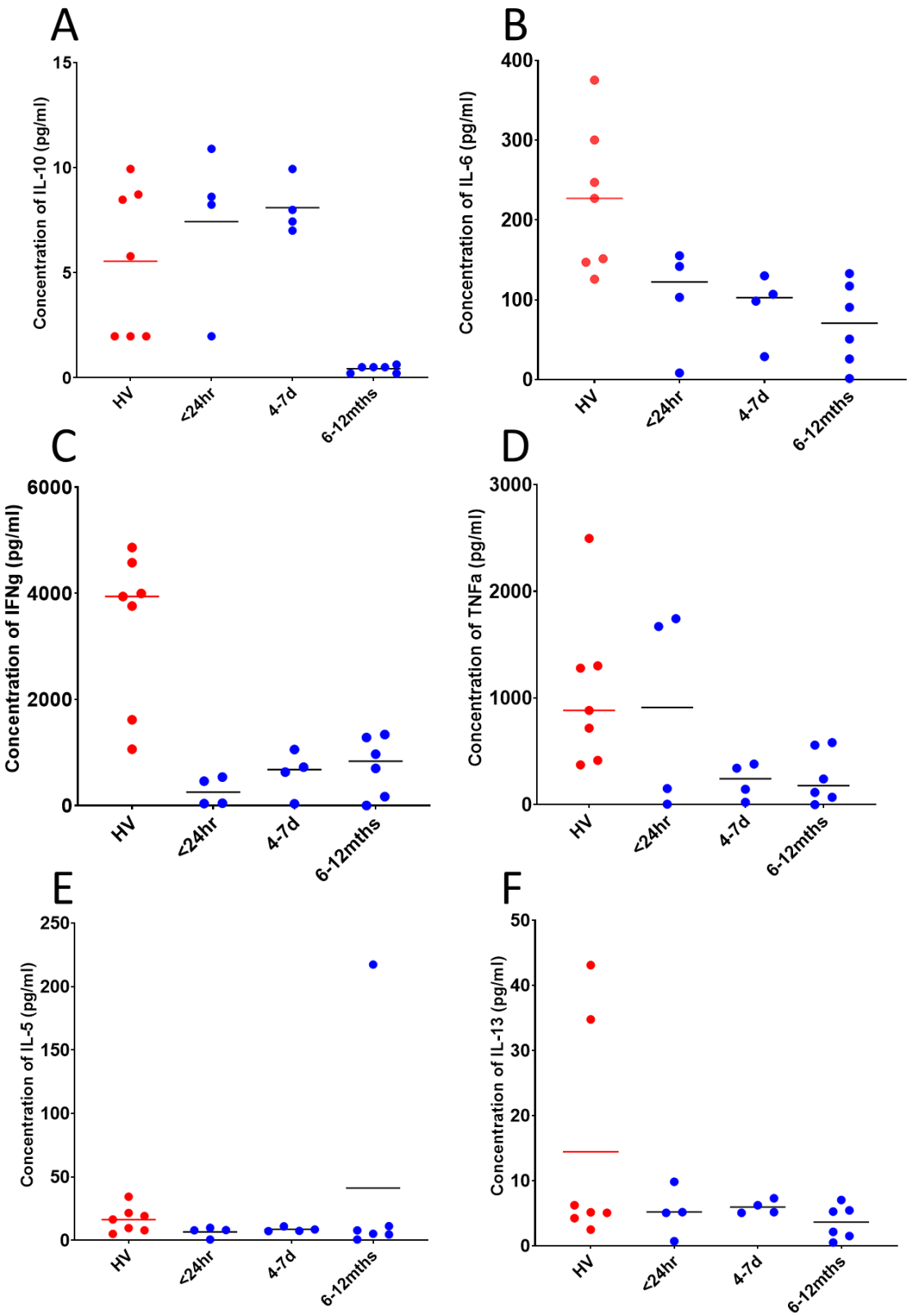

Key:	
HV= Healthy volunteer	<24hr= <24 hours post +blood culture
4-7d= 4-7 days post +blood culture	6-12mth= 6-12 months post hospital discharge

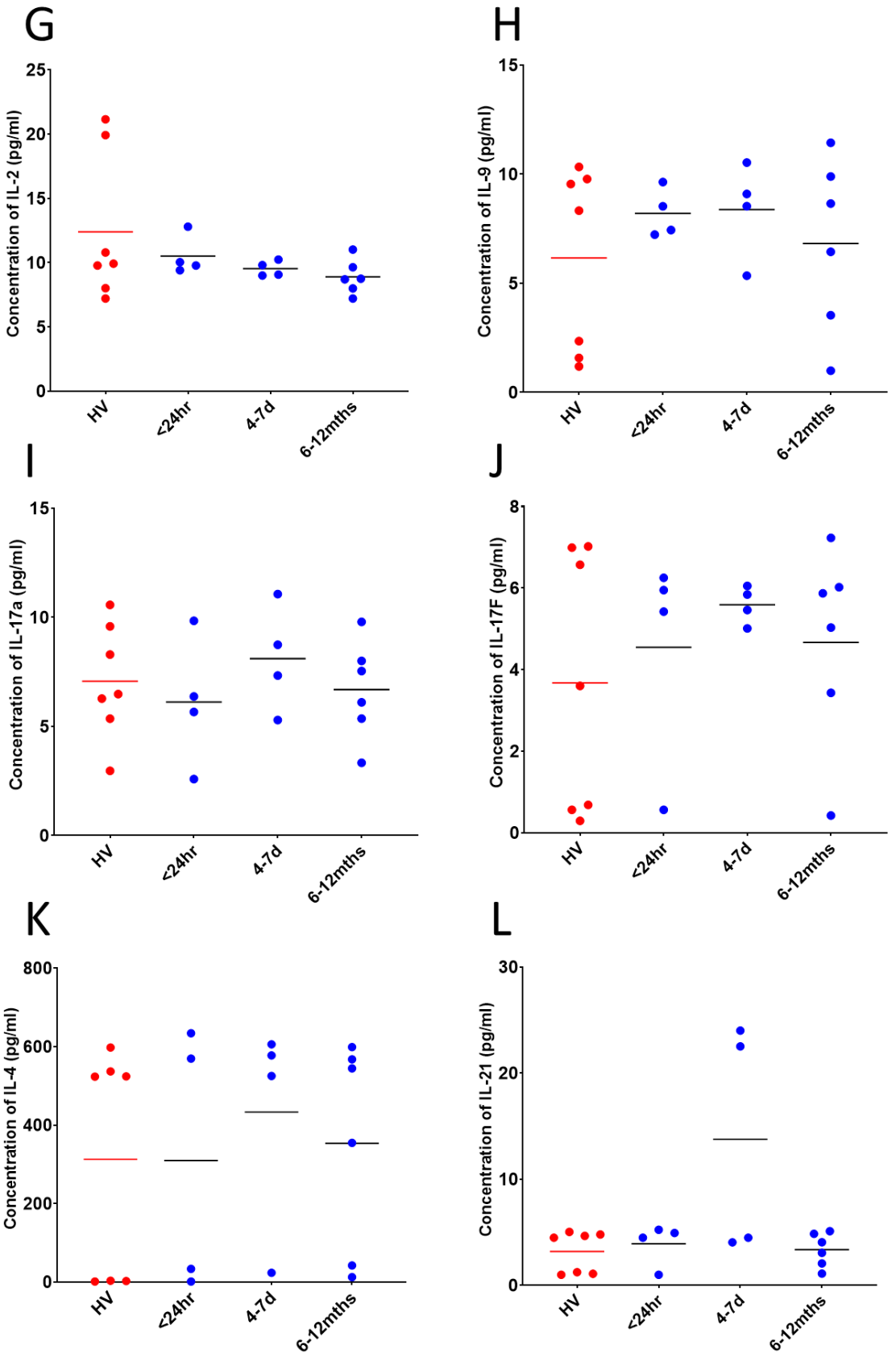

Key:

HV= Healthy volunteer

<24hr= <24 hours post +blood culture

4-7d= 4-7 days post +blood culture

6-12mth= 6-12 months post hospital discharge

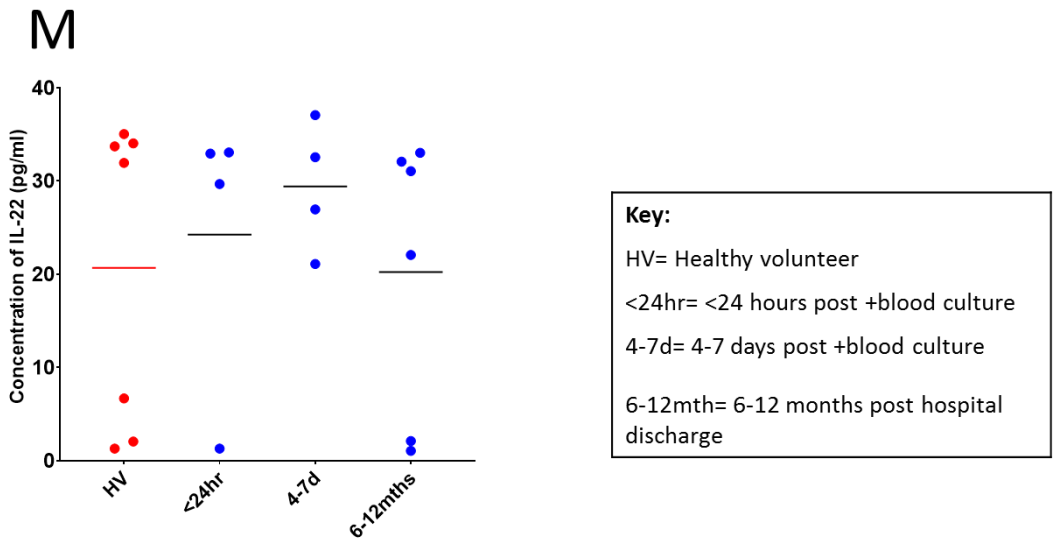

Figure 3.3.2.2 The concentration (pg/ml) of (A) IL-10, (B) IL-6, (C) IFNγ, (D) TNFα, (E) IL-5, (F) IL-13, (G) IL-2, (H) IL-9, (I) IL-17a, (J) IL-17F, (K) IL-4, (L) IL-21 and (M) IL-22 from supernatants of PBMCS rechallenged with PMA (30ng/µl) and ionomycin (1µM) for 24 hours *in vitro*. . Shown in blue, the PBMCs were extracted from septic patients at three time points, <24 hours post positive blood culture, 4-7 days post positive blood culture, and finally 6-12 months post hospital discharge. A comparator group of healthy volunteers is shown in red. Lines represent mean values.

.

Unstimulated controls

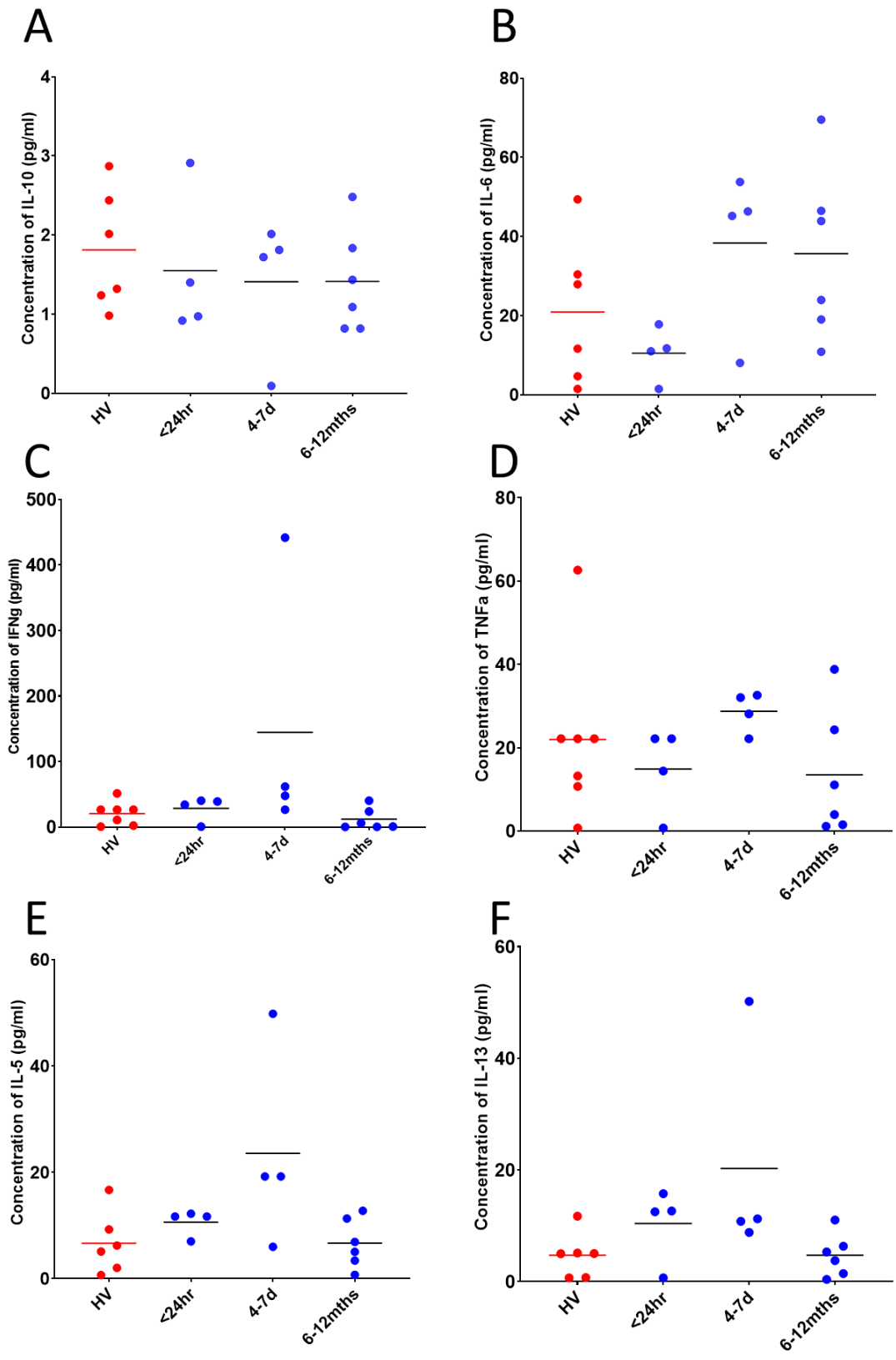

Key:	
HV= Healthy volunteer	<24hr= <24 hours post +blood culture
4-7d= 4-7 days post +blood culture	6-12mth= 6-12 months post hospital discharge

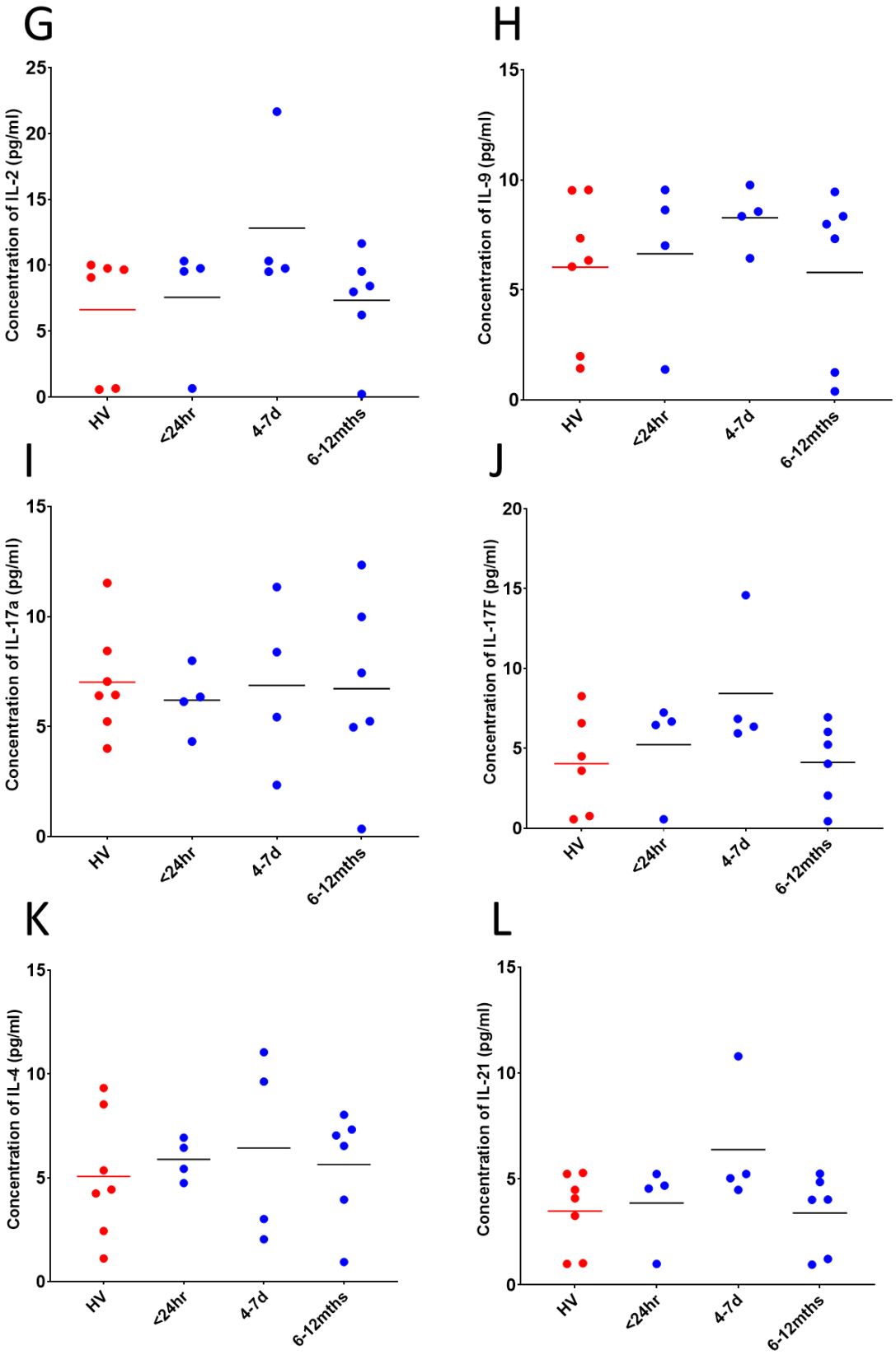

Key:

HV= Healthy volunteer

<24hr= <24 hours post +blood culture

4-7d= 4-7 days post +blood culture

6-12mth= 6-12 months post hospital discharge

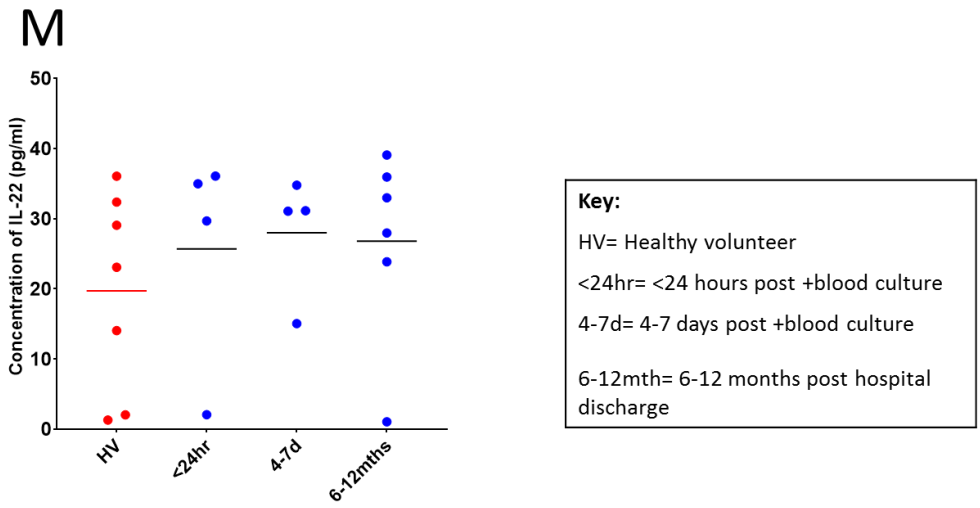

Figure 3.3.2.2 The concentration (pg/ml) of (A) IL-10, (B) IL-6, (C) IFNγ, (D) TNFα, (E) IL-5, (F) IL-13, (G) IL-2, (H) IL-9, (I) IL-17a, (J) IL-17F, (K) IL-4, (L) IL-21 and (M) IL-22 from supernatants of PBMCS unstimulated for 24 hours *in vitro*. Shown in blue, the PBMCs were extracted from septic patients at three time points, <24 hours post positive blood culture, 4-7 days post positive blood culture, and finally 6-12 months post hospital discharge. A comparator group of healthy volunteers is shown in red. Lines represent mean values.

Statistical analysis was not performed on these data sets as the sample size was too small. The concentrations of IL-10 and IFN-γ when restimulated with LPS, and the concentrations of IL-6 and IFN-γ when restimulated with PMA and ionomycin, may be reduced in cells drawn from septic patients compared to healthy volunteers. A larger samples size is required to investigate this further.

3.3.4 Gene expression of histone modifying enzymes in septic patients

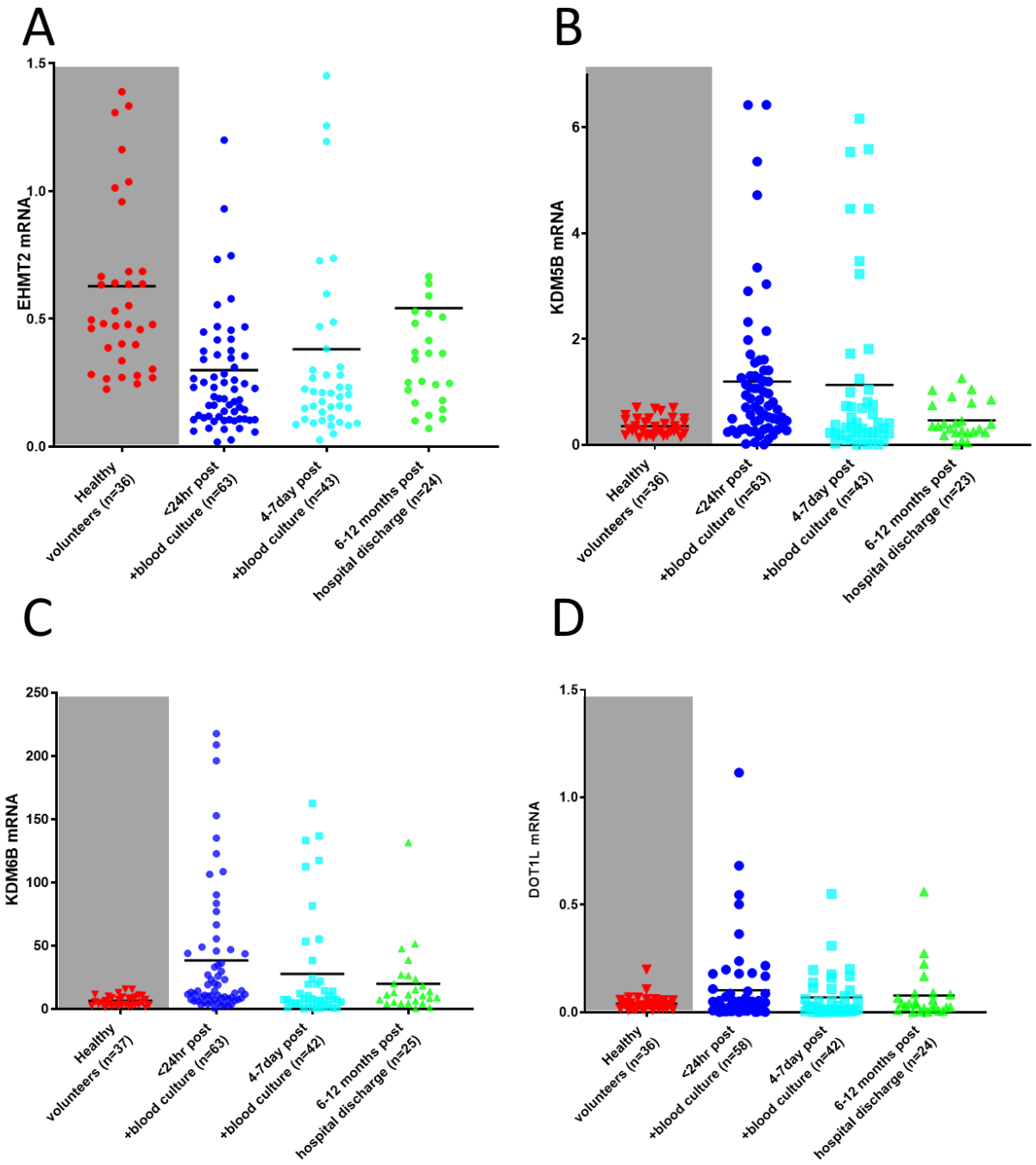

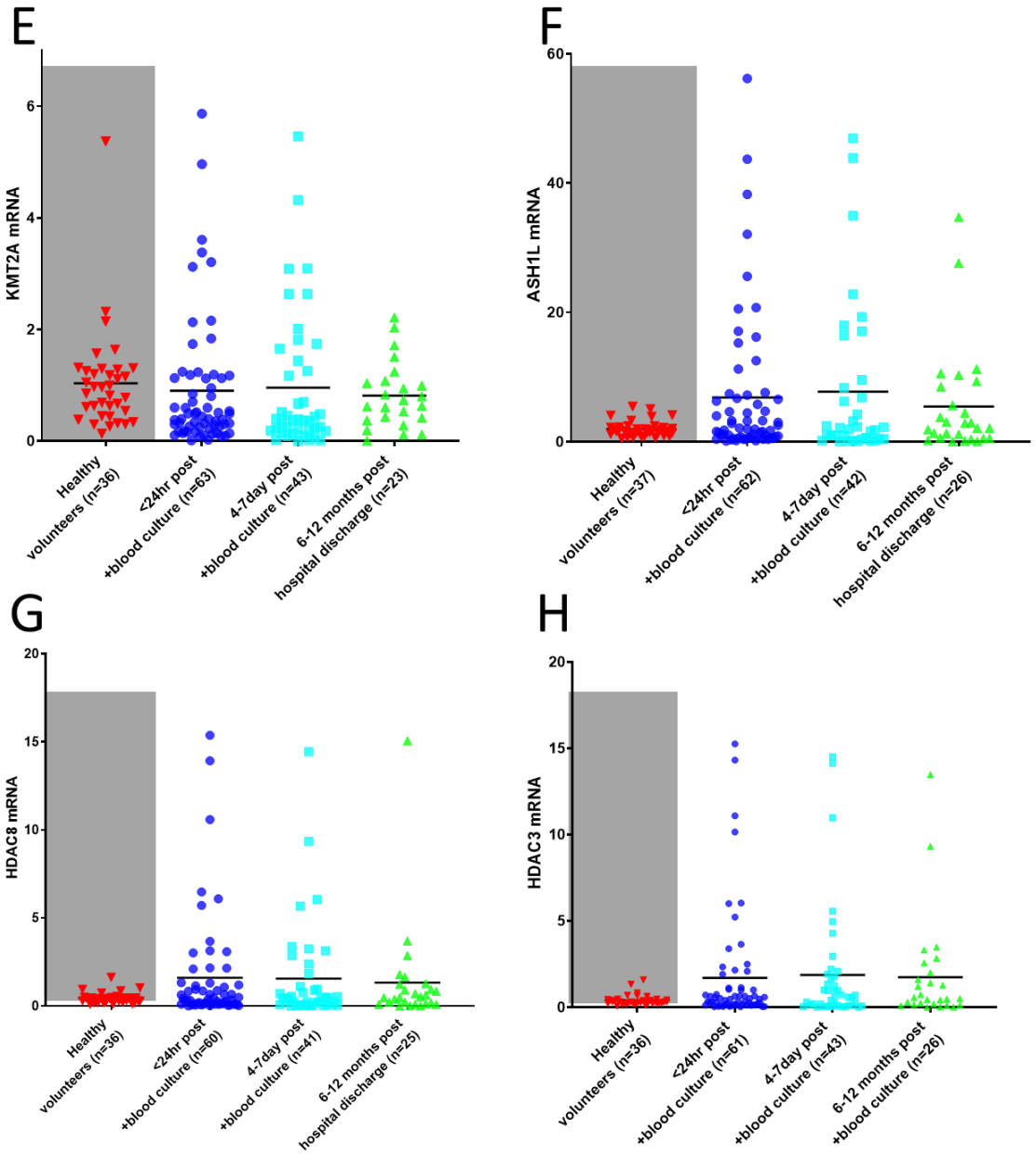

Figure 3.3.3 Gene expression of (A) EHMT2, (B) KDM5B, (C) KDM6B, (D) DOT1L, (E) KMT2A, (F) ASK1L, (G) HDAC8, and (H) HDAC3, derived from quantitative PCR data with two housekeeping genes UBC and HPRT. The expression of each of these genes were assessed for blood samples drawn from the same patient cohort at three time points, <24 hours post positive blood culture, 4-7 days post positive blood culture, and finally 6-12 months post hospital discharge, and from a comparator group of 37 healthy volunteers. Lines represent mean values. Friedman statistical test with Dunn post-hoc was performed on matched pairs from septic patients (n=18) with samples at all three time points.

The gene expression of histone modifying enzymes did not result in any significant differences (EHMT2 p=0.1273; KDM5B p=0.313; KDM6B p=0.8449; DOT1L p=0.3946; KMT2A p=0.396; ASH1L p=0.673; HDAC8 p=0.5349; HDAC3 p=0.3591). It is important to note that statistics were performed on matched pairs from septic patients (n=18) with samples at all three time points only and compared to full cohort of healthy volunteers.

3.3.5 Histone modifications in sepsis

Chromatin Immunoprecipitation optimisation for PBMCs

Both N-ChIP and X-ChIP were performed with the modifications H3K4me3, H3K27me3, H3K9Ac and H3K9me2 with IgG as a control. Optimisation was done on the following: cell lysis, cross-linking (X-ChIP), chromatin shearing (MNase concentration and reaction time for N-ChIP and sonication settings and time for X-ChIP), amount of chromatin to use per immunoprecipitation, antibody binding for the immunoprecipitation, the means to precipitate the chromatin-antibody complex (protein A/G or magnetic beads), amount of chromatin per immunoprecipitation, DNA purification and optimisation of specialised buffers.

Approximately 10 million PBMCs per ChIP were used in optimisation to reflect the number of cells for the patient samples. Optimisation was performed on PBMCs from healthy volunteers, frozen down in various ways. The first 65 patient PBMC samples were frozen in PBS 2% FBS; which is incompatible which subsequent ChIP analysis due to the cells bursting having been frozen without DMSO, and therefore damaging the DNA. Whilst the cell membrane does not necessarily need to be intact, the nucleus needs to be preserved. ChIP was attempted several times of these damaged samples to try to salvage them, but unfortunately they were too

damaged to work. A further 13 patient samples collected since the start of this PhD were frozen in FBS 10% DMSO, a way that is suitable for ChIP. Healthy donor samples were frozen in either PBS 2% FBS, or FBS 10% DMSO and used for optimisation.

A key point of optimisation for Chromatin Immunoprecipitation was the Chromatin shearing. Chromatin shearing was optimised for both N-ChIP using MNase and X-ChIP using sonication. Figure 3.3.5.1 below compares the DNA from each protocol run on a 2% agarose gel compared to a 1kb Plus DNA Ladder. The MNase digestion should return a band of DNA around 100-200bp because the enzyme cleaves in specific site between the histones, whereas in sonication the band will look like more of a smear. Non-sheared DNA will be a band at the top (12k bp) and DNA that is over-sheared will not show on the gel.

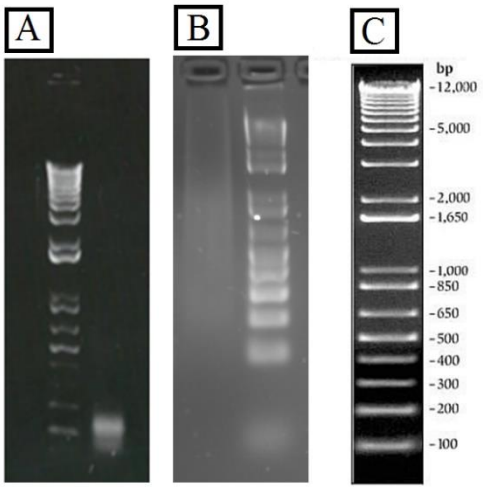

Figure 3.3.5.1 2% agarose gels showing A) histone-bound DNA digested by optimised 10U micrococcal nuclease enzyme (right) with 1kb DNA Plus Ladder (left), B) histone-bound DNA sheared by sonication (left) with 1kb DNA Plus Ladder (right) and C) 1kb DNA Plus Ladder from Thermo Fisher Scientific showing base-pairs (bp) per band.

To calculate relative enrichment, the Livak method was performed. First, average Cts were calculated for each gene. Then, the negative control gene mean Ct was subtracted from each

gene of interest; for H3K4me3 the negative control is HMGB1, and for H3K27me3 and H3K9me3 the negative control is GAPDH. This is the first 'delta' to get ΔCt. The input is then subtracted from each modification of interest (second 'delta' for ΔΔCt). Finally, 2 to the power of negative ΔΔCt was calculated to get the relative enrichment.

When cells were frozen in the way compatible for ChIP, N-ChIP was successful for H3K4me3 (Figure 3.3.4.2) and not for the other histone modifications of interest. X-ChIP was successful for all modifications, and the H3K4me3 showed greater enrichment than that of N-ChIP (Figure 3.3.4.3). N-ChIP did not work for samples frozen in the way that is unsuitable for ChIP to mimic patient samples.

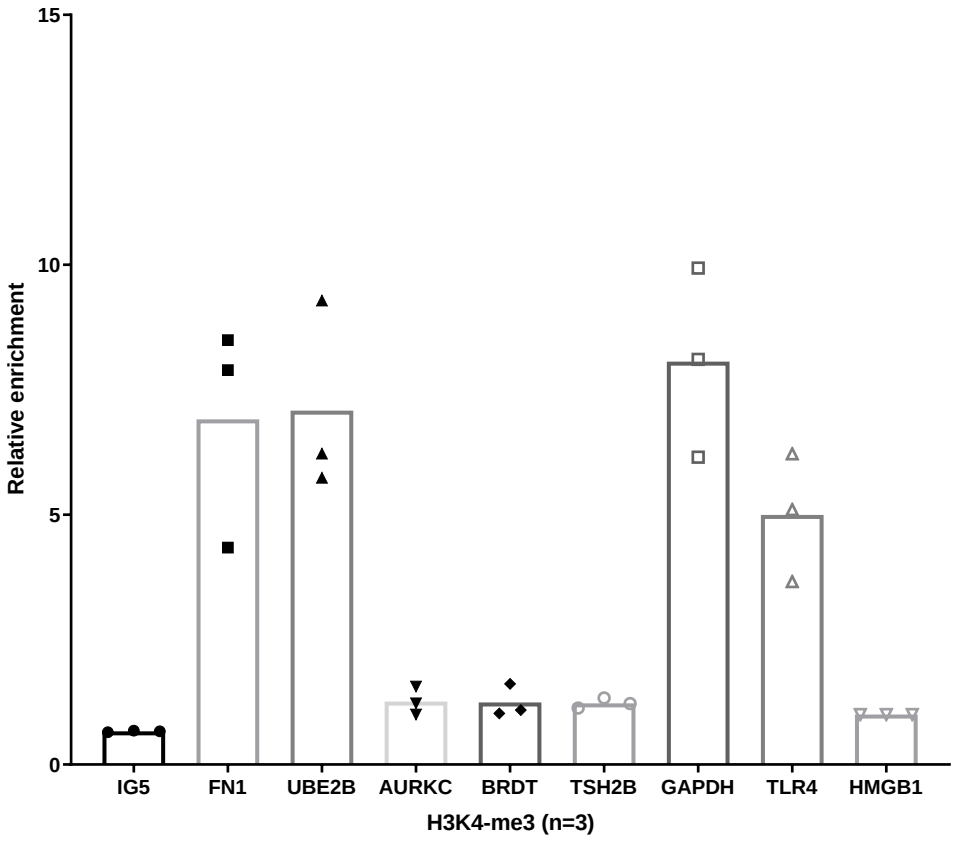

Figure 3.3.5.2 Working N-ChIP for H3K4me3 (n=3). IG5, AURKC, BRDT, TSH2B and HMGB1 are all negative controls for H3K4me3, and FN1, UBE2B, GAPDH and TLR4 are positive controls for H3K4me3. Bars represent the mean.

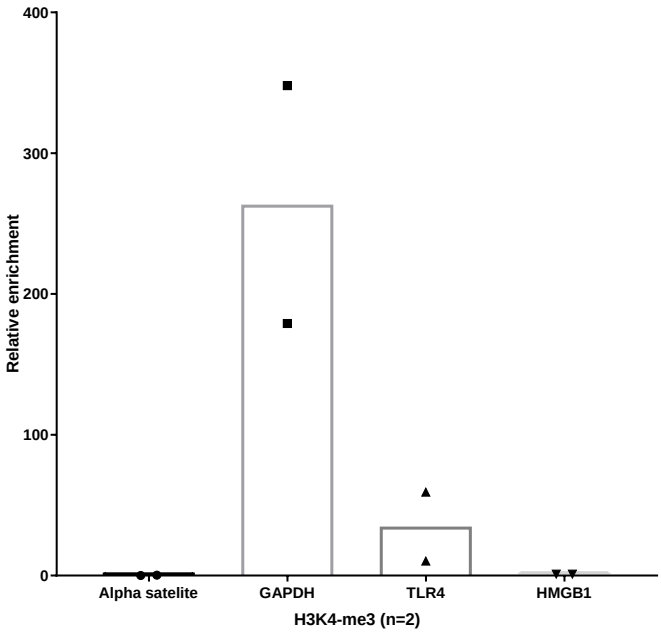

Figure 3.3.5.3 Working X-ChIP for H3K4me3. Alpha satellite and HMGB1 are negative controls for H3K4me3, and GAPDH and TLR4 are positive controls for H3K4me3. Bars represent the mean.

The best and most consistent ChIP to perform on the correctly frozen samples was X-ChIP of Active Motif ChIP-IT PBMC kit (cat no 53042). It was not possible to get ChIP working consistently for the incorrectly frozen samples, despite trying 6 different methodologies and attempting to troubleshoot and adapt. The methodologies attempted were from Weiterer et al, 2014; Sui et al, 2014; Arrigoni et al, 2016; Active Motif ChIP-IT® PBMC kit; Active Motif ChIP-IT High Sensitivity® kit; Epigentek, USA.

3.3.6 Chromatin Immunoprecipitation Experiment 1: Septic patient PBMCs

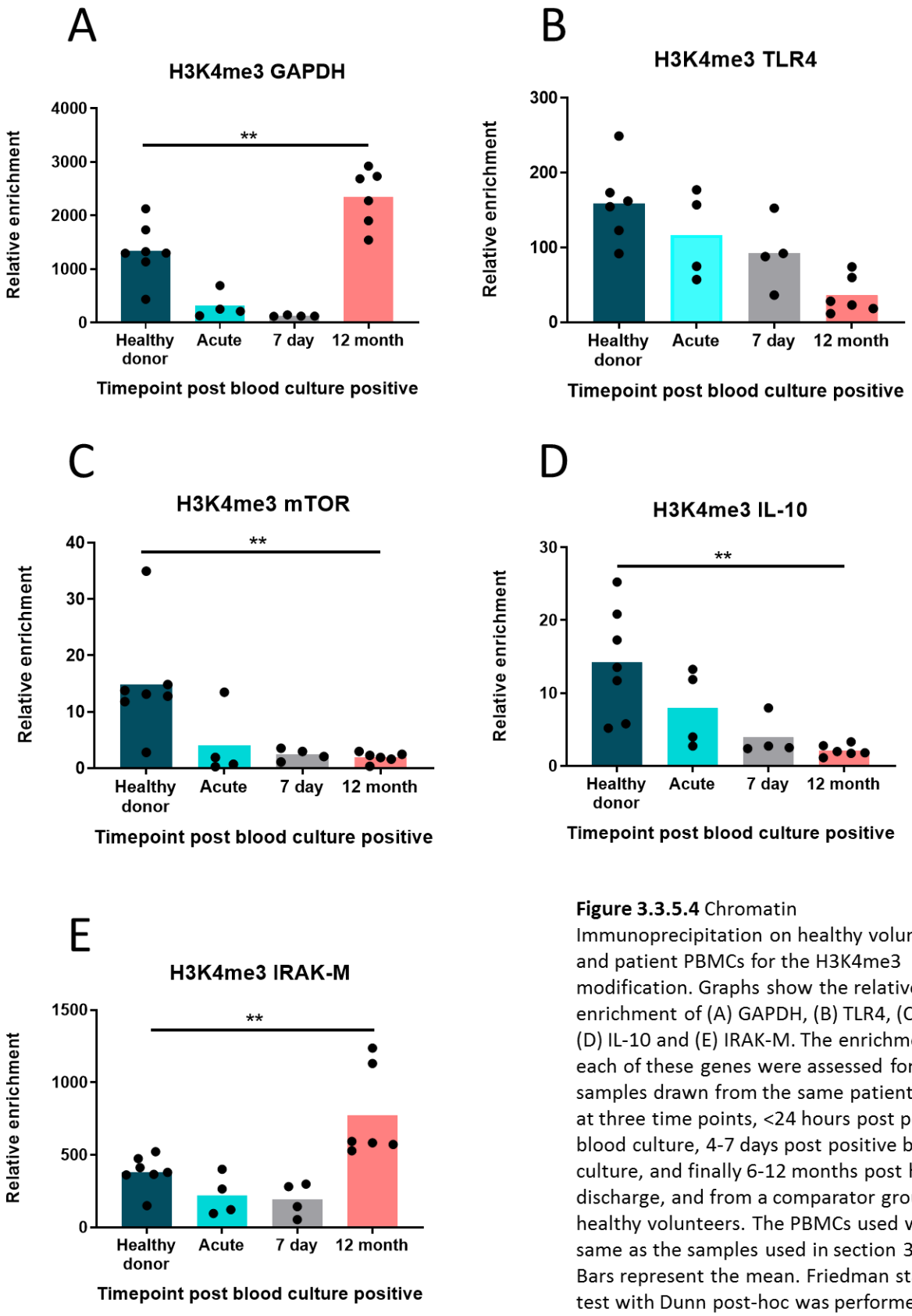

Figure 3.3.5.4 Chromatin Immunoprecipitation on healthy volunteer and patient PBMCs for the H3K4me3 modification. Graphs show the relative enrichment of (A) GAPDH, (B) TLR4, (C) mTOR, (D) IL-10 and (E) IRAK-M. The enrichment of each of these genes were assessed for blood samples drawn from the same patient cohort at three time points, <24 hours post positive blood culture, 4-7 days post positive blood culture, and finally 6-12 months post hospital discharge, and from a comparator group of healthy volunteers. The PBMCs used were the same as the samples used in section 3.3.2. Bars represent the mean. Friedman statistical test with Dunn post-hoc was performed

For H3K4me3, the gene activation marker, there was a significantly higher relative enrichment in patients 6-12 months post hospital discharge than healthy volunteers in GAPDH (p=0.0082) and IRAK-M (p=0.0012), and a significantly lower enrichment in IL-10 (p=0.0012) and mTOR (p=0.0023).

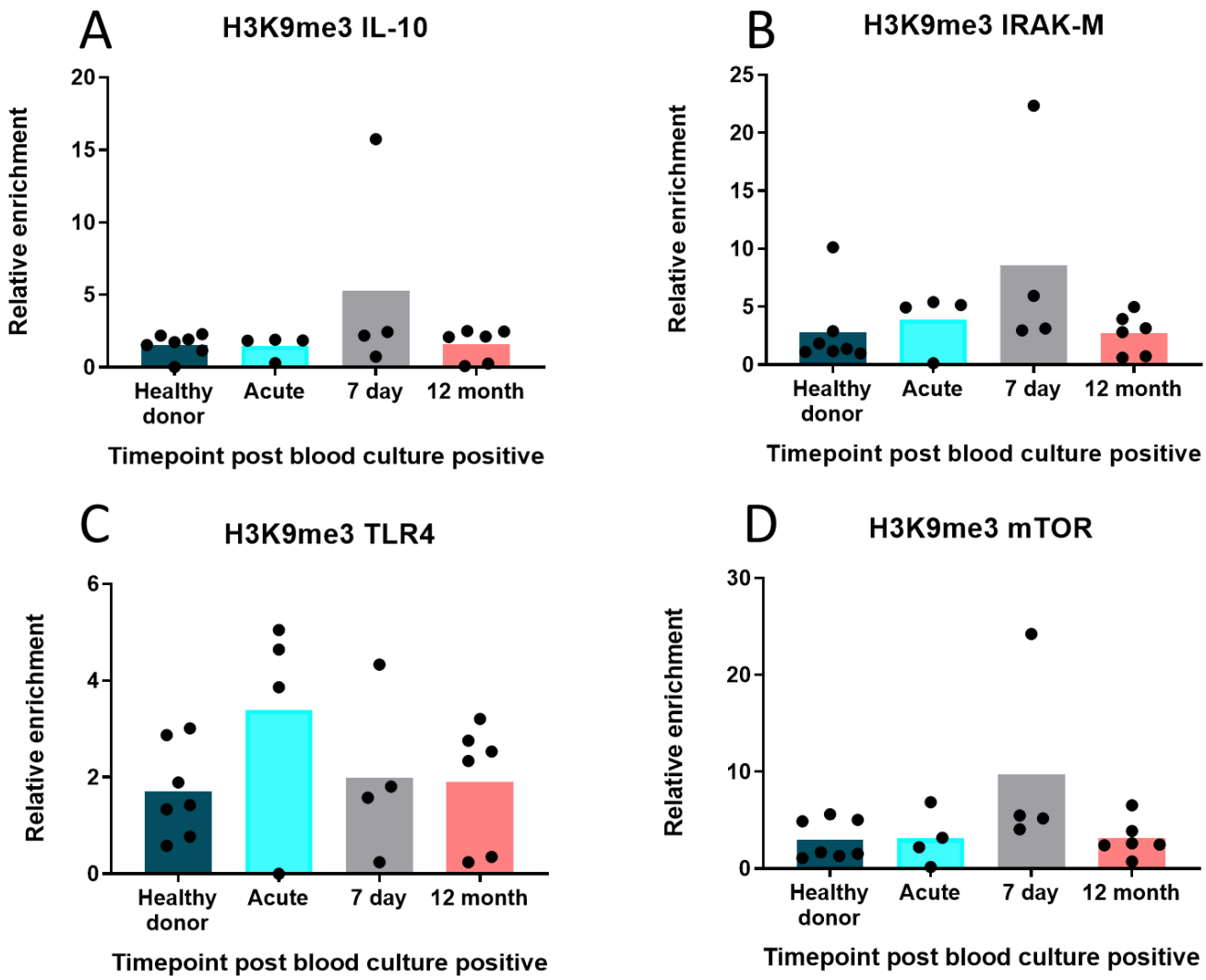

Figure 3.3.5.5 Chromatin Immunoprecipitation on healthy volunteer and patient PBMCs for the H3K9me3 modification. Graphs show the relative enrichment of (A) IL-10, (B) IRAK-M, (C) TLR4, and (D) mTOR. The enrichment of each of these genes were assessed for blood samples drawn from the same patient cohort at three time points, <24 hours post positive blood culture, 4-7 days post positive blood culture, and finally 6-12 months post hospital discharge, and from a comparator group of healthy volunteers. The PBMCs used were the same as the samples used in section 3.3.2. Bars represent the mean.

H3K9me3, known for gene inactivation, did not show any differences between any of the groups for the genes IL-10, IRAK-M, TLR4 and mTOR.

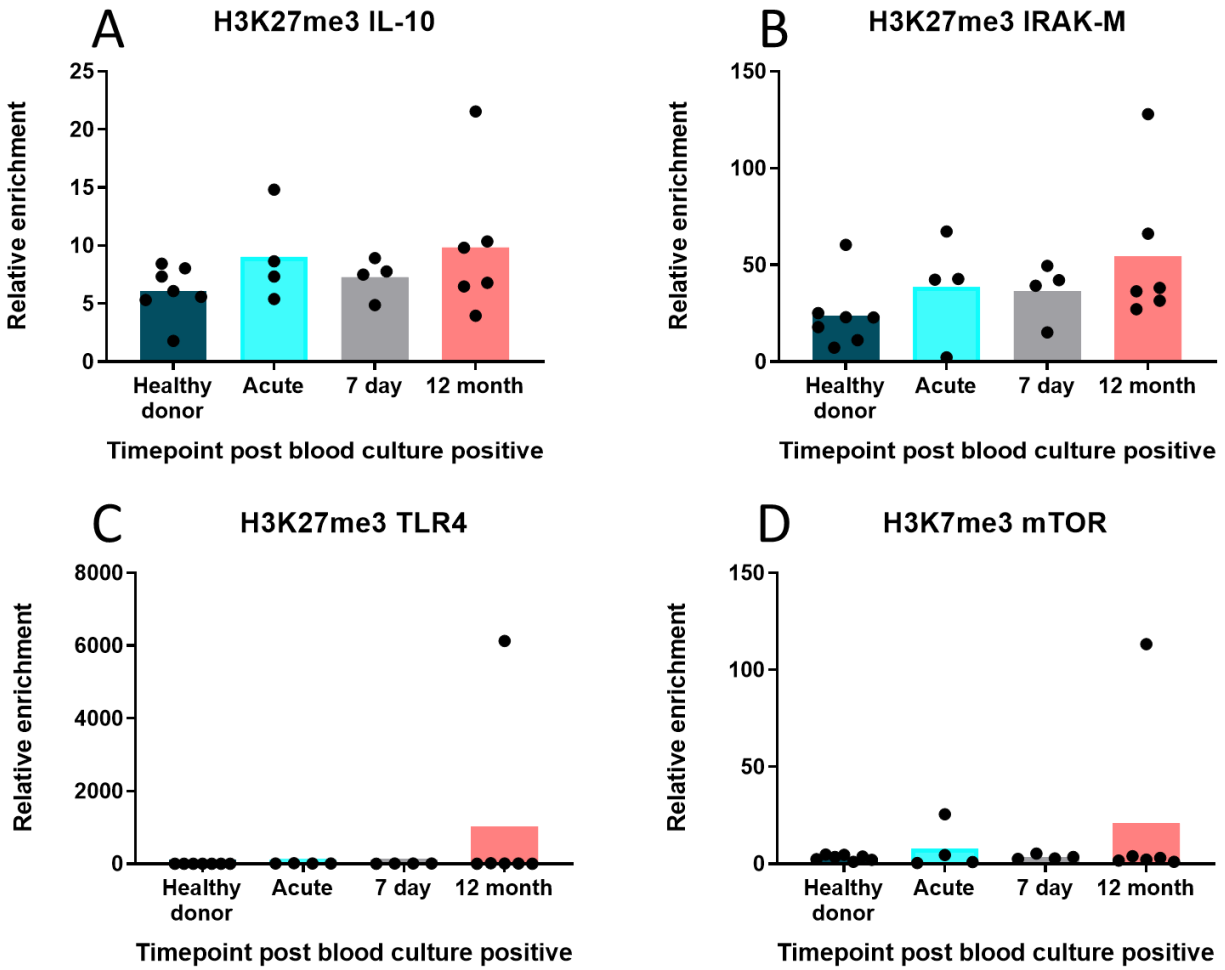

Figure 3.3.5.6 Chromatin Immunoprecipitation on healthy volunteer and patient PBMCs for the H3K27me3 modification. Graphs show the relative enrichment of (A) IL-10, (B) IRAK-M, (C) TLR4, and (D) mTOR. The enrichment of each of these genes were assessed for blood samples drawn from the same patient cohort at three time points, <24 hours post positive blood culture, 4-7 days post positive blood culture, and finally 6-12 months post hospital discharge, and from a comparator group of healthy volunteers. The PBMCs used were the same as the samples used in section 3.3.2. Bars represent the mean.

H3K27me3, also known for gene inactivation, returned similar results to H3K9me3. It did not show any differences between any of the groups for the genes IL-10, IRAK-M, TLR4 and mTOR.

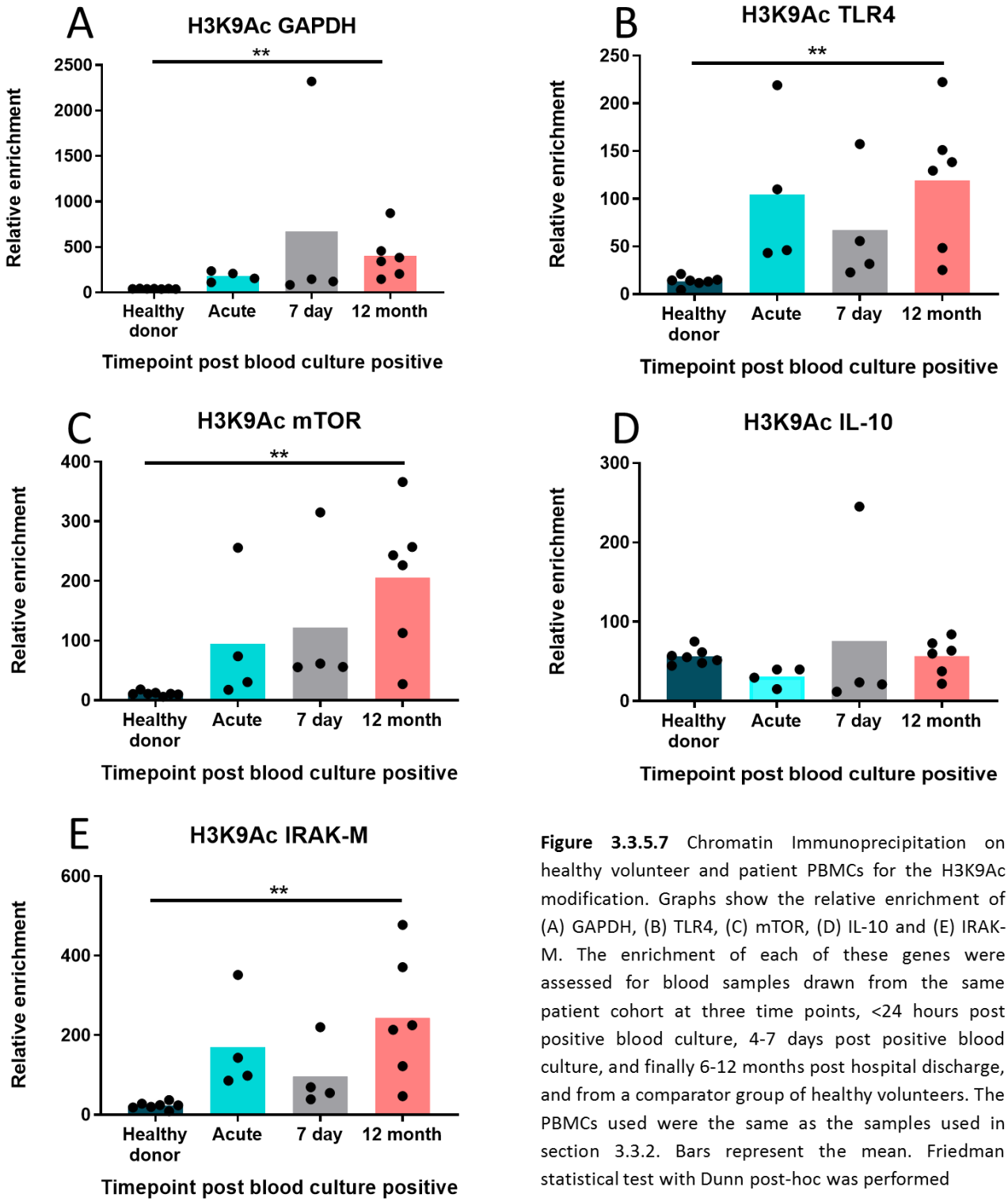

Figure 3.3.5.7 Chromatin Immunoprecipitation on healthy volunteer and patient PBMCs for the H3K9Ac modification. Graphs show the relative enrichment of (A) GAPDH, (B) TLR4, (C) mTOR, (D) IL-10 and (E) IRAK-M. The enrichment of each of these genes were assessed for blood samples drawn from the same patient cohort at three time points, <24 hours post positive blood culture, 4-7 days post positive blood culture, and finally 6-12 months post hospital discharge, and from a comparator group of healthy volunteers. The PBMCs used were the same as the samples used in section 3.3.2. Bars represent the mean. Friedman statistical test with Dunn post-hoc was performed

For the histone modification H3K9Ac, another activation marker, the relative enrichments were significantly higher in the 6-12 months post hospital discharge than the healthy volunteers for GAPDH, TLR4, IRAK-M and mTOR, all p=0.0012.

3.3.7 Chromatin Immunoprecipitation Experiment 2: Mimicking acute sepsis

For each of the three histone modifications- H3K4me3, H3K9me3, and H3K27me3- 20 genes were examined. These genes were: IRAK-M, GAPDH, mTOR, CD180, CD86, CD80, TNFα, IFNγ, IL-6, IL-10, IL-17α, TLR4, TLR2, CCL2, TREM1, EIR4EBPI, MyD88, PD1L, CIITA, and HIF1α.b Healthy volunteer PBMCs were cultured for 2 hours in pooled serum drawn from sepsis patients at different time points.

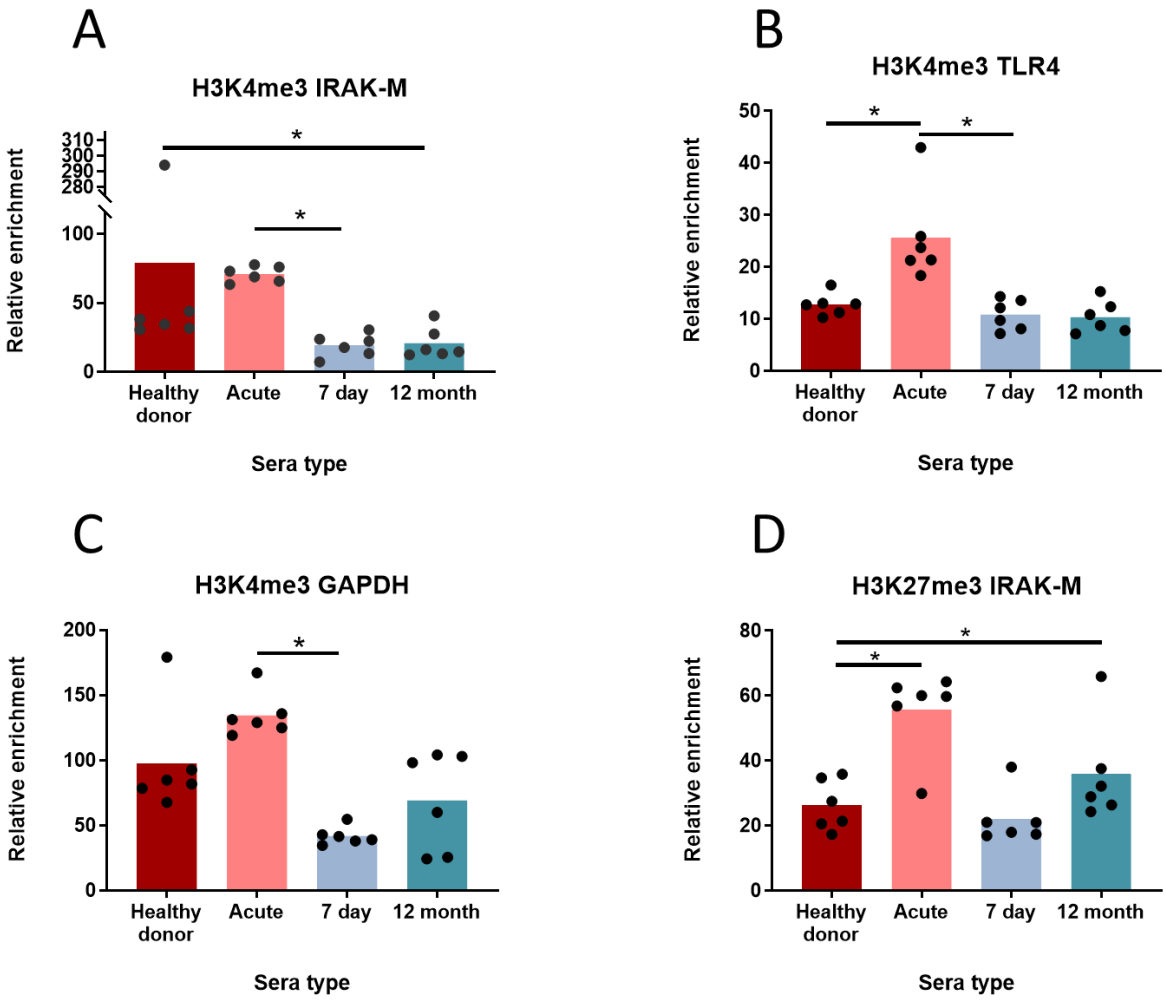

Figure 3.3.5.8 Chromatin Immunoprecipitation on healthy volunteer PBMCs that were cultured for 2 hours in 10% serum pooled from *e.coli* septic patients for the activation marker H3K4me3 (A-C) and repression marker H3K27me3 (D). Graphs show the relative enrichment of (A,D) IRAK-M (B) TLR4, and (C) GAPDH. The same healthy volunteers (n=6) were used in each serum condition. The enrichment of each of these genes were assessed for PBMCs cultured in pooled serum samples drawn from the same patient cohort at three time points, <24 hours post positive blood culture, 4-7 days post positive blood culture, and finally 6-12 months post hospital discharge, and from a comparator group of healthy volunteers. Bars represent the mean. A p-value less than 0.05 is flagged with one star (*), a p-value is less than 0.01 is flagged with two stars (**), a p-value is less than 0.001is flagged with three stars (***) and a p-value is less than 0.0001is flagged with four stars (****). Statistics calculated via Friedman test with Dunn post-hoc.

For H3K4me3, the gene activation marker, there was a lower relative enrichment in PBMCs when cultured in serum from 6-12 months post hospital discharge than serum from healthy volunteers in IRAK-M (p= 0.0232). For IRAK-M, there was also a drop in relative enrichment for 7 days post positive blood culture compared to when septic patients were sampled acutely (p= 0.0347). TLR4 displayed a rise in H3K4me3 relative enrichment when cells were

cultured in acute septic serum (healthy donor vs acute p=0.0347; acute vs 7 days post positive blood culture p=0.0347). For GAPDH, there was only a difference between acute and 7 days post positive blood culture p=0.0309.

For IRAK-M with repression marker H3K27me3, there was a lower relative enrichment when cells were cultured in healthy donor serum than acute septic serum (p=0.0347) or serum from 6-12 months post hospital discharge (p=0.0347).

For H3K9me3 repression marker, there were no differences in relative enrichment between serum conditions for any of the 20 genes analysed.

3.4 Discussion

Patient characteristics and demographics

The difficulty with these experiments is that the cohort is so varied with regards to pathophysiology and patient characteristics it is possible to miss more subtle findings. With more time to recruit patients that fit into specific subcategories (for example; 18-45 year old, *E.coli* sepsis, no chronic conditions, ICU patients) this could shed more light on the differences between the different patient groups. It is possible that the gram-positive versus the gram-negative bacteraemia could result in distinct phenotypes. In the gene expression experiments the statistics are performed only on patients who had a full set of samples, n=18. However, 14 of those were *E.coli* sepsis, which skews the results into this type of infection.

Pooled septic serum was collected from n=14 patients with *E.coli* sepsis from the full patient cohort who had samples at all timepoints. Pooled serum helps to create a normalised population for the subgroup it was selected for (in this case *E.coli* sepsis), and the more matched donors that are added the better it will be at fulfilling this goal. It helps reduce the impact of individual's variation in a sample. Ideally, this pooled serum should have been from a larger number of age and sex matched individuals without comorbidities.

Statistics and power

Some sample sizes within this body of work are too small to be able to perform statistical analysis, due to a high chance of a type II error. Results must be interpreted with this in mind, particularly where statistical power is lacking.

Rechallenging patient PBMCs may result in a reduced cytokine response

The main introduction discusses the evidence that T cells, monocytes and macrophages become exhausted when challenged with sepsis, and over time are less able to produce pro-inflammatory cytokines (immunoparalysis). This immune deficit can persist in sepsis survivors even long after the infection has cleared. The increased likelihood of sepsis survivors developing recurrent infections may be due to this dampening of the immune response from an exhaustion of leukocytes and inhibited cytokine production. The length of time a sepsis-induced immune deficit can persist is variable and has not been fully elucidated. The hypothesis of impaired immunity in survivors of sepsis was not adequately assessed in order to draw conclusions.

The biggest weakness to these experiments were the low sample size. It is not possible to perform statistical analysis on such small n numbers, and so any patterns that may emerge in the data are purely speculatory. Looking at the data, a trend suggests the concentrations of IL-10 and IFN-γ when restimulated with LPS, and the concentrations of IL-6 and IFN-γ when restimulated with PMA and ionomycin, may be reduced in cells drawn from septic patients compared to healthy volunteers. This would support research conducted by Boomer et. al., who found a global decrease in the secretion of TNF-α, IFN-γ, IL-6 and IL-10 in cells from patients who died from sepsis which were stimulated with LPS and α-CD3/28. Arens et. al. observed similar trends in their pilot study when restimulating septic patient PBMCs with α-CD3/28, LPS and zymosan.

If this is true, the samples suggest this immune deficit may persist for up to 12 months post hospital discharge in patients, making them vulnerable to further infections during this time.

However, this conclusion is too far-reaching with such a small sample size, and should only be taken as a pilot study to warrant further investigation.

The most extensively studied pro-inflammatory cytokines in sepsis are TNFα and IL-1, which are early mediators released during acute inflammation and have essential roles in the immune response (Schulte et al, 2013). TNFα is mostly produced by macrophages and monocytes, and to a lesser extent natural killer and B cells, and mediates a diverse set of reactions within the immune response (Sellati et al, 2014). TNFα regulated cell differentiation, proliferation and apoptosis (Parameswaran et al, 2010). It is considered a 'master regulator' of the immune response where it orchestrates the production of a pro-inflammatory cytokine cascade, and increases prostaglandins and platelet activating factor (Parameswaran et al, 2010; Maini et al, 1995; Vassalli, 1992). TNF has been shown to regulate transcription of the NLRP3 inflammasome components. A downstream reaction of TNFα results in the degradation of IκBα and activation of NF-κB (Parameswaran et al, 2010). TNFα cytokine concentration is higher in septic patients than healthy controls, and significantly increased in septic shock as compared with severe sepsis with higher levels associated with increased mortality (Schulte et al, 2013; Surbatovic et al, 2015).

Another essential pro-inflammatory cytokine is IL-6. A wide array of immune cells respond to and secrete IL-6, which can result in feedback loops to produce more IL-6 (Choy et al, 2017). IL-6 promotes the development of T-helper 17 (Th17) cells (which produce IL-17) and the maturation of B lymphocytes (Choy et al, 2017). IL-6 can help orchestrate a transition from acute to chronic inflammation through mediating the nature of leucocyte infiltrate (Gabay, 2006). IL-6 concentration is higher in septic patients than healthy controls, and is found to be associated with severity and organ dysfunction -higher IL-6 during the first 24 hours is

predictive of worsening organ dysfunction and mortality (Schulte et al, 2013; Bozza et al, 2007, Grealy et al, 2013). Th17 cells produce IL-6 and IL-17, which in turn induced fibroblasts to produce more IL-6 and amplifies the immune response (Otta et al, 2015).

IL-10 is an anti-inflammatory cytokine that has a crucial role in limiting host immune response to pathogens, and in produced by almost all leukocytes (Iyer et al, 2012). IL-10 concentration higher in septic patients than healthy controls, and could be associated with severity and organ dysfunction (Schulte et al, 2013; Bozza et al, 2007).

IL-10 and IL-4 help negatively regulate IFNγ production, whereas IL-12 and IL-18 help to positively regulate it (Salazar-Mather et al, 2000; Fukao et al, 2000; Sen, 2001).IFNγ has extendsive roles in the immune system, including regulating antigen processing and presentation by antigen presenting cells, causing apoptosis, production of NO, and leukocyte trafficking (Schroder et al, 2004; Cultraro et al, 1997).

IL-5 activates B cells and eosinophils and regulates the innate and acquired immune response (Takatsu et al, 2005). IL-13 reduces CD14 expression and blocks TNFα secretion by monocytes (Rink, 1998). IL-4 induces differentiation of naive helper T cells into Th2 cells, and in macrophages IL-4 along with IL-13 induce alternative macrophage activation (Junttila, 2008). IL-9, as well as being an immune regulator, is found to be able to mediate the JAK-STAT pathway (Bianchi et al, 2000). IL-2, IL-21 and IL-22 stimulate proliferation and enhances function of T-cells, natural killer cells and B-cells (Malek, 2003).

An oversight of the project was excluding the proinflammatory cytokines IL-1β and IL-18 from the panel. IL-1β in particular is a key proinflammatory cytokine in the immune response. The NLRP3 inflammasome is responsible for caspase-1-dependent maturation of IL-1β and IL-18 (by cleaving pro-IL-1β and pro-IL-18 into their secretory forms) (McGeough et al, 2017), and

therefore a crucial piece of the puzzle was omitted. Analysis of IL-1β and IL-18 would have helped ascertain the potential contributions from NLRP3 inflammasome-driven mechanisms. IL-1β concentration is higher in septic patients than healthy controls; and found to be associated with severity and organ dysfunction and a predictor of sepsis mortality (Bozza et al, 2007).

Clinical characteristics that likely modify immune function (age, sex, comorbidities) were not matched in this small sample size, further complicating the results. The healthy volunteers were not comparable to the septic patient cohort. Furthermore, a pre-sepsis sample of the patients was lacking, and therefore the immune profile of the patients pre-sepsis is unknown. Any immune deficits they may have may be due to differences in immune response from before a septic insult. Patients with a non-septic, sterile critical illness should have been matched to septic patients as a control, as it is currently not clear if these trends are due to patient comorbidities or a phenomenon of critical illness unrelated to infection. Patients were also not matched for the type of sepsis, as different infections may result in different changes to the immune response.

Cytokine gene expression in sepsis survivors- persistent presence of CCL2

As some of the cytokines' gene expression did not rise in acutely septic patients, in opposition to well established literature. A possible explanation is that the primer-probes in the experiment malfunctioned. A melt curve was not performed as the primers were Taqman rather than SYBR Green, however an additional method of quality control should have been carried out to ensure the primers were working correctly. This was a large oversight. It is also possible the samples had degraded during processing- cDNA should have been checking via

qPCR and agarose gel to determine if it was suitable before commencing the experiment. In general quality control is a large weakness of this thesis due to inexperience at the time.

Interindividual variability accounted for most of the lack of differences within the samples.

CCL2 was present in the samples of septic patients at all three time points but was not present in any of the controls. CCL2 is triggered in response to a variety of inflammatory stimuli, including Il-1, -4, -6, TNFα, IFNγ and LPS (Yoshimura *et al*, 2018; Choi *et al,* 2017). CCL2 is a chemokine involved in recruitment of monocytes, T memory cells and dendritic cells to sites of infection and inflammation and encourages monocytes differentiation into M2 macrophages. However, not only does CCL2 orchestrate chemotaxis in lymphoid and myeloid cells under normal physiological immune reactions, it is also involved in pathological reactions and diseases such as autoimmune diseases, inflammatory diseases, infectious diseases and some types of cancer (Gschwandtner *et al,* 2019). Indeed, it has been assessed as a potential biomarker for prostate and breast cancer (Tsaur *et al,* 2015; Lubowicka *et al,* 2018). When CCL2 levels persist they are known to exacerbate inflammation through continued cell recruitment in inflammatory conditions such as rheumatoid arthritis and atherosclerosis (Stankovic *et al,* 2009; Harrington *et al,* 2000). This suggests, if the findings are to be validated by a larger study, that CCL2 may be a lingering artifact of the sepsis-induced immune dysregulation and inflammation. It is possible CCL2 may play a more direct role in immune function; in certain contexts, it has be shown to induce macrophage polarisation (Ruytinx *et al*, 2018), an upregulation of CCL2 encouraging M1 polarisation (Wang *et al*, 2014; Mu *et al*, 2017; Sodhi *et al*, 2002) and a downregulation of CCL2 encouraging M2 polarisation (Gu *et al*, 2017; Nio *et al*, 2012). Whilst it may seem suggestive that CCL2 can act as an inflammatory stimulus, in reality there is still not enough evidence to draw this conclusion- only Sodhi *et al*

of those mentioned confirmed that the CCL2 could be blocked by an anti-CCL2 antibody and that their CCL2 was endotoxin-free, and changes observed may have been due to other contaminants or other cellular changes unrelated to CCL2.

CCL2 gene expression was also the only cytokine gene to have a persistent change in the 6-12 months post hospital discharge samples compared to healthy volunteer levels. This suggests there may be lingering inflammation after the infection has cleared, even 6-12 months later, or else it is indicative of a dysregulation in immune function in general. This change appears to not be controlled by histone modifications however, as the CCL2 relative enrichment for the modifications H3K4me3, H3K9me3 and H3K27me3 remain the same for samples at all three time points and healthy donors. It is possible that something upstream of CCL2 is epigenetically controlled, or that CCL2 is regulated by another modification that was not examined.

Although the expression of CCL2 is interesting, the finding is not very impactful in the context of the hypothesis. Several reasons may be attributed to the patients showing levels of CCL2, for example their comorbidities (that healthy volunteers did not have), or the heterogenous pathophysiology pf their condition, or perhaps even the stay in ICU itself (there were no sterile ICU patients as a control).

Without restimulation, the gene expression of the other cytokines in the full patient cohort all had returned to reflect that of the healthy volunteers by 6-12 months post hospital discharge. This was mirrored in the concentrations of IL-10 and IL-6 found in the patient plasma, which had returned to healthy volunteer levels by 6-12 months post hospital discharge. However, when a small sample of patient PBMCs were rechallenged with LPS or

PMA/ionomycin, there may have been an indication of a deficit in their ability to produce certain cytokines, and this persisted even 6-12 months post hospital discharge. This could be reflective of patients returning to hospital with recurrent infections, but the sample size is too small to draw conclusions. For further research on a larger patient cohort, it would be wise to conduct flow cytometry on the cells to enable mapping of markers and cytokines within the cell. It is possible that the cytokine production is normal, but the cytokines are not being released from within the cell for example.

Persistent changes in gene expression of histone modifying enzymes in sepsis survivors

The gene expression of the selected enzymes involved in histone modifications did not change in bacteraemia patients compared to healthy volunteers. Not finding any changes in gene expression levels of these enzymes does not necessarily mean the enzymes did not elicit changes in the patients cells when septic. Furthermore, particularly at the <24 hours post positive blood culture time point, there were often a few patients who had particularly high upregulation of the genes compared to the majority. There may have been different subsets of patients who respond differently to bacteraemia with regards to gene expression of certain histone modifying enzymes. The groups were split further for analysis- into sepsis severity via SOFA score and via Ward/ICU admission, patient outcome, type of bacteria of infection, age- but none of these revealed a clear distinction within any groups. The heterogeneity of the patient samples make it difficult to determine whether there really were no changes of if changes in a specific sub group were masked. To date there have not been any published studies examining the gene expression in histone modifying enzymes in septic patients or infection and so it is difficult to put it into context.

Chromatin Immunoprecipitation optimisation

Chromatin Immunoprecipitation could not be optimised on most of the patient cohort whose PBMCs were frozen in PBS 2% FBS, a way that it incompatible with ChIP due to the cells bursting and damaging the DNA. Many protocols were tried and adapted, however it was not possible to get a consistent result that would be needed for the patient PBMCs when practising with healthy donor PBMCs frozen in the same way as the patient samples. The Active Motif ChIP kit, which worked best for cells frozen in the correct way (DNA remaining intact), did not at all work for the incorrectly frozen samples despite alterations to the protocol. Several other protocols were employed, from the literature as well as novel ones, and stitched together to finally make a protocol that would mostly work for H3K4me3 but not the other modifications. Even then, the result of H3K4me3 was not consistent, working about 70% of the time only. There may have been a way to optimise ChIP for these incorrectly stored samples after continuously tweaking the protocols, however due to time constraints it was decided to not use them this time. It was a great shame that the 65 patient's samples could not be used, however it is best to store them for a time when a different compatible experiment makes sense. DNA methylation was also attempted on incorrectly stored controls, but again this did not work. The cells burst and their DNA is damaged, and so epigenetics studies are not suitable for these samples. It is possible that a western blot could be performed on proteins if they are not also damaged, but it was decided to instead go on with ChIP on the few samples that were stored correctly. For the correctly stored samples, the best protocol was the Active Motif ChIP kit, and so that was what was used.

Septic patient samples show persistent changes in histone modifications to certain genes.

ChIP performed on these correctly stored patient samples yielded interesting results. For the

gene activation marker H3K4me3, the promotors of GAPDH and IRAK-M were lower than healthy donors in the first few days of sepsis but by 12 months post hospital discharge they were higher than healthy donors. In recovery there appears to be a persistent overcompensation of GAPDH and IRAK-M. The promotors of IL-10, mTOR, and TLR4 had a reduction in relative enrichment of H3K4me3 compared to healthy donors, and this reduction persists even into recovery, significantly so for IL-10 and mTOR. Another activation marker, H3K9Ac, had a higher relative enrichment in patients than healthy donors that persisted even 12 months post hospital discharge for GAPDH, IRAK-M, and this time also for TLR4 and mTOR. For this modification there was also increased relative enrichment in the first few days of sepsis. For the patients, neither of the two gene repression makers H3K9me3 or H3K27me3 returned any differences.

When mimicking acute sepsis, different histone modification patterns were observed.

ChIP on healthy volunteer PBMCs that were cultured in septic serum returned different results. This may be due to the fact that the cells were only cultured in the serum for 2 hours prior to harvest, but these cells were cultured parallel to the seahorse experiments in the next chapter. They also utilised pooled *E.coli* septic serum which may account for differences.

The investigation used targeted ChIP due to budget constraints, however ChIP-Seq would provide a complete picture of the gene changes associated with each modification. On the other hand, targeted ChIP is a more suitable technique when the genes of interest are known, as they can be assessed more easily and accurately. The modifications selected were also the ones most associated with infection and sepsis, but an increased number of modifications could have been examined to gain a more complete understanding of the changes to histones. Furthermore, histone modifications are just one example of epigenetic changes, but it is the

most associated with sepsis and infections, whereas other epigenetic changes such as DNA methylation in sepsis returned very little results.

Further research

The extent of the immune defect persistence should be further examined, such as whether these epigenetic changes are lifelong and can be passed on via meiosis. An interesting experiment would be to examine offspring of sepsis survivors (murine/ human) to see if their immune function and epigenetic patterns are similar to their parents. In a murine model epigenetics can be examined before sepsis, after sepsis, then compared to the profile of the offspring- which can be born both before and after the parents were septic. Whether the specific changes in histone modifications detailed in this chapter would carry over into a murine model is not yet known. A further complicating factor in fully ascertaining the persistence of the effects of sepsis post hospital discharge is that most often the patients are older and have a plethora of comorbidities. They require a more complex management clinically which may itself effect epigenetics and will make it difficult to gather a large homogenous sample size to draw sepsis-specific conclusions from. A heterogenous sample was the biggest limitation of the gene expression data on the whole patient cohort, who had a variety of comorbidities, severities, and types of bacteria. Therefore, it resources and attainability allow it, study participants should be younger and without comorbid conditions, and with similar infections (e.g. all *E.coli* sepsis) in future work.

Summary

Patients recovered from an infectious insult display features of immune suppression which could be attributable to infection induced histone modifications. What was not yet clear, however, is whether this is due to the infection itself or its concomitant treatments. The

epigenetic impact of different clinical interventions in sepsis should be assessed, as the changes found may be partially attributable to these treatments rather than the infection itself. Key areas to assess would be sedatives, muscle relaxants, vasopressors, catecholamines, steroids, and antibiotic treatments. The sedative Propofol and the muscle relaxant Rocuronium are examined in subsequent chapters of this thesis.

Chapter 4: Epigenetics of sedation

4.1 Introduction

It is estimated that 55-70% of septic patients in intensive care require intubation and mechanical ventilation (Rivers et al, 2001), all of whom will therefore require sedation (Hogarth et al, 2004). The most widely used sedative in general anaesthesia is Propofol (Patel et al, 2012; Jakob et al, 2012).

Propofol has been demonstrated to elicit anti-inflammatory effects in human and animal models (Runzer et al, 2002; Murphy et al, 1992; Chen et al, 2002). In a murine model of bloodstream MRSA, Propofol increased populations of MDSCs and exacerbated the kidney pathology and dissemination of bacteria (Visvabharathy et al, 2017).

Furthermore, studies suggest that Propofol-induced suppression of immune function may be caused by Propofol inhibiting cells mitochondrial membrane potential (Chen et al, 2003). Growing evidence suggests that Propofol Infusion Syndrome (PRIS) may have a mitochondrial origin (Branca et al, 1991; Schenkman et al, 2000; Shimizu et al, 2019; Krajčová et al, 2018).

Broad defects in oxidative phosphorylation and glycolysis appear to underlie immunosuppression in sepsis (Cheng S *et al*, 2016). Both hyper- and hypo-inflammatory phases result in major shifts away from basal homeostasis. The phenotypic phase shifts of immune cells may in fact follow on from key metabolic shifts. These alterations in leukocyte metabolism may be attributable to concomitant treatments such as Propofol administration.

Hypothesis The administration of Propofol will contribute to immunometabolic changes in sepsis

Aims:

1: To assess immunometabolic changes when Propofol is administered to host cells

2: To determine if effects of Propofol persist in immune cells after the Propofol has been removed and cells left to recover

3: To describe the acquisition of histone modifications in immune cells as a result of Propofol exposure

4.2 Methods

4.2.1 Patient cohort

Peripheral blood mononuclear cells (PBMCs) from healthy donor volunteers (n=8) were exposed to 10% serum from patients who were blood culture positive with *Escherichia coli (E.coli*) sepsis and were either sedated or non-sedated, with serum from non-septic healthy volunteers serving as a control. The "sedated" patient was sedated with Propofol and was also treated with noradrenaline and fentanyl. Table 4.1 details the demographics of the sedated and non-sedated patient used in this research.

Table 4.2.1 Demographics of the septic patients from which the serum was drawn.

	Propofol-sedated patient	Non-sedated patient
Age	51	48
Sex	Male	Male
Sensitivity	Co-amoxiclav, Tazocin, Gentamicin, Amikacin	Co-amoxiclav, Tazocin, Gentamicin, Amikacin
Level of care	ICU	Ward
SOFA score	7	2
Ventilation days	3	-
Vasoactive Rx days	2	-
Chronic conditions	Nil	Nil

Serum was taken from the septic patients at two different time points; when they were acutely septic (<24 hours after blood culture positive result) and 7 days later when they had recovered from the infection but were still in hospital.

4.2.2 Immunometabolic profiling

The Seahorse extracellular flux analyser was utilised to read cells' immunometabolic profiles in real-time and assess their bioenergetic function.

Cell viability was assessed upon thawing and before the seahorse experiment via haemocytometer and Trypan Blue. Propofol concentration ascertained based on a Seahorse assay run with PBMCs at concentrations form 1-10µg/ml, and the concentration of 4µg/ml was chosen due to it being the highest dose to have an impact without reducing cell viability.

4.2.3 Seahorse Experiment 1: Donor PBMCs exposed to septic patient serum with and without Propofol

The healthy donor PBMCs (n=8) were freshly drawn and loaded into the Seahorse analyser. The cells were injected with either pooled healthy donor serum, serum from an acute sepsis Propofol-sedated patient, serum from the Propofol-sedated patient once recovered from sepsis, an acute sepsis non-sedated patient, or serum from the non-sedated patient once recovered from sepsis, and their immunometabolism was read in real-time. The recovered serum samples were taken 7 days after hospital admission when the infection was cleared, and the patient who had been receiving sedation had been off sedation for 4 days before the sample was taken. Figure 4.2.2.1 details the experimental design.

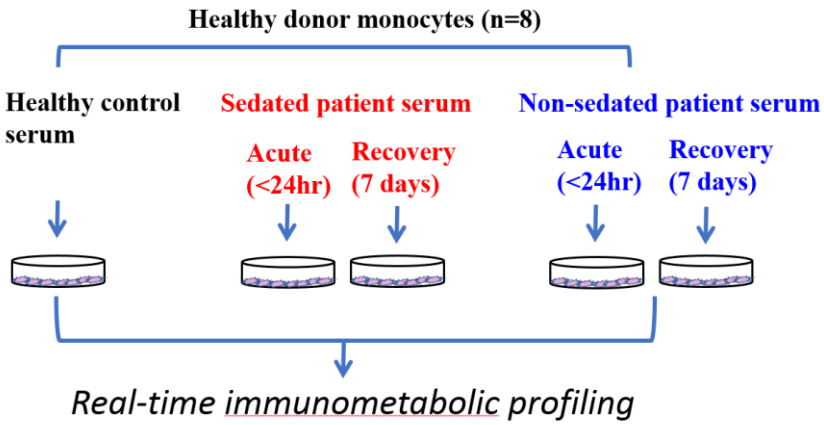

Figure 4.2.2.1 Methodology for culture of PBMCs with patient serum for seahorse assay.

The cells were exposed to the different sera in a Seahorse XFe96 assay, where their cellular respirometry was measured in real-time. The Seahorse XFe96 methodology is described in full in Chapter 2.

4.2.4 Seahorse Experiment 2: THP1 cell line Propofol exposure and recovery

THP1 Null and NLRP3-/- cells were divided into four testing categories each- 48 hour stimulation with 10% pooled serum that was either: acutely septic, acutely septic with Propofol (4µg/ml), healthy donor, or healthy donor with Propofol (4µg/ml). The acutely septic serum had been pooled from 15 *E.coli* septic patients who were all on Ward and were not sedated or administered any inotropes/ ventilation, and their bloods were drawn within 24 hours of a positive blood culture result. The healthy donor serum was pooled from 4 volunteers. After the 48 hours' incubation, cells were washed twice with pre-warmed PBS and then left to recover for two days in 10% healthy donor serum. After the recovery period, cells were transferred to FAO media and loaded into a Seahorse XFe analyser where the cells were rechallenged with either septic serum, healthy volunteer serum, or PMA.

Figure 4.2.2.2 depicts the four pre-treatment groups workflow.

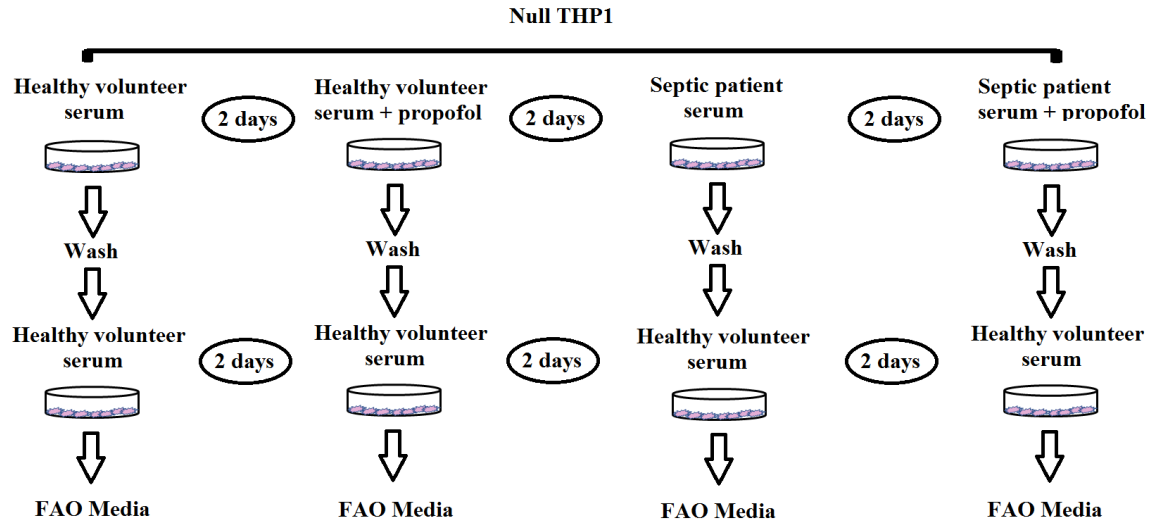

Figure 4.2.2.2 Null THP1 pre-treatment groups. The cells were divided into four pre-treatment groups; RPMI with 10% serum from either healthy volunteers or septic *E.coli* patients, and treated with or without Propofol at a final concentration of 4µg/ml. The cells were all cultured for two days then washed, and then all cells were cultured for a further two days in 10% healthy volunteer serum to recover. Finally, cells were transferred to FAO medium two hours before the Seahorse assay run.

4.2.5 Seahorse Experiment 3: Propofol recovered THP1 cells rechallenged with septic serum with and without Propofol

THP1 Null and NLRP3-/- cells were divided into two testing categories: 72 hour stimulation with 10% acutely septic serum that either contained Propofol (4µg/ml) or did not. The groups that were cultured in Propofol are referred to as “sedated” vs their “non-sedated” counterparts. After the 72 hours’ incubation, cells were washed twice with pre-warmed PBS and then left to recover for three days in 10% healthy donor serum. After the recovery period, cells were transferred to FAO media and loaded into a Seahorse XFe analyser where the cells were rechallenged with either septic serum alone, or septic serum with Propofol (4µg/ml).

4.2.6 Seahorse Experiment 4: Propofol recovery length time-course

The bioenergetic effect of the length of recovery time from Propofol administration was assessed in this experiment. THP1 Null cells were divided into three testing categories: 60 hour culture in healthy donor serum, healthy donor serum with Propofol, or no serum added (nil treatment). Cells were washed twice after their 60 hour pretreatments. Then, each pretreatment group was left for three different lengths of recovery before being run in the Seahorse: either 24 hour recovery after wash, 48 hour recovery after wash, or 72 hour recovery after wash. Cells were all initially plated at the same time, but the administration of the pretreatment was staggered depending on required recovery length so that they all went into the Seahorse at the same time. In the Seahorse, cells were all rechallenged with septic serum.

4.2.7 Seahorse Experiment 5: Propofol recovered cells rechallenged with Etomoxir in FAO study

THP1 Null cells were divided into the same four testing categories as Seahorse Experiment 2- 48 hour stimulation with 10% pooled serum that was either: acutely septic, acutely septic with Propofol (4μg/ml), healthy donor, or healthy donor with Propofol (4μg/ml). The layout can be found in Figure 4.2.2.2. After the 48 hours' incubation, cells were washed twice with pre-warmed PBS and then left to recover for two days in 10% healthy donor serum. After the recovery period, cells were transferred to FAO media. 15 minutes before the Seahorse assay run, cells were given either the inhibitor Etomoxir (40μM final) or assay buffer (control). Right before the run, each condition was given either Palmitate:BSA or BSA control.

Figure 4.2.2.3 depicts the workflow of inhibitor and palmitate treatment for each of the pre-treated conditions.

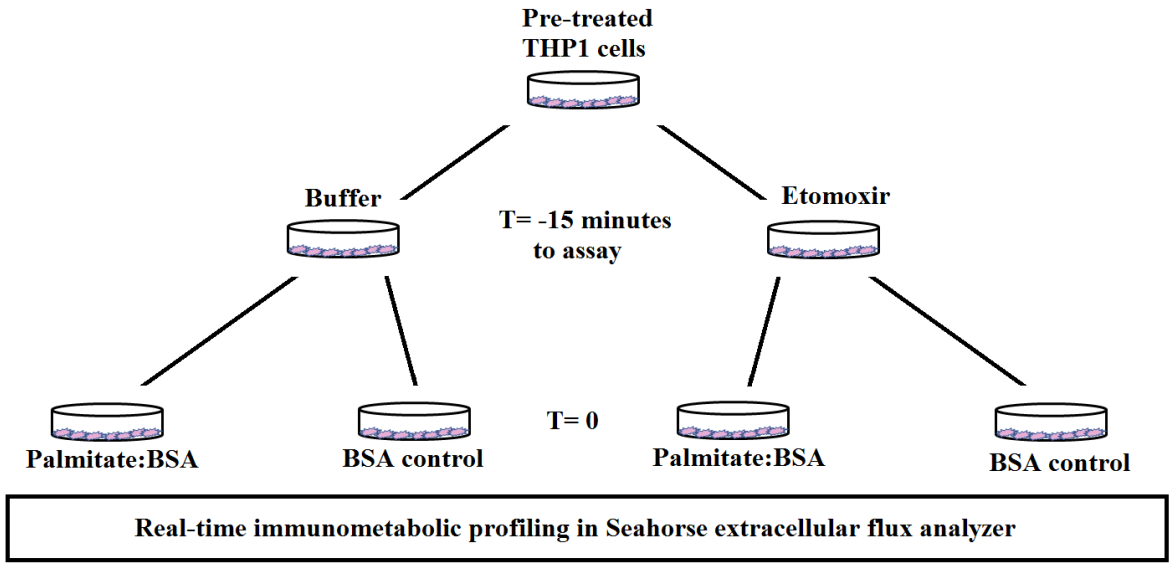

Figure 4.2.2.3 The pre-treated cells were divided so that half received Etomoxir or assay buffer (control) 15 minutes before the assay run. Right before the assay run, cells were administered either Palmitate:BSA or a BSA control.

4.2.8 Seahorse Experiment 6: Propofol recovered cells rechallenged with Etomoxir without Palmitate

THP1 Null and NLRP3-/- cells were divided into the same four testing categories as Seahorse Experiment 2- 48 hour stimulation with 10% pooled serum that was either: acutely septic, acutely septic with Propofol (4µg/ml), healthy donor, or healthy donor with Propofol (4µg/ml). The layout can be found in Figure 4.2.2.2. After the 48 hours' incubation, cells were washed twice with pre-warmed PBS and then left to recover for two days in 10% healthy donor serum. After the recovery period, cells were transferred to FAO media. In the Seahorse analyser, cells were rechallenged with septic serum with or without Etomoxir (40µM final).

4.2.9 Gene expression

THP1 Null (n=3) and NLRP3-/- (n=3) cells were cultured in 10% healthy volunteer serum either with or without Propofol (4μg/ml) for 24 hours. After 24 hours, the cells were washed twice in PBS and left to recover for three days. The gene expression of PINK1 and Parkin was then assessed via qPCR.

4.2.10 Histone modifications

Chromatin Immunoprecipitation was performed on THP1 Null cells that were cultured for three days in 10% serum with (n=6) or without (n=6) 4μg/ml Propofol, washed twice in PBS, then cultured for a further three days to recover before harvest. The histone modifications examined were H3K4me3, H3K27me3, and H3K9me3. Metabolic genes GAPDH, mTOR, HIF1α, EIR4EBP1, and IRAK-M were assessed using targeted qPCR.

4.3 Results

For quality control, the shapes of the normalised OCR and ECAR data for each Seahorse experiment was examined after the run to ensure the cells in each well were functioning correctly and reacting to the mitochondrial poisons. A representative figure is pictured below, from Seahorse experiment 1.

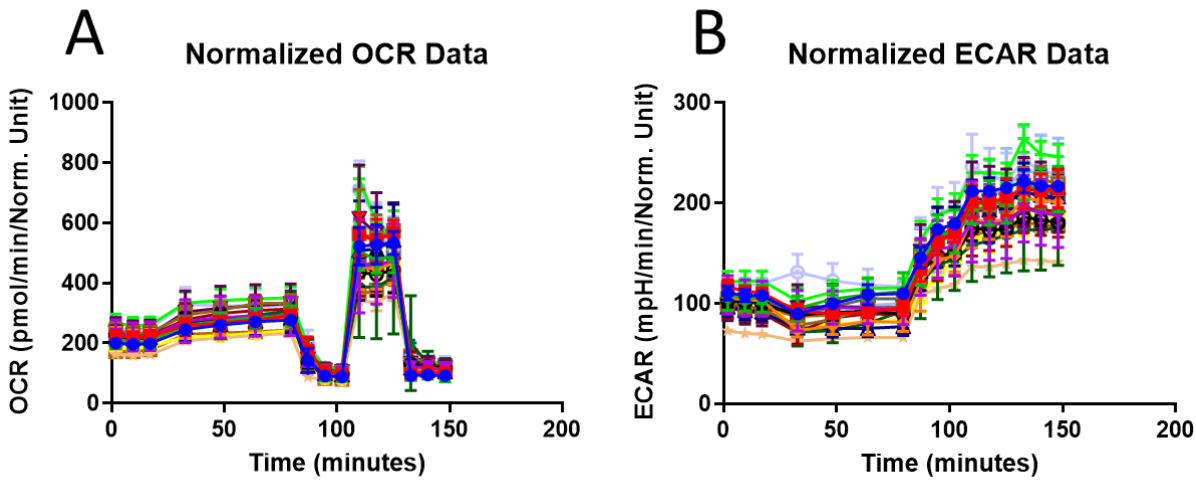

Figure 4.3 Normalised OCR (A) and ECAR (B) data from Seahorse experiment 1.

4.3.1 Seahorse Experiment 1: Donor PBMCs exposed to septic patient serum with and without Propofol

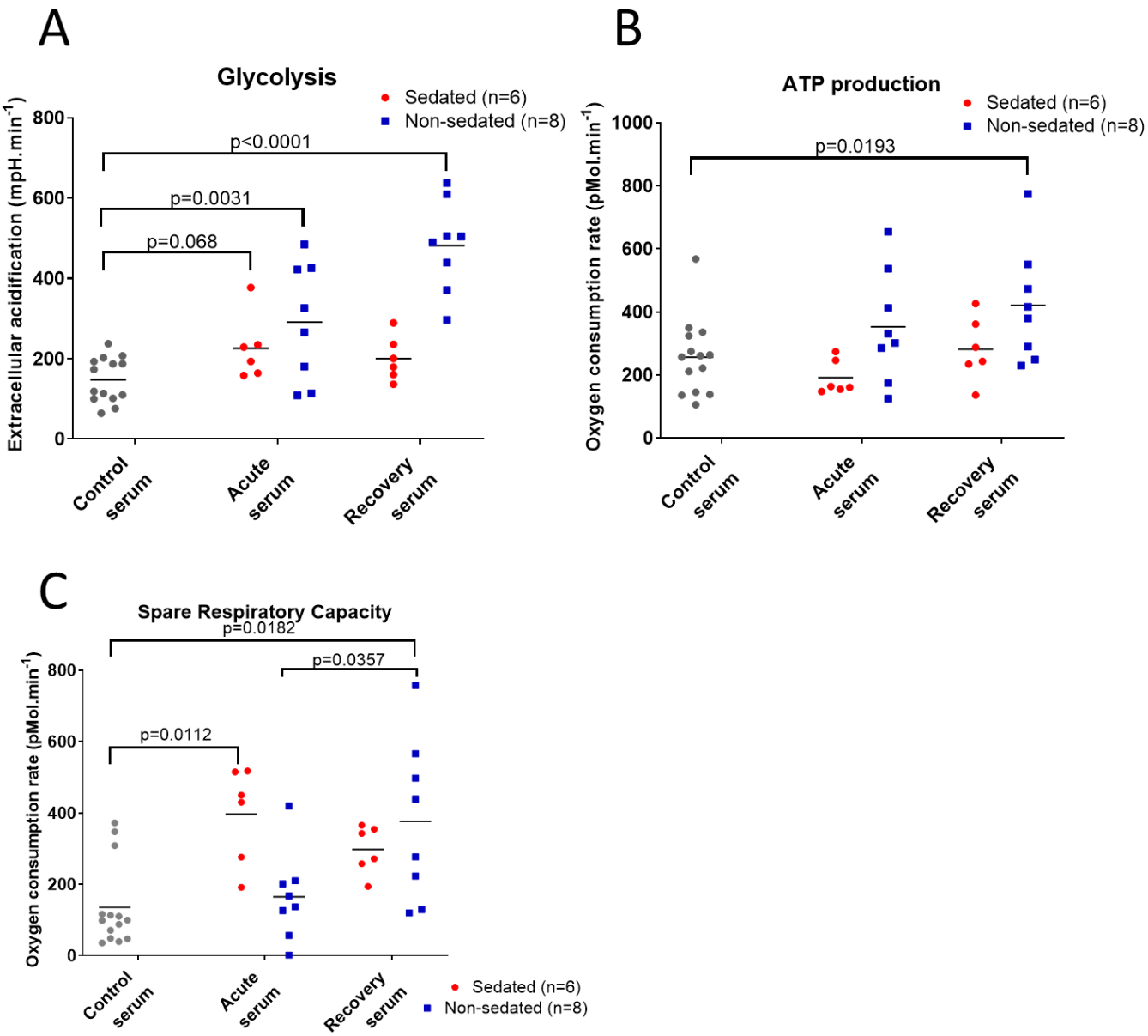

Figure 4.3.1.1 A) Glycolysis after treatment with serum collected at different stages of sepsis, from Propofol-sedated vs non-sedated patients. B) OCR after treatment with serum collected at different stages of sepsis, from Propofol-sedated vs non-sedated patients. C) Spare Respiratory Capacity after treatment with serum collected at different stages of sepsis, from Propofol-sedated vs non-sedated patients. All comparisons were made to healthy control serum (Friedman test with Dunn post-hoc test). Lines represent the means, with controls in grey, sedated patients in red, and non-sedated patients in blue. All values were standardised to µg.protein/well.

Glycolysis was higher in PBMCs cultured with non-sedated serum compared to controls, however serum from the Propofol-sedated patient appeared to not demonstrate this increase in glycolysis.

Sedation with Propofol on admission to hospital was associated with suppressed PBMC estimated ATP production which persisted even 7 days later when the patient was recovered from the infection.

While there is a marked increase in the SRC in recovered serum from the non-sedated patient compared to acute and control serum, this effect is not seen in the serum from the Propofol-sedated patient. In the Propofol-sedated patient, the SRC is higher in acute than recovery.

4.3.2 Seahorse Experiment 2: THP1 cell line Propofol exposure and recovery

THP1 Null and NLRP3-/- cell lines were exposed to septic or healthy volunteer serum with and without Propofol, washed and left to recover, then persistent changes to immunometabolism were assessed using the Seahorse XF methodology.

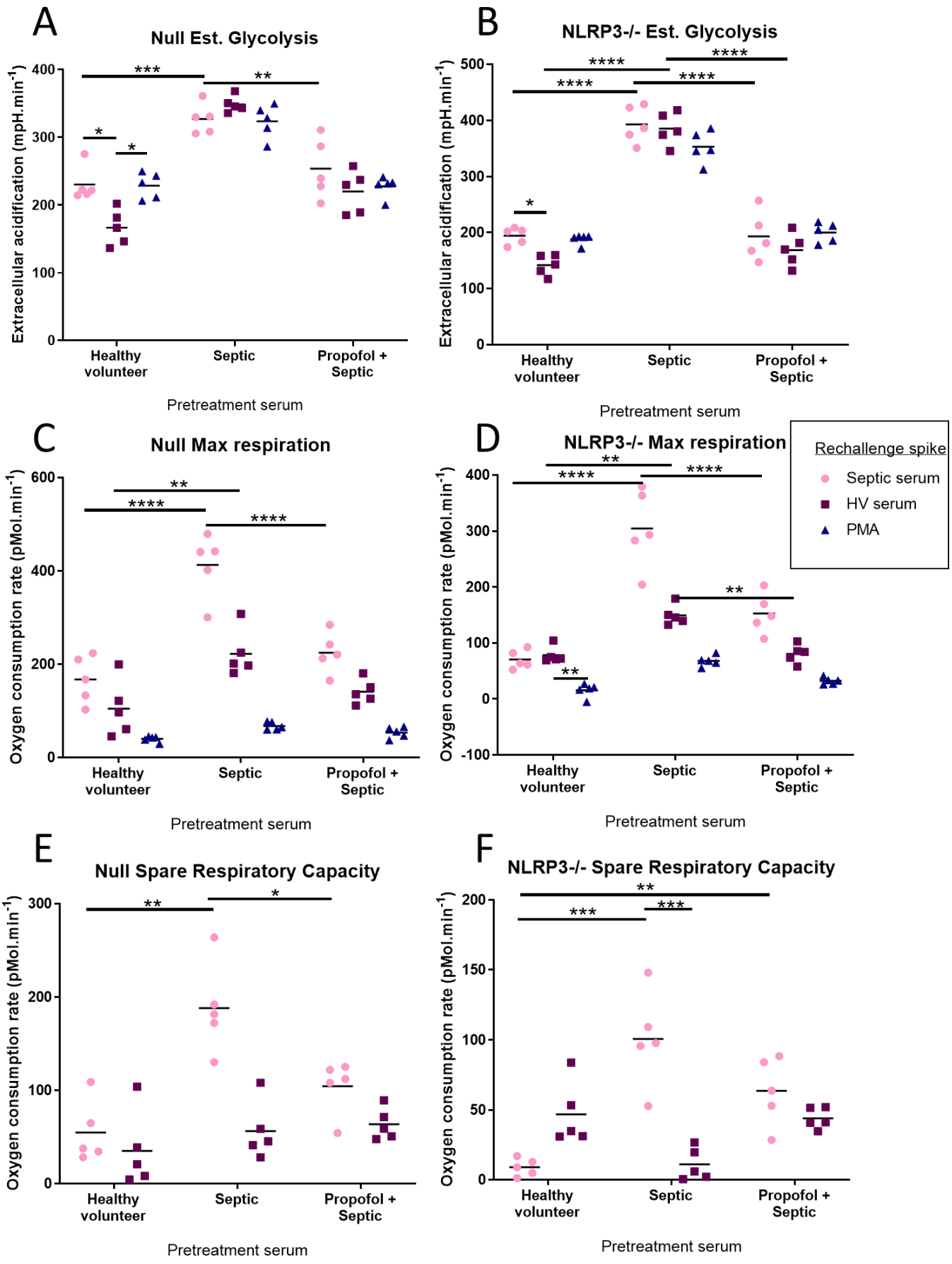
A
Null Est. Glycolysis
Extracellular acidification (mpH.min-1)
400
300
200
100
0
***
**
*
*
Healthy volunteer
Septic
Propofol + Septic
Pretreatment serum
B
NLRP3-/- Est. Glycolysis
Extracellular acidification (mpH.min-1)
500
400
300
200
100
0
****
****
****
****
*
Healthy volunteer
Septic
Propofol + Septic
Pretreatment serum
C
Null Max respiration
Oxygen consumption rate (pMol.min-1)
600
400
200
0
**
****
****
Healthy volunteer
Septic
Propofol + Septic
Pretreatment serum
D
NLRP3-/- Max respiration
Oxygen consumption rate (pMol.min-1)
400
300
200
100
0
-100
**
****
****
**
**
Healthy volunteer
Septic
Propofol + Septic
Pretreatment serum
Rechallenge spike
Septic serum
HV serum
PMA
E
Null Spare Respiratory Capacity
Oxygen consumption rate (pMol.min-1)
300
200
100
0
**
*
Healthy volunteer
Septic
Propofol + Septic
Pretreatment serum
F
NLRP3-/- Spare Respiratory Capacity
Oxygen consumption rate (pMol.min-1)
200
150
100
50
0
**
***
***
Healthy volunteer
Septic
Propofol + Septic
Pretreatment serum

Figure 4.3.2.1 The estimated A) and B) Glycolysis, C) and D) Maximum respiration, E) and F) Spare respiratory capacity for each THP1 pre-treatment group rechallenged with either septic serum (pink bars), healthy volunteer (HV) serum (maroon bars) or PMA (navy bars), for the THP1 genotypes Null (A, C, E) and NLRP3-/- (B,D,F). Pretreatments were cells cultured in 10% serum that was either healthy volunteer, septic, or septic plus propofol for two days then washed and left to recover for a further two days. Glycolysis was estimated from the extracellular acidification ($mpH.min^{-1}$) when exposed to serum prior to oligomycin injection. Maximum respiration was calculated from the oxygen consumption rate ($pMol.min^{-1}$) of the maximum rate measurement after FCCP injection minus the non-mitochondrial respiration. The SRC was calculated from the oxygen consumption rate ($pMol.min^{-1}$) of the maximal respiration minus the basal respiration after serum was added. A p-value less than 0.05 is flagged with one star (*), a p-value is less than 0.01 is flagged with two stars (**), a p-value is less than 0.001is flagged with three stars (***) and a p-value is less than 0.0001 is flagged with four stars (****). All comparisons were made Friedman test with Dunn post-hoc test. Lines represent the mean. All values were standardised to µg.protein/well.

For both the Null THP1 cells and NLRP3-/- THP1 cells, cells which were pretreated with septic serum had an overall higher estimated glycolysis when rechallenged than cells pretreated with healthy volunteer serum or with septic serum and propofol. In cells pretreated with healthy volunteer serum, a rechallenge of healthy volunteer serum resulted in lower extracellular acidification than when restimulated with septic serum or PMA.

Furthermore, the maximum respiration of both the Null and NLRP3-/- cells followed a similar pattern to the glycolysis, where the cells pretreated with septic serum had a higher overall oxygen consumption rate than cells pretreated with healthy volunteer serum and cells pretreated with septic serum with the addition of propofol. The cells responded to sepsis with an increase in oxidative phosphorylation.

From the maximum respiration the cells bioenergetic reserve, the Spare Respiratory Capacity (SRC), was calculated for rechallenge with septic or healthy volunteer serum. Cells pretreated with septic serum had a higher SRC when exposed to septic serum in both the Null and NLRP3-/- genotypes, and the response in cells pretreated with propofol was reduced.

4.3.3 Seahorse Experiment 3: Propofol recovered THP1 cells rechallenged with septic serum with and without Propofol

A similar experimental design was repeated. Cells were stimulated and recovered for three days each rather than two.

Glycolysis

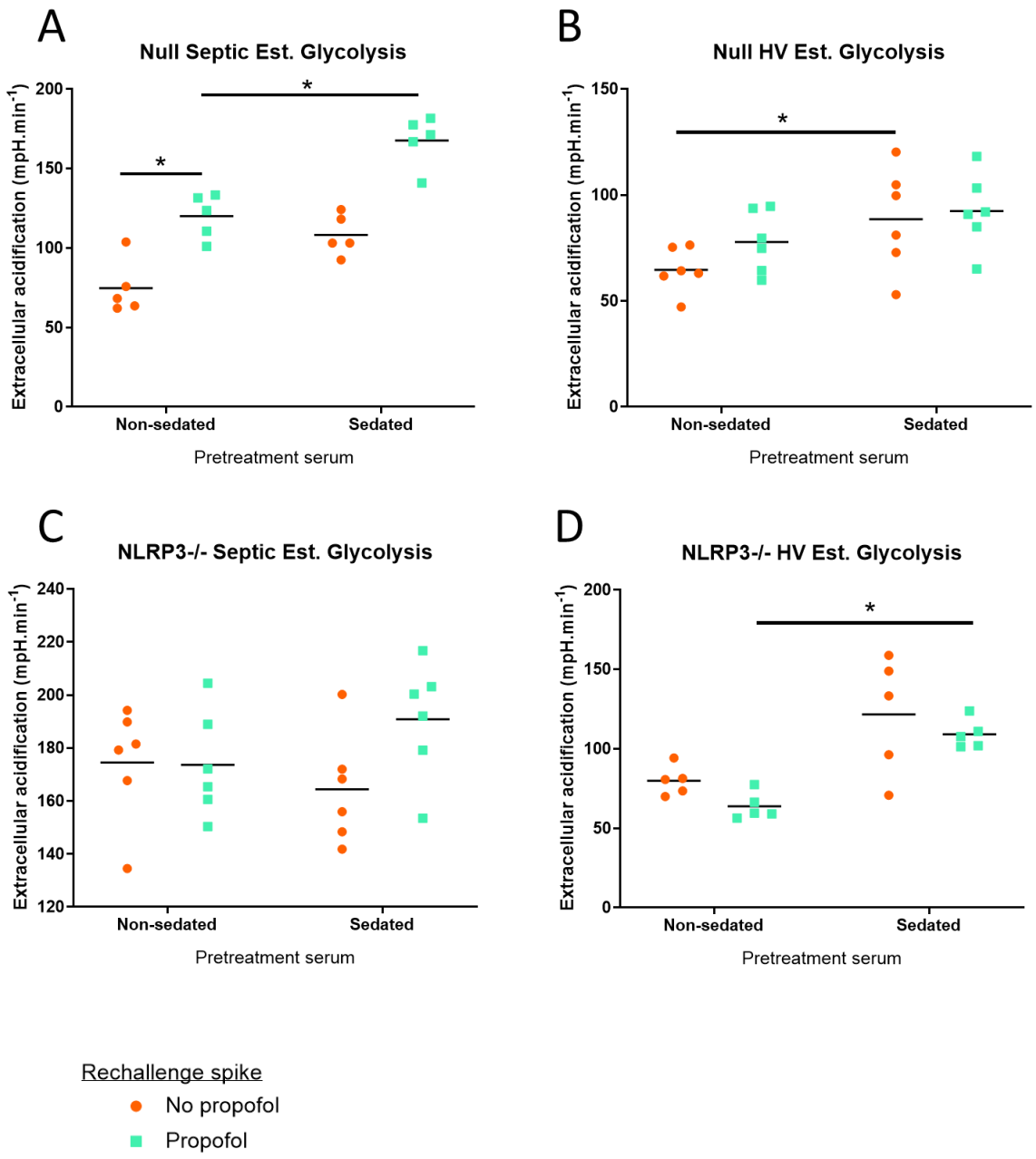

Figure 4.3.3.1 The estimated glycolysis for each THP1 pre-treatment group rechallenged with either septic serum (tangerine bars) or septic serum with propofol (mint bars), for the THP1 genotypes Null (A, B) and NLRP3-/- (C, D). Pretreatments were cells cultured in either 10% septic serum with propofol (sedated) or without propofol (non-sedated) (A, C) or with either 10% healthy volunteer serum serum with propofol (sedated) or without propofol (non-sedated) (B,D) for three days then washed and left to recover for a further three days. Glycolysis was estimated from the extracellular acidification ($mpH.min^{-1}$) when exposed to serum prior to oligomycin injection. A p-value less than 0.05 is flagged with one star (*), a p-value is less than 0.01 is flagged with two stars (**), a p-value is less than 0.001is flagged with three stars (***) and a p-value is less than 0.0001 is flagged with four stars (****). All comparisons were made with Freidman test with Dunn post-hoc test. Line represent the means. All values were standardised to µg.protein/well.

In the Null THP1s, when the cells were exposed to septic serum with propofol acutely glycolysis was higher than when exposed to septic serum alone, and was the case in both non-sedated (p=0.0399) and sedated (p= 0.0158) conditions. Furthermore, when cells were pretreated with propofol (sedated) and then rechallenged with propofol acutely, the glycolysis was higher than the non-sedated pretreated cells when exposed to propofol acutely (p=0.0340). In contrast, with the NLRP3-/- genotype there were no differences between any of the conditions.

When cells were pretreated with healthy volunteer serum, a similar increase in glycolysis was observed in the cells receiving propofol in their pretreatment serum (sedated), however this time the effect was translated to both Null and NLRP3-/- genotypes. Within the non-sedated conditions there was no difference in glycolysis between the healthy volunteer and healthy volunteer plus propofol rechallenges, and this effect was also seen in the sedated pretreatment and was observed in both genotypes.

Maximum respiration

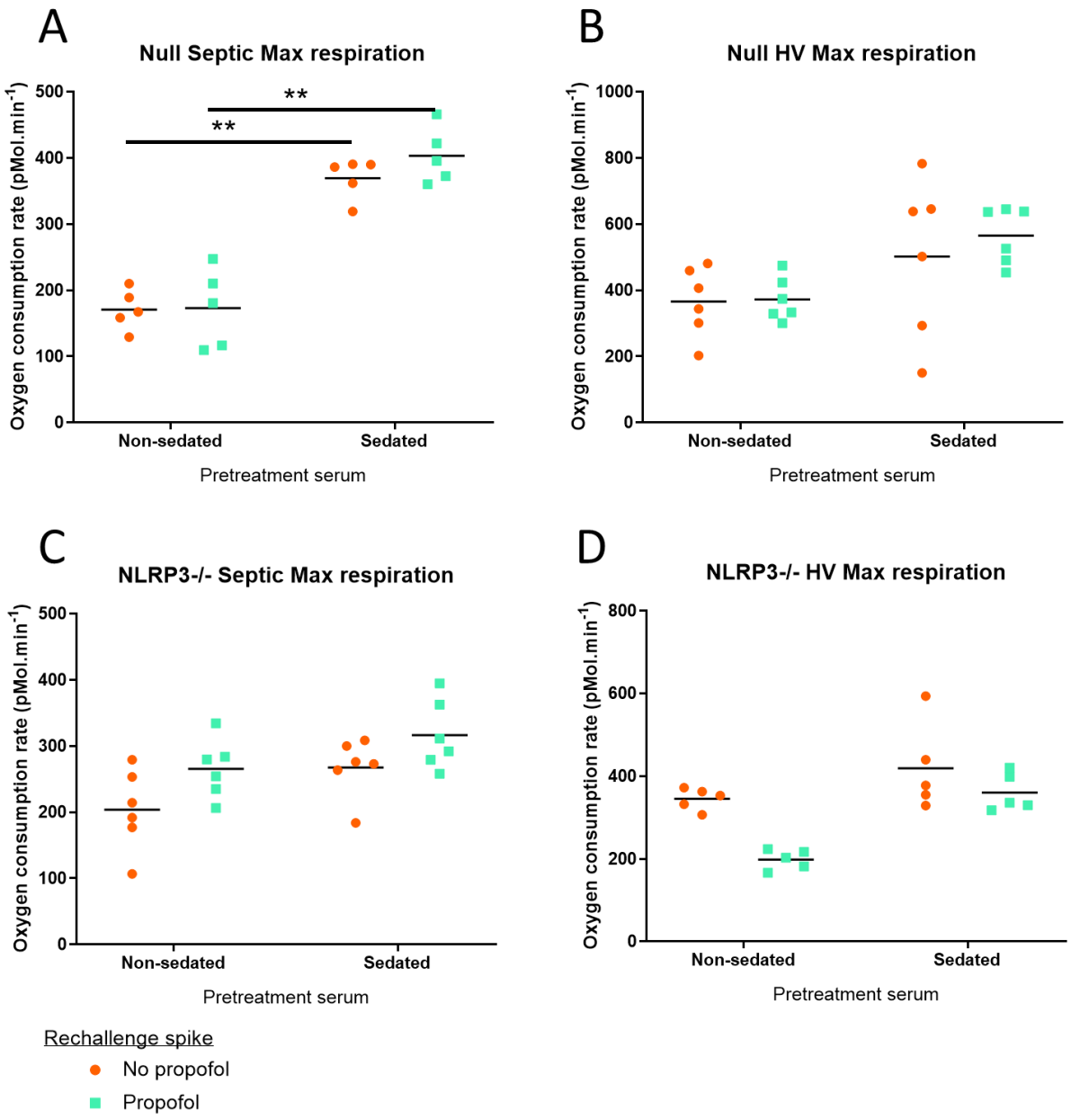

Figure 4.3.3.2 The maximum respiration for each THP1 pre-treatment group rechallenged with either septic serum (tangerine bars) or septic serum with propofol (mint bars), for the THP1 genotypes Null (A, B) and NLRP3-/- (C, D). Pretreatments were cells cultured in either 10% septic serum with propofol (sedated) or without propofol (non-sedated) (A, C) or with either 10% healthy volunteer serum serum with propofol (sedated) or without propofol (non-sedated) (B,D) for three days then washed and left to recover for a further three days. Glycolysis was estimated from the extracellular acidification ($mpH.min^{-1}$) when exposed to serum prior to oligomycin injection. A p-value less than 0.05 is flagged with one star (*), a p-value is less than 0.01 is flagged with two stars (**), a p-value is less than 0.001is flagged with three stars (***) and a p-value is less than 0.0001 is flagged with four stars (****). All comparisons were made with Freidman test with Dunn post-hoc test. Line represent the means. All values were standardised to µg.protein/well.

In the Null THP1s exposed to a septic serum rechallenge, there was a difference in maximum respiration between sedated and non-sedated pretreatments, which was also the case when rechallenged with septic serum with propofol acutely. Cells pretreated with propofol (sedated) had a higher maximum respiration with both rechallenged conditions than the non-sedated pretreatment. There were no differences between the non-sedated rechallenge spikes or the sedated rechallenge spikes. In contrast, with the NLRP3-/- genotype there were no differences between any of the conditions.

When cells were pretreated with health volunteer (HV) serum, there were no differences in maximum respiration between conditions in either genotype.

Estimated ATP production

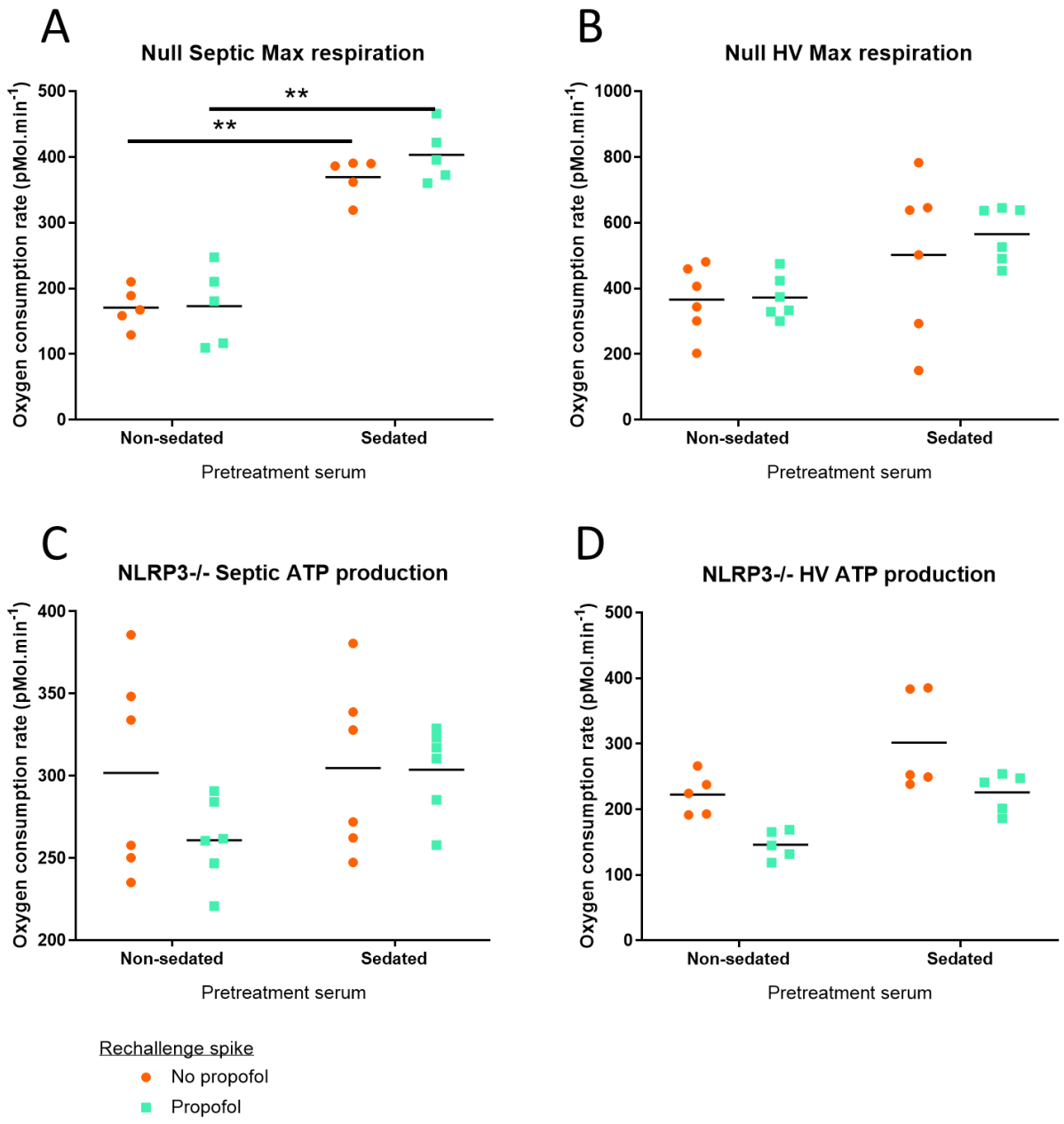

Figure 4.3.3.3 The ATP for each THP1 pre-treatment group rechallenged with either septic serum (tangerine bars) or septic serum with propofol (mint bars), for the THP1 genotypes Null (A, B) and NLRP3-/- (C, D). Pretreatments were cells cultured in either 10% septic serum with propofol (sedated) or without propofol (non-sedated) (A, C) or with either 10% healthy volunteer serum serum with propofol (sedated) or without propofol (non-sedated) (B,D) for three days then washed and left to recover for a further three days. Glycolysis was estimated from the extracellular acidification ($mpH.min^{-1}$) when exposed to serum prior to oligomycin injection. A p-value less than 0.05 is flagged

with one star (*), a p-value is less than 0.01 is flagged with two stars (**), a p-value is less than 0.001is flagged with three stars (***) and a p-value is less than 0.0001 is flagged with four stars (****). All comparisons were made with Freidman test with Dunn post-hoc test. Line represent the means. All values were standardised to µg.protein/well.

In the Null THP1s exposed to a septic serum rechallenge, there was a difference in ATP production between sedated and non-sedated pretreatments, which was also the case when rechallenged with septic serum with propofol acutely. Cells pretreated with propofol (sedated) had a higher ATP production with both rechallenge conditions than the non-sedated pretreatment. There was a difference between the rechallenge spike of either septic serum alone or septic serum with propofol acutely with cells in the sedated pretreatment condition (p=0.018). However, in the NLRP3-/- genotype there were no differences between pretreatment and rechallenge combinations.

Similarly, Null THP1s exposed to a healthy volunteer (HV) serum rechallenge had a difference in ATP production between sedated and non-sedated pretreatments, which was also the case when rechallenged with HV serum with propofol acutely. Cells pretreated with propofol (sedated) had a higher ATP production with both rechallenge conditions than the non-sedated pretreatment. The NLRP3-/- genotype again had no differences between pretreatment and rechallenge combinations.

4.3.4 Seahorse Experiment 4: Propofol recovery length time-course

To further investigate this phenomenon, a recovery timecourse experiment was performed. The bioenergetic function of Null THP1 cells of differing lengths of recovery period following a 48 hour pretreatment were compared.

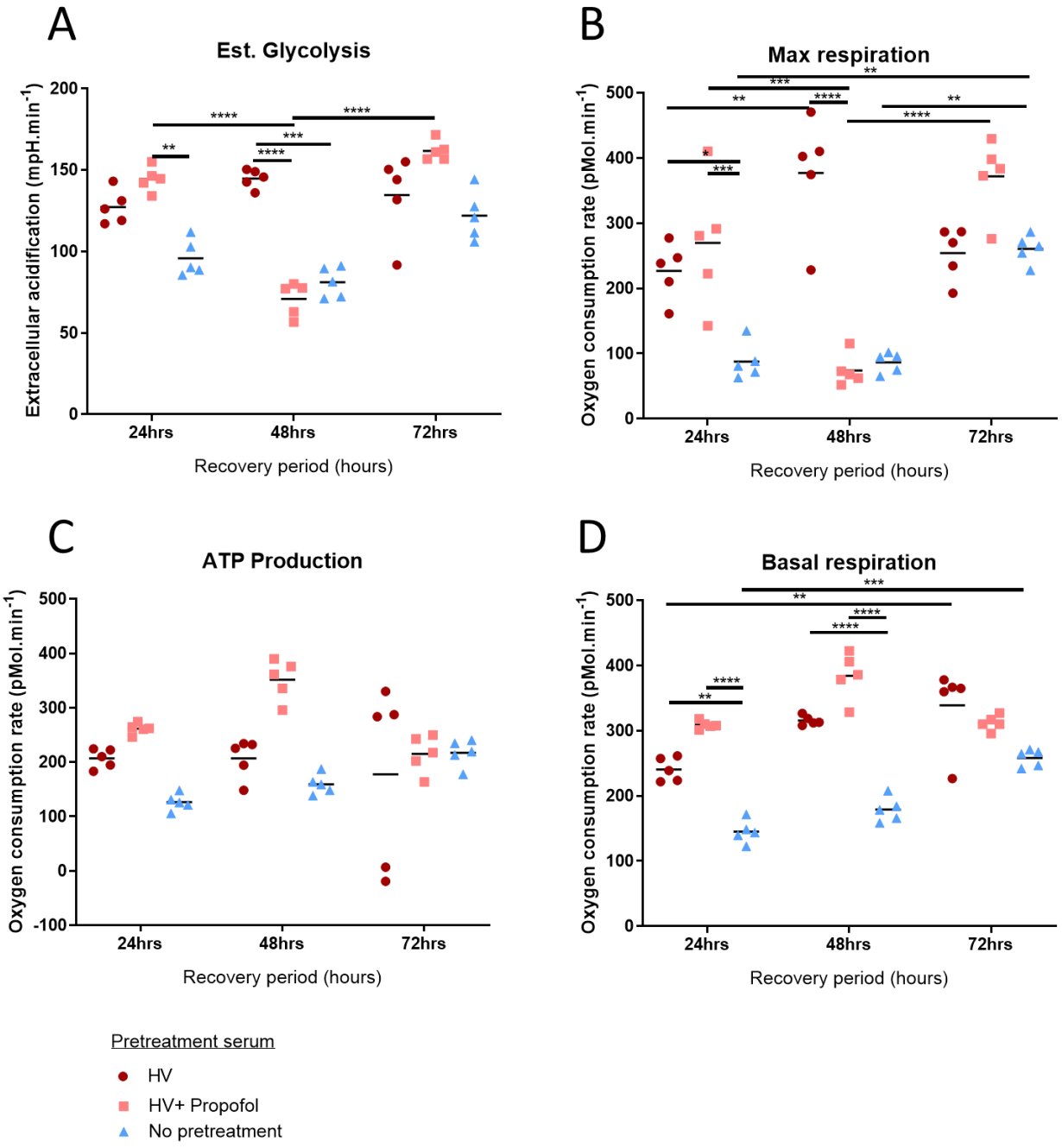

Figure 4.3.4 The (A) Glycolysis, (B) Maximum respiration, (C) ATP production and (D) Basal respiration of Null THP1 cells pretreated for 60 hours in either 10% healthy volunteer (HV) serum (red bars), 10% healthy volunteer serum plus 4μg/ml propofol (peach bars) or no pretreatment (blue bars). Cells were washed twice in PBS and left for a recovery period of either 24, 48 or 72 hours before being rechallenged with septic serum in the seahorse machine. Basal respiration was calculated from the oxygen consumption rate ($pMol.min^{-1}$) of the last measurement before the first injection minus the non-mitochondrial respiration. Maximum respiration was calculated from the oxygen consumption rate ($pMol.min^{-1}$) of the maximum rate measurement after FCCP injection minus the non-mitochondrial respiration. Glycolysis was estimated from the extracellular acidification ($mpH.min^{-1}$) when exposed to serum prior to oligomycin injection. ATP production was calculated from the oxygen consumption rate ($pMol.min^{-1}$) of the last rate measurement before Oligomycin injection minus the minimum rate measurement after Oligomycin injection. A p-value less than 0.05 is flagged with one star (*), a p-value is less than 0.01 is flagged with two stars (**), a p-value is less than 0.001is flagged with three stars (***) and a p-value is less than 0.0001is flagged with four stars (****). All comparisons were made with Freidman test with Dunn post-hoc test. Line represent the means. All values were standardised to μg.protein/well.

The basal respiration was different between each pretreatment group for 24 hour and 48 hour recovery times. For 24 hours, there was a difference between healthy volunteer (HV) and healthy volunteer plus propofol, healthy volunteer and no pretreatment, and healthy volunteer plus propofol and no pretreatment. For 48 hours, there was a difference between healthy volunteer (HV) and healthy volunteer plus propofol, healthy volunteer and no pretreatment, and healthy volunteer plus propofol and no pretreatment. However, for 72 hours there was only a difference between healthy volunteer and no pretreatment. There were also differences between the basal respirations of the same pretreatment groups at different lengths of recovery times. For healthy volunteer serum pretreatment groups, there was a difference between 24 hours recovery vs 48 hours recovery, and 24 hours vs 72 hours recovery. For healthy volunteer plus propofol pretreatment groups, there was a difference between 24 hours and 48 hours recovery, and 48 hours vs 72 hours recovery. For the no pretreatment groups there was a difference between 24 hours and 72 hours recovery and between 48 hours and 72 hours recovery.

The maximum respiration also had differences between each pretreatment group. For the healthy volunteer serum pretreatment groups, there were differences between 24 and 48 hours recovery, and 48 and 72 hours recovery. For the propofol plus healthy volunteer serum pretreatment groups, there were differences between 24 and 48 hours recovery, and 48 and 72 hours recovery. For the no pretreatment groups, there were differences between 24 hours and 72 hours recovery and 48 hours and 72 hours recovery. Within the 24 hour recovery group, there were differences between the pretreatments of healthy volunteer serum vs no pretreatment, and propofol plus healthy volunteer serum vs no pretreatment. The only condition where the maximum respiration decreased with the addition of propofol was the 48 hour recovery group. In the 48 hour recovery group, there were differences between the healthy volunteer serum and propofol plus healthy volunteer serum groups, and healthy volunteer serum vs no pretreatment. In the 72 hour recovery group, there were differences between the healthy volunteer serum and propofol plus healthy volunteer serum groups only.

The estimated glycolysis had differences between each pretreatment group and recovery time. For 24 hours, there was a difference between propofol plus healthy volunteer serum pretreatment and no pretreatment. The only condition where the glycolysis decreased with the addition of propofol was the 48 hour recovery group. For the 48 hour recovery group, the pretreatments with differences were the healthy volunteer serum and propofol plus healthy volunteer serum groups, and healthy volunteer serum vs no pretreatment. For the 72 hour recovery group, the pretreatments with differences were the propofol plus healthy volunteer serum and no pretreatment only.

The ATP production showed no differences between each recovery time and only one difference between pretreatments (propofol plus healthy volunteer serum vs no pretreatment at 48 hours recovery.

4.3.5 Seahorse Experiment 5: Propofol recovered cells rechallenged with Etomoxir in FAO study

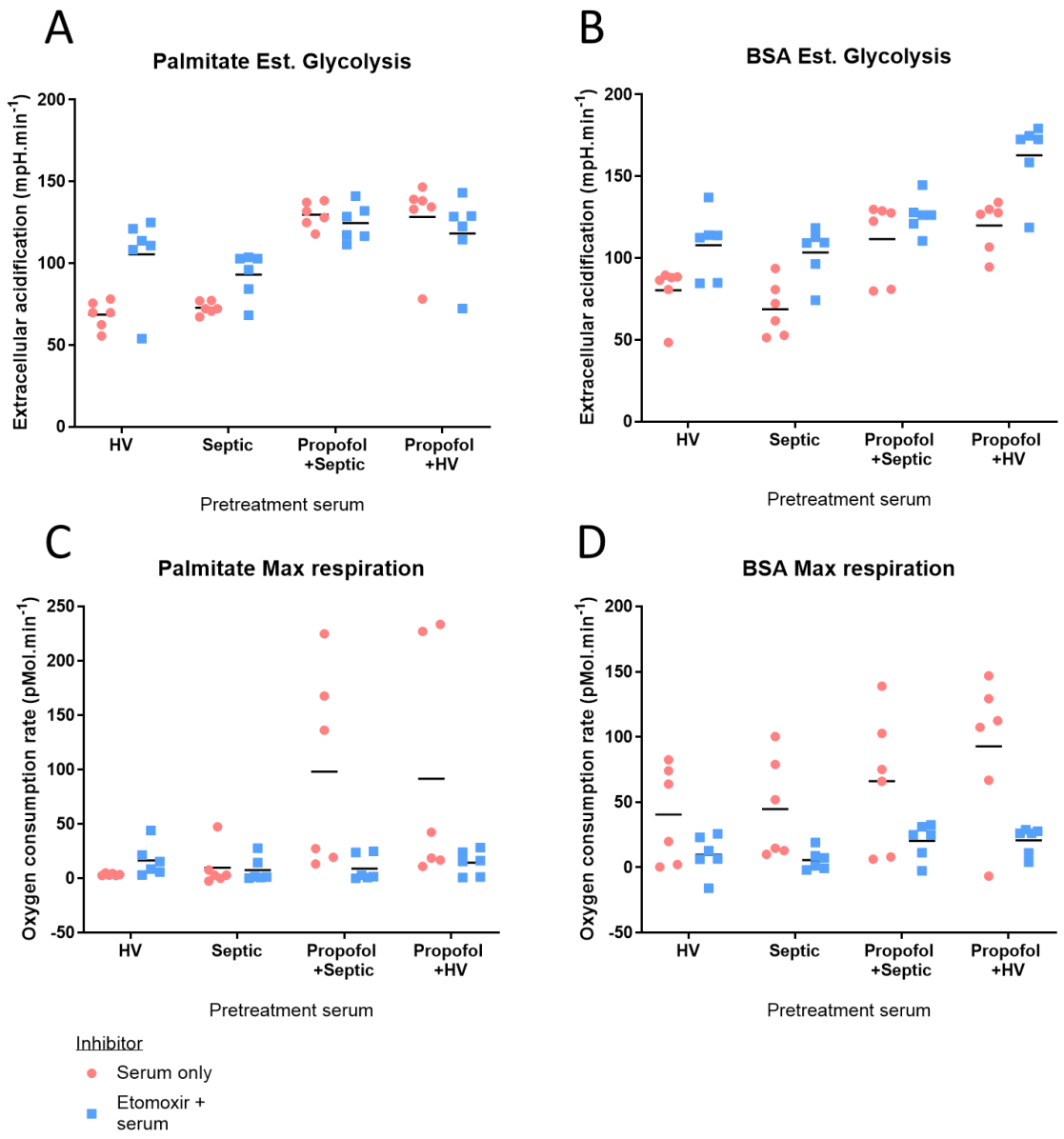

Figure 4.3.5 The estimated glycolysis (A, B) and max respiration (C, D) for THP1 Null pre-treatment groups exposed to either FAO buffer (peach bars) or etomoxir (blue bars), in the presence of (A, C) Palmitate:BSA or (B, D) BSA control. Glycolysis was estimated from the extracellular acidification (mpH.min^{-1}) when exposed to serum prior to oligomycin injection. "Healthy Volunteer" pre-treatment abbreviated to "HV". A p-value less than 0.05 is flagged with one star (*), a p-value is less than 0.01 is flagged with two stars (**), a p-value is less than 0.001is flagged with three stars (***) and a p-value is less than 0.0001is flagged with four stars (****). All comparisons were made with Freidman test with Dunn post-hoc test. Line represent the means. All values were standardised to µg.protein/well.

The BSA only did not work as a control; the estimated glycolysis of the BSA groups were similar to the Palmitate:BSA results. This is likely due to the THP1s generating their own fatty acids. The production

of their own fatty acids creating background noise means that it is not possible to interpret the results, and therefore the experimental design is not suitable.

The etomoxir did appear to dampen the maximum respiration of cells of both genotypes, and when exposed to palmitate in cell pretreated with propofol in both healthy volunteer (HV) serum and septic serum resulted in a higher maximum respiration without etomoxir.

Further experiments were conducted on THP1 Null and NLRP3-/- cells, with each cell type pre-treated in four serum conditions as previously described (either Healthy Volunteer, Healthy Volunteer plus Propofol, Sepsis, or Sepsis plus Propofol). In the Seahorse Extracellular Flux Analyzer, the cells were rechallenged with either septic serum or septic serum plus etomoxir. In one attempt, there were too few cells plated to distinguish the metabolic readings from the background noise, then in another attempt the freshly thawed vials of cells were too immature at the time of the experiment and reacted to neither Propofol nor etomoxir.

4.3.6 Seahorse Experiment 6: Propofol recovered cells rechallenged with Etomoxir without Palmitate

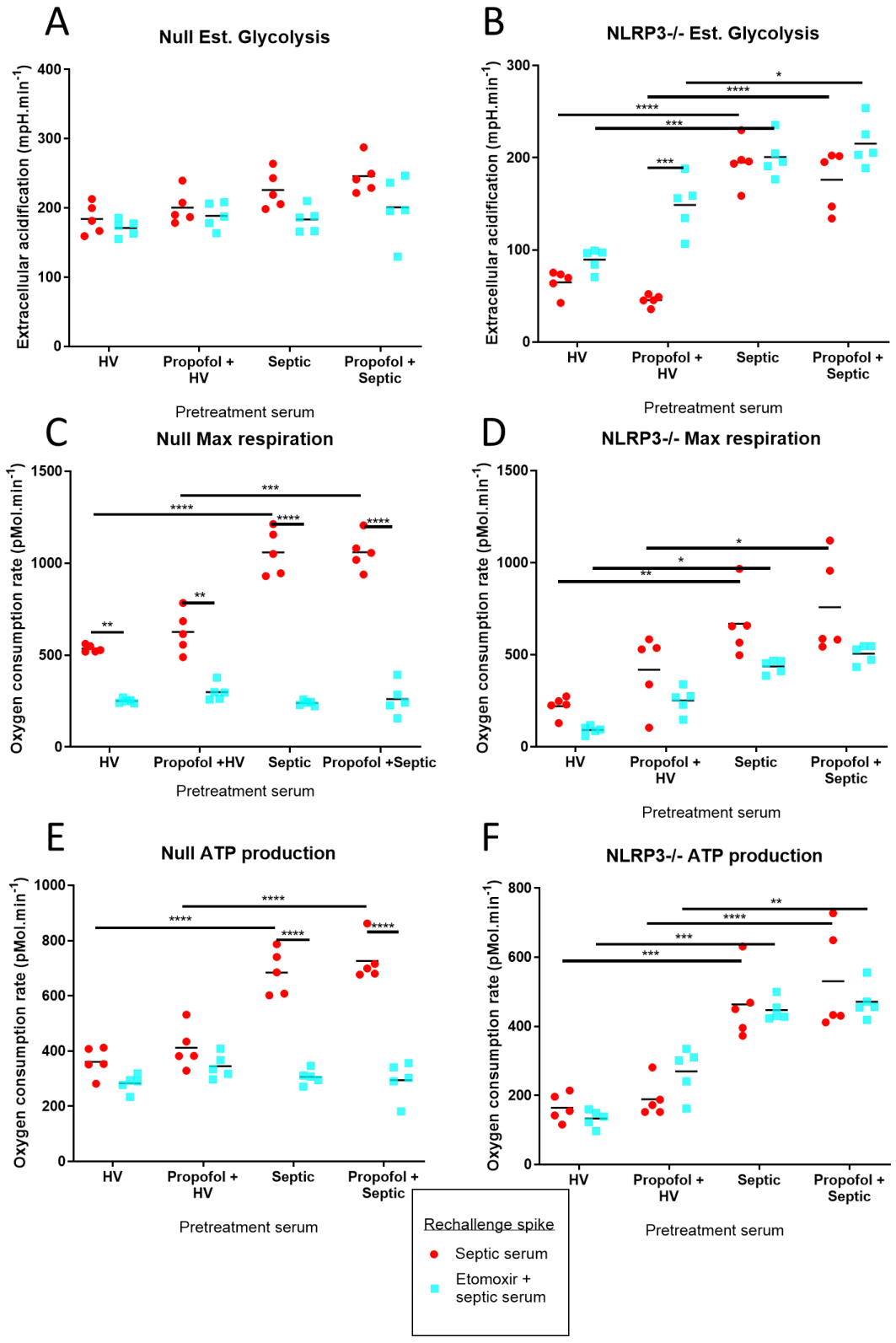

Figure 4.3.6 The estimated glycolysis of the THP1 genotypes (A) Null and (B) NLRP3-/-, the maximum respiration of the THP1 genotypes (C) Null and (D) NLRP3-/-, and the ATP production of the THP1 genotypes (E) Null and (F) NLRP3-/-. Pretreatments were cells cultured in 10% serum that was either healthy volunteer (HV), healthy volunteer plus propofol (4μg/ml), septic, or septic plus propofol 4μg/ml) for three days then washed and left to recover for a further three days. Glycolysis was estimated from the extracellular acidification (mpH.min^{-1}) when exposed to serum prior to oligomycin injection. Maximum respiration was calculated from the oxygen consumption rate (pMol.min^{-1}) of the maximum rate measurement after FCCP injection minus the non-mitochondrial respiration. ATP production was calculated from the oxygen consumption rate (pMol.min^{-1}) of the last rate measurement before Oligomycin injection minus the minimum rate measurement after Oligomycin injection. Cells were rechallenged in real-time with either 10% septic serum (red bars) or 10% septic serum plus etomoxir (40μM final) (blue bars). A p-value less than 0.05 is flagged with one star (*), a p-value is less than 0.01 is flagged with two stars (**), a p-value is less than 0.001is flagged with three stars (***) and a p-value is less than 0.0001is flagged with four stars (****). All comparisons were made with Freidman test with Dunn post-hoc test. Line represent the means. All values were standardised to μg.protein/well.

There were no differences observed in the Null cells for glycolysis within the different treatment groups. For NLRP3-/- cells, there were no differences between cells pretreated with propofol or non-propofol for each serum group. There were differences between cells pretreated with healthy volunteer serum alone vs septic serum alone. Similarly, there were differences between cells pretreated with healthy volunteer serum plus propofol vs septic serum plus propofol. However, etomoxir addition only had an effect in one condition; NLRP3-/- propofol plus healthy volunteer serum vs healthy volunteer serum alone.

For the Null genotype, the addition of etomoxir reduced the maximum respiration in each of the serum pretreatment conditions. This was not the case for the NLRP3-/- genotype, where the addition of etomoxir did not result in any effects. There were differences in the maximum respiration of each pretreatment group; for the Null cells when rechallenged with septic serum alone there were differences between healthy volunteer and septic pretreatments and propofol plus healthy volunteer and propofol plus septic pretreatments. For the NLRP3-/- cells, there were differences in the maximum

respiration when rechallenged with septic serum alone between healthy volunteer and septic pretreatments, propofol plus healthy volunteer and propofol plus septic pretreatments, and again healthy volunteer and septic pretreatments when rechallenged with septic serum plus etomoxir.

For NLRP3-/- THP1s, the addition of etomoxir did not have a effect on ATP production. For the Null THP1s there was an effect, but only for the septic and propofol plus septic pretreatments. There were no differences in the Null cells between pretreatment groups when rechallenged with septic serum plus etomoxir, but differences in serum pretreatment groups were observed when rechallenged with septic serum alone. Differences in ATP production between pretreatment groups were observed for both etomoxir and non-etomoxir septic serum rechallenges for the NLRP3-/- cells; for septic serum alone rechallenge there were pretreatment differences in healthy volunteer vs septic and propofol plus healthy volunteer vs propofol plus septic, and when rechallenged with etomoxir plus septic serum there were again pretreatment differences in healthy volunteer vs septic and propofol plus healthy volunteer vs propofol plus septic. The addition of septic serum in the pretreatment increased ATP production.

4.3.7 The effect of propofol on PINK1 and Parkin gene expression

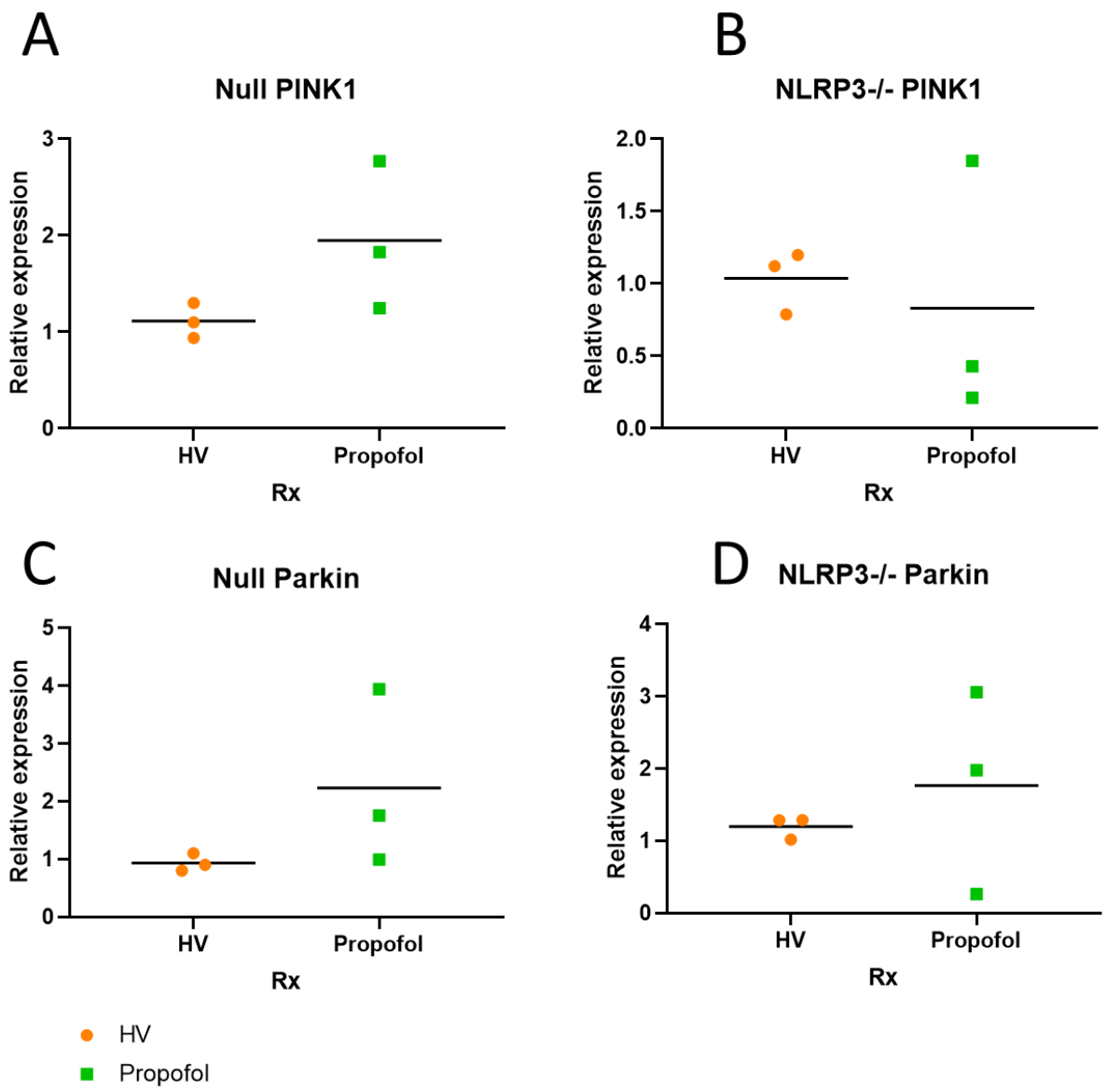

Figure 4.3.7 The gene expression of PINK1 in (A) Null THP1s (n=3), and (B) NLRP3-/- THP1s (n=3), and Parkin in (C) Null THP1s, and (D) NLRP3-/- THP1s, when normalised to housekeeping gene HPRT. Cells were exposed to either 10% healthy volunteer serum alone (HV) (mint bars) or propofol (4µg/ml) plus 10% healthy volunteer serum (orange bars) for 24 hours followed by twice PBS washing and a three days recovery period.

In Null and NLRP3-/- THP1 cells, no differences were observed in PINK1 gene expression when cells were exposed to propofol. In Null and NLRP3-/- THP1 cells, no differences were observed in Parkin gene expression when cells were exposed to propofol.

4.3.8 Histone modifications resulting from propofol administration

Chromatin Immunoprecipitation on NLRP3-/- THP1 cells could not be analysed as none of the panel of positive and negative gene controls for the ChIP-qPCR returned an appropriate reading (meaning that, for the NLRP3-/- THP1s, they did not act as a control but genes were influenced by experimental measures). DNA was amplified, but the positive and negative controls all returned similar readings. Due to time constraints, a suitable panel of gene controls could not be optimised for NLRP3-/- cells. However, the Null THP1 cells positive and negative controls for ChIP-qPCR worked and therefore results could be analysed. The control for H3K4me3 was HMGB1, and the control for H3K9me3 and H3K27me3 was GAPDH.

Gene activation marker H3K4me3

(A)

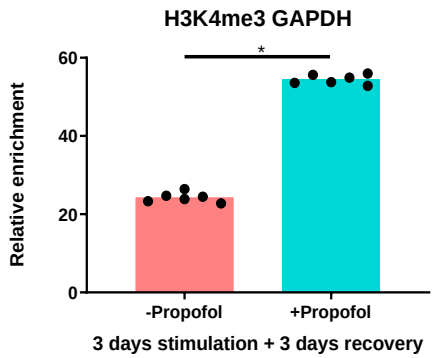

(D)

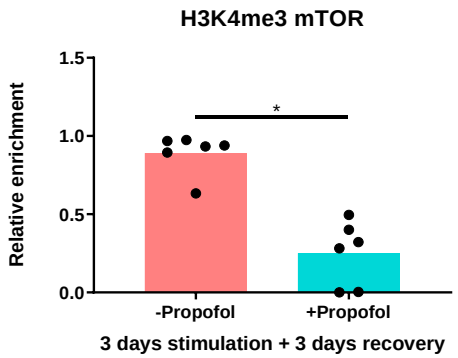

(B)

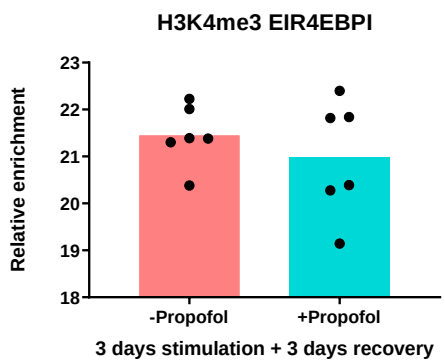

(E)

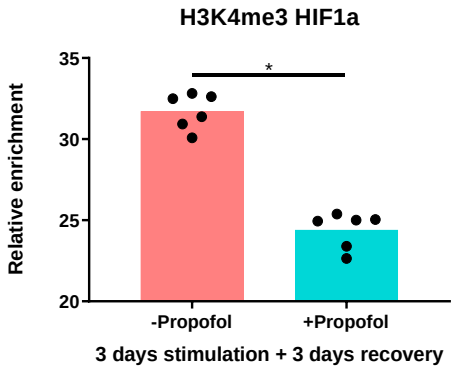

(C)

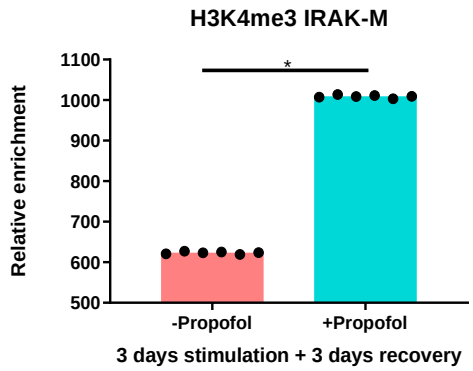

Figure 4.3.8.1 The H3K4me3 relative enrichment of the genes (A) GAPDH, (B) EIR4EBPI, (C) IRAK-M, (D) mTOR, and (E) HIF1α. THP1 Null cells were cultured for three days with or without Propofol, washed twice, then left to recover for a further three days before harvest. The orange bars represent THP1 Null cells cultured without Propofol, whereas the blue bars represent THP1 Null cells cultured with 4µg/ml Propofol. A p-value less than 0.05 is flagged with one star (*), a p-value is less than 0.01 is flagged with two stars (**), a p-value is less than 0.001is flagged with three stars (***) and a p-value is less than 0.0001is flagged with four stars (****). Groups were compared using the Wilcoxon signed-rank statistical test.

The addition of Propofol increased the H3K4me3 (gene activation) of GAPDH (p= 0.0313) and IRAK-M (p= 0.0313), and decreased the H3K4me3 of mTOR (p= 0.0313) and HIF1α (p= 0.0313). The addition of Propofol did not cause any changes to the H3K4me3 gene activation of EIR4EBPI.

Gene repression marker H3K9me3

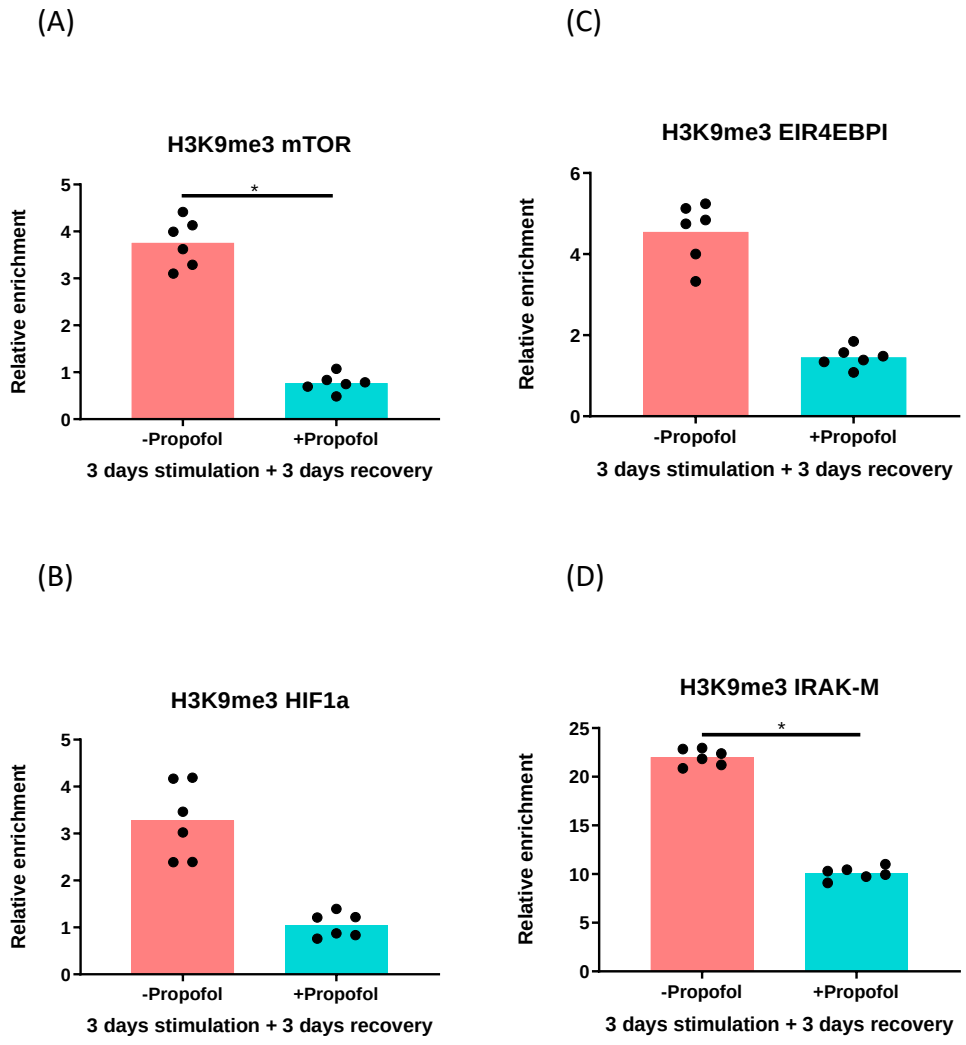

Figure 4.3.8.2 H3K9me3 relative enrichment of the genes (A) mTOR, (B) HIF1α (C) EIR4EBPI, and (D) IRAK-M. THP1 Null cells were cultured for three days with or without Propofol, washed twice, then left to recover for a further three days before harvest. The orange bars represent THP1 Null cells cultured without Propofol, whereas the blue bars represent THP1 Null cells cultured with 4µg/ml Propofol. A p-value less than 0.05 is flagged with one star (*), a p-value is less than 0.01 is flagged with two stars (**), a p-value is less than 0.001is flagged with three stars (***) and a p-value is less than 0.0001is flagged with four stars (****). Groups were compared using the Wilcoxon signed-rank statistical test.

The addition of Propofol decreased the H3K9me3 (gene repression) of mTOR (p= 0.0313) and IRAK-M (p= 0.0313). The addition of Propofol did not cause any changes to the H3K9me3 gene repression of EIR4EBPI or HIF1α.

Gene repression marker H3K27me3

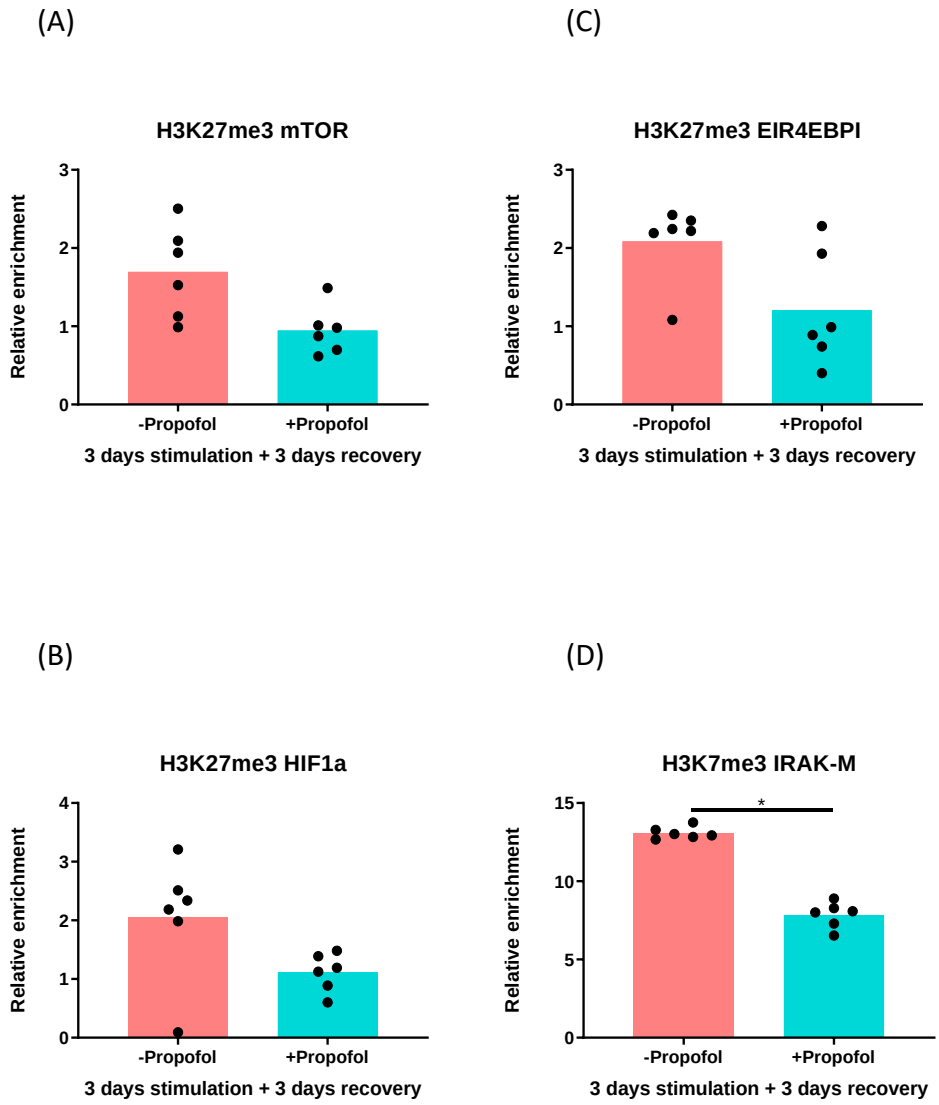

Figure 4.3.8.3 H3K27me3 relative enrichment of the genes (A) mTOR, (B) HIF1α (C) EIR4EBPI, and (D) IRAK-M. THP1 Null cells were cultured for three days with or without Propofol, washed twice, then left to recover for a further three days before harvest. The orange bars represent THP1 Null cells cultured without Propofol, whereas the blue bars represent THP1 Null cells cultured with 4µg/ml Propofol. A p-value less than 0.05 is flagged with one star (*), a p-value is less than 0.01 is flagged with two stars (**), a p-value is less than 0.001is flagged with three stars (***) and a p-value is less than 0.0001is flagged with four stars (****). Groups were compared using the Wilcoxon signed-rank statistical test.

The addition of Propofol decreased the H3K27me3 (polycomb gene repression) of only one gene, IRAK-M (p= 0.0313). Differences were not found for mTOR, HIF1α or EIR4EBPI.

4.4 Discussion

Acute Propofol sedation causes changes in PBMC immunometabolism

Healthy donor Peripheral Blood Mononuclear Cells (PBMCs) exposed to serum from septic patients who were either Propofol- sedated or non-sedated resulted in a change in these cells immunometabolism. These initial findings involving PBMCs were stumbled upon; the two patient's serums were selected to increase n numbers with patients of a similar demography with one being more severely ill and in ICU to potentially exaggerate the effects observed in the less ill ward patient. However, the contrast between the immunometabolism of cells exposed to the two serums suggested there was something else in the serum causing these distinct patterns, and the big difference between these patients was their treatments (sedation vs no sedation). Glycolysis when exposed to septic serum was suppressed when the patient serum contained Propofol, rather than increasing when exposed to non-sedated serum (in comparison to healthy volunteer serum), and likewise with ATP production.

The sepsis-induced glycolytic shift has been characterised in recent years, and this data supports it. Cytopathic hypoxia has been associated with sepsis (Fink, 2015; Suetrong and Walley, 2016), and the reduced capacity of tissues to utilise the oxygen from the bloodstream may contribute to this glycolytic shift. Septic cells do upregulate transcription and section of HIF-1α in a hypoxic response, which is a transcription factor that will upregulate several genes involved in glycolysis- including lactate dehydrogenase, which converts pyruvate into lactate (Marín-Hernández *et al*, 2009). Indeed, it is thought that an increase in lactate in sepsis results in this increased glycolysis. It was established in 1974 by Jones *et al* that the oxidation of lactate into pyruvate is defective in sepsis, and this may be due to dysfunction in mitochondrial transport systems being unable to transport protons of lactate oxygenation into the mitochondrial membrane (Jones, 1974). This means that in sepsis, along with an increase in lactate production, there is also ineffective lactate removal via these dysfunctional mitochondrial transport systems, leading to a build up of lactate. Mitochondrial dysfunction correlates

with a suppression in cytokine production, and is a predictor of mortality in sepsis (Brealey *et al*, 2002; Belikova *et al,* 2007). Cytokine production and metabolism seem to have a relationship; glycolysis has been shown to be downregulated by IL-10 (Martin *et al*, 2009) and the immune response can be influenced by inhibiting metabolic pathways (Chen *et al,* 2016). Studies tend to focus on a particular cell type; more research is needed to untangle the interplay of all the leukocytes *in vivo.*

The Propofol formulation consists of 1% Propofol in 10% soybean oil emulsion, which has been associated with allergies and inflammation (Baker *et al,* 2005). A suitable vehicle control for the intralipid soybean solution was not utilised, therefore it is not clear if any effects may actually be due to the emulsion rather than the propofol itself. However, it should be noted that Propofol is always supplied in this soybean emulsion, therefore any clinical impact will be the same whether changes are due to the Propofol itself or the emulsion.

Effects of Propofol on PBMC immunometabolism persist after Propofol is washed off and cells left to recover

These changes not only occurred in PBMCs exposed to “acute” serum taken within 24 hours of the blood culture positive sepsis result, but these changes also persisted when exposed to “recovered” serum taken one week post blood culture positive when the infection had cleared from the bloodstream, and where the Propofol-sedated patient had been free of receiving sedation for four days. This suggests that sedation induced changes that resulted in these alterations in immunometabolism, and that these changes persisted even when sedation had stopped being administered four days prior. It is possible that leukocyte immunometabolism may be modulated in part by epigenetics; the sedation may have caused epigenetic changes that resulted in immunometabolic alterations that were not reversed when sedation stopped being administered.

The Spare Respiratory Capacity (SRC) of these cells revealed two distinct characteristic patterns between acute and recovery serum in the presence or absence of sedation. A larger spare respiratory capacity is an indicator that the cells have more of an energy reserve to combat infection. The SRC in the acute sample is not different to the healthy control sample but rises in recovery serum in the patient who did not receive sedation. In contrast, the acute serum from a patient exposed to Propofol-sedation did have a higher SRC than the healthy control, but this had lowered by the time the recovery serum was taken. Each PBMC donor can be observed following this same pattern of an increase without sedation and decrease with sedation between the acute and recovery timepoints.

Indeed, these are just two patient serums that have been compared. Although the patients have very similar clinical characteristics, there were of course numerous factors that cannot be controlled for when using human donors, such background, diet etc. Therefore, the THP1 cell line was utilised in order to further investigate these phenomena.

The THP1 cell line was not compatible with the Seahorse Fatty Acid Oxidation assay

The cells respond to sepsis by increased oxidative phosphorylation, potentially due to the cells increasing their uptake of fatty acids. However, the THP1 cell line is cancerous, and appeared to be producing a lot of their own fatty acids which resulted in an estimated glycolysis for the BSA control comparable to the Palmitate condition in the Fatty Acid Oxidation Assay. Cancerous cell lines such as THP1 have been known to produce a lot of their own fatty acids which would interfere with the readings. Etomoxir appeared to vary in effectiveness between experiments. As discussed in the Introduction, etomoxir has been found to induce severe oxidative stress at commonly used concentrations, and etomoxir actions on Tregs are independent of CPT1a-mediated fatty acid oxidation.

The length of recovery time after Propofol administration has an effect on the immunometabolic profile of THP1 cells

The THP1 cell line was utilised in order to further examine the effects of Propofol on bioenergetic function. There were some differences between the experiments when it came two a two day stimulation with wash and two day recovery vs a three day stimulation, wash, and further three day recovery. In order to ascertain whether or not this was due to the length of days of recovery, THP1s were set up so that they underwent two and a half days of pretreatment culture then a recovery period of either one, two or three days before the bioenergetic function was measured to see if there were differences. The differences could be explained by the different vials of THP1 cells thawed, passage number of the cells, or length of time of stimulation/ recovery period. There were differences in the basal respiration, maximum respiration, and glycolysis of the different recovery time periods. The day two/ 48 hour time point did show a different pattern of results than both the day one/24 hour and day 3/ 72 hours recovery times; it is possible that approximately 48 hours after propofol/ a septic insult the cells display a different metabolic profile to 24 and 72 hours, however it is more likely that the 48 hour time point was measured during the cells' division. The cells in the sets of experiments from the first sets of experiments were younger, at passage 17, compared to the cells in later experiments which were passage 28. The younger THP1 cells are more likely to reflect the behaviour of primary cells and be consistent in results than older cells which may have mutated.

The use of primary cells and cell lines

The use of cell lines and primary cells each have their own sets of limitations, explored further in *Chapter 6: Discussion* in this thesis. A particular limitation was that the THP1s were not compatible with the Fatty Acid Oxidation assay. However, the fact that the donor primary cells and the cell line both respond to the addition of propofol is indicative of an independent effect of sedation when used in sepsis treatment.

There are some quality control limitations regarding the cell cultures in this thesis. The cell viability was assessed using a haemocytometer and Trypan Blue. Trypan Blue has been found to be inaccurate for cell viability under 80% (Chan *et al*, 2020), and it does not assess the functionality of the cells. A more accurate method would have been to measure the levels of the enzyme lactate dehydrogenase in the supernatant. Cells were not assessed for purity nor was power calculated to determine numbers of cells used; this was a massive oversight. Underpowered studies are not able to draw meaningful conclusions to answer the research question and introduces a high risk of type II errors, leading to biased conclusions. Purity assessment (potentially via flow cytometry) is critically important to ensure cells are not contaminated, and not assessing cell viability throws doubt into any conclusions drawn.

Propofol exposure appears to lead to changes in histone modifications

Chromatin Immunoprecipitation reveals epigenetic changes in key genes related to immunometabolism after exposure to Propofol, persisting to three days recovery after the Propofol was washed off. After Propofol exposure, IRAK-M (which specifically expresses in monocytes and macrophages) had a higher relative enrichment of H3K4me3 (gene activation) and a lower relative enrichment of H3K9me3 and H3K27me3 (both gene repression), suggesting Propofol may direct sepsis-induced chromatin modifications via IRAK-M modulations of the histone modifying machinery in the cell (Lyn-Kew K *et al*, 2010). Furthermore, IRAK-M is a negative regulator of Toll-like receptor signalling (Kobayashi K e*t al,* 2002), and over-expression of IRAK-M was seen to result in higher *Mycobacterium tuberculosis* bacterial load (Shen P *et al*, 2017). HIF1α, which acts on IRAK-M and appears to be upregulated in sepsis, interestingly had a lower relative enrichment of H3K4me3 when exposed to Propofol, potentially due to a negative feedback loop from the increase in IRAK-M. Collectively, these findings suggest a tight control of the expression of the IRAK-M pathway at the histone methylation level due to Propofol exposure.

For mTOR, Propofol exposure resulted in less relative enrichment for both H3K4me3 and H3K9me3, an activation and repression marker of genes, respectively. This is unusual, as these two modifications tend to seesaw with each other- you will most often find that when one of either H3K4me3 or H3K9me3 has a higher relative enrichment the other modification will have a lower relative enrichment. Again, this finding is possibly due to the involvement of a negative feedback loop, however it may also be due to a complexity that was first described in Chapter Three of this thesis. When gene expression was analysed of the full septic patient cohort (n=63), the patients displayed a reduction in the expression of EHMT2 compared to healthy volunteers (n=36), and this reduction persisted even 6-12 months post hospital discharge (p=0.0014). The EHMT2 gene encodes the protein G9a, a histone methyltransferase, which associates with promotors of genes to repress them by mediating H3K9me1, H3K9me2, and H3K9me3 (Osipovich *et al*, 2004; Yokochi *et al*, 2009). It is possible the Propofol administration mimics this, decreasing the gene expression of EHMT2 and thus protein G9a, and resulting in less H3K9me3 gene repression. Indeed, there appears to be a general trend of less H3K9me3 for all the genes examined in this chapter when exposed to Propofol. However, before a conclusion can be drawn the relationship between Propofol administration and protein G9a levels will need to be further established. Examination of these H3K9me3 results highlight the major complexity of the mechanisms involved in the control of gene repression due to Propofol exposure and warrant further investigation.

Despite the evidence in the literature for H3K27me3 involvement in sepsis, in this instance H3K27me3 observed stable enrichment at these examined genes with and without Propofol suggest that this epigenetic mark may not play a role in their expression. The exception being IRAK-M, as discussed above. It is possible that changes in H3K27me3, and indeed other modifications, may have occurred with acute drug exposure but recovered after washing and resting the cells.

GAPDH, a key gene in glycolysis, had a higher relative enrichment of H3K4me3 (gene activation) after Propofol exposure. This is perhaps not surprising, as it fits in with the seahorse data which revealed

higher levels of glycolysis when cells were exposed to Propofol even after washing and a recovery period.

Clinical implications

If further validated, these findings could result in implications clinically. In theory, if the treatments for sepsis, rather than the bacteraemia itself, is partially responsible for the immunosuppression associated with sepsis then use of these medicines would have consequences in several diseases requiring the same treatment. Particularly as these findings suggest that infection is not necessarily required in order for Propofol to illicit this immunometabolic change. Sedatives such as Propofol are widely used in intensive care medicine, and if it is able to induce these long lasting immunometabolic changes then patients receiving sedation should be monitored closely upon receiving this treatment with careful attention paid to their immune function. It may be that more drugs can affect patients' immunometabolism in a similar way, such as opioids for example.

Equally, it may not be all sedatives that illicit this response; as only Propofol was examined in these experiments. Midazolam, for example, may not result in the same immunometabolic changes, and further research into the exact mechanism of how Propofol induces these changes would help inform the breadth of sedatives that are likely to behave similarly.

However, at present it is far too early to draw such conclusions. This research has several major weaknesses, where further research is needed. At the moment the results serve as a pilot research piece which could help direct further study and results should not be taken as a conclusion.

Further research

The Fatty Acid Oxidation Seahorse assay could be performed on PBMCs or a cell line that produces less of its own fatty acids. The PBMCs would struggle to survive for the days required to wash and recover from Propofol exposure, but a 24 hour Propofol exposure could be easily performed.

The gene expression study had a sample size of only n=3, and it is far too small to draw conclusions from. A repeat of the experiment with a larger sample size would have been performed given the time, and a wider array of genes could have been examined. Similarly, the septic serum used on the donor PBMCs were only n=2, and the experiment should have ideally been repeated with pooled serum from several septic patients. Pooled serum was used in the THP1 experiments; but needs to be repeated with the PBMC experiments.

Propofol is just one type od sedative; experiments could be repeated on other sedatives to ascertain whether the observed effects are due to sedatives as a whole or only certain sedatives. For example, the changes recorded may not be due to the active molecule of Propofol, but maybe due to something else in the lipid suspension it is blended with.

Chromatin Immunoprecipitation could be performed on PBMCs that were cultured in Propofol and compared with the THP1 ChIP results.

Summary

The sedation and other clinical interventions in the treatment of bacteraemia and sepsis may be partly responsible for the metabolic reprogramming of leukocytes, diminishing the cells ability to elicit a bioenergetic response. There is without a doubt a need for further investigation to ascertain the role of Propofol exposure in histone modifications, however lasting epigenetic changes in key genes were clearly observed. The is a clear role of Propofol in the metabolic reprogramming of leukocytes, and this may translate to a clinical context where interventions such as sedation are used in the treatment

of sepsis. The failure to mount a bioenergetic response in cells previously exposed to Propofol suggest a potential role for genomic/epigenetic modulation of leukocyte metabolism.

Chapter 5: The effects of Rocuronium on immune function

5.1 Introduction

Patients in the ICU routinely receive neuromuscular blockade for various procedures; a standard used in anaesthesia for both surgical procedures and intubation (Brull SJ *et al*, 2017). Of patients undergoing general anaesthesia, approximately 80% receive neuromuscular blocking agents and 50% receive reversal agents (Ball L, 2017).

Despite their widespread use, patients who have received neuromuscular blocking agents have an increased risk of hospital readmission within 30 days due to pulmonary complications. The multicentre, prospective observational cohort study POPULAR (Kirmeier E *et al,* 2018) found that, irrespective of the use of reversal agents or neuromuscular monitoring, patients who have received neuromuscular blockade have a significant risk of developing postoperative pulmonary complications. The two most common clinical symptoms of the pulmonary complications were respiratory failure and respiratory infection. Due to the nature of the treatments, it is worth noting there may be a selection bias in the literature regarding pulmonary complications as this is what patients are expected to return to hospital with.

Neuromuscular blocking agents such as Rocuronium affect the nicotinic neuromuscular junction by acting on acetylcholine (ACh) and nicotinic acetylcholine (nAChR) receptors on the synapse. However, immune cells are also known to express cholinergic components such as muscarinic and nicotinic acetylcholine receptors (Fujii T *et al*, 2017). Indeed, immune cells are known to express several nicotinic acetylcholine receptors such as nAChR α7, and all of the

muscarinic acetylcholine receptors (mAChR) M1-M5 (Grando SA *et al*, 2015; Kawashima K *et al*, 2019).

What has yet to be considered is the potential effect of neuromuscular blockade on the immune system.

The study into mAChR and nAChR gene-knockout mice by Fujii T *et al* (2017) suggests that a functioning immune system is partially modulated by the immune cell cholinergic system. Manipulating the cholinergic activity of immune cells via neuromuscular blockade could therefore impact immune function.

Hypothesis: Administration of rocuronium will induce changes in immunometabolism and function of immune cells.

Aims:

1: Assess immunometabolism of cells in response to rocuronium

2: Assess changes in gene expression of immune cells in response to rocuronium

3: Explore role of Sugammadex in relation to (1) and (2) above.

5.2 Methods

5.2.1 Immunometabolic profiling

The Seahorse extracellular flux analyser was utilised to read cells' immunometabolic profiles in real-time. In the analyser, cells were spiked with either an assay buffer control or with pooled *E.coli* septic serum from acutely septic patient donors. Full details of Seahorse methodology can be found in the methods chapter, but as a refresher the readout of mitochondrial respiration OCR when spiked with the inhibitor drugs are shown in the figure below:

Seahorse Experiment 1 and 2: Rocuronium vs Propofol profiling

THP1 Null and NLRP3-/- cells were divided into four testing categories each- six hour stimulation with either Rocuronium (1.4µg/ml), Rocuronium (1.4µg/ml) + Propofol (4µg/ml), Propofol (4µg/ml), or cell media control. After the six hours' incubation, cells were washed twice with pre-warmed PBS and then left to recover for three days. After the recovery period, cells were split into a further two groups each and loaded into a Seahorse XFe analyser where they were rechallenged with either septic serum or assay buffer.

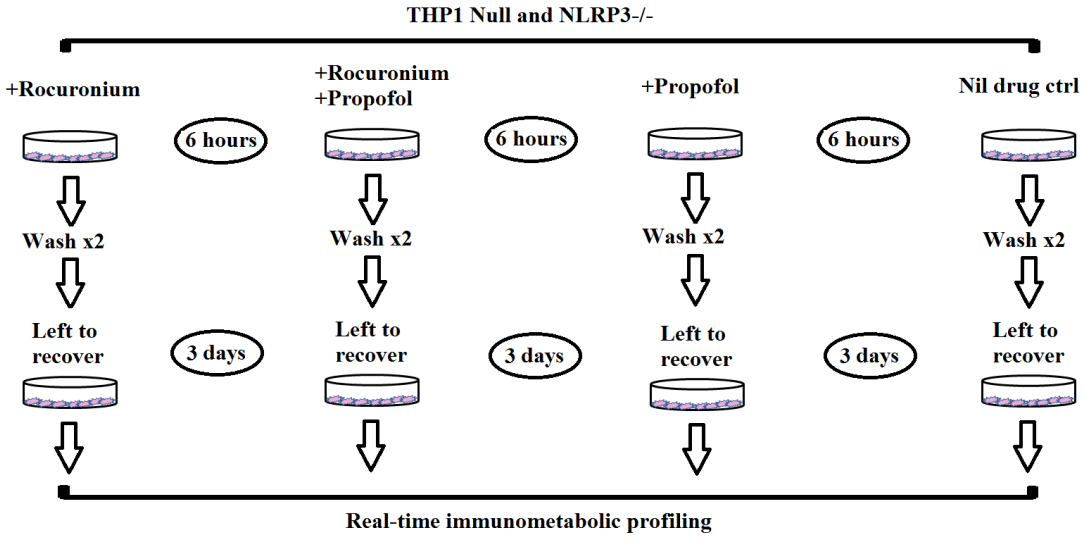

Figure 5.2.2 Methodology of Seahorse Experiment 1 on both Null and NLRP3-/- THP1 cells. Cells were rechallenged in the Seahorse XFe analyser with either septic serum or assay buffer and mitochondrial inhibitors.

Seahorse Experiment 3: Rocuronium serial dilution

THP1 Null and NLRP3-/- cells were divided into four testing conditions each. A serial dilution of Rocuronium was performed, beginning with Rocuronium at a clinical concentration of 1.4µg/ml, then a 1:10 and 1:100 dilution of this. Cells in the final condition were left as a control, having only cell media added in place of drugs. Cells were left to incubate for 6 hours with the drug, then were washed twice in pre-warmed PBS buffer. Cells were then left to recover for three days before being rechallenged in the Seahorse XFe analyser.

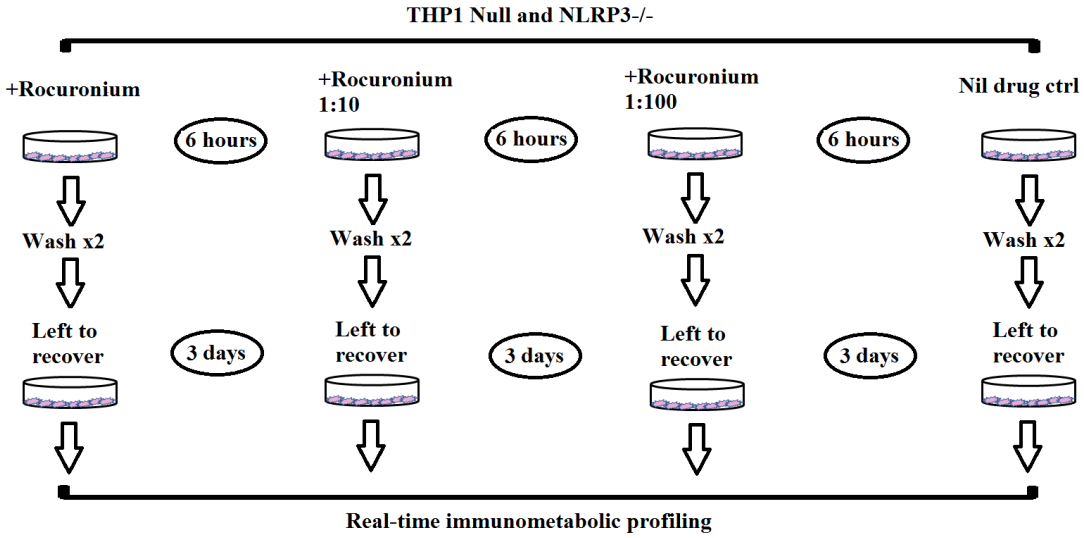

Figure 5.2.3 Methodology of Seahorse Experiment 3 on both Null and NLRP3-/- THP1 cells. Cells were rechallenged in the Seahorse XFe analyser with mitochondrial inhibitors.

Seahorse Experiment 4: Rocuronium and Vecuronium with Sugammadex reversal

THP1 Null and NLRP3-/- cells were divided into four conditions each. Two of the conditions were spiked with Rocuronium (1.4µg/ml) for 6 hours and two were spiked with Vecuronium (0.14µg/ml) for 6 hours. One Rocuronium condition and one Vecuronium condition were then reversed with the addition of 50µg/ml Sugammadex for 30 minutes. The other Rocuronium and Vecuronium conditions had only cell media added for 30 minutes. All cell conditions were then washed twice with pre-warmed PBS buffer and left to recover for three days. The cells were then loaded into the Seahorse XFe analyser and their immunometabolisms were read in real-time.

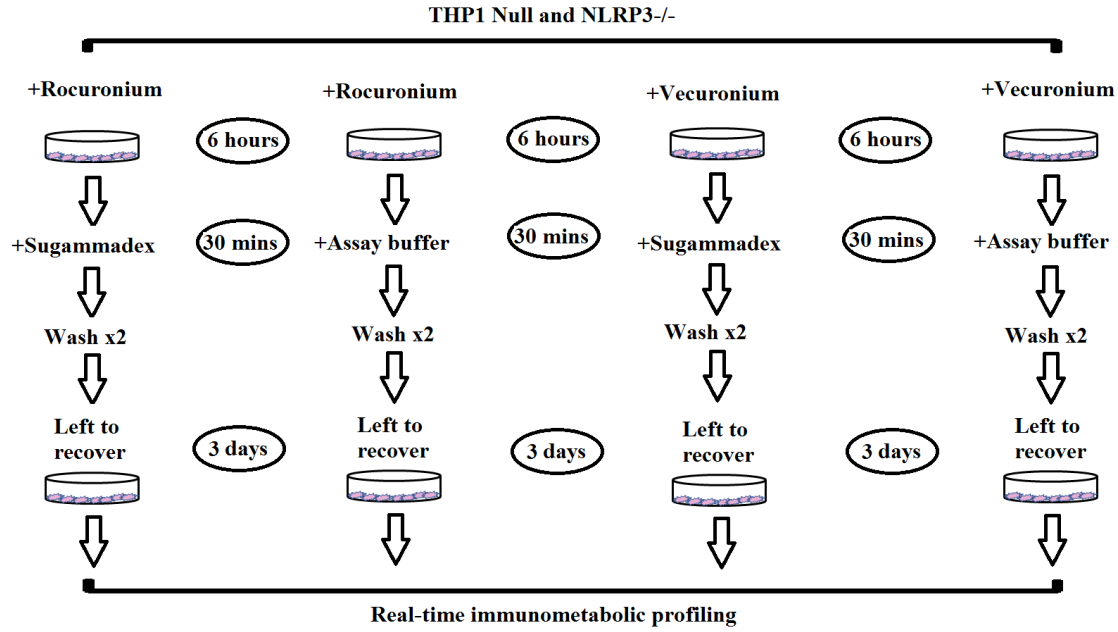

Figure 5.2.4 Methodology of Seahorse Experiment 4 on both Null and NLRP3-/- THP1 cells. Cells were rechallenged in the Seahorse XFe analyser with mitochondrial inhibitors.

5.2.2 Gene expression

Gene expression of the Rocuronium-spiked cells was ascertained using quantitative PCR. SYBR-Green Primers were designed and utilised as described in the Methods chapter. The cells analysed were HL-60, THP1 Null and NLRP3-/-, and PBMCs from healthy donors. The genes analysed were as following: GAPDH, VAChT, ChAT, PINK1, Parkin, TNFα, IFNγ, IL-10, IL-6, muscarinic receptors M1-M5, and nicotinic receptors α7, β2, γ, and ε. Three sets of primers for α4 nicotinic receptor were tested, but all appeared to be unstable and had a low efficiency, and so this gene was omitted from the study.

5.2.3 IL-10 and IL-6 concentration

The concentration of IL-6 and IL-10 in the supernatants of cells spiked with Rocuronium/ Sugammadex was read by ELISA assay. Five replicates each of THP1 Null, THP1 NLRP3-/-, HL-60, and donor Monocytes were analysed. The cells were divided into four treatment conditions each: Rocuronium (1.4µg/ml), Sugammadex (50µg/ml), Rocuronium and Sugammadex, or Nil drug control. Drugs were administered in a similar fashion to Figure 5.2.4 with cells being washed twice after exposure and left to recover for three days. After the recovery period, supernatants were aspirated and stored at -80°C until the ELISA assays were performed. Full details on ELISA methodology is found in the Methods Chapter.

5.2.4 Cell lines and donor monocytes

Three cell lines were utilised; THP1 Null, THP1 NLRP3-/-, and HL-60. Monocytes from five healthy donors (average age 34.5) were also utilised in the gene expression and ELISA experiments. Full details on cells used can be found in the Methods Chapter.

5.3 Results

5.3.1 Raw Seahorse analyser readout of Null cells exposed to Rocuronium, Vecuronium, and Nil drug control

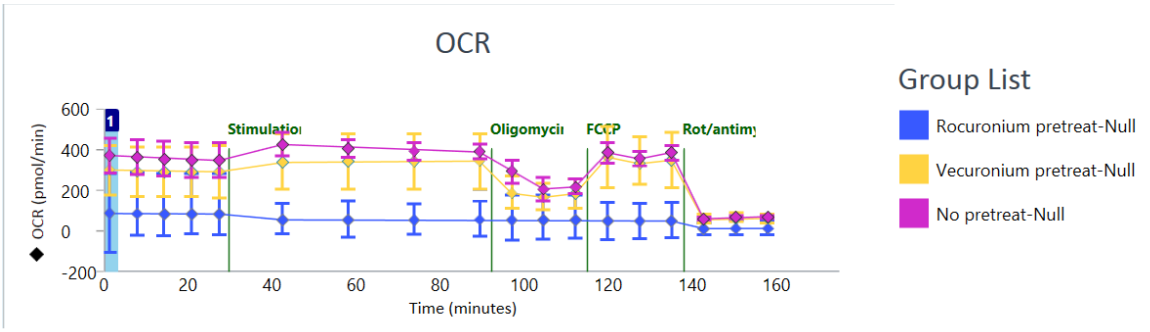

Figure 5.3.1.2 Raw readout from the Seahorse analyser of the oxygen consumption rate (OCR) over time for Null THP1 cells exposed to Rocuronium (blue), Vecuronium (yellow), or Nil drug control (purple). (NB: these are raw readouts, not normalised.)

Above is a typical readout from the Seahorse analyser showing oxygen consumption rate (OCR) over time. When exposed to the mitochondrial poisons, the cells treated with Vecuronium and Nil drug treated control cells exhibit the typical Seahorse OCR profile- OCR dropping with Oligomycin, rising with FCCP, and lowering with Rotenone/Antimycin A. Apart from a slight lowering of OCR when exposed to Rotenone/Antimycin A, cells exposed to Rocuronium had a steady low OCR which did not react to the addition of Oligomycin or FCCP.

5.3.2 Seahorse experiment 1: The immunometabolic effects of rocuronium in addition to Propofol in the presence or absence of septic serum

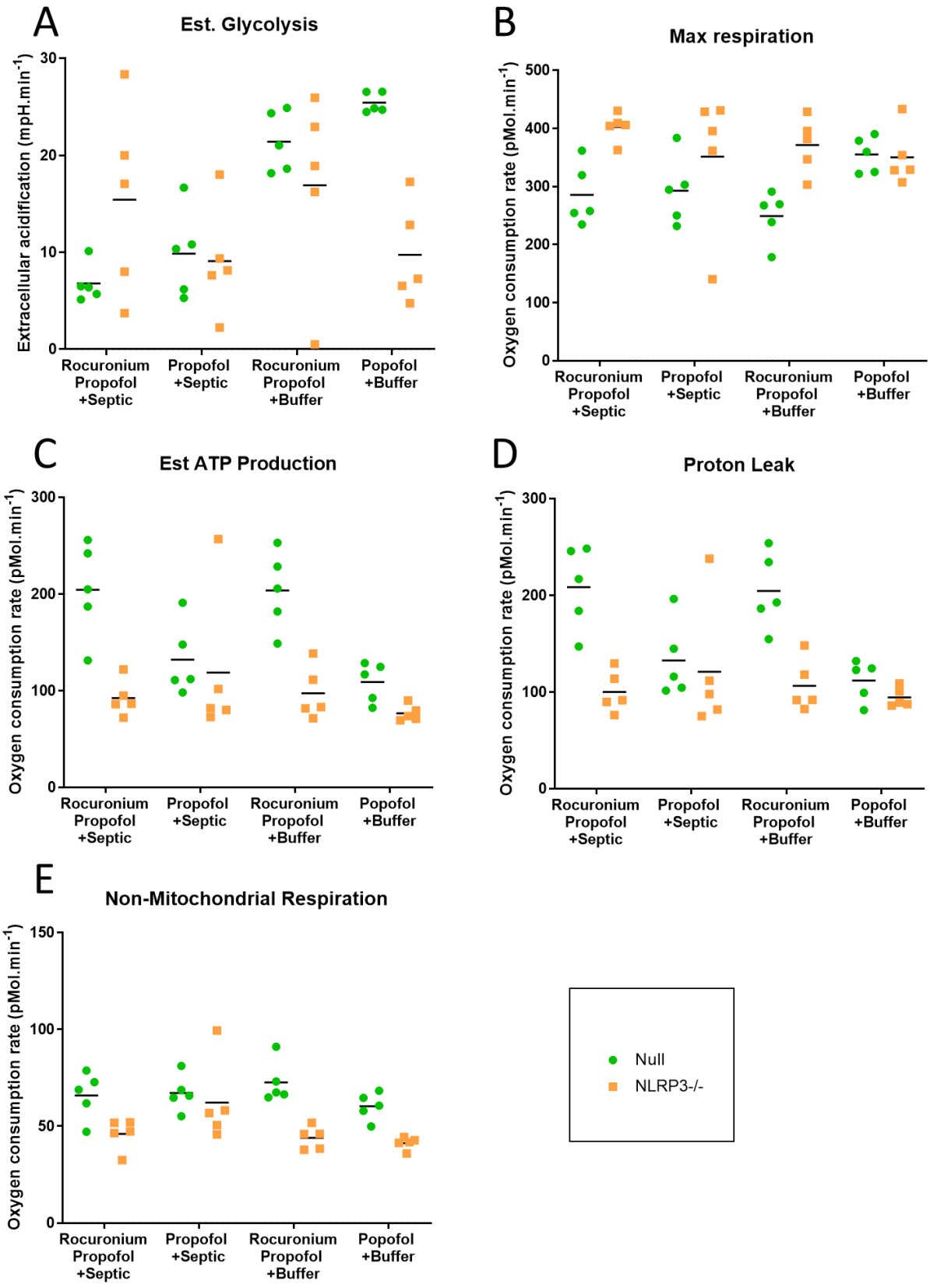

Figure 5.3.2. Estimated glycolysis (A), max respiration (B), ATP production (C), proton leak (D), and non-mitochondrial respiration (E) of THP1 Null (green) and THP1 NLRP3-/- (orange) cells after treatment with either Propofol (4μg/ml) on its own or Rocuronium (1.4μg/ml) + Propofol (4μg/ml). Cells were injected with either 10% pooled *E.coli* septic serum or assay buffer in the Seahorse analyser. All values were standardised to μg.protein/well.

A small sample size of n=5 per group precluded statistical analysis.

There are no visible differences in glycolysis, maximum respiration, ATP production, proton leak, or non-mitochondrial respiration between the different treatment conditions of NLRP3-/- cells.

In the Null cells, a trend appears to be emerging, and a larger sample size would be required to test differences. There is a trend in glycolysis between cells treated with Rocuronium and Propofol when exposed to either Septic serum of buffer, the septic serum possibly causing a reduction in glycolysis. Propofol on its own may result in lower glycolysis when restimulated with septic serum compared to buffer control in Null cells, as previously established in Chapter 4. There is a suggestion of a divide between cell type glycolysis in Propofol only exposure, with Null cells possibly being more glycolytic than NLRP3-/- cells.

There may be a difference between cell types when exposed to both Propofol and Rocuronium, with Null cells possibly displaying a lower max respiration when exposed to both septic serum and buffer. There may be differences trending between cell types when cells are treated with both Propofol and Rocuronium regarding ATP production and proton leak, with Null cells possibly having a higher estimated ATP production than NLRP3-/- cells both when restimulated to septic serum and buffer.

Rocuronium with and without septic serum

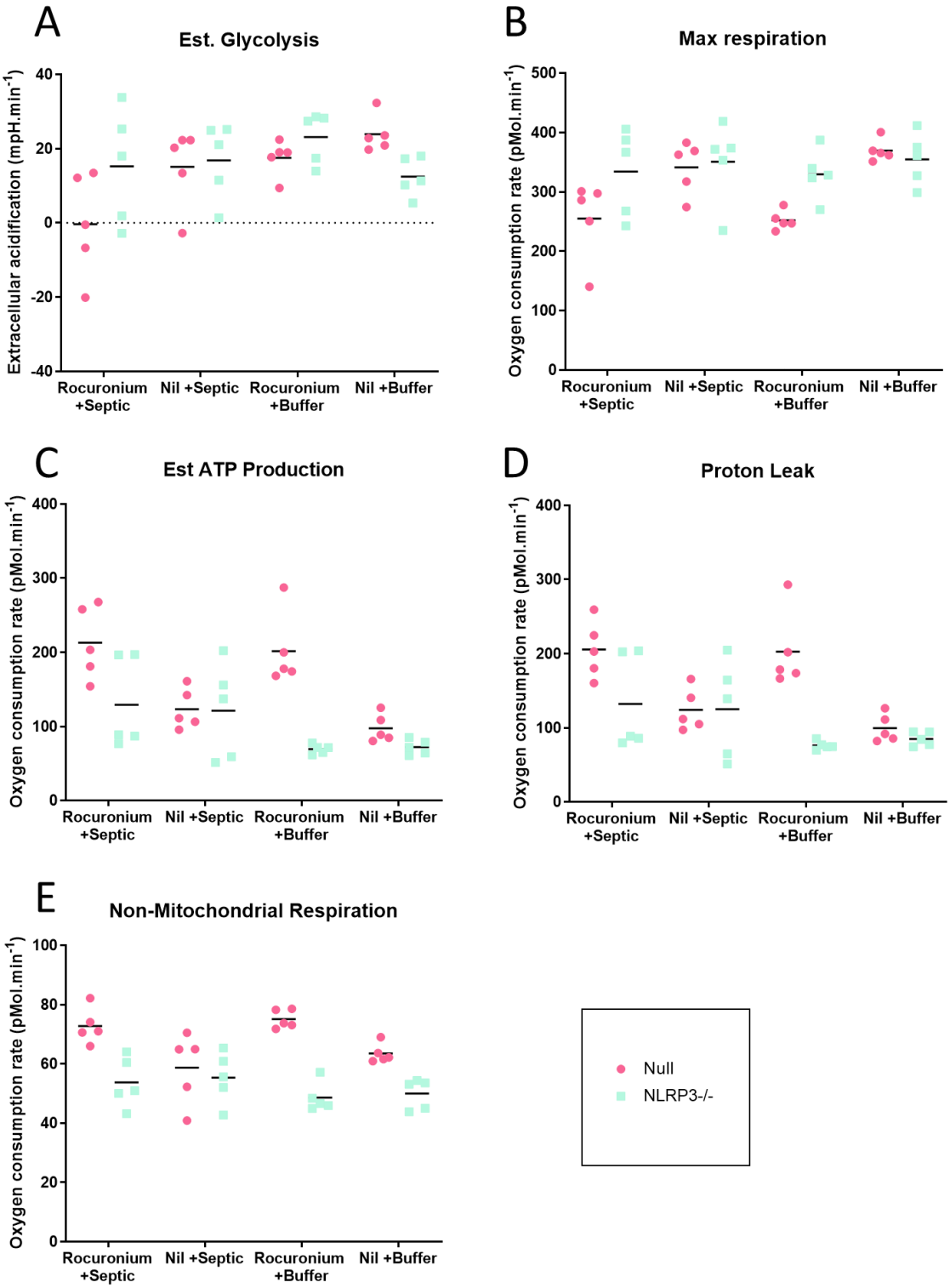

Figure 5.3.3 Estimated glycolysis (A), max respiration (B), ATP production (C), proton leak (D), and non-mitochondrial respiration (E) of THP1 Null (magenta) and THP1 NLRP3-/- (mint) cells after treatment with Rocuronium (1.4µg/ml) or Nil drug control. Cells were injected with

either 10% pooled *E.coli* septic serum or assay buffer in the Seahorse analyser. Lines represent the mean. All values were standardised to µg.protein/well.

A small sample size of n=5 per group precluded statistical analysis.

There are no visible differences in glycolysis, maximum respiration, ATP production, proton leak, or non-mitochondrial respiration between the different treatment conditions of NLRP3-/- cells.

In the Null cells, a trend appears to be emerging, and a larger sample size would be required to test differences. There is a trend in glycolysis of cells exposed to Rocuronium and restimulated with septic serum is lower than cells treated with Nil drugs and septic serum restimulation, or cells treated with Rocuronium but with a buffer control restimulation. When treated with Rocuronium and exposed to septic serum in the Seahorse analyser, Null cells may have a lower estimated glycolysis than NLRP3-/- cells.When restimulated with septic serum the cells treated with Rocuronium seem to have had a lower max respiration than cells that were treated with Nil drugs. Likewise, the Rocuronium treated Null cells seemed to have had a lower max respiration that Nil drug treated cells when restimulated with buffer only.

Septic Null cells may have had a higher ATP production and proton leak when treated with Rocuronium compared to Nil drug treatment and a higher ATP production and proton leak when stimulated with buffer compared to Nil drug treatment.

For non-mitochondrial respiration, there may be a difference between cell types for Rocuronium treatment condition; Null cells appear to have a higher non-mitochondrial respiration than NLRP3-/- when restimulated with septic serum or buffer.

5.3.3 Seahorse experiment 3: Rocuronium dose response

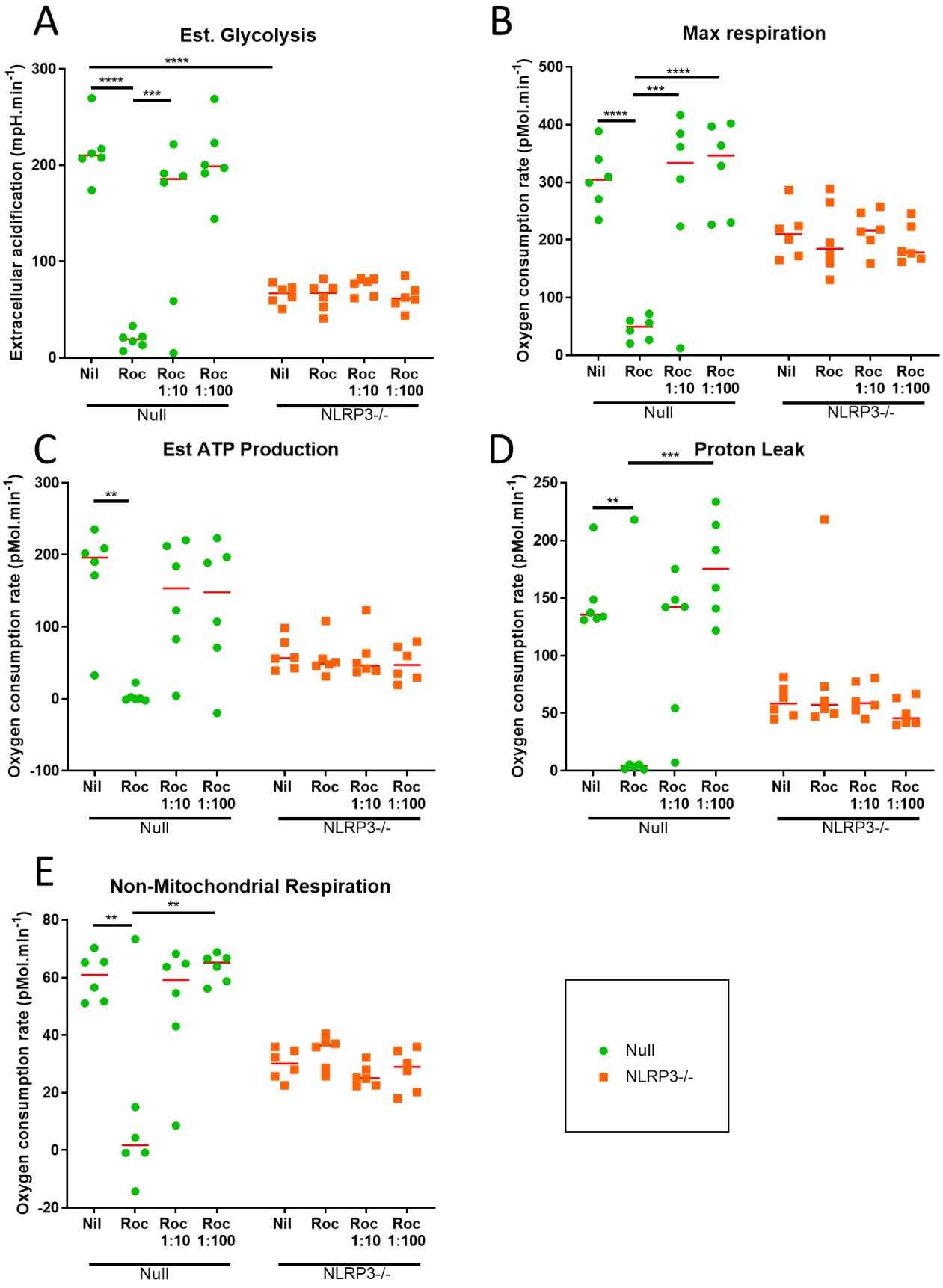

Figure 5.3.4 Estimated glycolysis of THP1 Null (green) and THP1 NLRP3-/- (orange) cells after treatment with serial dilution of Rocuronium, beginning at 1.4µg/ml, then 1:10 and 1:100 dilutions, or a Nil drug control. A p-value less than 0.05 is flagged with one star (*), a p-value is less than 0.01 is flagged with two stars (**), a p-value is less than 0.001is flagged with three stars (***) and a p-value is less than 0.0001is flagged with four stars (****). Statistics calculated via Friedman test with Dunn post-hoc test. Lines represent the mean. All values were standardised to µg.protein/well.

NLRP3-/- cells displayed no differences in estimated glycolysis, maximum respiration, ATP production, proton leak, or non-mitochondrial respiration between their different treatment conditions.

With the Nil drug treatment control, Null cells again demonstrated a higher estimated glycolysis than NLRP3-/- cell ($p<0.0001$). In Null cells, again treatment with Rocuronium at the highest concentration of 1.4µg/ml resulted in a far lower estimated glycolysis than the Null Nil drug treated cells ($p<0.0001$). However, with the drug dilutions the estimated glycolysis began to recover to the levels of the Nil drug; with the 1:10 Rocuronium higher ($p=0.0003$ compared to Rocuronium) and 1:100 Rocuronium dilution the same as the Nil drug glycolysis levels. In Null cells, treatment with Rocuronium at the highest concentration of 1.4µg/ml resulted in a far lower maximum respiration than the Null Nil drug treated cells ($p<0.0001$). When the Rocuronium was diluted 1:10, there was no longer a difference in maximum respiration compared to Nil drug control ($p=0.0002$ compared to Rocuronium 1.4µg/ml), and likewise with 1:100 Rocuronium dilution ($p<0.0001$ compared to Rocuronium 1.4µg/ml).

In Null cells, treatment with Rocuronium at the highest concentration of 1.4µg/ml resulted in a far lower estimated ATP production than the Null Nil drug treated cells ($p= 0.0023$). When the Rocuronium was diluted 1:10, there was no longer a difference in estimated ATP production compared to Nil drug control and likewise with 1:100 Rocuronium dilution.

In Null cells, treatment with Rocuronium at the highest concentration of 1.4µg/ml resulted in a far lower proton leak than the Null Nil drug treated cells (p= 0.0032). When the Rocuronium was diluted 1:10, there was no longer a difference in proton leak compared to Nil drug control, and likewise with 1:100 Rocuronium dilution.

In Null cells, treatment with Rocuronium at the highest concentration of 1.4µg/ml resulted in a far lower non-mitochondrial respiration than the Null Nil drug treated cells (p= 0.0042). When the Rocuronium was diluted 1:10, there was no longer a difference in non-mitochondrial respiration compared to Nil drug control, and likewise with 1:100 Rocuronium dilution.

5.3.4 Seahorse experiment 4: The immunometabolic effects of muscle relaxants Rocuronium and Vecuronium after administration of reversal agent Sugammadex.

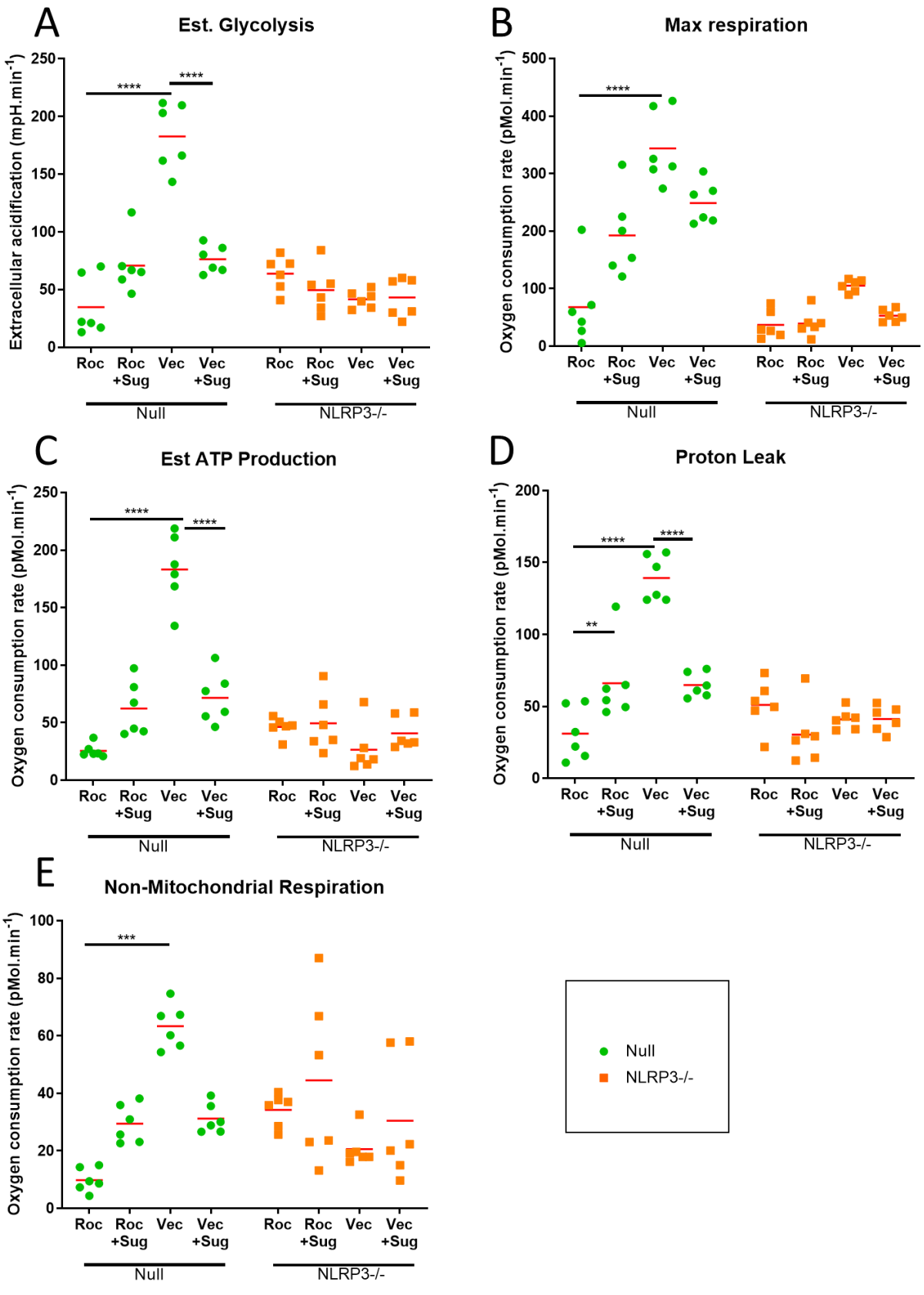

Figure 5.3.5 Estimated glycolysis of THP1 Null (green) and THP1 NLRP3-/- (orange) cells after treatment with either Rocuronium (1.4µg/ml) or Vecuronium (0.14µg/ml) with or without the reversal agent Sugammadex (50µg/ml). A p-value less than 0.05 is flagged with one star (*), a p-value is less than 0.01 is flagged with two stars (**), a p-value is less than 0.001is flagged with three stars (***) and a p-value is less than 0.0001is flagged with four stars (****). Statistics calculated via Friedman test with Dunn post-hoc. Line represent the means. All values were standardised to µg.protein/well.

NLRP3-/- cells displayed no differences in estimated glycolysis, maximum respiration, ATP production, proton leak, or non-mitochondrial respiration between their different treatment conditions.

In Null THP1s, cells treated with Vecuronium alone had a higher estimated glycolysis than cells treated with Vecuronium and then reversed with Sugammadex ($p<0.0001$). While there were no differences in estimated glycolysis between the two Sugammadex reversal treatments of Rocuronium and Vecuronium, cells which were treated only with Rocuronium had a lower glycolysis than Vecuronium treated cells ($p<0.0001$). Rocuronium treated cells also had a lower maximum respiration than Vecuronium treated cells ($p<0.0001$). There were no differences in maximum respiration between cells treated with Rocuronium + Sugammadex and Vecuronium + Sugammadex. There were also no differences in maximum respiration between cells treated with Vecuronium only and cells treated with Vecuronium and reversed with Sugammadex. In the Null cells, estimated ATP production was higher in the Vecuronium condition than both the Rocuronium condition ($p<0.0001$) and the Vecuronium + Sugammadex condition ($p<0.0001$). Proton leak was higher in the Vecuronium condition than both the Rocuronium condition ($p<0.0001$) and the Vecuronium + Sugammadex condition ($p<0.0001$). The cells treated with Rocuronium had a lower proton leak than cells treated with

Rocuronium + Sugammadex (p= 0.0032). Vecuronium treated cells had a higher non-mitochondrial respiration than Rocuronium (p= 0.0001).

5.3.5 The effects of rocuronium on cholinergic and cytokine gene expression.

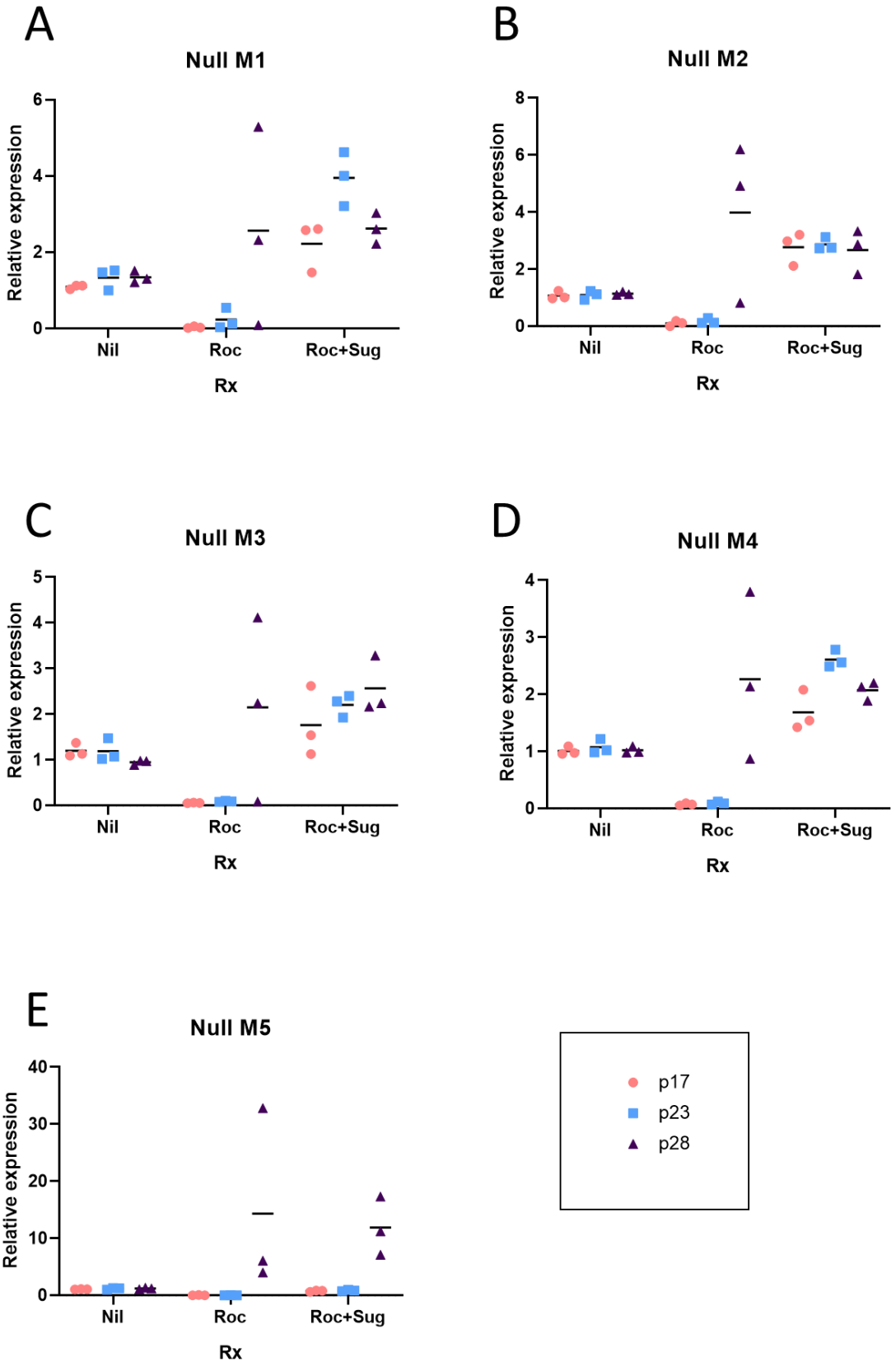

Figure 5.3.6.1 Relative expression of the M1, M2, M3, M4, and M5 genes for THP1 Null cells at passage 17 (peach), passage 23 (blue) and passage 28 (mauve). Cells of each passage were divided and treated with either Rocuronium (1.4µg/ml), Rocuronium (1.4µg/ml) and Sugammadex (50µg/ml), or Nil drug control, n=3 per treatment condition.

A small sample size of n=3 per group precluded statistical analysis. However, we can still observe trends with may warrant further investigation.

For passage 17and 23 Null THP1 cells, relative expression of the M1, M2, M3 and M4 genes appeared lower with Rocuronium treatment than treatment with Rocuronium and Sugammadex reversal. The additional of Sugammadex possibly raises expression relative to Rocuronium and nil. The M5 gene does not have any trends to observe.

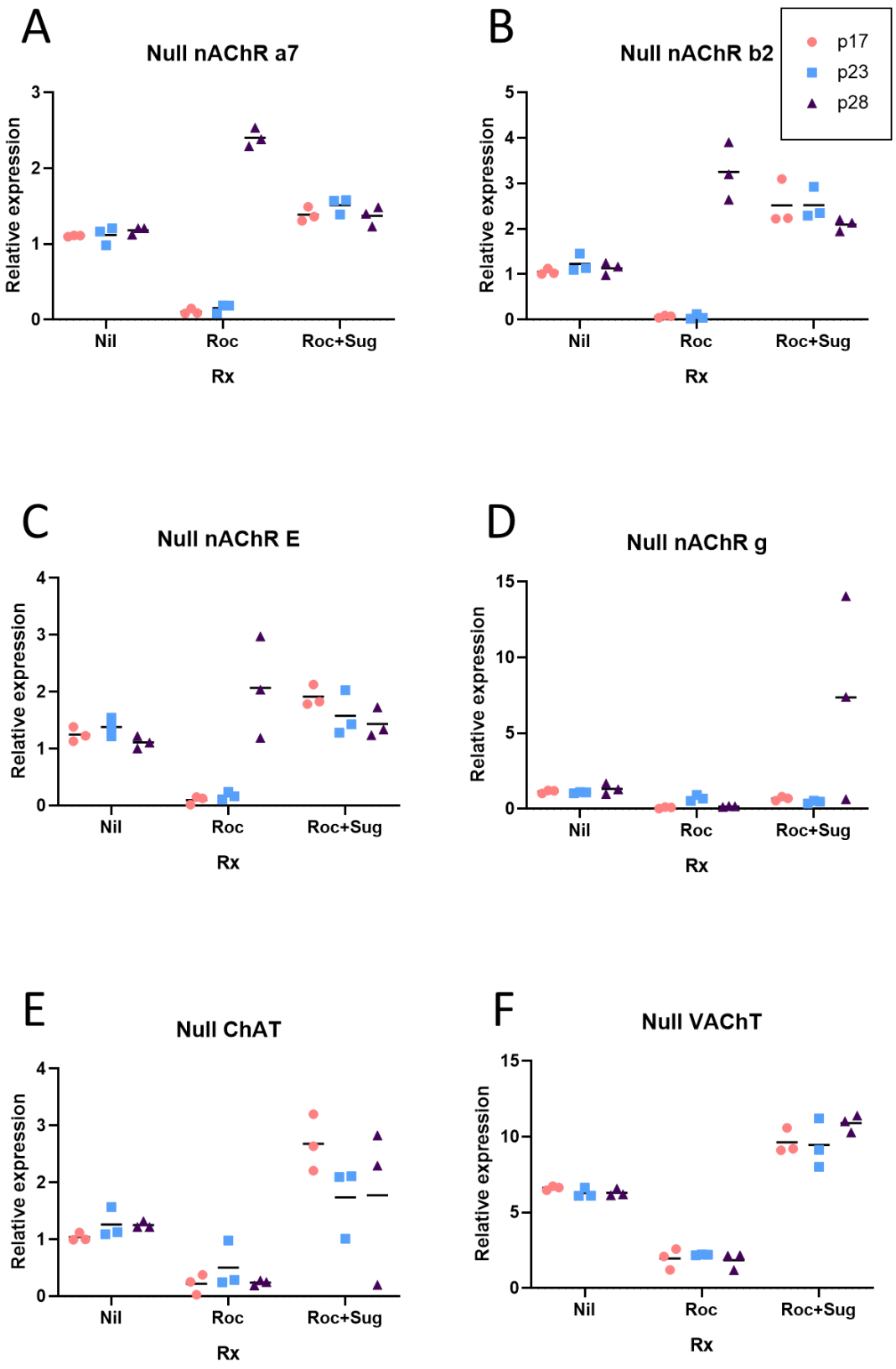
A
Null nAChR a7
Relative expression
0
1
2
3
Nil
Roc
Roc+Sug
Rx
B
Null nAChR b2
p17
p23
p28
Relative expression
0
1
2
3
4
5
Nil
Roc
Roc+Sug
Rx
C
Null nAChR E
Relative expression
0
1
2
3
4
Nil
Roc
Roc+Sug
Rx
D
Null nAChR g
Relative expression
0
5
10
15
Nil
Roc
Roc+Sug
Rx
E
Null ChAT
Relative expression
0
1
2
3
4
Nil
Roc
Roc+Sug
Rx
F
Null VAChT
Relative expression
0
5
10
15
Nil
Roc
Roc+Sug
Rx

Figure 5.3.6.2 Relative expression of A) nAChR α7 B) nAChRβ2, C) nAChRε, D) nAChRγ, E) ChAT, and F) AChT genes for THP1 Null cells at passage 17 (peach), passage 23 (blue) and passage 28 (mauve). Cells of each passage were divided and treated with either Rocuronium (1.4µg/ml), Rocuronium (1.4µg/ml) and Sugammadex (50µg/ml), or Nil drug control, n=3 per treatment condition.

In a similar trend to the M1-5 genes, most of these genes (with the exception of nAChRγ) appear to have less expression when treated with Rocuronium and more expression when treated with Rocuronium and Sugammadex compared to Nil treatment for the passages 17 and 23.

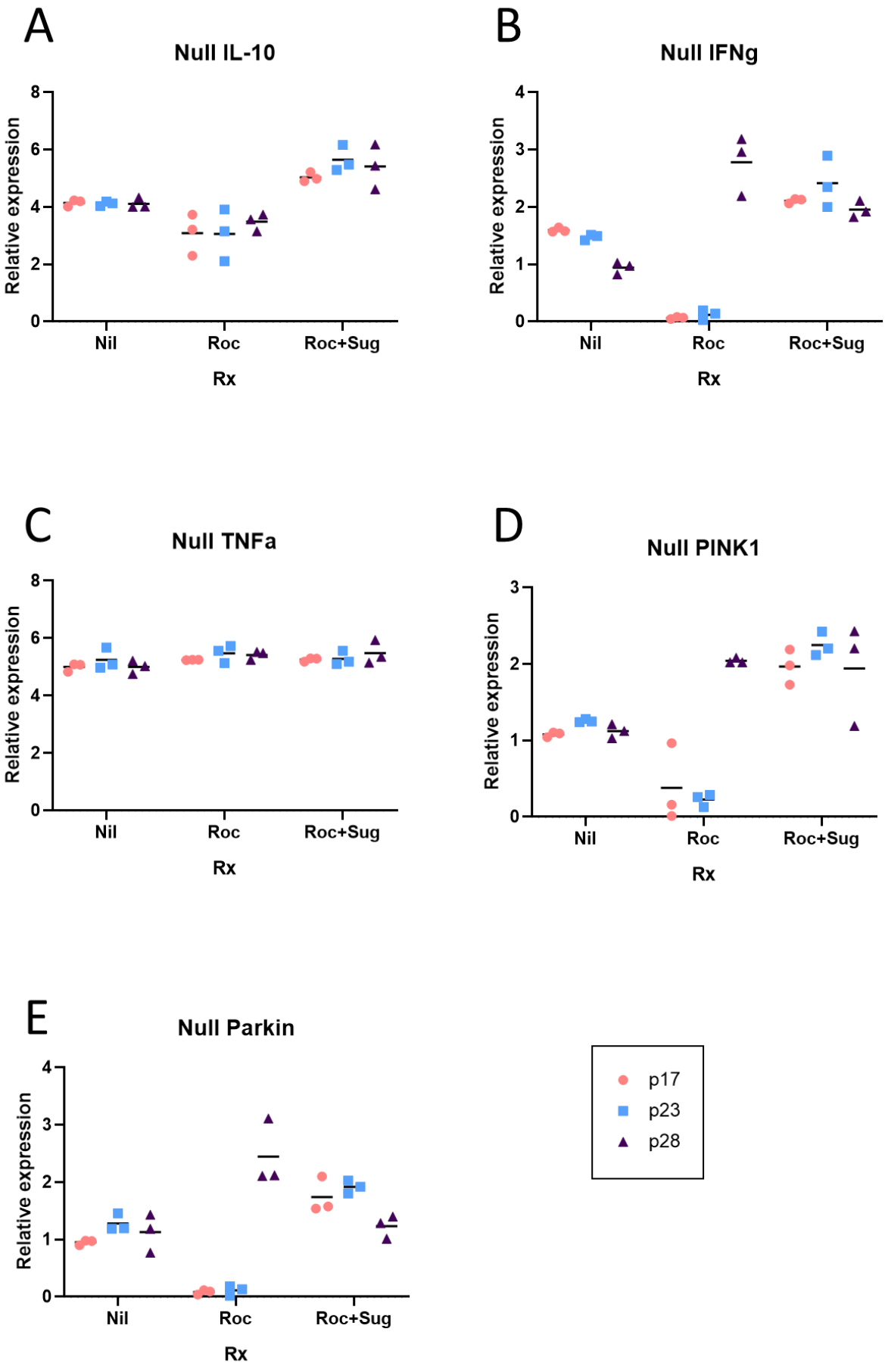
A
Null IL-10
Relative expression
0
2
4
6
8
Nil
Roc
Roc+Sug
Rx
B
Null IFNg
Relative expression
0
1
2
3
4
Nil
Roc
Roc+Sug
Rx
C
Null TNFa
Relative expression
0
2
4
6
8
Nil
Roc
Roc+Sug
Rx
D
Null PINK1
Relative expression
0
1
2
3
Nil
Roc
Roc+Sug
Rx
E
Null Parkin
Relative expression
0
1
2
3
4
Nil
Roc
Roc+Sug
Rx
p17
p23
p28

Figure 5.3.6.3 Relative expression of A) IL-10 B) IFNγ C) TNFα D) PINK1 E) Parkin genes for THP1 Null cells at passage 17 (peach), passage 23 (blue) and passage 28 (mauve). Cells of each passage were divided and treated with either Rocuronium (1.4µg/ml), Rocuronium (1.4µg/ml) and Sugammadex (50µg/ml), or Nil drug control, n=3 per treatment condition.

Relative expression of the PINK1, IFNγ and Parkin genes appeared to follow the previous trend of appearing lower in Rocuronium treated groups than groups treated with Nil drugs in both passage 17 and 23, higher in passage 28.

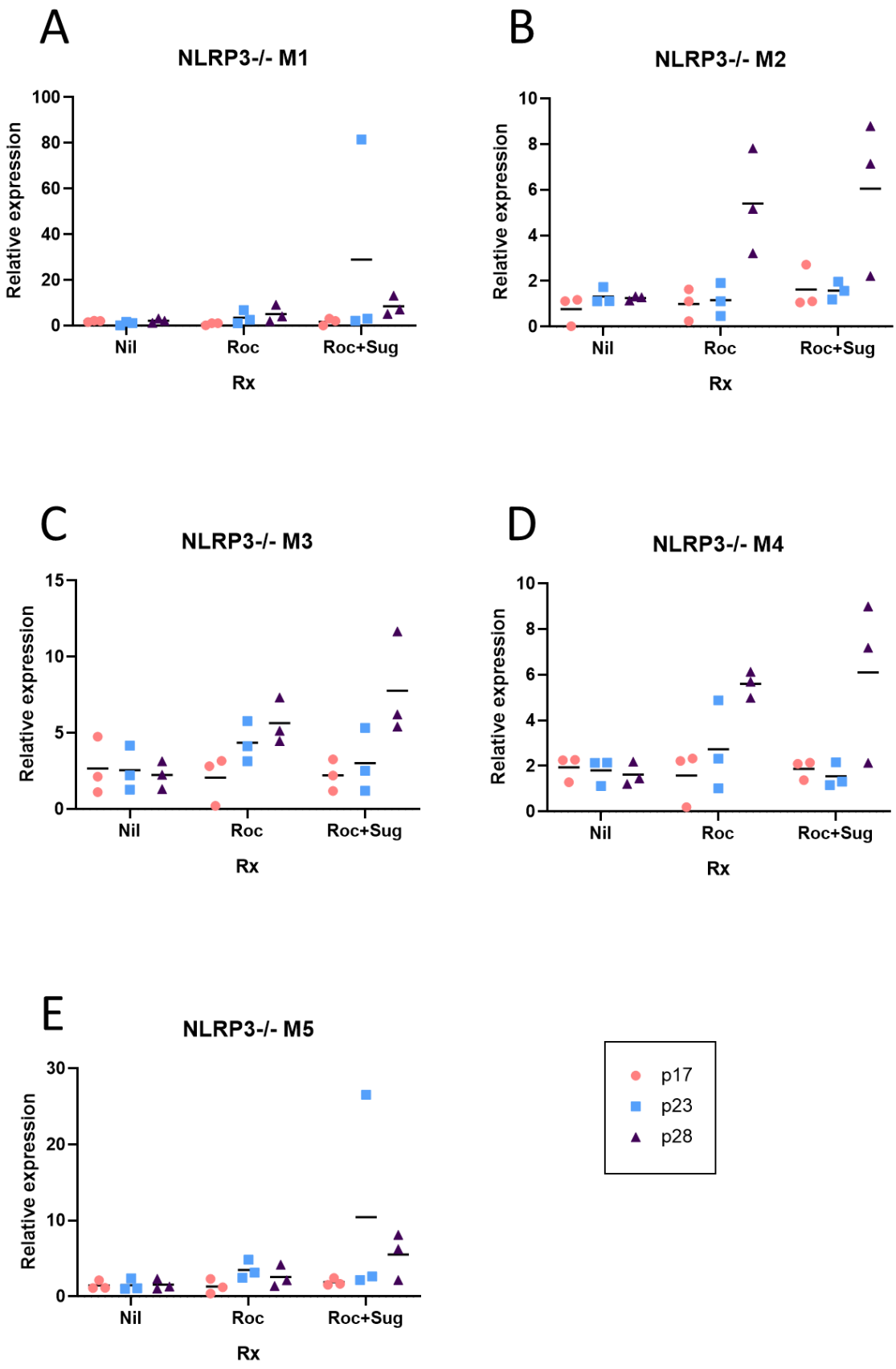
A
NLRP3-/- M1
Relative expression
100
80
60
40
20
0
Nil
Roc
Roc+Sug
Rx
B
NLRP3-/- M2
Relative expression
10
8
6
4
2
0
Nil
Roc
Roc+Sug
Rx
C
NLRP3-/- M3
Relative expression
15
10
5
0
Nil
Roc
Roc+Sug
Rx
D
NLRP3-/- M4
Relative expression
10
8
6
4
2
0
Nil
Roc
Roc+Sug
Rx
E
NLRP3-/- M5
Relative expression
30
20
10
0
Nil
Roc
Roc+Sug
Rx
p17
p23
p28

Figure 5.3.6.4 Relative expression of the M1, M2, M3, M4, and M5 genes for THP1 NLRP3-/- cells at passage 17 (peach), passage 23 (blue) and passage 28 (mauve). Cells of each passage were divided and treated with either Rocuronium (1.4µg/ml), Rocuronium (1.4µg/ml) and Sugammadex (50µg/ml), or Nil drug control, n=3 per treatment condition.

There appeared to be less of a trend in the NLRP3-/- cells than the Null cells. The expression of some genes appeared higher in some of the older passage strains.

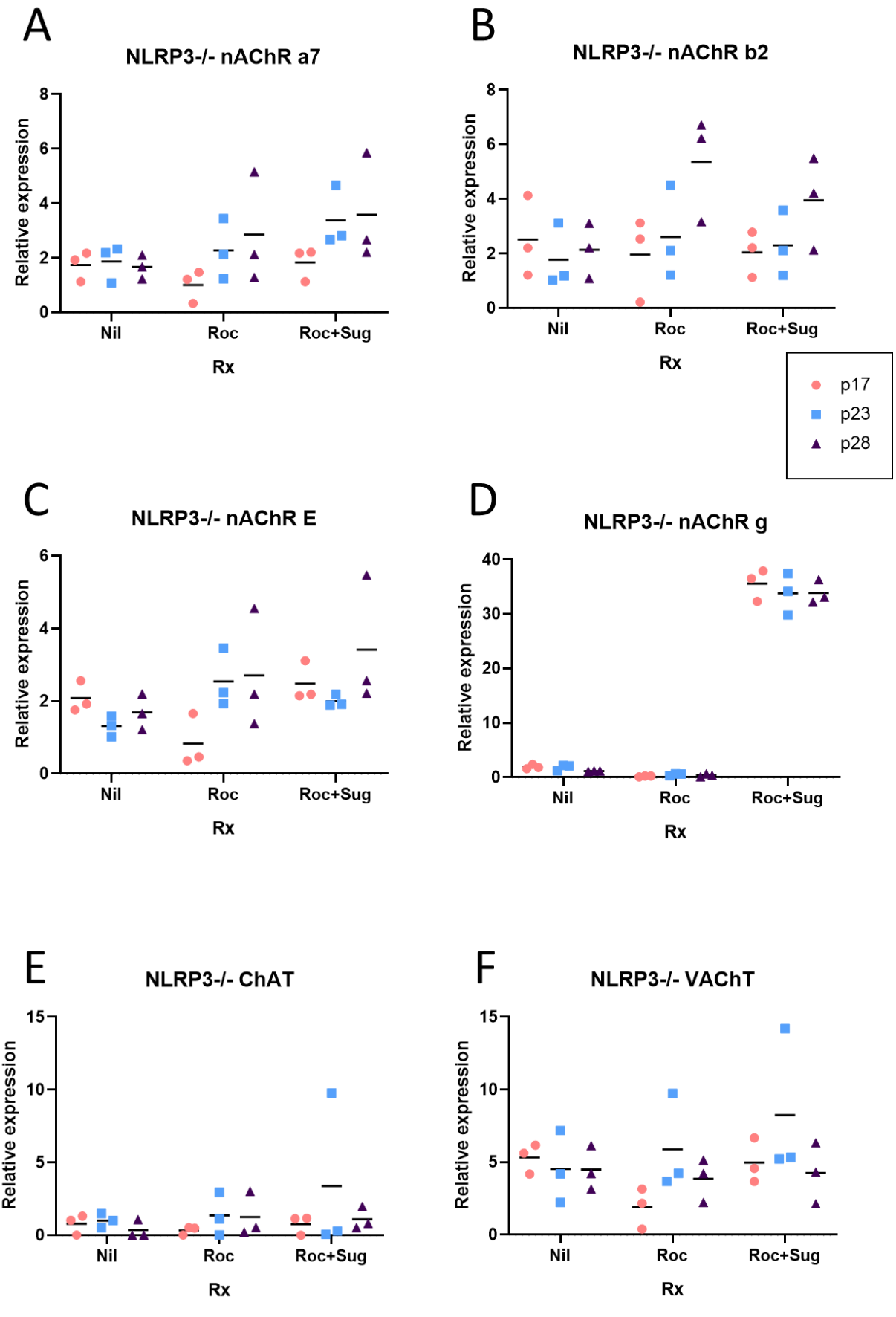
A
NLRP3-/- nAChR a7
Relative expression
0
2
4
6
8
Nil
Roc
Roc+Sug
Rx
B
NLRP3-/- nAChR b2
Relative expression
0
2
4
6
8
Nil
Roc
Roc+Sug
Rx
p17
p23
p28
C
NLRP3-/- nAChR E
Relative expression
0
2
4
6
Nil
Roc
Roc+Sug
Rx
D
NLRP3-/- nAChR g
Relative expression
0
10
20
30
40
Nil
Roc
Roc+Sug
Rx
E
NLRP3-/- ChAT
Relative expression
0
5
10
15
Nil
Roc
Roc+Sug
Rx
F
NLRP3-/- VAChT
Relative expression
0
5
10
15
Nil
Roc
Roc+Sug
Rx

Figure 5.3.6.5 Relative expression of A) nAChR α7 B) nAChRβ2, C) nAChRε, D) nAChRγ, E) ChAT, and F) AChT genes for THP1 NLRP3-/- cells at passage 17 (peach), passage 23 (blue) and passage 28 (mauve). Cells of each passage were divided and treated with either Rocuronium (1.4µg/ml), Rocuronium (1.4µg/ml) and Sugammadex (50µg/ml), or Nil drug control, n=3 per treatment condition.

There was a noticeable trend for the nAChRγ genes to have a higher expression when treated with Rocuronium and Sugammadex compared to Rocuronium alone or Nil treatment, however the other genes did not show any noticeable patterns.

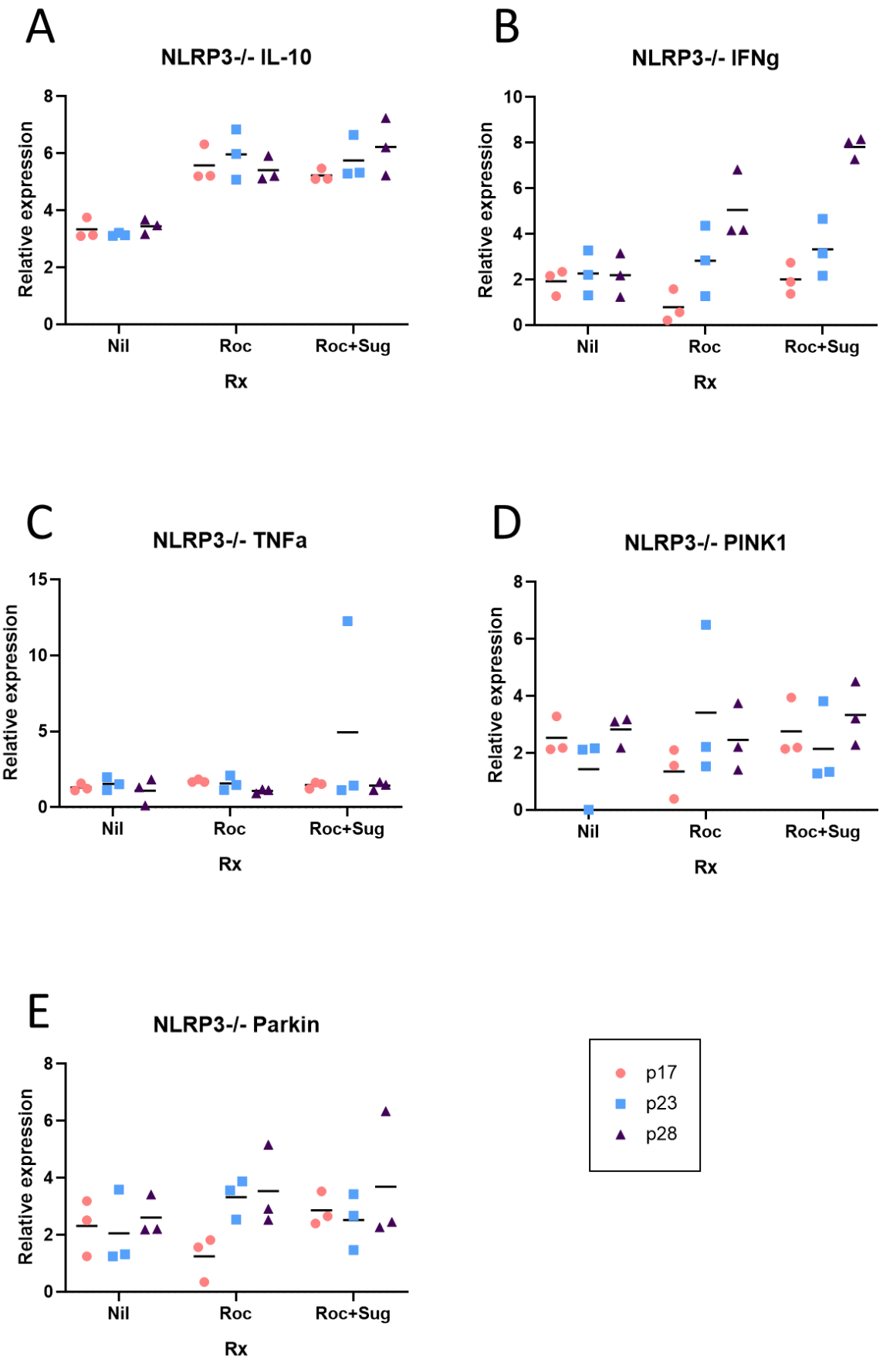
A
NLRP3-/- IL-10
Relative expression
0
2
4
6
8
Nil
Roc
Roc+Sug
Rx
B
NLRP3-/- IFNg
Relative expression
0
2
4
6
8
10
Nil
Roc
Roc+Sug
Rx
C
NLRP3-/- TNFa
Relative expression
0
5
10
15
Nil
Roc
Roc+Sug
Rx
D
NLRP3-/- PINK1
Relative expression
0
2
4
6
8
Nil
Roc
Roc+Sug
Rx
E
NLRP3-/- Parkin
Relative expression
0
2
4
6
8
Nil
Roc
Roc+Sug
Rx
p17
p23
p28

Figure 5.3.6.6 Relative expression of A) IL-10 B) IFNγ C) TNFα D) PINK1 E) Parkin genes for THP1 NLRP3-/- cells at passage 17 (peach), passage 23 (blue) and passage 28 (mauve). Cells of each passage were divided and treated with either Rocuronium (1.4µg/ml), Rocuronium (1.4µg/ml) and Sugammadex (50µg/ml), or Nil drug control, n=3 per treatment condition.

Again, most genes did not display any discernible pattern in their relative gene expression in NLRP3-/- cells. The IL-10 gene expression may be higher in cells treated with Rocuronium and Rocuronium with Sugammadex than the Nil treatment.

5.3.6 IL-10 production after Rocuronium and Sugammadex exposure.

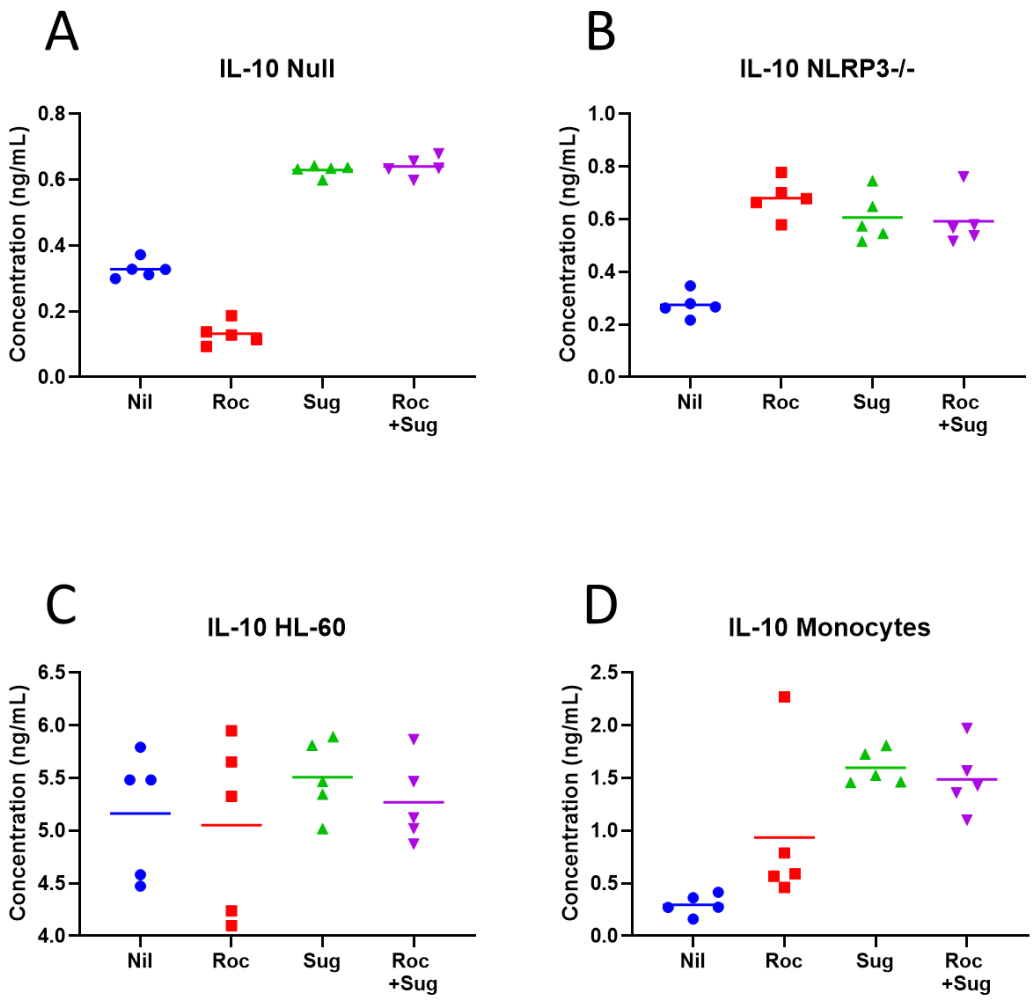

Figure 5.3.7.1 The concentration on IL-10 (ng/mL) in cell supernatants of A) THP1 Nulls, B) THP1 NLRP3-/-, C) HL-60, and D) Monocytes as determined via ELISA assay for cells treated with either Nil drugs control, Rocuronium 1.4µg/ml, Sugammadex 50µg/ml, or Rocuronium 1.4µg/ml and then reversed with Sugammadex 50µg/ml. N=5 per condition. Cells were treated with either Rocuronium for 6 hours or cell media control, then washed and treated with either Sugammadex or cell media control for a further 30 minutes before washing and being left to recover for three days, then supernatants harvested. Lines represent the median values.

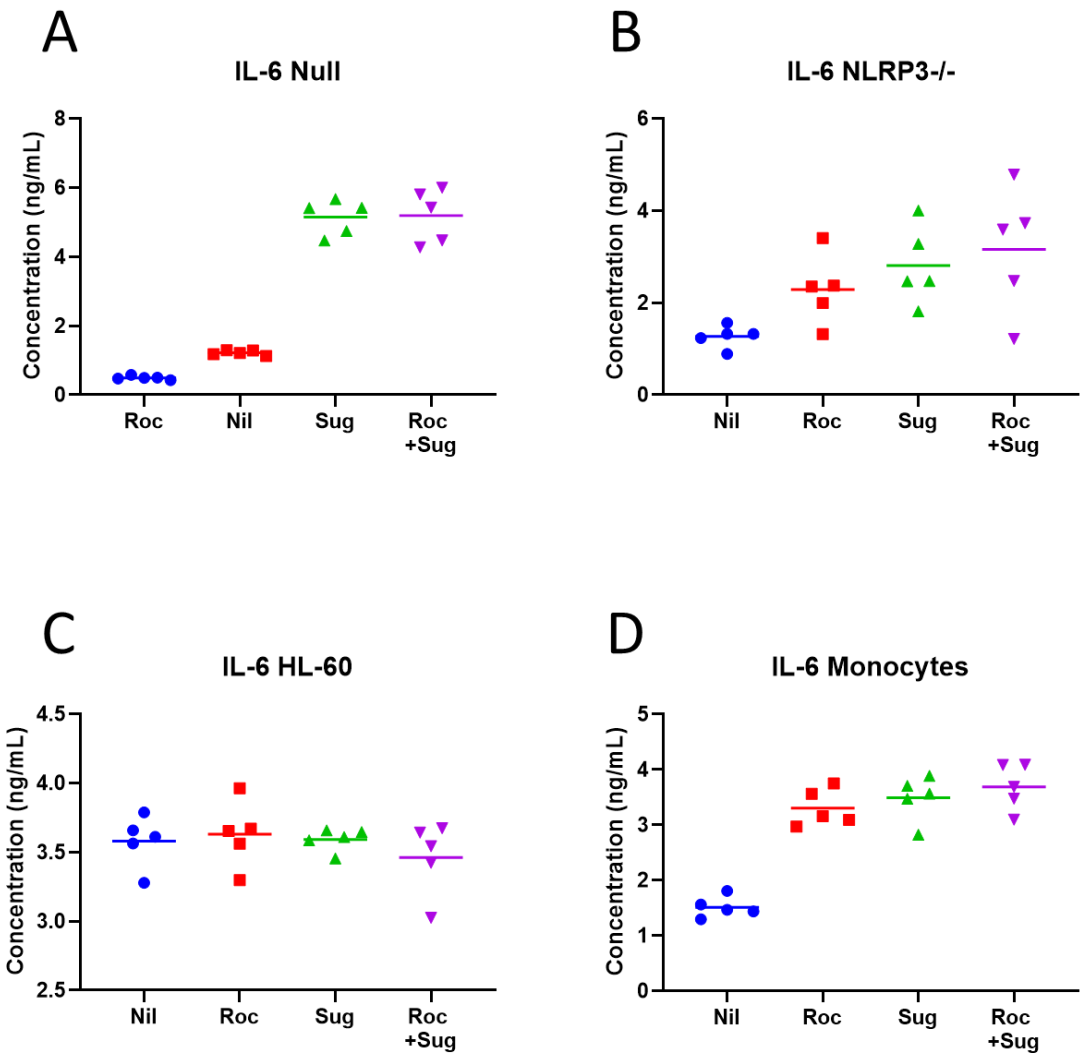

Figure 5.3.7.2 The concentration on IL-6 (ng/mL) in cell supernatants of A) THP1 Nulls, B) THP1 NLRP3-/-, C) HL-60, and D) Monocytes as determined via ELISA assay for cells treated with either Nil drugs control, Rocuronium 1.4µg/ml, Sugammadex 50µg/ml, or Rocuronium 1.4µg/ml and then reversed with Sugammadex 50µg/ml. N=5 per condition. Cells were treated with either Rocuronium for 6 hours or cell media control, then washed and treated with either Sugammadex or cell media control for a further 30 minutes before washing and being left to recover for three days, then supernatants harvested. Lines represent the median values.

A small sample size of n=5 per group precluded statistical analysis. However, we can still observe trends with may warrant further investigation. In Null cells, there appears to be a reduction in IL-10 and IL-6 in the Rocuronium treated samples. The NLRP3-/- THP1s and Monocytes appear to instead have lower levels of IL-10 and IL-6 in the Nil samples. HL-60 cells did not reveal any trends.

5.4 Discussion

Exposure to the muscle relaxant Rocuronium and its reversal agent Sugammadex results in changes in the immunometabolism of THP1 Null but not THP1 NLRP3-/- cells.

When THP1 Null cells are treated with Rocuronium, the cells appear to not respond to the mitochondrial poisons Oligomycin, FCCP, and Rotenone/Antimycin A that are injected in the Seahorse analyser. This is not the case when exposed to Vecuronium; and is not the case with NLRP3-/- cells which respond to the poisons with both Rocuronium and Vecuronium. The serial dilution of Rocuronium in Null cells diminishes this effect until the drug is diluted enough to return immunometabolic responses the same as control cells exposed to Nil drugs.

Rocuronium in Null cells results in a reduction of glycolysis and maximum respiration compared to Nil drug controls. A higher maximum respiration is an indicator that the cells have more of an energy reserve to combat infection. In Null cells, the addition of Sugammadex to Rocuronium results in an increase in maximum respiration and proton leak compared to Rocuronium alone. This is not observed in NLRP3-/- cells.

This suggests that the reactions in response to rocuronium are associated with the NLRP3 inflammasome. When acute respiratory distress syndrome (ARDS) patients, who present with pulmonary and systemic inflammation, were administered neuromuscular blocking agents their inflammatory response was decreased, specifically circulating levels of TNFα, IL-1β, and IL-6 (Forel *et al,* 2006). As previously discussed, IL-1β can mediate the NLRP3 inflammasome. A further ARDS study found that neuromuscular blockade results in a decrease in IL-8, which is used as a biomarker of systemic inflammation and epithelial and endothelial lung injury in

ARDS (Sottile *et al*, 2018). A meta-analysis in 2019 in ARDS found that neuromuscular blockade is associated with a lower 21-28 day mortality (Shao *et al,* 2019).

If neuromuscular blockade indirectly effects the NLRP3 inflammasome then this may explain why the NLRP3-/- THP1s react to rocuronium differently than the Null THP1s.

Rocuronium affects the immunometabolism of cells when exposed to infectious agents.

Unfortunately, the septic serum used to restimulate cells was old and therefore did not result in as large of a response as has been observed previously in Chapter 4. However, cells did still respond to it and Rocuronium in Null cells resulted in a lower glycolysis when exposed to septic serum than a buffer control. When exposed to septic serum, Rocuronium treated Null cells also had a higher proton leak, estimated ATP production, and non-mitochondrial respiration, and a lower glycolysis and maximum respiration, than the Nil drug control. When NLRP3-/- THP1 cells were exposed, the only difference observed in the presence of Rocuronium was that the cells had a higher estimated ATP production when restimulated with the septic serum instead of the buffer control.

This suggests that Rocuronium will affect the immunometabolism of cells when exposed to infectious agents. As discussed in previous chapters, changes to immunometabolism may contribute to immune suppression in recovered septic patients.

THP1 Null cells exposed to Propofol with the addition of Rocuronium have a different immunometabolic profile than cells exposed to Propofol alone.

The addition of Rocuronium will Propofol in Null THP1 cells results in a lower maximum respiration, and a higher estimated ATP production and proton leak, than in cells exposed to Propofol alone. NLRP3-/- cells do not display changes in immunometabolism when Rocuronium is added to Propofol compared to Propofol alone. This will have implications in a clinical setting, as patients are often given a combination of Propofol and Rocuronium in anaesthesia.

Vecuronium treatment results in a different immunometabolic profile than Rocuronium treatment in Null THP1 cells.

Despite being molecularly similar drugs, the immunometabolism of Null THP1 cells responds differently to Vecuronium than Rocuronium. It can be observed in the Seahorse readout that the cells exposed to Vecuronium still respond to the mitochondrial inhibitors in the Seahorse machine, unlike the cells exposed to Rocuronium.

In Null cells exposed to Rocuronium, glycolysis is lower than when exposed to Rocuronium + Sugammadex. However Null cells exposed to Vecuronium have a higher glycolysis than cells exposed to Rocuronium, and the addition of Sugammadex to the Vecuronium reduces glycolysis. The addition of Sugammadex to Rocuronium increases glycolysis, but the addition of Sugammadex to Vecuronium reduces it. Vecuronium treated Null cells also have a higher maximum respiration, estimated ATP production, proton leak, and non-mitochondrial respiration than Rocuronium treated cells.

The addition of Sugammadex to the Vecuronium in Null cells reduces the estimated ATP production, proton leak, and non-mitochondrial respiration compared to Vecuronium alone.

This is in contrast to Rocuronium treated Null cells, where the addition of Sugammadex results in an increase in maximum respiration and proton leak.

In NLRP3-/- THP1 cells, there are no differences in immunometabolism between cells treated with any of the drugs.

Rocuronium and Sugammadex affect the expression of key cholinergic and cytokine genes in THP1 cells.

In Null cells, Rocuronium caused a decrease in relative expression of the muscarinic receptor genes M1, M2, M3 and M4 compared to cells treated with Rocuronium and Sugammadex. M1 and M4 gene expression was higher in cells treated with Rocuronium and Sugammadex compared to the Nil drug control. In the nicotinic receptors, Rocuronium reduced the relative expression of the genes of nAChR α7, nAChR β2, and nAChR ε compared to Nil drug treatment and Rocuronium +Sugammadex treatment. This same pattern was observed in the relative expressions of ChAT, PINK1, Parkin, VAChT, and the cytokines IL-10 and IFNγ.

Despite the few differences in immunometabolism ad cytokine production, THP1 NLRP3-/- cells also demonstrated differences in gene expression when exposed to Rocuronium and Sugammadex. The relative expression of the nAChR γ gene was higher in cells exposed to Rocuronium and Sugammadex compared to Rocuronium alone or the Nil drug control, and exposure to Rocuronium related in an increased in expression of the IL-10 gene compared to the Nil drug control. A few more differences in gene expression were observed in old p28 NLRP3-/- cells but not the younger p17/p23 cells. For both THP1 Nulls and NLRP3-/- cells, older cells (p28) had a significantly different profile to the younger cells (p17 and p23).

HL-60 and n=5 donor monocytes were also assessed; however no differences were observed.

The addition of Sugammadex results in an increase in concentration of IL-6 and IL-10 in THP1 Null cells.

The cells had had the Rocuronium/Sugammadex washed from them and were left to recover for three days prior to supernatant samples being taken. Furthermore, cells were not restimulated with an infectious agent, therefore all concentrations of IL-6 and IL-10 released by cells were low and indicative of the cells' healthy resting state. Nevertheless, monocytes and Null THP1 cells released a higher concentration of IL-10 cytokine when exposed to Sugammadex alone or combination Rocuronium + Sugammadex three days prior. The same was observed in Null THP1 cells with IL-6 concentrations rising when exposed to Sugammadex alone or combination Rocuronium + Sugammadex three days prior. It is worth noting that there was a high cell death in monocytes after the three days of recovery, cell viability being 68% when the supernatant samples were taken. HL-60 and NLRP3-/- THP1 cells showed no differences between treatment conditions for concentrations of IL-10 or IL-6. Sugammadex is thought to not interact directly with the cell, this data suggests that it may do.

Different cell types and passage numbers respond to Rocuronium and Sugammadex in different ways.

In THP1 cells, the Null cells had a very particular response to Rocuronium and Sugammadex, affecting immunometabolism, cytokine production and expression of certain genes. The addition of Rocuronium appeared to prevent cells from responding to the mitochondrial

poisons injected in the Seahorse machine. These responses were not observed in NLRP3-/- cells, which were largely unaffected by the addition of Rocuronium and Sugammadex. This suggests that the response to Rocuronium in Null cells may involve the NLRP3 inflammasome. However, HL-60 cells (which contain the inflammasome) did not reveal any effects of Rocuronium on cytokine production of IL-10 and IL-6 or gene expression. There may be another mechanism preventing the HL-60 cells from being affected by the drug, and these were not assessed in the Seahorse and so immunometabolic changes in HL-60 cannot be assessed. It is also possible that the HL-60 cells recovered faster from the drugs during their three-day rest period. Different cell types may require different lengths of recovery time. Although, this is not likely to be the case where Rocuronium was administered without the Sugammadex reversal agent, which would likely still be bound to receptors even after washing the cells.

Whilst HL-60 cells were a young passage 12, a selection of different passage numbers were assessed in the gene expression in THP1 Null and NLRP3-/- cells. Old cells, at passage 28, had a different profile of gene expression when exposed to the drugs compared to younger cells (p17 and p23). There were also some differences in gene expression between passage 17 and passage 23 when exposed to the drugs. It is therefore important to maintain a consistent cell passage number when performing experiments.

Only a small number (n=5) of human donors was assessed and only monocytes were examined, however the results of the IL-10 cytokine production experiments indicate that Rocuronium and Sugammadex have a lasting effect on monocytes. A larger sample population and a greater variety of immune cell types will be required in order to inform cause and effect.

Further research

All experiments were performed after a three-day rest period from the drug exposure. A comparison of these results to cells which did not have a period of rest may reveal larger differences induced by Rocuronium and Sugammadex. Cells such as the HL-60 line may have had changes due to the drugs which were missed if they had fully recovered during the three-day period. This would also be of benefit to cells from human donors which gradually die off over the period of rest. It would equally be interesting to have a longer recovery period with the THP1 cell line to see how long the changes persist.

Seahorse experiments were performed only on THP1 Null and THP1 NLRP3-/- cells. Immunometabolism of HL-60 cells and donor monocytes should be assessed in the presence of Rocuronium and Sugammadex. Further to this, different peripheral blood mononuclear cell types should be examined as well as monocytes. Particularly lymphocytes should be assessed, which make up the bulk of peripheral blood mononuclear cells.

Due to time constraints it was not possible to perform Chromatin Immunoprecipitation experiments to analyse changes in histone modifications as a result of Rocuronium and Sugammadex. It would be interesting to relate these changes, if any, to the histone modifications induced by exposure of Propofol and sepsis.

Other commonly used neuromuscular blocking agents (such as Atracurium) and reversal agents (such as Neostigmine) should also be assessed on their impact on immune function. Time constraints prevented Atracurium from being assessed in this research.

Summary

Rocuronium and Sugammadex directly interact with immune cells via their muscarinic and nicotinic receptors and induce changes in the cells' gene expression, cytokine production, and immunometabolism. The immunometabolic changes may involve an interaction between the drugs and the NLRP3 inflammasome. It is possible that these cellular changes induced by Rocuronium and Sugammadex contribute to features of immune suppression and therefore the recurrent hospitalisation of patients who have received such treatments. This research adds to the evidence that neuromuscular blocking agents during anaesthesia may result in postoperative complications, and therefore until further research is conducted into the pathophysiology of neuromuscular blockade the deferral of their use should be considered where clinically feasible.

Chapter 6: Discussion

6.1 Novel findings in this thesis

Sepsis-induced histone modifications of peripheral blood mononuclear cells

Several novel insights have been gained into the long-term effects in post sepsis recovery. Gene expression for the chemokine CCL2 was present in septic patient PBMCs, and it persist at least 6-12 months following hospital discharge. CCL2 was not present in any of the healthy volunteer PBMCs. Septic patient PBMCs cultured *in vitro* displayed defects in their ability to produce certain cytokines when restimulated with LPS or PMA/ionomycin. Furthermore, this defect persisted in cells obtained 6-12 months post hospital discharge. In the literature, ChIP-seq has been performed on a small number of septic patients' PBMCs, but targeted ChIP had not been performed on septic patient PBMCs, and nor were patients followed up for up to 12 months post hospital discharge. Targeted ChIP revealed patterns in the activation and repression of several genes including GAPDH, IRAK-M, mTOR, IL-10, and TLR4, spanning from acute sepsis to up to a year after sepsis recovery.

The effects of Propofol on immune function

Propofol's influence on septic patient's immunometabolism is a novel discovery. Key areas of the immunometabolic profile of septic cells would change when exposed to Propofol, this included glycolysis, ATP production, maximum respiration and spare respiratory capacity. These Propofol-induced differences were also observed in cells exposed to serum from patients who had seemingly "recovered" from the infection (7 days post blood culture positive, minimum 4 days since Propofol treatment stopped). This suggests that Propofol induced cellular changes that resulted in these alterations in immunometabolism, and that

these effects persisted even when sedation had stopped being administered four days prior. It is possible that leukocyte immunometabolism may be modulated in part by epigenetics. The sedation may have influenced epigenetic changes that resulted in immunometabolic alterations that were not reversed when sedation stopped being administered. The exposure to Propofol appears to result in persistent changes to gene activation and expression of genes involved in the glycolytic pathway and immune response. This effect persisted even when the cells had been washed and recovered from Propofol for three days. Chromatin Immunoprecipitation reveals epigenetic changes in key genes related to immunometabolism after exposure to Propofol, persisting to three days recovery after the Propofol was washed off.

The effects of Rocuronium on immune function

It has been previously established that (i) patients who have received neuromuscular blocking agents have an increased risk of hospital readmission within 30 days due to pulmonary complications (Kirmeier E *et al*, 2018), and (ii) immune cells are also known to express cholinergic components such as muscarinic and nicotinic acetylcholine receptors (Fujii T *et al*, 2017). However, the potential effect of neuromuscular blockade on the immune system had not been previously established in the literature. Several novel findings into the effects of neuromuscular blocking agent Rocuronium and its reversal agent Sugammadex on immune cells were elucidated in this thesis. Rocuronium appears to suppress the immunometabolism of THP1 Null cells, whereas Sugammadex administration reverses it- often to an overcompensation compared to Nil drug treated cells. As the NLRP3-/- cells did not display the same effects, it is possible (but not conclusive) that the interactions of Rocuronium may involve the NLRP3 inflammasome. Exposure to Rocuronium and Sugammadex results in

changes in the immunometabolism of THP1 Null but not THP1 NLRP3-/- cells. Rocuronium also affects the immunometabolism of cells when exposed to infectious agents, and when Null THP1 cells treated with Propofol were spiked with Rocuronium the cells' immunometabolic profile were altered. The expression of key cholinergic and cytokine genes were affected by Rocuronium and Sugammadex in THP1 cells. Sugammadex resulted in an increase in concentration of IL-6 and IL-10 in THP1 Null supernatants. Despite similarities in molecular structure to Rocuronium, Vecuronium induces a different immunometabolic profile.

6.2 Relevance of findings

The sample sizes and various limitations to this body of work must be fully taken into account. Results should be viewed as pilot studies to warrant larger studies on the topic, and are certainly not conclusive.

T cells, monocytes and macrophages become exhausted during a septic insult, and after a while are less able to produce pro-inflammatory cytokines (immunoparalysis). This immune deficit can persist in sepsis survivors even long after the infection has cleared. The reprogramming of these cells during sepsis may be due to the epigenetic control of gene expression. The results of these studies do not contradict this theory.

NLRP3 is activated by a broad range of stimuli, consisting of both PAMPs and DAMPs, in contrast to most other PRRs. The various stimuli are unrelated, however all induce cellular stress. It is possible that cells' response to rocuronium may be associated with the NLRP3 inflammasome. The literature details several ARDS patients studies who had a decreased

inflammatory response when given neuromuscular blockade infusions (Forel *et al*, 2006; Sottile *et al*, 2018; Shao *et al,* 2019).

The upstream mechanisms regarding NLRP3 activation have not been fully elucidated, but are believed to include mitochondrial dysfunction, changes in metabolism, calcium ion flux, and potassium or chloride ion efflux. A by-product of oxidative phosphorylation is the production of ROS by the mitochondria, and in times of cellular stress the release of mitochondrial ROS into the cytosol is greatly increased, which in turn will trigger NLRP3 to activate (Swanson *et al*, 2019; Cruz *et al,* 2007). In addition, there evidence that mitochondria may be used as a docking site for NLRP3 inflammasome assembly, due to activated NLRP3 and caspase-1 independently associating with the mitochondria via the mitochondrial phospholipid cardiolipin (Zhong *et al*, 2018; Dudek *et al,* 2017; Zhou *et al*, 2011; Subramanian *et al*, 2013; Iyer *et al*, 2013; Elliott *et al*, 2018). It is possible that the mitochondrial dysfunction described in sepsis overlaps with mitochondrial link to the inflammasome, however without knowing the full mechanisms of action it requires further research.

Results found a glycolytic shift in cells when they were exposed to sepsis. NLRP3 inflammasome activation is speculated to have a role in glycolysis. Sanman *et al* (2016) found that the NLRP3 inflammasome will be activated, as well as IL-1β production and pyroptosis, by a disruption of glycolytic flux, triggered by a decrease in NADH levels and an induction of mitochondrial ROS production. However, NLRP3 priming was also shown to inhibit glycolysis and therefore inhibit LPS-induced IL1β gene transcription (Tannahill *et al,* 2013).

The data in this thesis is not robust enough to warrant further research based on these results alone, instead a larger repeat of these experiments with a more robust quality control and methodology is required.

6.3 Strengths of this thesis

Appropriate methodologies

The methodologies in the thesis were considered and appropriate. The Seahorse methodology for measuring bioenergetics in cells is a new technology that has many advantages over traditional metabolic assays, and has in-built quality control measures. Only a small number of cells are required, and both glycolysis and mitochondrial respiration can be measured simultaneously in real-time. Chromatin Immunoprecipitation is a complex epigenetic technique and was fully optimised to the samples used.

Patient sampling up to one year post hospital discharge

Patients were sampled up to 12 months post hospital discharge; it is challenging to follow up with patients over such a long period of time from a logistical standpoint and patient mortality; it is therefore unusual to have access to such samples. The research provides a unique look into the genotype and phenotype of patient samples that have had such a long recovery time since sepsis. The three sampling timepoints provide a valuable insight into the stages of patient recovery: acute sepsis, sepsis cleared from system but still in hospital, and finally sepsis cleared from system and out of hospital for several months.

Cell lines corroborating primary cell data

No model is perfect, but the fact that the donor primary cells and the cell line both respond in similar ways in experiments strengthens the evidence for the hypothesis; for example both PBMCs and THP1 cells display a comparable phenotype with the addition of propofol is indicative of an independent effect of sedation when used in sepsis treatment.

6.4 Limitations of this thesis

Varied patient cohort

The use of patient samples presents several limitations. The cohort recruited have many variations in pathophysiology and patient characteristics; there is a trade-off to using a larger more heterogenous sample size vs a small sample size of clinically and characteristically similar patients. The small sample sizes will not necessarily produce findings that will apply to the majority of patients. Patients also were all recruited at the same hospital; and may not represent patients from hospitals worldwide. A varied cohort could also result in more subtle findings being lost where they relate to only a specific pathophysiology. More time is required to recruit more patients that fit into specific subcategories, such as *E.coli* sepsis ICU patients who are 18-45 years old with no chronic conditions.

Small sample sizes/ underpowered study

Many of the studies included in this thesis are done on very small sample sizes. Power analysis was not calculated before beginning research, resulting in an underpowered study with limited reach. Statistical analysis could not be performed on many of the samples as their n numbers were too low and therefore the probability of a type II error was high. The results

detail some interesting observations, however they should only be taken as a pilot study in order to warrant further investigation. Such limited sample sizes will not provide an accurate snap shot of the patient landscape.

Healthy volunteers as comparator group

A further thing to note is that healthy volunteers are used as a comparator group to the septic patients. It can be argued that this is not an effective comparator group. Firstly, the healthy volunteers on average were younger than the septic full cohort, and they did not have any chronic conditions frequently found in the septic cohort. It is not if patients who go on to develop sepsis have a pre-existing phenotype that makes them susceptible to sepsis and bacteraemia, in which case this would be absent in the healthy volunteers. Non-bacteraemic perioperative patients may be a better comparator group in this regard. The best comparator group would be if the patients had a pre-sepsis sample taken, but of course this requires a prediction of which patients will go on to become septic. This would be possible given enough time and resources: patient groups who are at high risk of bacteraemia could be approached for a pre-sepsis sample and subsequent blood culture positive sampling can then be taken from the patients who go on to develop sepsis. One such group at higher risk of developing sepsis are patients undergoing abdominal surgery for example.

Cell lines not always representative of primary cells

The use of cell lines presents its own set of limitations, various factors mean that cell lines may not adequately represent primary cells. It is well established that there are genotypic and phenotypic differences between primary cells and cancer-derived immortal cell lines. As demonstrated in Chapters 4 and 5, significant changes to the cells' phenotypes and genotypes occur with serial passage of cell lines. It would be preferable to use the same (young) passage

number for all experiments. Genetic drift can also result in heterogeneity in cell line cultures grown at the same time. The different cell lines will also behave differently, as demonstrated in Chapter 5 between THP1 cells and HL-60 cells, and so care must be taken when selecting a suitable cell line for study.

Lack of quality control and study controls

In several places an adequate quality control is lacking. Examples include the lack of purity testing of cell cultures, and not assessing the quality of the cDNA and Taqman primer probes; all of which make it impossible to confidently identify potential mechanisms.

6.5 Further research

Extent of persistence of immune defects

Firstly, taking this data as a pilot, it should be repeated with appropriate controls and quality controls on a larger sample size to analyse correlations.

The extent of the immune defect persistence should be further examined, such as whether these epigenetic changes are lifelong and can be passed on via meiosis. An interesting experiment would be to examine offspring of sepsis survivors (murine/ human) to see if their immune function and epigenetic patterns are similar to their parents. In a murine model epigenetics can be examined before sepsis, after sepsis, then compared to the profile of the offspring- which can be born both before and after the parents were septic. Whether the specific changes in histone modifications detailed in this chapter would carry over into a murine model is not yet known. A further complicating factor in fully ascertaining the persistence of the effects of sepsis post hospital discharge is that most often the patients are

older and have a plethora of comorbidities. They require a more complex management clinically which may itself effect epigenetics and will make it difficult to gather a large homogenous sample size to draw sepsis-specific conclusions from. A heterogenous sample was the biggest limitation of the gene expression data on the whole patient cohort, who had a variety of comorbidities, severities, and types of bacteria. Therefore, it resources and attainability allow it, study participants should be younger and without comorbid conditions, and with similar infections (e.g. all *E.coli* sepsis) in future work.

Examine other drugs in general anaesthesia

It may be that more drugs can affect patients' immunometabolism in a similar way to Propofol and Rocuronium/ Sugammadex. The effects of other drugs typically used in general anaesthesia should also be further examined, like opioids such as fentanyl and adrenaline/ noradrenaline. It is possible that not be all sedatives that illicit this response; Midazolam, for example, may not result in the same immunometabolic changes as Propofol, and this may inform clinicians on the best drugs to administer to certain patients. Further research into the exact mechanism of how Propofol and Rocuronium/ Sugammadex induces these changes would help inform the breadth of drugs that are likely to behave similarly.

Acute Rocuronium exposure

All the Rocuronium experiments were performed after a three-day rest period from the drug exposure. A comparison of these results to cells which did not have a period of rest may reveal larger differences induced by Rocuronium and Sugammadex. Cells such as the HL-60 line may have had changes due to the drugs which were missed if they had fully recovered during the three-day period. This would also be of benefit to cells from human donors which gradually

die off over the period of rest. It would equally be interesting to have a longer recovery period with the THP1 cell line to see how long the changes persist.

Immunometabolism of HL-60 and primary cell subtypes

Seahorse experiments were performed on THP1 Null and THP1 NLRP3-/- cells, and in Propofol experiments on PBMCs. Immunometabolism of HL-60 cells and different primary cell subtypes should be assessed when exposed to Propofol and Rocuronium/ Sugammadex and can be compared to THP1 data. Immunometabolism can be assessed with both acute exposure to the drugs and after a period of recovery.

Chromatin Immunoprecipitation of Rocuronium exposed cells

Due to time constraints it was not possible to perform Chromatin Immunoprecipitation experiments on the Rocuronium exposed cells. It would be interesting to relate these changes, if any, to the histone modifications induced by exposure of Propofol and sepsis. Chromatin Immunoprecipitation will inform on whether or not Rocuronium/ Sugammadex results in epigenetic changes or not.

References

1. Abraham E. Nuclear factor–kB and its role in sepsis–associated organ failure. J Infect Dis. (2003) 187:364–9. doi: 10.1086/374750

2. Amin OAI, Salah HE. The effect of general or spinal anaesthesia on pro- and anti-inflammatory intracellular cytokines in patients undergoing appendicectomy using flow cytometric method. Egypt J Anaesth. 2011;27:121–5.

3. An R, Feng J, Xi C, Xu J, Sun L. miR-146a attenuates sepsis-induced myocardial dysfunction by suppressing IRAK1 and TRAF6 via targeting ErbB4 expression. Oxid Med Cell Longev. (2018) 2018:1–9. doi: 10.1155/2018/7163057

4. Angus DC, Opal S. Immunosuppression and Secondary Infection in Sepsis: Part, Not All, of the Story. JAMA. 2016;315(14):1457-1459. doi:10.1001/jama.2016.2762.

5. Arens, C., Bajwa, S. A., Koch, C., Siegler, B. H., Schneck, E., Hecker, A., … Uhle, F. (2016). Sepsis-induced long-term immune paralysis - results of a descriptive, explorative study. Critical Care, 20(1), 10–13. https://doi.org/10.1186/s13054-016-1233-5

6. Arrigoni L, Richter AS, Betancourt E, et al. Standardizing chromatin research: a simple and universal method for ChIP-seq. Nucleic Acids Res. 2016;44(7):e67. doi:10.1093/nar/gkv1495

7. Aune TM et al. Epigenetic activation and silencing of the gene that encodes IFN-γ. Front Immunol. 2013;4:112

8. Aung HT et al. LPS regulates proinflammatory gene expression in macrophages by altering histone deacety lase expression. FASEB J. 2006; 20:1315-27

9. Auten, R., Davis, J. Oxygen Toxicity and Reactive Oxygen Species: The Devil Is in the Details. Pediatr Res 66, 121–127 (2009).

10. Baker MT, Naguib M. Propofol: the challenges of formulation. Anesthesiology. 2005 Oct;103(4):860-76. doi: 10.1097/00000542-200510000-00026. PMID: 16192780.

11. Ball, L., de Abreu, M. G., Schultz, M. J., & Pelosi, P. (2019). Neuromuscular blocking agents and postoperative pulmonary complications. The Lancet Respiratory Medicine, 7(2), 102–103. https://doi.org/10.1016/S2213-2600(18)30363-1

12. Barnes PJ, Adcock IM, Ito K. Histone acetylation and deacetylation: importance in inflammatory lung diseases. Eur Respir J. (2005) 25:552–63. doi: 10.1183/09031936.05.00117504

13. Barton K, Hiener B, Winckelmann A, Rasmussen TA, Shao W, Byth K, et al. Broad activation of latent HIV-1 in vivo. Nat Commun. (2016) 7:12731. doi: 10.1038/ncomms12731

14. Bataille A, Galichon P, Ziliotis M-J, Sadia I, Hertig A. Epigenetic changes during sepsis: on your marks! Crit Care. (2015) 19:358. doi: 10.1186/s13054-015-1068-5

15. Bazzoni F, Rossato M, Fabbri M, Gaudiosi D, Mirolo M, Mori L, et al. Induction and regulatory function of miR-9 in human monocytes and neutrophils exposed to proinflammatory signals. Proc Natl Acad Sci. (2009) 106:5282–7. doi: 10.1073/pnas.0810909106

16. Belikova, I. et al. Oxygen consumption of human peripheral blood mononuclear cells in severe human sepsis. Crit. Care Med. 35, 2702–2708 (2007)

17. Benjamim CF et al. Septic m ice are susceptible to pulmonary aspergillosis. Am J Pathol. 2003; 163:2605-17

18. Berg JM, Tymoczko JL, Stryer L. Biochemistry. 5th edition. New York: W H Freeman; 2002. Chapter 18, Oxidative Phosphorylation.

19. Bhaskar SB. Emergence from anaesthesia: Have we got it all smoothened out? Indian J Anaesth. 2013;57:1–3.

20. Bianchi M., Meng C., Ivashkiv L.B. Inhibition of IL-2-induced Jak-STAT signaling by glucocorticoids. Proc. Natl. Acad. Sci. USA. 2000;97:9573–9578.

21. Bom A, Bradley M, Cameron K, et al. A novel concept of reversing neuromuscular block: chemical encapsulation of rocuronium bromide by a cyclodextrin-based synthetic host. Angew Chem Int Ed Engl 2002; 41: 266–70

22. Bomsztyk K, Mar D, An D, Sharifian R, Mikula M, Gharib SA, et al. Experimental acute lung injury induces multi-organ epigenetic modifications in key angiogenic genes implicated in sepsis-associated endothelial dysfunction. Crit Care. (2015) 19:225. doi: 10.1186/s13054-015-0943-4

23. Bone RC. A piece of my mind. Maumee: my Walden pond. JAMA. 1996 Dec;276:1931

24. Boomer, J. S., To, K., Chang, K. C., Takasu, O., Osborne, D. F., Walton, A. H., … Hotchkiss, R. S. (2011). Immunosuppression in patients who die of sepsis and multiple organ failure. JAMA - Journal of the American Medical Association, 306(23), 2594–2605. https://doi.org/10.1001/jama.2011.1829

25. Bozza FA, Salluh JI, Japiassu AM, Soares M, Assis EF, Gomes RN, Bozza MT, Castro-Faria-Neto HC, Bozza PT: Cytokine profiles as markers of disease severity in sepsis: a multiplex analysis. Crit Care. 2007, 11: R49-10.1186/cc5783

26. Branca D, Roberti MS, Lorenzin P, Vincenti E, Scutari G. Influence of the anesthetic 2,6-diisopropylphenol on the oxidative phosphorylation of isolated rat liver mitochondria. Biochem Pharmacol 1991;42:87–90

27. Brealey, D. et al. Association between mitochondrial dysfunction and severity and outcome of septic shock. Lancet 360, 219–223 (2002).

28. Busslinger M, Tarakhovsky A. Epigenetic control of immunity. Cold Spring Harb Perspect Biol. (2014) 6:a019307. doi: 10.1101/cshperspect.a019307

29. Byrne, M. F., Chiba, N., Singh, H., Sadowski, D. C., & Clinical Affairs Committee of the Canadian Association of Gastroenterology (2008). Propofol use for sedation during endoscopy in adults: a Canadian Association of Gastroenterology position statement. Canadian journal of gastroenterology =Journal canadien de gastroenterologie, 22(5), 457–459. https://doi.org/10.1155/2008/268320

30. Calao M, Burny A, Quivy V, Dekoninck A, Lint CV. A pervasive role of histone acetyltransferases and deacetylases in an NF-κB-signaling code. Trends Biochem Sci. (2008) 33:339–49. doi: 10.1016/j.tibs.2008.04.015

31. Carson WF et al. Epigenetic regulation of immune cell functions during post-septic immunosuppression. Epigenetics. 6:3;273-283 (2011)

32. Chan C et al. Endotoxin to lerance disrupts chromatin remodelling and NFkappaB transactivation at the IL -1beta promoter. J I mmunol. 2005;175:461-8

33. Chan LLY, Rice WL, Qiu J (2020) Observation and quantification of the morphological effect of trypan blue rupturing dead or dying cells. PLOS ONE 15(1): e0227950. https://doi.org/10.1371/journal.pone.0227950

34. Chan, J. K. et al. Alarmins: awaiting a clinical response. J. Clin. Invest. 122, 2711–2719 (2012).

35. Chang DW, Tseng C-H, Shapiro MF. Rehospitalizations following sepsis: common and costly. Crit Care Med. (2015) 43:2085–93. doi: 10.1097/CCM.0000000000001159

36. Chen J, Sahakian E, Powers JJ, LienlafMoreno M, Xing L, Deng S, et al. Histone deacetylase 11 (HDAC11) as a novel transcriptional regulator of C/EBP-β, in immature myeloid cell to myeloid derived suppressor cell transition. Blood. (2014) 124:225.

37. Chen Y, Wang D, Zhao Y, Huang B, Cao H, Qi D. p300 promotes differentiation of Th17 cells via positive regulation of the nuclear transcription factor RORγt in acute respiratory distress syndrome. Immunol Lett. (2018) 202:8–15. doi: 10.1016/j.imlet.2018.07.004

38. Chen, R. M. et al. Anti-inflammatory and antioxidative effects of propofol on lipopolysaccharide-activated macrophages. Ann N Y Acad Sci (2002) 1042, 262–271

39. Chen, R. M., Wu, C. H., Chang, H. C., Wu, G. J., Lin, Y. L., Sheu, J. R., & Chen, T. L. (2003). Propofol suppresses macrophage functions and modulates mitochondrial membrane potential and cellular adenosine triphosphate synthesis. Anesthesiology, 98(5), 1178–1185. https://doi.org/10.1097/00000542-200305000-00021

40. Cheng S.-C., Scicluna B.P., Arts R.J.W., Gresnigt M.S., Lachmandas E., Giamarellos-Bourboulis E.J., Kox M., Netea M.G. Broad defects in the energy metabolism of leukocytes underlie immunoparalysis in sepsis. Nature Immunology, 17 (4) , pp. 406-413 (2016)

41. Cheng S-C, Quintin J, Cramer RA, Shepardson KM, Saeed S, Kumar V, et al. mTOR- and HIF-1α-mediated aerobic glycolysis as metabolic basis for trained immunity. Science. (2014) 345:1250684. doi: 10.1126/science.1250684

42. Choi K-C, Jung MG, Lee Y-H, Yoon JC, Kwon SH, Kang H-B, et al. Epigallocatechin-3-gallate, a histone acetyltransferase inhibitor, inhibits EBV-induced B lymphocyte transformation via suppression of RelA acetylation. Cancer Res. (2009) 69:583–92. doi: 10.1158/0008-5472.CAN-08-2442

43. Choi S, You S, Kim D, Choi SY, Kwon HM, Kim H-S, et al. Transcription factor NFAT5 promotes macrophage survival in rheumatoid arthritis. J Clin Investig. (2017) 127:954–69. doi: 10.1172/JCI87880

44. Choi SW, Braun T, Henig I, Gatza E, Magenau J, Parkin B, et al. Vorinostat plus tacrolimus/methotrexate to prevent GVHD following myeloablative conditioning unrelated donor HCT. Blood. (2017) 130:1760–7. doi: 10.1182/blood-2017-06-790469

45. Choy E, Rose-John S. Interleukin-6 as a Multifunctional Regulator: Inflammation, Immune Response, and Fibrosis. Journal of Scleroderma and Related Disorders. 2017;2(2_suppl):S1-S5.

46. Christou NV, Meakins JL, Gordon J, Yee J, Hassan-Zahraee M, Nohr CW, et al. The delayed hypersensitivity response and host resistance in surgical patients. 20 years later. Ann Surg. (1995) 222:534–46. doi: 10.1097/00000658-199522240-00011

47. Clifford KM, Dy-Boarman EA, Haase KK, Maxvill K, Pass S, Alvarez CA. Challenges with diagnosing and managing sepsis in older adults. Expert Rev Anti Infect Ther. (2016) 14:231–41. doi: 10.1586/14787210.2016.1135052

48. Collier SP et al. Cutting edge: influence of Tmevpg1, a long intergenic noncoding RNA, on the expression of IFNγ by Th1 cells. J Immunol. 2012. Sept 1;189(5):2084-8

49. Colucci D, Harvey G, Gayol MC, Elena G, Puig N. Halothane anesthesia in mice: effect on the phagocytic activity and respiratory burst of peritoneal macrophages. Neuroimmunomodulation. 2011;18:11–18

50. Colucci DG, Puig NR, Hernandez PR. Influence of anesthetic drugs on immune response: from inflammation to immunosuppression. OA Anesthetics. 2013;1:21–38

51. Corcoran, T. B. et al. The effects of propofol on lipid peroxidation and inflammatory response in elective coronary artery bypass grafting. Journal of cardiothoracic and vascular anesthesia 18, 592–604 (2004).

52. Cordero P et al. Leptin and TNF-alpha promoter methylation levels measured by MSP could predict the response to a low-calorie diet. Journal of physiology and biochemistry. Apr 2011;67(3):463-70

53. Corrales-Medina, V. F., Alvarez, K. N., Weissfeld, L. A., Angus, D. C., Chirinos, J. A., Chang, C. C. H., … Yende, S. (2015). Association between hospitalization for pneumonia and subsequent risk of cardiovascular disease. JAMA - Journal of the American Medical Association, 313(3), 264–274.

54. Cross D, Drury R, Hill J and Pollard AJ (2019) Epigenetics in Sepsis: Understanding Its Role in Endothelial Dysfunction, Immunosuppression, and Potential Therapeutics. Front. Immunol. 10:1363. doi: 10.3389/fimmu.2019.01363

55. Cultraro, C. M., Bino, T., Segal, S. (1997) Function of the c-Myc antagonist Mad1 during a molecular switch from proliferation to differentiation. Mol. Cell. Biol. 17, 2353– 2359.

56. Cummings M, Sarveswaran J, Homer-Vanniasinkam S, Burke D, Orsi NM. Glyceraldehyde-3-phosphate dehydrogenase is an inappropriate housekeeping gene for normalising gene expression in sepsis. Inflammation. 2014;37(5):1889-1894. doi:10.1007/s10753-014-9920-3

57. Czaja AS et al. Readmission and late mortality after paediatric severe sepsis. Paediatrics. 2009;123:849

58. Damuth, E., Mitchell, J. A., Bartock, J. L., Roberts, B. W., & Trzeciak, S. (2015). Long-term survival of critically ill patients treated with prolonged mechanical ventilation: A systematic review and meta-analysis. The Lancet Respiratory Medicine, 3(7), 544–553. https://doi.org/10.1016/S2213-2600(15)00150-2

59. De Backer D, Ortiz JA, Salgado D. Coupling microcirculation to systemic hemodynamics. Curr Opin Crit Care. (2010) 16:250. doi: 10.1097/MCC.0b013e3283383621

60. De Santa F, Narang V, Yap ZH, Tusi BK, Burgold T, Austenaa L, et al. Jmjd3 contributes to the control of gene expression in LPS-activated macrophages. EMBO J. (2009) 28:3341–52. doi: 10.1038/emboj.2009.271

61. De Santa F, Totaro MG, Prosperini E, Notarbartolo S, Testa G, Natoli G. The histone H3 lysine-27 demethylase Jmjd3 links inflammation to inhibition of polycomb-mediated gene silencing. Cell. (2007) 130:1083–94. doi: 10.1016/j.cell.2007.08.019

62. Delano, M. J., & Ward, P. A. (2016). Sepsis-induced immune dysfunction: Can immune therapies reduce mortality? Journal of Clinical Investigation, 126(1), 23–31. https://doi.org/10.1172/JCI82224

63. Deng JC et al. Sepsis-induced suppression of lung innate immunity is mediated by IRAK -M. J Clin Invest. 2006; 116:2532-42

64. Denstaedt SJ, Singer BH, Standiford TJ. Sepsis and nosocomial infection: patient characteristics, mechanisms, and modulation. Front Immunol. (2018) 9:2446. doi: 10.3389/fimmu.2018.02446

65. Deutschman, C. S. & Tracey, K. J. Sepsis: current dogma and new perspectives. Immunity 40, 463–475 (2014)

66. Dimick, JB, Chen, SL, Taheri, PA, Henderson, WG, Khuri, SF, Campbell, DAJr Hospital costs associated with surgical complications: A report from the private-sector National Surgical Quality Improvement Program.. J Am Coll Surg. (2004). 199 531–7

67. Drury RE, O'Connor D, Pollard AJ. The clinical application of microRNAs in infectious disease. Front Immunol. (2017) 8:1182. doi: 10.3389/fimmu.2017.01182

68. Dupont C, Armant R, Brenner CA. Epigenetics: definition, mechanisms and clinical perspective. Semin Reprod Med. (2009) 27:351–7. doi: 10.1055/s-0029-1237423.Epigenetics

69. Eduardo, C. R. C., Alejandra, T. I. G., Guadalupe, D. R. K. J., Herminia, V. R. G., Lenin, P., Enrique, B. V., … Iván, G. P. M. (2019). Modulation of the extraneuronal cholinergic system on main innate response leukocytes. Journal of Neuroimmunology, 327(January), 22–35. https://doi.org/10.1016/j.jneuroim.2019.01.008

70. Egger G. et al. Epigenetics in human disease and prospects for epigenetic therapy. Nature 429, 457-463 (2004).

71. El Gazzar M et al. Chromatin -specific remodelling by HMGB1 and linker histone H1 silences proinflammatory genes during endotoxin tolerance. Mol Cell Biol. 2009;29:1959-71

72. El Gazzar M, Yoza B, Chen X, Hu J, Hawkins G, McCall C. G9a and HP1 couple histone and DNA methylation to TNFα transcription silencing during endotoxin tolerance. J Biol Chem. (2008) 283:198–208. doi: 10.1074/jbc.M803446200

73. Engelmann, B. & Massberg, S. Thrombosis as an intravascular effector of innate immunity. Nat. Rev. Immunol. 13, 34–45 (2013)

74. Epemolu O, Bom A, Hope F, Mason R. Reversal of neuromuscular blockade and simultaneous increase in plasma rocuronium concentration after the intravenous infusion of the novel reversal agent Org 25969. Anesthesiology 2003; 99: 632–7

75. Farhan H, Moreno-Duarte I, McLean D, Eikermann M. Residual paralysis: does it influence outcome after ambulatory surgery? Curr Anesthesiol Rep 2014; 4: 290–302

76. Fazi F, Rosa A, Fatica A, Gelmetti V, De Marchis ML, Nervi C, et al. A minicircuitry comprised of microRNA-223 and transcription factors NFI-A and C/EBPalpha regulates human granulopoiesis. Cell. (2005) 123:819–31. doi: 10.1016/j.cell.2005.09.023

77. Fernández-Morera JL, Calvanese V, Rodríguez-Rodero S, Menéndez-Torre E, Fraga MF. Epigenetic regulation of the immune system in health and disease. Tissue Antigens. (2010) 76:431–9. doi: 10.1111/j.1399-0039.2010.01587.x

78. Fink MP (2015) Cytopathic hypoxia and sepsis: Is mitochondrial dysfunction pathophysiologically important or just an epiphenomenon. Pediatr Crit Care Med 16: 89–91

79. Fink, H., Luppa, P., Mayer, B., Rosenbrock, H., Metzger, J., Martyn, J. A. J., & Blobner, M. (2003). Systemic inflammation leads to resistance to atracurium without increasing membrane expression of acetylcholine receptors. Anesthesiology, 98(1), 82–88. https://doi.org/10.1097/00000542-200301000-00016

80. Forel JM, Roch A, Marin V, Michelet P, Demory D, Blache JL, Perrin G, Gainnier M, Bongrand P, Papazian L. Neuromuscular blocking agents decrease inflammatory response in patients presenting with acute respiratory distress syndrome. Crit Care Med. 2006 Nov;34(11):2749-57. doi:

81. Foster, S. L., Hargreaves, D. C. & Medzhitov, R. Gene-specific control of inflammation by TLR-induced chromatin modifications. Nature 447, 972–978 (2007).

82. Fragou P et al. Major gastrointestinal surgery is associated with a specific gene expression profile that is quantitatively associated with infectious complications. Eur J Anesthesiol. June 2014;31 e supplement 52:14

83. Fragou P et al. Perioperative blood transfusion is associated with a characteristic immune response, excess infectious complications and death in patients undergoing scheduled major gastrointestinal surgery. Eur J Anesthesiol. June 2014;31 e supplement 52:91

84. Fujii, T., Mashimo, M., Moriwaki, Y., Misawa, H., Ono, S., Horiguchi, K., & Kawashima, K. (2017). Physiological functions of the cholinergic system in immune cells. Journal of Pharmacological Sciences, 134(1), 1–21. https://doi.org/10.1016/j.jphs.2017.05.002

85. Fujiwara Y, Ito H, Asakura Y, Sato Y, Nishiwaki K, Preoperative Ultra Short-Term Entropy Predicts Arterial Blood Pressure Fluctuation During the Induction of Anesthesia, Anesthesia & Analgesia: April 2007 - Volume 104 - Issue 4 - p 853-856 doi: 10.1213/01.ane.0000258756.41649.2d

86. Fukao, T., Matsuda, S., Koyasu, S. (2000) Synergistic effects of IL-4 and IL-18 on IL-12-dependent IFN-gamma production by dendritic cells. J. Immunol. 164, 64–71.

87. Gabay, C. Interleukin-6 and chronic inflammation. Arthritis Res Ther 8, S3 (2006). https://doi.org/10.1186/ar1917

88. Gabrilovich DI, Nagaraj S. Myeloid-derived suppressor cells as regulators of the immune system. Nat Rev Immunol. (2009) 9:162–74. doi: 10.1038/nri2506

89. Gaertner, F & Massberg, S. Blood coagulation in immunothrombosis—At the frontline of intravascular immunity. Seminars in Immunology. Volume 28, Issue 6, 561-569 (2016)

90. Galli M, Salmoiraghi S, Golay J, Gozzini A, Crippa C, Pescosta N, et al. A phase II multiple dose clinical trial of histone deacetylase inhibitor ITF2357 in patients with relapsed or progressive multiple myeloma. Ann Hematol. (2010) 89:185–90. doi: 10.1007/s00277-009-0793-8

91. Gao M, Wang X, Zhang X, Ha T, Ma H, Liu L, et al. Attenuation of cardiac dysfunction in polymicrobial sepsis by microRNA-146a is mediated via targeting of IRAK1 and TRAF6 expression. J Immunol Baltim Md 1950. (2015) 195:672–82. doi: 10.4049/jimmunol.1403155

92. Gao, L., Ramzan, I., & Baker, B. (2002). Rocuronium plasma concentrations during three phases of liver transplantation: Relationship with early postoperative graft liver function. British Journal of Anaesthesia, 88(6), 764–770. https://doi.org/10.1093/bja/88.6.764

93. geNorm. (2002). Normalization of real-time PCR expression data.

94. Ghizzoni M, Haisma HJ, Maarsingh H, Dekker FJ. Histone acetyltransferases are crucial regulators in NF-κB mediated inflammation. Drug Discov Today. (2011) 16:504–11. doi: 10.1016/j.drudis.2011.03.009

95. Ghosh SK, Perrine SP, Williams RM, Faller DV. Histone deacetylase inhibitors are potent inducers of gene expression in latent ebv and sensitize lymphoma cells to nucleoside antiviral agents. Blood. (2012) 119:1008–17. doi: 10.1182/blood-2011-06-362434

96. Gijsenbergh F, Ramael S, Houwing N, van Iersel T. First human exposure of Org 25969, a novel agent to reverse the action of rocuronium bromide. Anesthesiology. 2005;103:695–703

97. Goodwin AJ, Guo C, Cook JA, Wolf B, Halushka PV, Fan H. Plasma levels of microRNA are altered with the development of shock in human sepsis: an observational study. Crit Care. (2015) 19:440. doi: 10.1186/s13054-015-1162-8

98. Grealy, White, Stordeur, et al., "Characterising Cytokine Gene Expression Signatures in Patients with Severe Sepsis," Mediators of Inflammation, vol. 2013, Article ID 164246, 8 pages, 2013. doi:10.1155/2013/164246

99. Gschwandtner M., Derler R., Midwood K. S.More Than Just Attractive: How CCL2 Influences Myeloid Cell Behavior Beyond Chemotaxis. Frontiers in Immunology. Vol10. 2019. DOI=10.3389/fimmu.2019.02759

100. Gu W, Yao L, Li L, Zhang J, Place AT, Minshall RD, et al. ICAM-1 regulates macrophage polarization by suppressing MCP-1 expression via miR-124 upregulation. Oncotarget. (2017) 8:111882. doi: 10.18632/oncotarget.22948

101. Gyawali, B., Ramakrishna, K., & Dhamoon, A. S. (2019). Sepsis: The evolution in definition, pathophysiology, and management. SAGE open medicine, 7, 2050312119835043. https://doi.org/10.1177/2050312119835043

102. Harrington JR. The role of MCP-1 in atherosclerosis. Stem Cells. (2000) 18:65–6. doi: 10.1634/stemcells.18-1-65

103. Harrison DA et al. Relation between volume and outcome for patients with severe sepsis in United Kingdom : a retrospective cohort study. BMJ. 2012 May 29;344:e3394

104. Hawkins RB, Raymond SL, Stortz JA, Horiguchi H, Brakenridge SC, Gardner A, et al. Chronic critical illness and the persistent inflammation, immunosuppression, and catabolism syndrome. Front Immunol. (2018) 9:1511. doi: 10.3389/fimmu.2018.01511

105. Hemmerling TM, Zaouter C, Geldner G, Nauheimer D. Sugammadex: A short review and clinical recommendations for the cardiac anesthesiologist. Ann Card Anaesth. 2010;13:206–16

106. Henning DJ, Carey JR, Oedorf K, Day DE, Redfield CS, Huguenel CJ, et al. The absence of fever is associated with higher mortality and decreased antibiotic and Iv fluid administration in emergency department patients with suspected septic shock. Crit Care Med. (2017) 45:575–82.

107. Ho J, Chan H, Wong SH, Wang MHT, Yu J, Xiao Z, et al. The involvement of regulatory non-coding RNAs in sepsis: a systematic review. Crit Care. (2016) 20:383. doi: 10.1186/s13054-016-1555-3

108. Hogarth DK, Hall J. Management of sedation in mechanically ventilated patients. Curr Opin Crit Care. 2004;10:40–6.

109. Hotchkiss RS et al. The pathophysiology and treatment of sepsis. N Engl J Med. 2003 Jan 9;348(2):138-50

110. Hotchkiss RS et al. The sepsis seesaw: tilting towards immunosuppression. Nat Med. 2009 May;15(5):496-7

111. Huang J, Wan D, Li J, Chen H, Huang K, Zheng L. Histone acetyltransferase PCAF regulates inflammatory molecules in the development of renal injury. Epigenetics. (2015) 10:62–72. doi: 10.4161/15592294.2014.990780

112. Huggett J, Dheda K, Bustin S, Zumla A. Real-time RT-PCR normalisation; strategies and considerations. Genes Immun. 2005;6(4):279-284. doi:10.1038/sj.gene.6364190

113. Hull E, Montgomery M, Leyva K. HDAC inhibitors as epigenetic regulators of the immune system: impacts on cancer therapy and inflammatory diseases. BioMed Res Int. (2016) 2016:8797206. doi: 10.1155/2016/8797206

114. Illingworth RS, Bird AP. CpG islands–"A rough guide." FEBS Lett. (2009) 583:1713–20. doi: 10.1016/j.febslet.2009.04.012

115. Ince C, Mik EG. Microcirculatory and mitochondrial hypoxia in sepsis, shock, and resuscitation. J Appl Physiol. (2015) 120:226–35. doi: 10.1152/japplphysiol.00298.2015

116. Ishii, M., Wen, H., Corsa, C. A. S., Liu, T., Coelho, A. L., Allen, R. M., … Kunkel, S. L. (2009). Epigenetic regulation of the alternatively activated macrophage phenotype. Blood, 114(15), 3244–3254. https://doi.org/10.1182/blood-2009-04-217620

117. Iyer, S. S., & Cheng, G. (2012). Role of interleukin 10 transcriptional regulation in inflammation and autoimmune disease. Critical reviews in immunology, 32(1), 23–63. https://doi.org/10.1615/critrevimmunol.v32.i1.30

118. Jakob SM, Ruokonen E, Grounds RM, et al. Dexmedetomidine vs Midazolam or Propofol for Sedation During Prolonged Mechanical Ventilation: Two Randomized Controlled Trials. JAMA. 2012;307(11):1151–1160. doi:10.1001/jama.2012.304

119. Jing Y, Ai Q, Lin L, Dai J, Jia M, Zhou D, et al. Protective effects of garcinol in mice with lipopolysaccharide/D-galactosamine-induced apoptotic liver injury. Int Immunopharmacol. (2014) 19:373–80. doi: 10.1016/j.intimp.2014.02.012

120. Joehanes R, Just AC, Marioni RE, Pilling LC, Reynolds LM, Mandaviya PR, et al. Epigenetic signatures of cigarette smoking. Circ Cardiovasc Genet. (2016) 9:436–47. doi: 10.1161/CIRCGENETICS.116.001506

121. Jones GRN (1974) Ionic shuttles in shock. Lancet 11: 905

122. Kafer, ER, Marsh, HM The effects of anesthetic drugs and disease on the chemical regulation of ventilation.. Int Anesthesiol Clin. (1977). 15 1–38

123. Kahn, J. M., Le, T., Angus, D. C., Cox, C. E., Hough, C. L., White, D. B., … Carson, S. S. (2015). The epidemiology of chronic critical Illness in the United States. Critical Care Medicine, 43(2), 282–287. https://doi.org/10.1097/CCM.0000000000000710

124. Kane BA, Bryant KJ, McNeil HP, Tedla NT. Termination of immune activation: an essential component of healthy host immune responses. J Innate Immun. (2014) 6:727–38. doi: 10.1159/000363449

125. Kaufmann E, Sanz J, Dunn JL, Khan N, Mendonça LE, Pacis A, et al. BCG educates hematopoietic stem cells to generate protective innate immunity against tuberculosis. Cell. (2018) 172:176–90.e19. doi: 10.1016/j.cell.2017.12.031

126. Kawahara T, Michishita E, Adler A, Damian M, Berber E, Lin M, et al. SIRT6 links histone H3 lysine 9 deacetylation to NF-κB-dependent gene expression and organismal life span: cell. Cell. 136:62–74. doi: 10.1016/j.cell.2008.10.052

127. Kawasaki T, Kawai T. Toll-like receptor signaling pathways. Front Immunol. (2014) 5:461. doi: 10.3389/fimmu.2014.00461

128. Ke R, Lewin SR, Elliott JH, Perelson AS. Modeling the effects of vorinostat in vivo reveals both transient and delayed HIV transcriptional activation and minimal killing of latently infected cells. PLoS Pathog. (2015) 11:e1005237. doi: 10.1371/journal.ppat.1005237

129. Kennedy BC, Hall GM. Neuroendocrine and inflammatory aspects of surgery: do they affect outcome? Acta Anaesthesiol Belg. 1999;50:205–9

130. Kheterpal S, Vaughn MT, Dubovoy TZ, Shah NJ, Bash LD, Colquhoun DA, Shanks AM, Mathis MR, Soto RG, Bardia A, Bartels K, McCormick PJ, Schonberger RB, Saager L; Sugammadex versus Neostigmine for Reversal of Neuromuscular Blockade and Postoperative Pulmonary Complications (STRONGER): A Multicenter Matched Cohort Analysis. Anesthesiology 2020;132(6):1371-1381.

131. Khuri, SF, Henderson, WG, DePalma, RG, Mosca, C, Healey, NA, Kumbhani, DJ Participants in the VA National Surgical Quality Improvement Program, Determinants of long-term survival after major surgery and the adverse effect of postoperative complications.. Ann Surg. (2005). 242 326–41; discussion 341–3

132. Kim M-J, Seong A-R, Yoo J-Y, Jin C-H, Lee Y-H, Kim YJ, et al. Gallic acid, a histone acetyltransferase inhibitor, suppresses β-amyloid neurotoxicity by inhibiting microglial-mediated neuroinflammation. Mol Nutr Food Res. (2011) 55:1798–808. doi: 10.1002/mnfr.201100262

133. Kirmeier, E., Eriksson, L. I., Lewald, H., Jonsson Fagerlund, M., Hoeft, A., Hollmann, M., … Zupanĕič, D. (2019). Post-anaesthesia pulmonary complications after use of muscle relaxants (POPULAR): a multicentre, prospective observational study. The Lancet Respiratory Medicine, 7(2), 129–140. https://doi.org/10.1016/S2213-2600(18)30294-7

134. Kleinnijenhuis J, Quintin J, Preijers F, Joosten LAB, Ifrim DC, Saeed S, et al. Bacille calmette-guerin induces NOD2-dependent non-specific protection from reinfection via epigenetic reprogramming of monocytes. Proc Natl Acad Sci. (2012) 109:17537–42. doi: 10.1073/pnas.1202870109

135. Klose RJ et al. Regulation of histone methylation by demethylimination and demethylation. Nat Rev Mol Cell Biol 2007;8:307-18

136. Kopman AF, Neostigmine versus Sugammadex: Which, When, and How Much?. Anesthesiology 2010;113(5):1010-1011.

137. Kotani Y., Shimazawa M., Yoshimura S., Iwama T., Hara H. The experimental and clinical pharmacology of propofol, an anesthetic agent with neuroprotective properties. CNS Neuroscience and Therapeutics. 2008;14(2):95–106.

138. Krajčová, A., Løvsletten, N. G., Waldauf, P., Frič, V., Elkalaf, M., Urban, T., … Duška, F. (2018). Effects of Propofol on Cellular Bioenergetics in Human Skeletal Muscle Cells. Critical Care Medicine, 46(3), e206–e212. https://doi.org/10.1097/CCM.0000000000002875

139. Kumar, GV, Nair, AP, Murthy, HS, Jalaja, KR, Ramachandra, K, Parameshwara, G Residual neuromuscular blockade affects postoperative pulmonary function.. Anesthesiology. (2012). 117 1234–44

140. Kurosawa S, Kato M. Anesthetics, immune cells, and immune responses. J Anesth. 2008;22:263–77.

141. Lahiri R et al. Systemci Inflammatory Response Syndrome after major abdominal surgery predicted by early upregulation of TLR4 and TLR5. Ann Surg 2015 May 27 (epub ahead of print)

142. Lal G et al. Epigenetic mechanisms of regulation of Foxp3 expression. Blood 2009;114:3727-35

143. Lawrence T . The nuclear factor NF-kappaB pathway in inflammation. Cold Spring Harb Perspect Biol 2009

144. Lee C, Jahr JS, Candiotti KA, Warriner B, Zornow MH, Naguib M. Reversal of profound neuromuscular block by sugammadex administered three minutes after rocuronium: A comparison with spontaneous recovery from succinylcholine. Anesthesiology. 2009;110:1020–5

145. Lee H. FDA approval: belinostat for the treatment of patients with relapsed or refractory peripheral T-cell lymphoma. Clin Cancer Res. (2015) 11:1659–64. doi: 10.2217/fon.15.62.

146. Lee HH, Sanada S, An SM, Ye BJ, Lee JH, Seo Y-K, et al. LPS-induced NFκB enhanceosome requires tonEBP/NFAT5 without DNA binding. Sci Rep. (2016) 6:24921. doi: 10.1038/srep24921

147. Leligdowicz A, Richard-Greenblatt M, Wright J, Crowley VM, Kain KC. Endothelial activation: the ang/tie axis in sepsis. Front Immunol. (2018) 9:838. doi: 10.3389/fimmu.2018.00838

148. Leone M, Boutière B, Camoin-Jau L, Albanèse J, Horschowsky N, Mège J-L, et al. Systemic endothelial activation is greater in septic than in traumatic-hemorrhagic shock but does not correlate with endothelial activation in skin biopsies. Crit Care Med. (2002) 30:808–814.

149. Leoni F, Zaliani A, Bertolini G, Porro G, Pagani P, Pozzi P, et al. The antitumor histone deacetylase inhibitor suberoylanilide hydroxamic acid exhibits antiinflammatory properties via suppression of cytokines. Proc Natl Acad Sci. (2002) 99:2995–3000. doi: 10.1073/pnas.052702999

150. Li, X., Egervari, G., Wang, Y., Berger, S. L., & Lu, Z. (2018). Regulation of chromatin and gene expression by metabolic enzymes and metabolites. Nature Reviews Molecular Cell Biology, 19(9), 563–578. https://doi.org/10.1038/s41580-018-0029-7

151. Limaye AP et al. Cytomegalovirus reactivation in critically ill immunocompetent patients. JAMA. 2008;300(4):413-22

152. Liu TF, Yoza BK, Gazzar ME, Vachharajani VT, McCall CE. NAD+-dependent SIRT1 deacetylase participates in epigenetic reprogramming during endotoxin tolerance. J Biol Chem. (2011) 286:9856–64. doi: 10.1074/jbc.M110.196790

153. Liu, L., Min, S., Li, W., Wei, K., Luo, J., Wu, G., … Wang, Z. (2014). Pharmacodynamic changes with vecuronium in sepsis are associated with expression of 7-and γ-nicotinic acetylcholine receptor in an experimental rat model of neuromyopathy. British Journal of Anaesthesia, 112(1), 159–168. https://doi.org/10.1093/bja/aet253

154. Liu, V.; Escobar, G. J.; Greene, J. D.; Soule, J.; Whippy, A.; Angus, D. C.; Iwashyna, T. J. Hospital Deaths in Patients With Sepsis From 2 Independent Cohorts. JAMA 2014,312, 90– 92, DOI: 10.1001/jama.2014.5804

155. Livak, K. J., & Schmittgen, T. D. (2001). Analysis of relative gene expression data using real-time quantitative PCR and the 2-ΔΔCT method. Methods, 25(4), 402–408. https://doi.org/10.1006/meth.2001.1262

156. Long C, Lai Y, Li J, Huang J, Zou C. LPS promotes HBO1 stability via USP25 to modulate inflammatory gene transcription in THP-1 cells. Biochim Biophys Acta BBA Gene Regul Mech. (2018) 1861:773–82. doi: 10.1016/j.bbagrm.2018.08.001

157. Longbottom ER et al. Post-operative immune suppression is reversible with interferon gamma and independent of IL-6 pathways. Ann Surg. 2015

158. Longbottom ER, Torrance HD, Owen HC, et al. Features of Postoperative Immune Suppression Are Reversible With Interferon Gamma and Independent of Interleukin-6 Pathways. Ann Surg. 2016;264(2):370-377.

159. Lubowicka E, Przylipiak A, Zajkowska M, Piskór BM, Malinowski P, Fiedorowicz W, et al. Plasma chemokine CCL2 and its receptor CCR2 concentrations as diagnostic biomarkers for breast cancer patients. BioMed Res Int. (2018) 2018:2124390. doi: 10.1155/2018/2124390

160. Lyn-Kew et al. IRAK-M regulates chromatin remodelling in lung macrophages during experimental sepsis. PLoS ONE. 2010;5:11145

161. Maini RN, Elliott MJ, Brennan FM, Feldmann M. Beneficial effects of tumour necrosis factor-alpha (TNF-alpha) blockade in rheumatoid arthritis (RA) Clin Exp Immunol. 1995 Aug;101(2):207–212.

162. Malek TR. The main function of IL-2 is to promote the development of T regulatory cells. J Leukoc Biol. 2003 Dec;74(6):961-5.

163. Mann BS, Johnson JR, Cohen MH, Justice R, Pazdur R. FDA approval summary: vorinostat for treatment of advanced primary cutaneous T-cell lymphoma. Oncologist. (2007) 12:1247–52. doi: 10.1634/theoncologist.12-10-1247

164. Marik PE. Don't miss the diagnosis of sepsis! Crit Care. (2014) 18:529. doi: 10.1186/s13054-014-0529-6

165. Marín-Hernández A, Gallardo-Pérez JC, Ralph SJ, Rodríguez-Enríquez S, Moreno-Sánchez R (2009) HIF-1alpha modulates energy metabolism in cancer cells by inducing over-expression of specific glycolytic isoforms. Mini Rev Med Chem 9: 1084–101

166. Markovic-Bozic, J. et al. Effect of propofol and sevoflurane on the inflammatory response of patients undergoing craniotomy. BMC anesthesiology (2016) 16, 18,

167. Marmorstein R, Zhou M-M. Writers and readers of histone acetylation: structure, mechanism, and inhibition. Cold Spring Harb Perspect Biol. (2014) 6:a018762. doi: 10.1101/cshperspect.a018762

168. Martin, F.P. et al. Metabolic assessment of gradual development of moderate experimental colitis in IL-10 deficient mice. J. Proteome Res. 8, 2376–2387 (2009).

169. Martínez-García, J. J., Martínez-Banaclocha, H., Angosto-Bazarra, D., de Torre-Minguela, C., Baroja-Mazo, A., Alarcón-Vila, C., … Pelegrin, P. (2019). P2X7 receptor induces mitochondrial failure in monocytes and compromises NLRP3 inflammasome activation during sepsis. Nature Communications, 10(1). https://doi.org/10.1038/s41467-019-10626-x

170. McClure C, Brudecki L, Ferguson DA, Yao ZQ, Moorman JP, McCall CE, et al. MicroRNA 21 (miR-21) and miR-181b couple with NFI-A to generate myeloid-derived suppressor cells and promote immunosuppression in late sepsis. Infect Immun. (2014) 82:3816–25. doi: 10.1128/IAI.01495-14

171. McGeough, M. D., Wree, A., Inzaugarat, M. E., Haimovich, A., Johnson, C. D., Peña, C. A., Goldbach-Mansky, R., Broderick, L., Feldstein, A. E., & Hoffman, H. M. (2017). TNF regulates transcription of NLRP3 inflammasome components and inflammatory molecules in cryopyrinopathies. The Journal of clinical investigation, 127(12), 4488–4497. https://doi.org/10.1172/JCI90699

172. McLean, D. J., Diaz-Gil, D., Farhan, H. N., Ladha, K. S., Kurth, T., & Eikermann, M. (2015). Dose-dependent Association between Intermediate-acting Neuromuscular-blocking Agents and Postoperative Respiratory Complications. Anesthesiology, 122(6), 1201–1213. https://doi.org/10.1097/ALN.0000000000000674

173. Meisel C et al. Granulocyte-macrophage colony-stimulating factor to reverse sepsis-associated immunosuppression: a double-blind, randomized, placebo-controlled multicentre trial. Am J Respir Crit Care Med. 2009 Oct 1;180(7):640-8

174. Minarovits J, Niller HH. Patho-Epigenetics of Infectious Disease. 1st ed. New York, NY: Springer International Publishing (2016).

175. Mira JC, Gentile LF, Mathias BJ, Efron PA, Brakenridge SC, Mohr AM, et al. Sepsis pathophysiology, chronic critical illness and PICS. Crit Care Med. (2017) 45:253–62. doi: 10.1097/CCM.0000000000002074

176. Mira JC, Gentile LF, Mathias BJ, et al. Sepsis Pathophysiology, Chronic Critical Illness, and Persistent Inflammation-Immunosuppression and Catabolism Syndrome. Crit Care Med. 2017;45(2):253-262

177. Mitroulis I, Ruppova K, Wang B, Chen L-S, Grzybek M, Grinenko T, et al. Modulation of myelopoiesis progenitors is an integral component of trained immunity. Cell. (2018) 172:147–61.e12. doi: 10.1016/j.cell.2017.11.034

178. Mu J. RhoA signaling in CCL2-induced macrophage polarization. J Allergy Clin Immunol. (2018) 141:AB114. doi: 10.1016/j.jaci.2017.12.363

179. Murphy, GS, Brull, SJ Residual neuromuscular block: Lessons unlearned. Part I: Definitions, incidence, and adverse physiologic effects of residual neuromuscular block.. Anesth Analg. (2010). 111 120–8

180. Murphy, P. G., Myers, D. S., Davies, M. J., Webster, N. R. & Jones, J. G. The antioxidant potential of propofol (2,6-diisopropylphenol). British journal of anaesthesia 68, 613–618 (1992)

181. Namgaladze, D., Lips, S., Leiker, T. J., Murphy, R. C., Ekroos, K., Ferreiros, N., … Brüne, B. (2014). Inhibition of macrophage fatty acid β-oxidation exacerbates palmitate-induced inflammatory and endoplasmic reticulum stress responses. Diabetologia, 57(5), 1067–1077. https://doi.org/10.1007/s00125-014-3173-4 Nature.com. (2017). Cell Culture. Retrieved from https://www.nature.com/subjects/cell-culture

182. Netea MG, Joosten LAB, Latz E, Mills KHG, Natoli G, Stunnenberg HG, et al. Trained immunity: a program of innate immune memory in health and disease. Science. (2016) 352:aaf1098. doi: 10.1126/science.aaf1098

183. Netea MG, Quintin J, Van Der Meer JWM. Trained immunity: a memory for innate host defense. Cell Host Microbe. (2011) 9:355–61. doi: 10.1016/j.chom.2011.04.006

184. Nguyen C et al. Susceptibility of Nonpromoter CpG Islands to De Novo Methylation in Normal and Neoplastic Cells. J Natl Cancer Institute (2001) 93 (19):1465-1472

185. Nicholson WT, Sprung J, Jankowski CJ. Sugammadex: A novel agent for the reversal of neuromuscular blockade. Pharmacotherapy. 2007;27:1181–8.

186. Nio Y, Yamauchi T, Iwabu M, Okada-Iwabu M, Funata M, Yamaguchi M, et al. Monocyte chemoattractant protein-1 (MCP-1) deficiency enhances alternatively activated M2 macrophages and ameliorates insulin resistance and fatty liver in lipoatrophic diabetic A-ZIP transgenic mice. Diabetologia. (2012) 55:3350–8. doi: 10.1007/s00125-012-2710-2

187. Novakovic B, Habibi E, Wang S-Y, Arts RJW, Davar R, Megchelenbrink W, et al. β-glucan reverses the epigenetic state of LPS-induced immunological tolerance. Cell. (2016) 167:1354–68.e14. doi: 10.1016/j.cell.2016.09.034

188. Nunez Lopez O, Cambiaso-Daniel J, Branski LK, Norbury WB, Herndon DN. Predicting and managing sepsis in burn patients: current perspectives. Ther Clin Risk Manag. (2017) 13:1107–17. doi: 10.2147/TCRM.S119938

189. O'Dwyer MJ et al. The human response to infection is associated with distinct patterns of interleukin 23 and interleukin 27 expression. I ntensive Care Med. 2008 Apr;34(4):683-91

190. O'Dwyer MJ et al. The occurrence of severe sepsis and septic shock are related to distinct patterns of cytokine gene expression. Shock. 2006 Dec;26(6):544-50

191. Oda, Y. (2018). Rocuronium bromide: clinical application of single-dose pharmacokinetic models to continuous infusion. Journal of Anesthesia, 32(1), 1–2. https://doi.org/10.1007/s00540-017-2401-8

192. Oeckinghaus A, Ghosh S . The NF-kappaB family of transcription factors and its regulation. Cold Spring Harb Perspect Biol 2009

193. Osuchowski MF, Welch K, Siddiqui J, Remick DG. Circulating cytokine/inhibitor profiles reshape the understanding of the SIRS/CARS continuum in sepsis and predict mortality. J Immunol Baltim Md 1950. (2006) 177:1967–74. doi: 10.4049/jimmunol.177.3.1967

194. Ota, M Yanagisawa, M Tachibana, H et al. A significant induction of neutrophilic chemoattractants but not RANKL in synoviocytes stimulated with interleukin 17. J Bone Miner Metab 201533 140–47

195. Ou S-M, Chu H, Chao P-W, Lee Y-J, Kuo S-C, Chen T-J, et al. Long-term mortality and major adverse cardiovascular events in sepsis survivors. A nationwide population-based study. Am J Respir Crit Care Med. (2016) 194:209–17. doi: 10.1164/rccm.201510-2023OC

196. Owen HC et al. Immune related micro RNAs are associated with nosocomial pneumonia following severe trauma in ICU patients: An exploration of potential epigenetic regulatory pathways. J Trauma Acute Care Surg. 2015. In press

197. Palmer, C. S., Cherry, C. L., Sada-Ovalle, I., Singh, A., & Crowe, S. M. (2016). Glucose Metabolism in T Cells and Monocytes: New Perspectives in HIV Pathogenesis. EBioMedicine, 6, 31–41. https://doi.org/10.1016/j.ebiom.2016.02.012

198. Parameswaran, N., & Patial, S. (2010). Tumor necrosis factor-α signaling in macrophages. Critical reviews in eukaryotic gene expression, 20(2), 87–103. https://doi.org/10.1615/critreveukargeneexpr.v20.i2.10

199. Patel SB, Kress JP. Sedation and analgesia in the mechanically ventilated patient. Am J Respir Crit Care Med. 2012;185:486–97.

200. Perl TM et al. Long term survival and function after suspected gram-negative sepsis. JAMA 1995;274:338-45

201. Petronis A. Epigenetics as a unifying principle in the aetiology of complex traits and diseases. Nature. 2010. Jun 10;465, 721-7

202. Pfaffl M. W. A new mathematical model for relative quantification in real-time RT-PCR. Nucleic acids research 2001, 29(9), e45. https://doi.org/10.1093/nar/29.9.e45

203. Placek, K., Schultze, J. L., & Aschenbrenner, A. C. (2019). Epigenetic reprogramming of immune cells in injury, repair, and resolution. Journal of Clinical Investigation, 129(8), 2994–3005. https://doi.org/10.1172/JCI124619

204. Prescott H.C., Langa K.M., & Iwashyna T.J., (2015). Readmission diagnoses after hospitalization for severe sepsis and other acute medical conditions. JAMA - Journal of the American Medical Association, 313(10), 1055–1057.

205. Prescott HC, Angus DC. Enhancing recovery from sepsis: a review. JAMA. (2018) 319:62–75. doi: 10.1001/jama.2017.17687

206. Prescott HC, Osterholzer JJ, Langa KM, Angus DC, Iwashyna TJ. Late mortality after sepsis: propensity matched cohort study. BMJ. (2016) 353:i2375. doi: 10.1136/bmj.i2375

207. Pühringer, F. K., Gordon, M., Demeyer, I., Sparr, H. J., Ingimarsson, J., Klarin, B., … Heeringa, M. (2010). Sugammadex rapidly reverses moderate rocuronium- or vecuronium-induced neuromuscular block during sevoflurane anaesthesia: A dose - Response relationship. British Journal of Anaesthesia, 105(5), 610–619. https://doi.org/10.1093/bja/aeq226

208. Quartin AA et al. Magnitude and duration of the direct effect of sepsis on survival. Department of Veterans Affairs Systemic Sepsis Cooperative Studies Group. JAMA 1997;277:1058-63

209. Quintin J, Saeed S, Martens JH a, Giamarellos- EJ, Ifrim DC, Logie C, et al. Candida albicans infection affords protection against reinfection via functional reprogramming of monocytes. Cell Host Microbe. (2013) 12:223–32. doi: 10.1016/j.chom.2012.06.006.Candida

210. Raedler LA. Farydak (Panobinostat): first HDAC inhibitor approved for patients with relapsed multiple myeloma. Am Health Drug Benefits. (2016) 9:84–87.

211. Raja M et al, Long-term follow-up of sepsis induced immunoparalysis. Intensive Care Med Exper. 2015 in press

212. Rhee, C., Jones, T. M., Hamad, Y., Pande, A., Varon, J., O'Brien, C., … Klompas, M. (2019). Prevalence, Underlying Causes, and Preventability of Sepsis-Associated Mortality in US Acute Care Hospitals. JAMA Network Open, 2(2), e187571. https://doi.org/10.1001/jamanetworkopen.2018.7571

213. Ricklin D, Hajishengallis G, Yang K, Lambris J. Complement: a key system for immune surveillance and homeostasis. Nat Immunol. (2019) 11:785–97. doi: 10.1038/ni.1923.

214. Rink, L. Tumor Necrosis Factor α. Editor(s): Peter J. Delves, Encyclopedia of Immunology (Second Edition), Elsevier 1998, Pages 2435-2440, ISBN 9780122267659

215. Rivers E, Nguyen B, Havstad S, Ressler J, Muzzin A, Knoblich B, et al. Early goal-directed therapy in the treatment of severe sepsis and septic shock. N Engl J Med. 2001;345:1368–77

216. Roger T, Lugrin J, Roy DL, Goy G, Mombelli M, Koessler T, et al. Histone deacetylase inhibitors impair innate immune responses to toll-like receptor agonists and to infection. Blood. (2011) 117:1205–17. doi: 10.1182/blood-2010-05-284711

217. Roh, G.U., Song, Y., Park, J. et al. Effects of propofol on the inflammatory response during robot-assisted laparoscopic radical prostatectomy: a prospective randomized controlled study. Sci Rep 9, 5242 (2019).

218. Royse CF, Liew DFL, Wright CE, Royse AG, Angus JA; Persistent Depression of Contractility and Vasodilation with Propofol but Not with Sevoflurane or Desflurane in Rabbits. Anesthesiology 2008;108(1):87-93.

219. Runzer, T. D., Ansley, D. M., Godin, D. V. & Chambers, G. K. Tissue antioxidant capacity during anesthesia: propofol enhances in vivo red cell and tissue antioxidant capacity in a rat model. Anesthesia and analgesia 94, 89–93, table of contents (2002).

220. Rusting, R. Scientific American. Illustrations by AXS Biomedical Animation Studio. (2011)

221. Ruytinx P, Proost P, Van Damme J, Struyf S. Chemokine-induced macrophage polarization in inflammatory conditions. Front Immunol. (2018) 9:1930. doi: 10.3389/fimmu.2018.01930

222. Ryan QC, Headlee D, Acharya M, Sparreboom A, Trepel JB, Ye J, et al. Phase I and pharmacokinetic study of MS-275, a histone deacetylase inhibitor, in patients with advanced and refractory solid tumors or lymphoma. J Clin Oncol. (2005) 23:3912–22. doi: 10.1200/JCO.2005.02.188

223. Saeed, S., Quintin, J., Kerstens, H. H. D., Rao, N. A., Aghajanirefah, A., Matarese, F., … Stunnenberg, H. G. (2014). Epigenetic programming of monocyte-to-macrophage differentiation and trained innate immunity. Science, 345(6204). https://doi.org/10.1126/science.1251086

224. Salazar-Mather, T. P., Hamilton, T. A., Biron, C. A. (2000) A chemokine-to-cytokine-to-chemokine cascade critical in antiviral defense. J. Clin. Invest. 105, 985–993.

225. Sapienza C, Issa J-P. Diet, nutrition, and cancer epigenetics. Annu Rev Nutr. (2016) 36:665–81. doi: 10.1146/annurev-nutr-121415-112634

226. Saraiva, M., & O'Garra, A. (2010). The regulation of IL-10 production by immune cells. Nature Reviews Immunology, 10(3), 170–181. https://doi.org/10.1038/nri2711

227. Schenkman KA, Yan S. Propofol impairment of mitochondrial respiration in isolated guinea pig hearts determined by reflectance spectroscopy. Crit Care Med 2000;28:172–177

228. Schläpfer, M., Piegeler, T., Dull, R.O. et al. Propofol increases morbidity and mortality in a rat model of sepsis. Crit Care 19, 45 (2015).

229. Schmidt F, Gasparoni N, Gasparoni G, Gianmoena K, Cadenas C, Polansky JK, et al. Combining transcription factor binding affinities with open-chromatin data for accurate gene expression prediction. Nucleic Acids Res. (2017) 45:54–66. doi: 10.1093/nar/gkw1061

230. Schneemilch CE, Schilling T, Bank U. Effects of general anaesthesia on inflammation. Best Pract Res Clin Anaesthesiol. 2004;18:493–507

231. Schrijver IT, Théroude C, Roger T. Myeloid-derived suppressor cells in sepsis. Front Immunol. (2019) 10:327. doi: 10.3389/fimmu.2019.00327

232. Schroder, Hertzog, Ravasi, Hume. Interferon-gamma: an overview of signals, mechanisms and functions. J. Leukoc. Biol., 75 (2004), pp. 163-189

233. Schulte, W., Bernhagen, J., and Bucala, R. (2013). Cytokines in sepsis: potent immunoregulators and potential therapeutic targets–an updated view. Med. Inflamm. 2013:165974. doi: 10.1155/2013/165974

234. Seeley JJ, Baker RG, Mohamed G, Bruns T, Hayden MS, Deshmukh SD, et al. Induction of innate immune memory via microRNA targeting of chromatin remodelling factors. Nature. (2018) 559:114. doi: 10.1038/s41586-018-0253-5

235. Sellati, T, Sahay, B. Cells of Innate Immunity: Mechanisms of Activation. Editor(s): Linda M. McManus, Richard N. Mitchell, Pathobiology of Human Disease, Academic Press 2014, Pages 258-274, ISBN 9780123864574.

236. Sen, G. C. (2001) Viruses and interferons. Annu. Rev. Microbiol. 55, 255–281.

237. Seong A-R, Yoo J-Y, Choi K, Lee M-H, Lee Y-H, Lee J, et al. Delphinidin, a specific inhibitor of histone acetyltransferase, suppresses inflammatory signaling via prevention of NF-κB acetylation in fibroblast-like synoviocyte MH7A cells. Biochem Biophys Res Commun. (2011) 410:581–6. doi: 10.1016/j.bbrc.2011.06.029

238. Serpa Neto A, Hemmes SNT, Barbas CSV, et al. Incidence of mortality and morbidity related to postoperative lung injury in patients who have undergone abdominal or thoracic surgery: a systematic review and meta-analysis. Lancet Respir Med 2014; 2: 1007–15.

239. Seto E, Yoshida M. Erasers of histone acetylation: the histone deacetylase enzymes. Cold Spring Harb Perspect Biol. (2014) 6:a018713. doi: 10.1101/cshperspect.a018713

240. Shao S, Kang H, Tong Z. Early neuromuscular blocking agents for adults with acute respiratory distress syndrome: a systematic review, meta-analysis and meta-regression. BMJ Open 2020;10:e037737. doi: 10.1136/bmjopen-2020-037737

241. Shimizu, J., Tabata, T., Tsujita, Y., Yamane, T., Yamamoto, Y., Tsukamoto, T., Ogawa, N., Kim, H., Urushitani, M. and Eguchi, Y. (2020), Propofol infusion syndrome complicated with mitochondrial myopathy, encephalopathy, lactic acidosis, and stroke-like episodes: a case report. Acute Med Surg, 7: e473.

242. Singer M, Deutschman CS, Seymour CW, Shankar-Hari M, Annane D, Bauer M, et al. The third international consensus definitions for sepsis and septic shock (Sepsis-3). JAMA. (2016) 315:801–10. doi: 10.1001/jama.2016.0287

243. Sodhi A, Biswas SK. Monocyte chemoattractant protein-1-induced activation of p42/44 MAPK and c-Jun in murine peritoneal macrophages: a potential pathway for macrophage activation. J Interferon Cytokine Res. (2002) 22:517–26. doi: 10.1089/10799900252981990

244. Sônego F, Castanheira FV e S, Ferreira RG, Kanashiro A, Leite CAVG, Nascimento DC, et al. Paradoxical roles of the neutrophil in sepsis: protective and deleterious. Front Immunol. (2016) 7:155. doi: 10.3389/fimmu.2016.00155

245. Sottile, P.D., Albers, D. & Moss, M.M. Neuromuscular blockade is associated with the attenuation of biomarkers of epithelial and endothelial injury in patients with moderate-to-severe acute respiratory distress syndrome. Crit Care 22, 63 (2018). https://doi.org/10.1186/s13054-018-1974-4

246. Stankovic A, Slavic V, Stamenkovic B, Kamenov B, Bojanovic M, Mitrovic D. Serum and synovial fluid concentrations of CCL2 (MCP-1) chemokine in patients suffering rheumatoid arthritis and osteoarthritis reflect disease activity. Bratisl. Lek. Listy. (2009) 110:641–6.

247. Storgaard M et al. Short and long term mortality in patients with community acquired severe sepsis and septic shock. Scand J Infect Dis. 2013 Aug;45(8):577-83

248. Suetrong B, Walley KR (2016) Lactic acidosis in sepsis: It's Not All anaerobic: implications for diagnosis and management. Chest 149: 252–261

249. Sui WG, He HY, Yan Q, Chen JJ, Zhang RH, Dai Y. ChIP-seq analysis of histone H3K9 trimethylation in peripheral blood mononuclear cells of membranous nephropathy patients. Braz J Med Biol Res. 2014;47(1):42-49. doi:10.1590/1414-431X20132809

250. Sun SC, Liu ZG . A special issue on NF-kappaB signaling and function. Cell Res 2011; 21: 1–2.

251. Sun X, Icli B, Wara AK, Belkin N, He S, Kobzik L, et al. MicroRNA-181b regulates NF-κB–mediated vascular inflammation. J Clin Invest. (2012) 122:1973–90. doi: 10.1172/JCI61495

252. Sutterwala FS, Haasken S, Cassel SL . Mechanism of NLRP3 inflammasome activation. Ann N Y Acad Sci 2014; 1319: 82–95.

253. Suy K, Morias K, Cammu G, et al. Sugammadex, a selective relaxant binding agent, offers effective reversal of moderate rocuronium- or vecuronium-induced neuromuscular block. Anesthesiology 2007; 106: 283–8

254. Sweeney, T. E., Shidham, A., Wong, H. R., & Khatri, P. (2015). A comprehensive time-course-based multicohort analysis of sepsis and sterile inflammation reveals a robust diagnostic gene set. Science Translational Medicine, 7(287), 1–16. https://doi.org/10.1126/scitranslmed.aaa5993

255. Tak PP, Firestein GS . NF-kappaB: a key role in inflammatory diseases. J Clin Invest 2001; 107: 7–11.

256. Takatsu, Moon, Itakura, Tsukamoto, Horikawa, Ikutani, Kouro, Takaki. Role of IL-5 in the innate immune system and disease control. International Congress Series, Volume 1285, 2005, Pages 145-154,

257. Tang D, Kang R, Coyne CB, Zeh HJ, Lotze MT. PAMPs and DAMPs: signal 0s that spur autophagy and immunity. Immunol Rev. (2012) 249:158–75. doi: 10.1111/j.1600-065X.2012.01146.x

258. Tian J, Rui K, Tang X, Ma J, Wang Y, Tian X, et al. MicroRNA-9 regulates the differentiation and function of myeloid-derived suppressor cells via targeting runx1. J Immunol. (2015) 195:1301–11. doi: 10.4049/jimmunol.1500209

259. Tompkins, R. G. (2015). Genomics of injury. Journal of Trauma and Acute Care Surgery (Vol. 78). https://doi.org/10.1097/ta.0000000000000568

260. Torrance HD et al. Association between gene expression biomarkers of immunosuppression and blood transfusion in severely injured trauma patients. Ann Surg 2015. Apr;261(4):751-9

261. Tsaur I, Noack A, Makarevic J, Oppermann E, Waaga-Gasser AM, Gasser M, et al. CCL2 chemokine as a potential biomarker for prostate cancer: a pilot study. Cancer Res Treat. (2015) 47:306. doi: 10.4143/crt.2014.015

262. Uhel F, Azzaoui I, Grégoire M, Pangault C, Dulong J, Tadié J-M, et al. Early expansion of circulating granulocytic myeloid-derived suppressor cells predicts development of nosocomial infections in patients with sepsis. Am J Respir Crit Care Med. (2017) 196:315–27. doi: 10.1164/rccm.201606-1143OC

263. Unsinger J et al. IL-7 promotes T cell viability, trafficking, and functionality and improves survival in sepsis. J Immunol. 2010 Apr ; 184(7):3768-79

264. van der Poll T, van de Veerdonk FL, Scicluna BP, Netea MG. The immunopathology of sepsis and potential therapeutic targets. Nat Rev Immunol. (2017) 17:407–20. doi: 10.1038/nri.2017.36

265. van Vught LA, Klein Klouwenberg PMC, Spitoni C, et al; MARS Consortium. Incidence, risk factors, and attributable mortality of secondary infections in the intensive care unit after admission for sepsis. JAMA. doi:10.1001/jama.2016.2691. (2016)

266. Vandesompele, J., De Preter, K., Pattyn, F. et al. Accurate normalization of real-time quantitative RT-PCR data by geometric averaging of multiple internal control genes. Genome Biol 3, research0034.1 (2002). https://doi.org/10.1186/gb-2002-3-7-research0034

267. Vassalli P. The pathophysiology of tumor necrosis factors. Annu Rev Immunol. 1992;10:411–452.

268. Vincent J, Moreno R, Takala J, Willatts S, De Mendonça A, Bruining H, et al. (1996) The SOFA (Sepsis-related Organ Failure Assessment) score to describe organ dysfunction/failure. on behalf of the working group on sepsis-related problems of the European society of intensive care medicine. Intensive Care Med.

269. Vincent J-L. The clinical challenge of sepsis identification and monitoring. PLoS Med. (2016) 13:17–8. doi: 10.1371/journal.pmed.1002022

270. Visvabharathy, L., & Freitag, N. E. (2017). Propofol Sedation Exacerbates Kidney Pathology and Dissemination of Bacteria during Staphylococcus aureus Bloodstream Infections, Infection and Immunity 85(7), 1–15.

271. Vojinovic J, Damjanov N. HDAC inhibition in rheumatoid arthritis and juvenile idiopathic arthritis. Mol Med. (2011) 17:397–403. doi: 10.2119/molmed.2011.00030

272. Wallner, S., Schröder, C., Leitão, E., Berulava, T., Haak, C., Beißer, D., … Horsthemke, B. (2016). Epigenetic dynamics of monocyte-to-macrophage differentiation. Epigenetics and Chromatin, 9(1), 1–17. https://doi.org/10.1186/s13072-016-0079-z

273. Walton AH, Muenzer JT, Rasche D, Boomer JS, Sato B, Brownstein BH, et al. Reactivation of multiple viruses in patients with sepsis. PLoS ONE. (2014) 9:e98819. doi: 10.1371/journal.pone.0098819

274. Wang B, Lin L, Ai Q, Zeng T, Ge P, Zhang L. HAT inhibitor, garcinol, exacerbates lipopolysaccharide-induced inflammation in vitro and in vivo. Mol Med Rep. (2016) 13:5290–6. doi: 10.3892/mmr.2016.5189

275. Wang Q, Ren J, Morgan S, Liu Z, Dou C, Liu B. Monocyte chemoattractant protein-1 (MCP-1) regulates macrophage cytotoxicity in abdominal aortic aneurysm. PLoS ONE. (2014) 9:e92053. doi: 10.1371/journal.pone.0092053

276. Wang X, Yu Y. MiR-146b protect against sepsis induced mice myocardial injury through inhibition of Notch1. J Mol Histol. (2018) 49:411–7. doi: 10.1007/s10735-018-9781-4

277. Wang Z, Zang C, Cui K, Schones DE, Barski A, Peng W, et al. Genome-wide mapping of HATs and HDACs reveals distinct functions in active and inactive genes. Cell. (2009) 138:1019–31. doi: 10.1016/j.cell.2009.06.049

278. Wang, L., Ko, K. W. S., Lucchinetti, E., Zhang, L., Troxler, H., Hersberger, M., … Zaugg, M. (2010). Metabolic Profiling of Hearts Exposed to Sevoflurane and Propofol Reveals Distinct Regulation of Fatty Acid and Glucose Oxidation. Anesthesiology, (3), 1. https://doi.org/10.1097/aln.0b013e3181e2c1a1

279. Wang, Z. M., Zhang, P., Lin, M. J., Tan, B., Qiu, H. B., & Yu, W. F. (2013). Influence of Obstructive Jaundice on Pharmacodynamics of Rocuronium. PLoS ONE, 8(10), 3–7. https://doi.org/10.1371/journal.pone.0078052

280. Warnock C, Totterdell P, Tod AM, Mead R, Gynn JL, Hancock B. The role of temperature in the detection and diagnosis of neutropenic sepsis in adult solid tumour cancer patients receiving chemotherapy. Eur J Oncol Nurs. (2018) 37:12–8. doi: 10.1016/j.ejon.2018.10.001.

281. Wei J, Dong S, Bowser RK, Khoo A, Zhang L, Jacko AM, et al. Regulation of the ubiquitylation and deubiquitylation of CREB-binding protein modulates histone acetylation and lung inflammation. Sci Signal. (2017) 10:eaak9660. doi: 10.1126/scisignal.aak9660

282. Weiser, TG, Regenbogen, SE, Thompson, KD, Haynes, AB, Lipsitz, SR, Berry, WR, Gawande, AA An estimation of the global volume of surgery: A modelling strategy based on available data.. Lancet. (2008). 372 139–44

283. Weiterer S, Uhle F, Bhuju S, Jarek M, Weigand MA, et al. (2014) From Human Monocytes to Genome-Wide Binding Sites - A Protocol for Small Amounts of Blood: Monocyte Isolation/ChIP-Protocol/Library Amplification/Genome Wide Computational Data Analysis. PLOS ONE 9(4): e94164

284. Weiterer S, Uhle F, Lichtenstern C, Siegler BH, Bhuju S, et al. (2015) Sepsis Induces Specific Changes in Histone Modification Patterns in Human Monocytes. PLOS ONE 10(3): e0121748

285. Wen H et al. Epigenetic regulation of dendritic cell-derived interleukin-12 facilitates immunosuppression after a severe innate immune response. Blood; 111:1797-804 (2008)

286. Wheeler AP, Bernard GR. Treating patients with severe sepsis. N Engl J Med. 1999;340:207–14.

287. Wiersinga WJ. Current insights in sepsis: from pathogenesis to new treatment targets. Curr Opin Crit Care. (2011) 17:480–6. doi: 10.1097/MCC.0b013e32834a4aeb

288. Windt, Gerritje J.W. van der et al. Measuring Bioenergetics in T Cells Using a Seahorse Extracellular Flux Analyzer. Current protocols in immunology 113 (2016): 3.16B.1-3.16B.14

289. Wolf, M, Weir P, Segar P, Stone J, Shield J, (2001). Impaired fatty acid oxidation in propofol infusion syndrome. Lancet. 357. 606-7. 10.1016/S0140-6736(00)04064-2.

290. Xiao G, Harhaj EW, Sun SC . NF-kappaB-inducing kinase regulates the processing of NF-kappaB2 p100. Mol Cell 2001;

291. Yang, S., Chou, W. P. & Pei, L. Effects of propofol on renal ischemia/reperfusion injury in rats. Exp Ther Med (2013) 6, 1177–1183

292. Yoshimura T. The chemokine MCP-1 (CCL2) in the host interaction with cancer: a foe or ally? Cell Mol Immunol. (2018) 15:335–45. doi: 10.1038/cmi.2017.135

293. Young PJ, Bellomo R. Fever in sepsis: is it cool to be hot? Crit Care. (2014) 18:109. doi: 10.1186/cc13726

294. Yu T, Peng X, Liu L, et al. Propofol increases preload dependency in septic shock patients. J Surg Res. 2015;193(2):849-855. doi:10.1016/j.jss.2014.08.050

295. Yuan Z, Syed MA, Panchal D, Rogers D, Joo M, Sadikot RT. Curcumin mediated epigenetic modulation inhibits TREM-1 expression in response to lipopolysaccharide. Int J Biochem Cell Biol. (2012) 44:2032–43. doi: 10.1016/j.biocel.2012.08.001

296. Zhang C, Wang Z, Zhang J, et al. Competitive inhibition of the nondepolarizing muscle relaxant rocuronium on nicotinic acetylcholine receptor channels in the rat superior cervical ganglia. J Cardiovasc Pharmacol. 2014;63(5):428-433.

297. Zhang L, Jin S, Wang C, Jiang R, Wan J. Histone deacetylase inhibitors attenuate acute lung injury during cecal ligation and puncture-induced polymicrobial sepsis. World J Surg. (2010) 34:1676–83. doi: 10.1007/s00268-010-0493-5

298. Zhang M-Q. Drug-specific cyclodextrins: the future of rapid reversal? Drugs Future 2003; 28: 347–54

299. Zhang Q, Cao X. Epigenetic regulation of the innate immune response to infection. Nat Rev Immunol. (2019) doi: 10.1038/s41577-019-0151-6. [Epub ahead of print].

300. Zhang R, Erler J, Langowski J. Histone acetylation regulates chromatin accessibility: role of H4K16 in inter-nucleosome interaction. Biophys J. (2017) 112:450–9. doi: 10.1016/j.bpj.2016.11.015

301. Zhao Y, Yi W, Wan X, Wang J, Tao T, Li J, et al. Blockade of ICAM-1 improves the outcome of polymicrobial sepsis via modulating neutrophil migration and reversing immunosuppression. Mediators Inflamm. (2014) 2014:195290. doi: 10.1155/2014/195290